Founded 1897 • New Series

Vol. 129 • No. 6/2026 • November

Romanian Journal of Military Medicine



REVISTA DE MEDICINĂ MILITARĂ

- *Aging of the skin. From molecular mechanisms and clinical aspects to chronic skin failure and social impact*
- *AI in Drug Discovery and Precision Medicine*
- *Artificial Intelligence for Radiographic Assessment of Peri-Implant Marginal Bone Loss: Current Evidence, Clinical Interpretation, and Limitations*
- *Association of [18F]FDG PET/CT radiomic features with Ki-67 in untreated primary breast carcinoma*
- *Deep Brain Stimulation for Parkinson's Disease: Current state and perspectives – a narrative review*
- *Design and validation of a questionnaire regarding the occupational risk of cancer for clinical practice in Romania*
- *Discordance between coronary CT angiography and invasive coronary angiography at low Agatston scores: a bicentric cohort of 124 Romanian patients*
- *Psychiatric disorders due to brain tumors: A perspective on diagnostic vigilance and integrated care*
- *Rethinking Interleukin-11 in Metabolic Liver Disease: A Critical Reappraisal of Biomarker Directionality*
- *Unravelling the serum calcium-to-magnesium ratio: a study in 474 individuals with/without adrenal tumors in relationship with central DXA results*

CLARIVATE ANALYTICS
EMERGING SOURCES CITATION INDEX
INDEXED

Editorial Board of the Romanian Journal of Military Medicine

Under the patronage of	Romanian Academy Carol Davila University of Medicine and Pharmacy, Romania
Honorary Editor	Acad. Victor Voicu, MD, Ph.D.
Editors-in-Chief	Florentina Ioniță Radu, MD, Ph.D. Dan Mischianu, MD, Ph.D.
Executive Editor	Octavian Vasiliu, MD, Ph.D.
Associate Editor	Mariana Jinga, MD, Ph.D., MBA
Medical Editors	Ana M.A. Stănescu, MD, Ph.D. Clara Ursescu, MD Ștefan Ion, MD, Ph.D. Florentina Pleșa, MD, Ph.D. Vasile Balaban, MD, Ph.D. Camelia Diaconu, MD, Ph.D. Mihaiță Pătrășescu, MD, Ph.D.
Surgical Editors	Adrian Ciuche, MD, Ph.D. Remus Nica, MD, Ph.D. Dan Spînu, MD, Ph.D. Ana Căruntu, MD, Ph.D.
Paraclinical Editors	Raluca Mititelu, MD, Ph.D. Valentina Uivarosi, MD, Ph.D. Constantin Căruntu, MD, Ph.D.
Editorial Assistants	Cristina Licurici, Teodora Mititelu, Gabriel Ilinoiu
Technical Secretary	Bogdan Ciubotaru
Publisher	The Carol Davila University of Medicine and Pharmacy Publishing House

International Editorial Board

Dinu V. Bălănescu (USA)
Natan Børnstein (Israel)
Silviu Brill (Israel)
Cris S. Constantinescu (UK)
Daniel Dănilă (USA)
Stergios Ganatsios (Greece)
Mihai Moldovan (Denmark)
Gerard Roul (France)
Erwin Santo (Israel)
Radu Ţuţuian (Switzerland)
Shyam Varadarajulu (USA)
Peter Vilmann (Denmark)

Scientific Publishing Committee

Mihaela Banu (Anatomy and Morphology)
Adrian G Barbilian (Traumatology)
Anda Băicuş (Microbiology)
Cristian R Băicuş (Internal Medicine)
Andra R Bălănescu (Rheumatology)
Șerban M Bălănescu (Cardiology)
Șerban VG Berteșteanu (ENT)
Mircea Beuran (Surgery)
Daciana E Brănișteanu (Dermatology)
Mihai Ciocârlan (Gastroenterology)
Cătălin F Cîrstoiu (Traumatology)
Gabriel Constantinescu (Gastroenterology)
Magda M Constantin (Dermatology)
Silviu M Constantinoiu (Surgery)
Lucian George Eftimie (Pathology)
Alice Munteanu (Cardiology)
Dan Corneci (Intensive Care)
Cristina E Dinu Pirvu (Pharmacology)
Carmen G Fierbințeanu (Gastroenterology)
Florin M Filipoiu (Anatomy and Morphology)
Mihai E Hinescu (Molecular Biology)
Radu C Jecan (Plastic Surgery)
Viorel Jinga (Urology)
Ruxandra O Jurcuț (Cardiology)
Mara M. Mihai (Dermatology)
Marian Mitrică (Neurosurgery)
Dafin F Mureșanu (Neurology)
Monica Neagu (Immunology)
Claudiu Nistor (Thoracic Surgery)
Lucian E Negreanu (Internal Medicine)
Diana C Nuță (Pharmacology)
Silviu-Ionel Dumitrescu (Cardiology)
Diana L Păun (Endocrinology)
Cătălina Poiană (Endocrinology)
Alexandru B Popescu (Cardiology)
Andreea C Popescu (Cardiology)
Bogdan O Popescu (Neurology)
Victor L Purcărea (Management)
Aurelian E Ranetti (Endocrinology)
Andrada Seicean (Gastroenterology)
Carmen A Sîrbu (Neurology)
Horia Stanca (Ophthalmology)
Silviu M Stanciu (Internal Medicine)
Victor Strambu (Surgery)
Alina Tănase (Biochemistry)
Călin Tătaru (Ophthalmology)
Dragoş Vinereanu (Cardiology)
Ana-Maria Oproiu (Plastic Surgery)

REDACTION
Strada Mircea Vulcanescu, Nr. 88, Sector 1, București, Email: office@rjmm.ro
www.revistamedicinamilitara.ro

Romanian Journal of Military Medicine, New Series, vol. 129, No 6/2026, November
ISSN-L1222-5126; eISSN 2501-2312; pISSN 1222-512

Romanian Journal of
Military Medicine

Founded 1897•New Series
Vol. 129 • No. 6/2026, November

Contents

1. Mihail A. Badea, Andrei C. Costache, Adrian B. Ghigolea, Bara Monica Angela, Bugnariu Anca Iulia, Daniel O. Costache, Ștefan Laurian Maxim
● ***Aging of the skin. From molecular mechanisms and clinical aspects to chronic skin failure and social impact*** **589**

2. Richa Sharma, Richa Saxena, Rakshith Maneshwar Hoskeri, Ekadashi Rajni, Teju Lal Chaurasia
● ***AI in Drug Discovery and Precision Medicine*** **600**

3. Vladimir Năstasie, Ioan Sîrbu, Andreea Mihaela Custură , Elisei Adelin Radu , Dragoș Epistatu, Alexandra Tuță, Valentin Daniel Sîrbu
● ***Artificial Intelligence for Radiographic Assessment of Peri-Implant Marginal Bone Loss: Current Evidence, Clinical Interpretation, and Limitations*** **610**

4. Alexandru Mitoi, Raluca-Mihaela Mititelu, Cosmin Medar, Vlad-Octavian Bolocan, Ciprian Constantin, Ioan-Nicolae Mateș
● ***Association of [18F]FDG PET/CT radiomic features with Ki-67 in untreated primary breast carcinoma*** **624**

5. Gabriel-Sebastian Donea, Miruna-Cătălina Maftei, Andreea-Ramona Treteanu, Octavian Andronic, Octavian Mihai Sîrbu, Maria Mirabela Manea
● ***Deep Brain Stimulation for Parkinson's Disease: Current state and perspectives – a narrative review*** **636**

6. Cristina Mandanach, Alice Elena Munteanu, Alexandru Ștefan Cătălin Rașcu, Ștefan Dumitrache-Rujinski, Mihai Teodor Georgescu, Andreea Maftei, Claudia Lucia Toma, Marina Ruxandra Oțelea
● ***Design and validation of a questionnaire regarding the occupational risk of cancer for clinical practice in Romania*** **652**

7. Andra-Maria Barota-Bebeselea, Doru-Florian Cornel Moga, Ioan Manitiu
● ***Discordance between coronary CT angiography and invasive coronary angiography at low Agatston scores: a bicentric cohort of 124 Romanian patients*** **687**

8. Cristian Năstase, Bogdan M. Petrescu, Octavian Vasiliu, Cristian A. Cândea, Andrei G. Mangalagiu
● ***Psychiatric disorders due to brain tumors: A perspective on diagnostic vigilance and integrated care*** **696**

9. Ion Mereuță, Diana Mihaela Ciuc, Cristina Octaviana Daia, Madalina Codruta Verenca, Vladimir Cărăuș, Ion Bălan, Nicolae Roșca, Valeriu-Gabi Dincă, Cristian Daniel Marica, Gabriel Petre Gorecki
● ***Rethinking Interleukin-11 in Metabolic Liver Disease: A Critical Reappraisal of Biomarker Directionality*** **709**

10. Mihai-Lucian Ciobica, Mihai Costachescu, Anda Dumitrascu, Ana-Maria Gheorghe, Gabi Voicu, Dana Manda, Sorina Violeta Schiopor, Mara Carsote, Luminita Suveica, Alexandra-ioana Trandafir
● ***Unravelling the serum calcium-to-magnesium ratio: a study in 474 individuals with/without adrenal tumors in relationship with central DXA results*** **725**

Guidelines for authors **741**

https://doi.org/10.55453/rjmm.2026.129.6.1

Review

Aging of the skin. From molecular mechanisms and clinical aspects to chronic skin failure and social impact

Mihail A. Badea[1,2], Andrei C. Costache[3,*], Adrian B. Ghigolea[1,*], Bara Monica Angela[1], Bugnariu Anca Iulia[1], Daniel O. Costache[4], Ștefan Laurian Maxim[5]

[1] Department of Social Sciences, 1 December 1918 University of Alba Iulia, Romania
[2] Natural Skin Târgu Mureș, Mureș, Romania
[3] Carol Davila University of Medicine and Pharmacy, Bucharest, Romania
[4] Dermatology Department, Carol Davila Military University Emergency Hospital, Carol Davila University of Medicine and Pharmacy, Bucharest, Romania
[5] Emergency Clinical County Hospital Brașov, Faculty of Medicine, Transilvania University of Brașov, Romania
*Correspondence: ACC, andrei-catalin.costache2023@stud.umfcd.ro, and ABG, adrian.ghigolea@uab.ro

Abstract: The process of aging population is increasing the relevance of comprehending age-related changes in skin structure and function, as well as their implications for clinical care. This narrative review explores aspects of the intrinsic and extrinsic mechanisms of skin aging, their molecular and morphological consequences, and their clinical expression, with particular attention to chronic cutaneous insufficiency. The intrinsic aging process is reflecting declining cellular functionality, impaired tissue homeostasis, and endocrine changes, especially regarding estrogen deficiency after menopause. These processes are reducing collagen synthesis, hydration, and elasticity and thus contributing to epidermal and dermal atrophy and barrier dysfunction. On the other hand, extrinsic aging is driven mainly by cumulative ultraviolet exposure, with additional contributions from pollution, smoking, diet, and behavioral and psychosocial factors. Processes such as oxidative stress, inflammation, DNA damage, glycation, and increased matrix metalloproteinase activity promote extracellular matrix degradation, linking the environmental exposure to the photoaging and cutaneous carcinogenesis. Main clinical manifestations include xerosis, chronic pruritus, pigmentary changes, benign lesions, actinic keratoses, and basal cell and squamous cell carcinomas. Inflammatory, allergic, autoimmune, and drug-induced dermatoses, including psoriasis, lichen planus, and bullous pemphigoid, are complicating healthcare in older adults, while systemic comorbidities and medication use are influencing clinical presentation and treatment. Dermatoporosis is characterized by cutaneous atrophy, purpura, pseudoscars, and susceptibility to injury after minor trauma. Reduced hyaluronic acid availability and CD44 expression contribute to impaired hydration and mechanical resilience, potentially leading to ulceration and deep dissecting hematomas. Management measures are emphasizing the role of photoprotection, skin hydration, trauma prevention, and reduction of modifiable exposures, with corticosteroid use warranting reassessment in secondary dermatoporosis. Other discussed approaches are topical hyaluronic acid, retinoids, alpha-hydroxy acids, and vitamin C, but the proposed interventions have limited supporting evidence. Therefore, it is considered that early recognition of these interconnected changes may be supportive for planning prevention, a timely diagnosis, and individualized care, based on considerations like skin fragility, associated disease, and treatment burden in older patients.

Keywords: skin aging; endocrine aging; sun exposureȘ dermatoporosis; photoaging; oxidative stress; skin barrier dysfunction

EPIDEMIOLOGICAL ASPECTS OF POPULATION AGING

According to recent statistics, 10% of the world's population is over the age of 60, and this percentage is expected to double by the end of the 21st century. Aging is considered a global phenomenon with an estimated increase in the number of individuals aged 80 and above in the near future. The researchers describe it as "aging of the elderly." Worldwide, the elderly are the fastest-growing population group. By the year 2050, it is expected that the percentage of the elderly will surpass that of children. Economic growth and rising education levels have some consequences, such as significant disruption in the children-to-elderly ratio, particularly in Western Europe and the United States [1,2].

Citation: Badea MA, Costache AC, Ghigolea AB, Bignariu AI, Costache DO, Maxim SL. *Aging of the skin. From molecular mechanisms and clinical aspects to chronic skin failure and social impact.* R. J. Mil. Med. 2026, CXXIX(6): 589-599. https://doi.org/10.55453/rjmm.2026.129.6.1

Academic Editor: Octavian Vasiliu

Received: 30 September 2026
Revised: 21 October 2026
Accepted: 29 October 2026

The situation in Romania aligns with the global aging trend, especially in the past two decades. In 2018, the country's population reached 22,194,000 citizens. The phenomenon of demographic aging has increased, with the elderly population aged 65 years and older exceeding the population aged 0–14 years by 350,000 people, according to the National Institute of Statistics (INS). Life expectancy approximately doubled, from 36.4 years at the beginning of the 20th century to 75 years by 2015. Romania ranks 67th in terms of life expectancy, with Monaco in 1st place, and Angola and Sierra Leone in last place (source: WHO, 2016).

In Romania, we are facing a decrease in the population aged 0–14 years and an increase in the population over 65 years old; this aspect is attributed to the decrease in the birth rate, rising economic levels, and improvements in the quality of healthcare services. This gap between the two groups is found especially in rural areas due to migration toward urban areas and outside the country (about 10% of Romania's population has emigrated, particularly following the country's accession to the European Union). This phenomenon also has an impact on the birth rate, with most of the children of those who emigrated being born outside the country, especially in Germany, Spain and Italy. Based on these data, it is not difficult to conclude that in about three decades, the Romanian medical system is likely to face a real problem regarding treatment for the elderly (according to the INS, as of January 1, 2018, the largest age group in Romania was composed of those aged 45–49 years) [3,4].

INTRINSIC SKIN AGING

Intrinsic, or endogenous, aging results from the sum of two major factors. The first involves a slow and gradual decline in physiological cellular functions; it has individual variations and is genetically determined. On top of these gradually accumulated changes sits the reduction in the activity of the endocrine glands, especially involving the gonads. Skin aging due to endogenous factors is a slow and inevitable process, unlike extrinsic aging, which can be significantly delayed by avoiding the factors involved in its genesis, such as exposure to the sun [5].

The genetic component has an important influence on the skin aging process. Thus, gender, ethnicity, and individual variations in the composition of the hydrolipidic film bring significant differences in the degree of skin aging. Women have lower amounts of dermal collagen compared to men; these levels remain constant up until menopause, after which a sudden and marked reduction is observed. In men, collagen decreases gradually by 1% per year. This steady decline also affects other skin functions such as elasticity and hydration. While men experience chronological aging directly proportional to age, in women there is a sudden onset of these skin manifestations based on the estrogen deficiency induced by menopause. Ethnicity plays an important role in the clinical degree of chronological cutaneous aging. This is directly related to the level of skin pigmentation, leading to different responses to ultraviolet radiation. Thus, the elderly with Fitzpatrick phototype VI (African Americans) do not show significant differences between extrinsic and endogenous skin aging due to the protective role of high pigmentation. There are large differences in skin morphology and physiology between Caucasians, Asians, and African Americans [6,7].

Endocrine factors play an important role in the aging process of the human body. Menopause is the period characterized by the permanent loss of ovarian function (meno = month in Greek, pause = stop). It represents the transition from the cyclical, monthly secretion of estradiol to a constant and diminished hormonal output. It is a process that sets in gradually, being preceded by a period with polymorphous clinical manifestations called perimenopause or climacteric. These changes are followed by an increased risk of developing cardiovascular disease, osteoporosis, and cognitive impairment. The onset of menopause significantly impacts the skin aging process. Menopause leads to a significant acceleration in skin aging due to a 30% reduction in dermal collagen during the first 5 years after its onset. Estrogen deficiency predisposes to cutaneous xerosis and accentuation of wrinkles, as well as to a reduction in mechanical function, which is clinically observed in the appearance of bruises after minimal trauma. Cutaneous xerosis is caused by a decrease in epidermal hydration, as well as a reduction in the skin's barrier function. Androgenic alopecia can be found in menopausal women and has clinical aspects similar to those found in men. It manifests as hair thinning in the frontal and parietal regions. Unlike in men, androgenic alopecia in menopausal women rarely becomes complete and is frequently associated with hirsutism. Another manifestation linked to menopause is frontal fibrosing alopecia, characterized by the loss of hair in the frontotemporal regions and a fibrotic aspect of the underlying skin. This condition is permanent and irreversible [8,9]. Andropause sets in slowly after the age of 40. The signs are usually subtle and are caused by reduced levels of free testosterone. Clinical manifestations include decreased libido, bone and muscle fragility, and sleep disorders. Reduced testosterone levels correlate with reduced skin elasticity and the formation of wrinkles [10].

EXTRINSIC SKIN AGING

Ultraviolet radiation (UVR) was discovered in 1801 by Johann Wilhelm Ritter. The first correlations between exposure to UVR and the acceleration of skin aging were made by Unna in 1894. Thirteen years later, Dubreuilh made the first observation linking sun exposure to the development of skin cancer (1907). UVR is absorbed into the skin through high-affinity molecules called chromophores. Following absorption, photochemical reactions occur at the cellular level. The main chromophores for UVR in the skin include melanin, beta-carotene, proteins, 7-dehydrocholesterol, protoporphyrin IX, and nuclear DNA. These chromophores absorb radiation depending on its wavelength; for example, nuclear DNA, proteins, and protoporphyrin IX absorb predominantly ultraviolet B (UVB), while beta-carotene and 7-dehydrocholesterol have an affinity for the absorption of ultraviolet A (UVA). Melanin acts as a chromophore for both UVA and UVB. The absorption of UVR initiates photochemical reactions that are central

to the pathophysiological mechanisms involved in acute effects (such as sunburn) or chronic conditions (such as aging and skin cancer) [11]. Exposure to UVR leads to the formation of reactive oxygen species (ROS) that cause oxidative stress, inflammation, DNA lysis or decreased DNA repair capacity, as well as malignant transformation at the cellular level. Although the skin has its own defense mechanisms against these molecules (antioxidant enzymes), chronic exposure to UVR disrupts the balance between aggressors and protective mechanisms. This type of aggression can be quantified by some laboratory techniques such as chemiluminescence, photon emission detection or immunohistochemistry. Immunohistochemical analysis used to evaluate the oxidative stress induced by ROS focuses on measuring the expression of 8-hydroxy-2-deoxyguanosine (8-OHdG), a compound produced by the interaction between the hydroxyl radical (-OH) and the skin [11,12]. Bernerd highlights the fact that UVB has a harmful effect on the epidermis, while UVA radiation reaches deeper layers and alters dermal structures by quantifying pyrimidine dimers that behave as chromophores for ultraviolet radiation at the skin level. Detection of photon emission seems to be a reliable method for assessing the cellular stress induced by ROS [13]. Khabiri investigated these effects by measuring the emission of photons resulting from the oxidation of amino acids such as tryptophan, cysteine, phenylalanine, lysine, or threonine. These amino acids emit photons at various intensities when exposed to ROS [14].

Air pollution has serious consequences for the skin, including an accelerated aging process, delayed wound healing, the appearance of precancerous and/or malignant lesions and, last but not least, the triggering of dermatological diseases in predisposed individuals (psoriasis, atopic dermatitis). The skin is the second organ through which the pollutants can penetrate into the body after the respiratory system. Air pollution exerts its harmful effects on the skin system through ozone (O3). Although ozone has no harmful effects per se, its interaction with substances resulting from industrial processes leads to the formation of ROS. O3 is a pale blue, unstable gas with a sharp smell detectable at concentrations of 0.01 ppb (parts per billion). It has great oxidative properties and is normally found in the stratosphere (12-55 km above the ground), where it forms the "air filter" with a protective role against UVR. On the other hand, its presence in the troposphere becomes toxic to living organisms. In highly industrialized areas, ozone concentrations can exceed 1000 ppb (normally the tropospheric concentration is approximately 80 ppb), particularly during the summer months when UVR levels are elevated. It is estimated that during the 21st century the concentration of O3 will increase about fivefold, due to the large number of cars as well as urban crowding. O3 reduces the number of antioxidants present in the epidermis, destroys the lipid film, and activates collagenase-like proteins. The skin's defense mechanisms against these harmful effects include antioxidants (vitamins E and C, glutathione, ubiquinol) and enzymes (peroxidases, superoxide dismutase and catalase). However, the distribution of these substances is not uniform throughout the epidermis, so they are found in lower concentrations at the most superficial layer of the skin, partly because the area is directly exposed to the environment, and partly due to the epidermal turnover. O3 has a pro-inflammatory effect on the skin by activating the nuclear factor kappa B (NF-κB), which determines the expression of pro-inflammatory molecules such as IL-8, TNF-α, as well as adhesion molecules (ICAM, VCAM). Additionally, it also leads to the activation of cyclooxygenase-2 (COX2). It has been demonstrated that these pro-inflammatory molecules can be inhibited by topical application of antioxidants (tocopherol) in both laboratory animals and human subjects. In the deeper layers of the epidermis, ozone activates heat shock proteins (HSP) 32, 27, 70 that are involved in apoptosis, cell proliferation and inflammation. O3 also has effects on the extracellular matrix by activating metalloproteinases (MMPs) 2, 9, which are responsible for the degradation of the extracellular components of the skin. These changes occur both through increasing the expression of these enzymes and decreasing their inhibitors (TIMPs). It seems that the effects of O3 are amplified when acting on previously sun-damaged skin; as a result, wound healing in elderly people is delayed. In summary, O3 accelerates the aging process by disrupting the lipid film, degrading extracellular components, decreasing antioxidants, and inducing pathophysiological mechanisms such as inflammation, apoptosis, and cell proliferation. While UVR affects rural populations with chronic occupational sun exposure, ozone exerts its harmful effects on people from urban and highly industrialized areas. To date, the negative impact of O3 can be decreased by therapeutic or preventive measures such as topical application of antioxidants, especially vitamin E, as well as a diet rich in fruits and vegetables [15–18].

Smoking is believed to have a negative influence on the skin aging process. The role of smoking is still debated, as the impact of this habit on the skin system is most likely related to a multitude of other factors such as age, sex, genetic predisposition, phototype, as well as cofactors: sun exposure, alcohol consumption, stress, or chronic organic diseases. The primary molecular mechanism by which cigarette smoke accelerates skin aging is represented by the increased expression of metalloproteinases (MMPs) 1, 3, 7. MMP 1 is responsible for collagen degradation, while MMPs 3 and 7 have a role in decreasing elastin and proteoglycans. This leads to damage to extracellular matrix components, especially collagen, elastin, and proteoglycans [19,20]. Yin and colleagues demonstrated that fibroblasts exposed to cigarette smoke have reduced synthesis of collagen and its precursors, procollagen I and III. Cigarette smoke directly induces dehydration of the epidermis, which promotes the formation of wrinkles. Smoking is also associated with the development of cutaneous elastosis and telangiectasia [21]. Studies on identical twins with the same lifestyle have shown the influence of smoking on the aging process after a history of more than 20 years of smoking, with more visible clinical signs in men [22,23]. Daniell observed a particular morphology and distribution of wrinkles in smokers, with more defined lines on the lateral parts of the eyes, the temples, as well as around the lips, due to the specific movements of the facial muscles during smoking [24]. It is important to highlight that smoking is a cofactor in the skin aging process in the case of chronic sun exposure, the best example being Favre-Racouchot syndrome. The adverse effects of smoking

on the skin can be prevented by topical application of vitamin C, which decreases the expression of smoking-induced metalloproteinases in fibroblasts [19,20].

Diet has some impact on the degree of skin aging. Thus, sugar consumption accelerates the skin aging process, particularly by deepening wrinkles and promoting skin elastosis. The effects are linked to the formation of advanced glycation end products (AGEs). Certain cooking methods, such as frying, lead to the formation of large amounts of AGEs [25]. Increased consumption of carbohydrates and animal fats increases the risk of wrinkles and skin atrophy. Nutrition also plays a role in developing non-melanocytic skin cancer; therefore, increasing the intake of fruits and vegetables containing vitamins C and E and glutathione significantly reduces the risk of squamous cell carcinoma [26]. Similarly, selenium, zinc, and green tea extract have been shown to be effective in preventing skin tumors, most likely through their photoprotective effects [27]. Other compounds that can reduce the risk of skin cancer, as well as slow down the skin aging process, include tomatoes, curcumin, beta-carotene and genistein. These substances act by reducing inflammation, oxidative stress, and degradation of nuclear DNA. A vitamin C-rich diet significantly reduces the risk of wrinkles [28]. Interestingly, studies carried out on isolated substances have failed to demonstrate significant preventive benefits regarding skin cancer or aging. Only a diet based on combinations of antioxidant and photoprotective nutrients is effective, probably because these substances act through multiple different mechanisms [29].

Alcohol consumption could be a precipitating factor of skin aging, but data from the scientific literature remain limited. Twin studies describe a more youthful appearance in those who have not consumed alcohol during their lifetime without specifying a direct link between the quantity of alcohol consumed and the degree of aging [30]. Most likely, alcohol consumption works as a cofactor often associated with smoking, psychosocial events, and even occupational sun exposure.

Psychosocial events with a negative emotional impact play an important role in accelerating the skin aging process. Direct correlations have been made with experiences such as divorce, death of the spouse, financial situation, or depression [31].

MOLECULAR AND MORPHOLOGICAL ASPECTS

There are clear differences between the two types of skin aging, intrinsic and extrinsic. These differences arise from distinct etiological factors involved in their genesis. Thus, the photoexposed skin will develop changes due to the chronic effects of the sun, pollutants and behavior (diet, smoking, alcohol consumption). By contrast, the photoprotected skin will develop slow changes due to a physiological decrease in homeostasis and endocrine factors. The sun-exposed skin in elderly people shows specific changes in the epidermis and dermis, as well as the selective reduction of subcutaneous fat in areas such as the face, the backs of the hands and the anterior calves. The upper part of the epidermis frequently displays a compact appearance or contains vesicles with fibrillar protein material, along with the disappearance of the transition zone. The number of melanosomes in the basal layer is increased. The dermo-epidermal junction tends to flatten. Dysplastic changes, vacuolization and necrosis can occur within the squamous layer, accompanied by a reduction in the number of Langerhans cells. The papillary dermis develops elastotic changes with the formation of amorphous material, fragmentation of collagen fibers, along with a decreased number of fibroblasts. Aging of the photoprotected skin is characterized by epidermal atrophy, a flattened basement membrane and decreased melanocytes. At the dermal level, there is a noticeable reduction and degeneration of elastic fibers and a slight decrease in proteoglycans and blood vessels in the papillary dermis. Collagen synthesis is also reduced due to diminished fibroblast activity. In contrast to sun-exposed skin, photoprotected skin shows no inflammatory infiltrate [32,33].

CLINICAL ASPECTS OF SKIN AGING

Aging skin is clinically notable for its polymorphic manifestations. Skin aging reflects the sum of chronological changes due to chronic exposure to UVR and other exogenous factors such as pollution, smoking and diet. The intensity of the manifestations is generally correlated with extrinsic factors, especially in males, where hormonal changes associated with old age do not have such an obvious clinical impact as in females [34].

Degenerative skin changes

Solar elastosis occurs as a result of the accumulation of degraded elastin fibers under the dermal-epidermal junction, accompanied by disorganized, non-functional collagen. This condition is more evident in smokers, manifests as a thickened and yellowish appearance of the facial skin with deepening of wrinkles, and has a chronic evolution. On the neck, these wrinkles intersect to form rhomboidal areas, often referred to as rhomboidal neck skin or sailor's neck. Other rare manifestations of solar elastosis include elastic nodules of the helix and Raimer's bands on the dorsal surfaces of the forearms [35,36].

Senile or solar comedones occur in the elderly, being located predominantly on the nose and zygomatic region. They are not related to acne or seborrheic syndrome. They appear as open (black) or closed (white) lesions that do not become inflamed, being directly related to aging, sun exposure and smoking. These lesions result from cellular degradation and enlargement of pilosebaceous orifices caused by ROS under the long-term action of ultraviolet rays [37,38]. Favre-Racouchot syndrome is a chronic, asymptomatic dermatosis associated with smoking, long-term sun exposure and male sex. Its incidence of 1.4% is reported in individuals over 50 years of age and it increases to 2.8–5% in patients with chronic kidney disease. It presents as cysts

appearing on plaques of solar elastosis and is frequently located on the face, especially in both temporal regions [39]. The lesions require periodic evaluation, and cases of squamous cell carcinoma have been described [40].

Sebaceous hyperplasia (SH) is commonly found on the facial skin of individuals with chronic sun exposure. Typically located in areas such as the forehead, infraorbital region or temporal region, it occurs around the age of 40, its incidence increasing with age. SH appears as centrally umbilicated papules, yellowish in color, with a diameter of about 2-6 mm. Long-term exposure to UVR, advanced age, or immunosuppressive therapy (cyclosporine A, corticosteroid therapy) are considered to be contributing factors. The diagnosis is based on clinical assessment, with dermatoscopy and confocal microscopy playing an important role in differential diagnosis with basal cell carcinoma. SH treatment is indicated, most often, for aesthetic reasons [41,42].

Idiopathic guttate hypomelanosis (IGH) is characteristic of older women, occurring as hypopigmented macules on the forearms and calves. It can also be found in other areas such as the anterior chest or shoulder region. At the molecular level, the condition is associated with atrophy and focal disappearance of melanocytes. From a pathophysiological point of view, a decrease in the melanogenesis process has been identified both in terms of melanin synthesis and its transport to keratinocytes [43]. Recently, it has been described that IGH melanocytes have an increased volume, contain more melanin than normal ones and have reduced dendritic extensions (Rani et al., 2018). These findings clearly suggest an impairment in melanin transportation to keratinocytes, this being the principal mechanism involved in the genesis of IGH lesions. The disease implies only aesthetic risks [44].

Lentigines are benign flat lesions formed by the proliferation of melanocytes induced by UVR action. They appear as pigmented macules that persist during the cold season (unlike ephelides), being located on the face, the backs of the forearms and hands, as well as the posterior thorax. A solitary lesion is called a solar lentigo and should be differentiated from lentiginous melanoma and lentigo maligna [45].

Skin tumors

Seborrheic keratoses are benign skin lesions that are caused by the proliferation of basal epidermal cells (basal cell papilloma). They are asymptomatic and appear predominantly on the seborrheic areas (on the face and posterior thorax), developing after the age of 30 and mainly affecting women. They are never found on the mucous membranes or at the palmoplantar level. Seborrheic keratoses are usually multiple lesions and their number tends to increase with age. Clinically, they appear as pigmented macules or plaques, some with a rough surface. While the lesions are asymptomatic, some patients report pruritus. Their etiology remains uncertain, the only demonstrated cause being skin aging. It is extremely rare that seborrheic keratoses appear before the age of 20 [46,47].

Actinic or solar keratoses are the result of the proliferation of the squamous layer of the epidermis due to chronic exposure to UVR. Histologically, they are characterized by epidermal dysplasia without involvement of the basal layer of the epidermis with hyperkeratosis, nuclear pleomorphism and sometimes with mitoses. Lesions present as erythematous spots or erythematous-squamous plaques, usually less than 2 cm in size. While asymptomatic, some may be associated with mild itching. They are located on the face and back of the hands, less often in other areas, occurring most frequently in patients with Fitzpatrick skin phototypes I and II. The condition begins in the form of erythematous macules that over time enlarge and become covered with adherent scales. Interestingly, spontaneous remission of these lesions has been described [48].

A cutaneous horn is a hyperkeratotic lesion and is considered a precursor to squamous cell carcinoma. It often occurs in elderly patients (over the age of 70) and is located in photoexposed areas such as the face, forearms, decolletage or the back of the hands. The condition is more prevalent in people with skin phototypes I and II, and the risk of malignant transformation into squamous cell epithelioma is higher among male individuals [49,50].

Keratoacanthoma is considered an early form of squamous cell carcinoma, presents as a nodular formation with central ulceration and tends to develop on the face or back of the hands. The risk of progression to squamous cell carcinoma is about 15%. It has a sudden onset and shows rapid growth over a few weeks or months. The treatment of choice is surgical excision, especially to rule out an invasive squamous cell carcinoma [51,52].

Basal cell carcinoma is the most common type of skin cancer [53] and develops from epidermal basal cells or cutaneous adnexal structures, without affecting the mucous membranes. While it is considered to be only locally malignant, histologically it has the characteristics of a cancer such as cell dysplasia, pleomorphic nuclei and atypical mitoses. Clinically, it frequently occurs after the age of 50, especially in people with a light phototype. Chronic exposure to UVR is the primary risk factor for its development [54]. The mechanism by which UVR induces BCC includes inactivation of tumor suppressor genes (e.g., the p53 gene with a role in inducing apoptosis) and changes in DNA manifesting as pyrimidine dimers. Therefore, mutation of the p53 gene is found in more than half of the patients with basal cell epithelioma, regardless of the clinical or histopathological form. UVB also induces mutations in the PTCH1 gene, which controls cell growth and differentiation [55]. BCC is often located on the face and less commonly on the chest or limbs. The lesion begins as a papule, nodule, erythematous plaque or an ulceration covered by a hemorrhagic crust [56].

Squamous cell carcinoma typically develops on chronically irritated or damaged skin, particularly in areas exposed over time to external noxious agents such as UVR, toxic substances, radiotherapy, cigarette smoking, or post-burn scarring. It is highly aggressive, and it spreads via both lymphatic and hematogenous routes. It frequently arises after the age of 65 in people with fair skin, being more common among men (male-to-female ratio of 2-3:1). Unlike BCC, this condition can affect the mucosal and semimucous membranes, frequently affecting the lower lip (in patients with a history of chronic solar cheilitis or heavy smoking). Clinically, it has polymorphism, being characterized by nodular or ulcerated lesions, sometimes covered by scales and having no tendency for spontaneous resolution. The lesions are frequently located on the head and neck areas. It metastasizes to the visceral organs like the brain, the liver and the lungs [55–57]. Alterations in EGFR/MAPK signaling have also been investigated in cutaneous squamous cell carcinogenesis [58].

Senile angiomas (cherry angiomas, Campbell de Morgan spots) are vascular proliferations with a benign nature that present as asymptomatic papules, predominantly on the trunk. They frequently begin after the age of 30 and have been linked with pregnancy and exposure to pollutants (bromides), as well as genetics. As patients age, they can spread to the limbs, face and scalp. Some clinical variations of the classical form have been described, such as ruby spots and senile hemangioma of the lip. Ruby spots represent small, sometimes palpable vascular proliferations, frequently found on the trunk and limbs among people over 80. Senile angioma of the lip appears as a soft, painless, reddish-purple nodule of the lower lip, more often observed in females. All clinical forms are closely related to chronological aging rather than extrinsic factors [59,60].

Aspects of inflammatory, allergic, autoimmune or idiopathic dermatoses in elderly patients

Pruritus is one of the most common skin symptoms in older patients, with a prevalence of approximately 20%. It can have various causes, ranging from underlying dermatological conditions (e.g., xerosis) and medications to systemic diseases like anemia, thyroid diseases, liver or renal disease and malignancies. Pruritus in the elderly is most often a chronic condition (over six weeks). The approach requires a careful clinical examination, as well as paraclinical and laboratory investigations to identify an underlying cause. Despite investigations, 30% of cases do not have a clear cause, and treatment remains symptomatic with topical antipruritic agents [61,62].

Skin xerosis is clinically important, not only because of the constant association with pruritus, but also because it predisposes to the development of secondary dermatoses (eczema, skin infections). Although xerosis presents with a widespread distribution, it is better outlined on the extremities, especially on the anterior area of the calves, where it exhibits the characteristic appearance of cracked eczema. Exacerbating factors include excessive washing and chronic use of certain medications such as diuretics and antihyperlipidemic drugs. Therapeutic management is focused on preventing dryness and ensuring skin hydration [63,64].

Atopic dermatitis is characterized by the presence of pruritus, xerosis and eczema and is associated with a personal or family history of atopic conditions such as bronchial asthma, allergic rhinitis and a high incidence of food allergies. It is considered a disease of children and adolescents; its appearance in the elderly is not very well defined. When it comes to older patients, atopic dermatitis is more common in males (male-to-female ratio of 3:1). In general, the clinical features resemble those found in adults, in the form of cutaneous xerosis and eczematous areas with lichenification. In most older individuals, the condition is a continuation of the symptoms first experienced in early childhood, adolescence or adulthood [65,66].

Contact dermatitis manifests differently in the elderly, having a milder clinical appearance and an extended duration. It appears as subtle erythematous lesions with a tendency toward lichenification, while bullous forms are rare. The condition can have both allergic and irritative mechanisms, developing in patients with a history of skin xerosis. The most frequent sensitizers described are topical medications and detergents. Elderly people with urinary incontinence frequently develop contact dermatitis of the inguinal area [67].

Granulomatous dermatoses are defined by the presence of a chronic inflammatory infiltrate as part of a delayed-type immune response. The most common skin lesions with granuloma formation are cutaneous sarcoidosis, granuloma annulare, interstitial granulomatous dermatitis and gouty tophi. They are more frequently encountered in the elderly secondary to therapeutic interventions (drug therapy or surgery), systemic diseases (gout, systemic sarcoidosis, diabetes) or even malignancies [68,69].

Drug-induced cutaneous reactions tend to occur more frequently in elderly patients than in other population groups. Certain clinical features are relatively specific, such as eczematous reactions in response to angiotensin-converting enzyme inhibitors and calcium channel blockers or reactions associated with chemotherapy (hand-foot syndrome, flagellate erythema, follicular or acneiform eruptions). Also, lichenoid drug eruption is particularly common in the elderly due to its tendency to occur after prolonged administration of certain medications [68–70].

Psoriasis presents some specific aspects in the elderly. Due to its chronic nature, the disease tends to be at least more pronounced, if not more severe, in the elderly. This can be attributed to a higher risk of developing psoriatic arthropathy, as well as superimposed factors such as comorbidities and use of antihypertensives (beta-blockers, angiotensin-converting enzyme inhibitors) or nonsteroidal anti-inflammatory drugs (NSAIDs). Although the condition appears after the age of 70 years in only 3% of cases, about 10% of patients with psoriasis are older than 70 years and often present with secondary conditions like type II

diabetes, hypertension and dyslipidemia. Older adults with psoriasis are more likely to develop certain forms or complications such as inverse psoriasis, guttate, pustular, or erythrodermic psoriasis [71,72]. In a study of 90 patients with psoriasis, hepatic steatosis was present in 58.9% and was more frequent in older patients and those with diabetes [73].

Lichen planus is a chronic inflammatory disease that affects the skin, appendages and mucous membranes. The incidence varies between 0.2 and 5%, being more common among the elderly and female patients. The increased frequency in the elderly is largely due to the presence of some triggering factors such as viral infection with hepatitis B or C, psychiatric disorders, immunosuppression and certain medications. Specific forms in the elderly include verrucous lichen (associated with chronic venous insufficiency) and oral mucosal lichen planus (favored by various denture materials) [74]. Lichen planopilaris occurs more frequently in older women and manifests as frontal fibrosing alopecia that is linked with postmenopausal estrogen deficiency or Graham-Little-Piccardi-Lassueur syndrome, which combines scarring alopecia of the scalp with follicular rash and non-scarring alopecia of the large folds [75,76]. Lichenoid drug eruptions are more common in older patients due to the use of antihypertensive medication (ACE inhibitors, beta-blockers, diuretics) and nonsteroidal anti-inflammatory drugs (NSAIDs) [77].

Bullous pemphigoid is the most common autoimmune blistering dermatosis in the elderly population. Its incidence increases significantly after the age of 60, with the average age of patients in Europe with bullous pemphigoid varying between 77 and 83 years [78]. Although no direct causal link has been made, the increase in the number of cases among the elderly is associated with other comorbidities. Thus, most patients with bullous pemphigoid suffer from diabetes mellitus or neurological diseases such as dementia, Parkinson's disease or multiple sclerosis, or have a history of stroke. Neurological pathology is present in 30% of patients with bullous pemphigoid. Many cases of localized bullous pemphigoid begin in hemiplegic areas. Additionally, orthopedic prostheses are reported in 25% of cases. The disease has an increased incidence in patients with bipolar psychiatric disorders [79]. The role of certain medications such as spironolactone and neurological drugs has also been discussed [80].

Aging of the mucous and semi-mucous membranes

Like the skin, the mucous membranes suffer a decrease in wound healing ability as part of the aging process. The risk of oral mucosal lesions of any type in the elderly increases significantly when the patient also has diabetes, smokes, or has poorly fitted or morphologically inadequate dental prostheses. The most common changes are xerostomia and sublingual varicosity.

Stomatitis due to dental prostheses occurs in 10% of the elderly, with squamous cell carcinoma being the most common tumor of the oral cavity. Angular cheilitis is commonly encountered in the elderly and its appearance is influenced by several factors such as the deepening of commissural wrinkles, weakening of the facial muscles, as well as alterations in the dental apparatus. Actinic cheilitis occurs more frequently in men and is mainly caused by chronic exposure to UVR, but also by smoking.

In the genital mucosa, atrophy appears with age, particularly in women. Atrophy of the vulva and vagina correlates with postmenopausal estrogen deficiency. There is also a higher incidence of urinary incontinence and perineal dermatitis in women. Genital lichen sclerosus et atrophicus is the most frequent cause of circumcision in older men [81–83].

Nail aging

Due to keratinocyte turnover disorders as well as decreased blood flow in the nail bed, the elderly develop certain dystrophic nail changes. Changes in coloration of the nail plate that mimic onychomycosis are frequently encountered. The nails become thickened and dull in appearance and sometimes onychogryphosis can be present. Changes associated with medication or repeated trauma may also be encountered in the context of distal sensory impairment. With age, nails lose their length and become more convex. Their resistance decreases, and they become friable, especially toward the distal ends. A particular manifestation seen in senile nails is the arrangement of three horizontal bands, which are white, pink and opaque from proximal to distal. Other features associated with age are localized hypertrophy of the nail (onychauxis), subungual clavus formation, and an increase in subungual hemorrhages and hematomas compared to the young population. These dystrophic changes contribute to a higher incidence of onycholysis [84,85].

Clinical aspects of hair aging

Hair aging involves two aspects: physiological canities (graying) and diffuse alopecia (hair thinning). Men with androgenic alopecia have an earlier tendency to exhibit graying. It is a gradual physiological process that frequently begins after the age of 35, caused by a reduction in the melanogenesis process. So far, canities remains an irreversible condition. Diffuse alopecia of the elderly occurs after the age of 60 and is linked especially to hormonal status. In women, the process is slower and becomes noticeable at a more advanced age. In men, hypertrichosis can be observed in the eyebrows and external auditory canal. Furthermore, hair density on the limbs decreases with age in both sexes [86,87].

Chronic cutaneous insufficiency or dermatoporosis

We are witnessing an increase in the average life expectancy in developing countries. This aspect has amplified both intrinsic and extrinsic factors involved in the skin aging process. Up until recently, we could not discuss chronic organ insufficiency when it comes to the skin, but the term chronic cutaneous insufficiency or fragility has emerged in recent years. Kaya and Saurat were

the first to introduce the term dermatoporosis in 2007, describing it as the association between senile purpura and pseudoscars that developed on atrophic skin of the elderly [88]. Injuries occur as a result of minimal trauma caused by decreased mechanical function of the skin. However, the clinical features of senile purpura had been described as early as two centuries ago by Thomas Bateman, while Colomb described the stellate pseudoscars on the forearms in the elderly in 1967 [88–90]. The main pathophysiological mechanism is based on the reduction in extracellular matrix components, particularly hyaluronic acid (HA) and its main receptor, CD44 [88]. Based on this phenomenon, viscoelasticity and skin hydration decline [91]. Clinical changes include skin atrophy, purpura, pseudoscars, hyperpigmentation and skin ulcerations. These clinical aspects lead to an increased risk of developing deep dissecting hematomas (DDHs) due to the accumulation of blood between the hypodermis and the muscular fascia after minimal trauma [88,92]. The lesions are mainly located on the forearms and calves [88]. Other locations can include the presternal region and the dorsum of the hands, as well as the face and scalp in some isolated cases [93,94].

The prevention of dermatoporosis lesions begins with eliminating or reducing the patient's exposure to the triggering factor. Thus, it is necessary to use photoprotection strategies and avoid trauma in patients with primary dermatoporosis. In cases of secondary dermatoporosis, prevention may be achieved by reducing the dose and/or duration of corticosteroid therapy [88,94].

The first therapeutic measures were developed by Kaya in 2007, along with the initial description of the disease. Topical application of 1% hyaluronic acid leads to improvement of the lesions [88]. Topical retinoids have proven effective in the treatment of dermatoporosis, and their role is to restore the cellular differentiation process. Combining hyaluronic acid and retinaldehyde is more effective than the separate application of either compound [93]. Alpha-hydroxy acids (AHAs) work in reducing the degree of skin atrophy [95]. Humbert et al. claim that dermatoporosis, especially Bateman's senile purpura, is related to vitamin C deficiency in the skin, and they demonstrate a reduction in lesions following topical application of 5% vitamin C [96]. Kluger suggests that systemic administration of vitamin C is also effective [97]. There are limited data on the efficacy of topical applications of epidermal growth factor or dehydroepiandrosterone [98,99].

Conflicts of interest and sources of funding

The authors declare no conflicts of interest.

This research received no external funding.

Authors' contribution

Conceptualization, MAB and MLS; methodology, BAM; software, BAI; validation, DOC, ACC and MAB; formal analysis, ABG; investigation, MAB; resources, MAB; data curation, DOC; writing—original draft preparation, MAB; writing—review and editing, MAB; visualization, DOC and ACC; supervision, DOC and MLS. All authors have read and agreed to the published version of the manuscript.

Ethics approval and consent to participate

Not applicable.

References

1. Ward SA, Parikh S, Workman B. Health perspectives: international epidemiology of ageing. Best Pract Res Clin Anaesthesiol. 2011;25:305–317.

2. Berrío Valencia MI. Envejecimiento de la población: un reto para la salud pública. Rev Colomb Anestesiol. 2012;40:192–194.

3. Cucerzan M. Dimensions of population ageing in Romania. Agriculture: Science and practice. 2016;3-4:99-100.

4. Lutz W, Sanderson W, Scherbov S. The coming acceleration of global population ageing. Nature 2008;451:716-719.

5. Addor FAS. Beyond photoaging: additional factors involved in the process of skin aging. Clin Cosmet Investig Dermatol. 2018;11:437-443.

6. Vierkötter A, Krutmann J. Environmental influences on skin aging and ethnic-specific manifestations. Dermatoendocrinol. 2012;4(3):227–231.

7. Rittié L, Fisher GJ. Natural and sun-induced aging of human skin. Cold Spring Harb Perspect Med. 2015;5(1):a015370.

8. Herman J, Rost-Roszkowska M, Skotnicka-Graca U. Skin care during the menopause period: noninvasive procedures of beauty studies. Postepy Dermatol Alergol. 2013;30(6):388-395.

9. Genazzani AR, Gambacciani M, Simoncini T. Menopause and aging, quality of life and sexuality. Climacteric 2007;10:88-96.

10. Keaney TC. Aging in the Male Face: Intrinsic and Extrinsic Factors. Dermatol Surg. 2016 Jul;42(7):797-803.

11. Shah P, He YY. Molecular regulation of UV-induced DNA repair. Photochem Photobiol. 2015;91(2):254-264.

12. Poon F, Kang S, Chien AL. Mechanisms and treatments of photoaging. Photodermatol Photoimmunol Photomed. 2015;31(2):65-74.

13. Bernerd F, Marionnet C, Duval C. Solar ultraviolet radiation induces biological alterations in human skin in vitro: relevance of a well-balanced UVA/UVB protection. Indian J Dermatol Venereol Leprol. 2012;78 Suppl 1:S15-23.

14. Khabiri F, Hagens R, Smuda C, et al. Non-invasive monitoring of oxidative skin stress by ultraweak photon emission (UPE)-measurement. I: mechanisms of UPE of biological materials. Skin Res Technol. 2008;14(1):103-111.

15. Puri P, Nandar SK, Kathuria S, et al. Effects of air pollution on the skin: A review. Indian J Dermatol Venereol Leprol. 2017;83(4):415-423.

16. Kampa M, Castanas E. Human health effects of air pollution. Environ Pollut 2008;151:362-367.

17. English JS, Dawe RS, Ferguson J. Environmental effects and skin disease. Br Med Bull 2003;68:129-142.

18. Madronich S, Wagner M, Groth P. Influence of tropospheric ozone control on exposure to ultraviolet radiation at the surface. Environ Sci Technol 2011;45:6919-6923.

19. Morita A. Tobacco smoke causes premature skin aging. J Dermatol Sci. 2007;48(3):169-175.

20. Vierkötter A, Schikowski T, Sugiri D, et al. MMP-1 and -3 promoter variants are indicative of a common susceptibility for skin and lung aging: results from a cohort of elderly women (SALIA). J Invest Dermatol. 2015;135(5):1268-1274.

21. Yin L, Morita A, Tsuji T. Alterations of extracellular matrix induced by tobacco smoke extract. Arch Dermatol Res. 2000;292(4):188-194.

22. Ichibori R, Fujiwara T, Tanigawa T, et al. Objective assessment of facial skin aging and the associated environmental factors in Japanese monozygotic twins. J Cosmet Dermatol. 2014;13(2):158-163.

23. Skinner AL, Woods A, Stone CJ, et al. Smoking status and attractiveness among exemplar and prototypical identical twins discordant for smoking. R Soc Open Sci. 2017;4(12):161076.

24. Daniell HW. Smoking and wrinkling. Arch Dermatol. 1993;129(7):907.

25. Danby F. Nutrition and aging skin: sugar and glycation. Clin Dermatol. 2010;28(4):409–411.

26. Dearlove R, Greenspan P, Hartle D, et al. Inhibition of protein glycation by extracts of culinary herbs and spices. J Med Food. 2008;11:275–281.

27. Chan S, Gerson B, Subramaniam S. The role of copper, molybdenum, selenium, and zinc in nutrition and health. Clin Lab Med. 1998;18(4):673-685.

28. Pullar JM, Carr AC, Vissers MCM. The Roles of Vitamin C in Skin Health. Nutrients. 2017;9(8). pii: E866.

29. Katta R, Desai SP. Diet and dermatology: the role of dietary intervention in skin disease. J Clin Aesthet Dermatol. 2014;7(7):46-51.

30. Nilsson P, et al. Adverse social factors predict early ageing in middle-aged men and women: the Ebeltoft Health Study, Denmark. Scand J Public Health. 2003;31(4):255–260.

31. Demakakos P, Nazroo J, Breeze E, et al. Socioeconomic status and health: the role of subjective social status. Soc Sci Med. 2008;67(2):330–340.

32. Khavkin J, Ellis DA. Aging skin: histology, physiology, and pathology. Facial Plast Surg Clin North Am. 2011;19(2):229-234.

33. Bonta M, Daina L, Muţiu G. The process of ageing reflected by histological changes in the skin. Rom J Morphol Embryol. 2013;54(3 Suppl):797-804.

34. Hadi H, Awadh AI, Hanif NM, et al. The investigation of the skin biophysical measurements focusing on daily activities, skin care habits, and gender differences. Skin Res Technol. 2016;22(2):247-254.

35. Tsukahara K, Tamatsu Y, Sugawara Y, et al. Morphological study of the relationship between solar elastosis and the development of wrinkles on the forehead and lateral canthus. Arch Dermatol. 2012;148(8):913-917.

36. Sellheyer K. Pathogenesis of solar elastosis: synthesis or degradation? J Cutan Pathol. 2003;30(2):123-127.

37. Sayal SK, Rajbhandari S, Malik AK, et al. A study of dermatological disorders in geriatric age group. Indian J Dermatol Venereol Leprol. 1998;64(6):270-272.

38. Izumi AK, Marples RR, Kligman AM. Senile (solar) comedones. J Invest Dermatol. 1973;61(1):46-50.

39. Sonthalia S, Arora R, Chhabra N, et al. Favre-Racouchot syndrome. Indian Dermatol Online J. 2014;5(Suppl 2):S128-129.

40. Leeuwis-Fedorovich NE, Starink M, van der Wal AC. Multifocal squamous cell carcinoma arising in a Favre-Racouchot lesion - report of two cases and review of the literature. J Dermatol Case Rep. 2015;9(4):103-106.

41. Zouboulis CC, Boschnakow A. Chronological ageing and photoageing of the human sebaceous gland. Clin Exp Dermatol. 2001;26(7):600-607.

42. Eisen DB, Michael DJ. Sebaceous lesions and their associated syndromes: part I. J Am Acad Dermatol. 2009;61(4):549-560.

43. Juntongjin P, Laosakul K. Idiopathic Guttate Hypomelanosis: A Review of its Etiology, Pathogenesis, Findings, and Treatments. Am J Clin Dermatol. 2016;17(4):403-411.

44. Rani S, Kumar R, Kumarasinghe P, et al. Melanocyte abnormalities and senescence in the pathogenesis of idiopathic guttate hypomelanosis. Int J Dermatol. 2018;57(5):559-565.

45. Praetorius C, Sturm RA, Steingrimsson E. Sun-induced freckling: ephelides and solar lentigines. Pigment Cell Melanoma Res. 2014;27(3):339-350.

46. Hafner C, Vogt T. Seborrheic keratosis. J Dtsch Dermatol Ges. 2008;6(8):664-677.

47. Noiles K, Vender R. Are all seborrheic keratoses benign? Review of the typical lesion and its variants. J Cutan Med Surg. 2008;12(5):203-210.

48. Siegel JA, Korgavkar K, Weinstock MA. Current perspective on actinic keratosis: a review. Br J Dermatol. 2017;177(2):350-358.

49. Sathyanarayana SA, Deutsch GB, Edelman M, et al. Cutaneous horn: a malignant lesion? A brief review of the literature. Dermatol Surg. 2012;38(2):285-287.

50. Fernandes NF, Sinha S, Lambert WC, et al. Cutaneous horn: a potentially malignant entity. Acta Dermatovenerol Alp Pannonica Adriat. 2009;18(4):189-193.

51. Kwiek B, Schwartz RA. Keratoacanthoma (KA): An update and review. J Am Acad Dermatol. 2016;74(6):1220-1233.

52. Gleich T, Chiticariu E, Huber M, et al. Keratoacanthoma: a distinct entity? Exp Dermatol. 2016;25(2):85-91.

53. Porosnicu AL, Jebreen KA, Riza SM, Cepi PA, Sinescu RD. Evaluating arbitrary and histological margins in high-risk nonmelanoma skin cancers: a one-center experience. Rom J Mil Med. 2025;128(6):546-553. doi: 10.55453/rjmm.2025.128.6.8.

54. Verkouteren JAC, Ramdas KHR, Wakkee M, et al. Epidemiology of basal cell carcinoma: scholarly review. Br J Dermatol. 2017;177(2):359-372.

55. Emmert S, Schön MP, Haenssle HA. Molecular biology of basal and squamous cell carcinomas. Adv Exp Med Biol. 2014;810:234-252.

56. Marzuka AG, Book SE. Basal cell carcinoma: pathogenesis, epidemiology, clinical features, diagnosis, histopathology, and management. Yale J Biol Med. 2015;88(2):167-179.

57. Kallini JR, Hamed N, Khachemoune A. Squamous cell carcinoma of the skin: epidemiology, classification, management, and novel trends. Int J Dermatol. 2015;54(2):130-140.

58. Dobre EG, Căruntu A, Munteanu AN, Surcel M, Constantin C, et al. Investigating EGFR, BRAF, and RAS mutations in oral and cutaneous squamous cell neoplasms: a preliminary report on Romanian patients. Rom J Mil Med. 2024;127(5):341-350. doi: 10.55453/rjmm.2024.127.5.2.

59. Karadag AS, Parish LC. Campbell de Morgan Spot, Better Known As a Cherry Angioma. Skinmed. 2016;14(5):331-333.

60. Borghi A, Minghetti S, Battaglia Y, et al. Predisposing factors for eruptive cherry angiomas: New insights from an observational study. Int J Dermatol. 2016;55(11):e598-e600.

61. Valdes-Rodriguez R, Stull C, Yosipovitch G. Chronic pruritus in the elderly: pathophysiology, diagnosis and management. Drugs Aging. 2015;32(3):201-215.

62. Clerc CJ, Misery L. A Literature Review of Senile Pruritus: From Diagnosis to Treatment. Acta Derm Venereol. 2017;97(4):433-440.

63. Reszke R, Pełka D, Walasek A, et al. Skin disorders in elderly subjects. Int J Dermatol. 2015;54(9):e332-338.

64. White-Chu EF, Reddy M. Dry skin in the elderly: complexities of a common problem. Clin Dermatol. 2011;29(1):37-42.

65. Tanei R, Hasegawa Y. Atopic dermatitis in older adults: A viewpoint from geriatric dermatology. Geriatr Gerontol Int. 2016;16 Suppl 1:75-86.

66. Garmhausen D, Hagemann T, Bieber T, et al. Characterization of different courses of atopic dermatitis in adolescent and adult patients. Allergy. 2013;68(4):498-506.

67. Balato A, Balato N, Di Costanzo L, et al. Contact sensitization in the elderly. Clin Dermatol. 2011;29(1):24-30.

68. Magro CM, Crowson AN. Lichenoid and granulomatous dermatitis. Int J Dermatol. 2000;39(2):126-133.

69. Badea MA, Buicu CF, Sin AI, et al. The value of histopathological diagnosis in the elderly patients with granulomatous dermatoses. Case series. Rom J Morphol Embryol. 2016;57(2):525-529.

70. Heng YK, Lim YL. Cutaneous adverse drug reactions in the elderly. Curr Opin Allergy Clin Immunol. 2015;15(4):300-307.

71. Yosipovitch G, Tang MB. Practical management of psoriasis in the elderly: epidemiology, clinical aspects, quality of life, patient education and treatment options. Drugs Aging. 2002;19(11):847-863.

72. Phan C, Sigal ML, Estève E, et al. Psoriasis in the elderly: epidemiological and clinical aspects, and evaluation of patients with very late onset psoriasis. J Eur Acad Dermatol Venereol. 2016;30(1):78-82.

73. Tamer F, Atliya O, Polat M, Adisen E. Hepatic steatosis is the most common finding in abdominal ultrasonography performed in patients with psoriasis before biological agent treatment. Rom J Mil Med. 2024;127(3):237-242. doi: 10.55453/rjmm.2024.127.3.9.

74. Fazel N. Cutaneous lichen planus: A systematic review of treatments. J Dermatolog Treat. 2015;26(3):280-283.

75. Baibergenova A, Donovan J. Lichen planopilaris: update on pathogenesis and treatment. Skinmed. 2013;11(3):161-165.

76. Badea MA, Buicu F, Ţilea AM, et al. Graham Little-Lassueur Syndrome with Hypertrophic Lichen Planus in a Patient with Chronic Hepatitis C. Acta Medica Marisiensis 2016;62(1):149-151.

77. Fessa C, Lim P, Kossard S, et al. Lichen planus-like drug eruptions due to β-blockers: a case report and literature review. Am J Clin Dermatol. 2012;13(6):417-421.

78. de Quatrebarbes J, Joly P. Bullous pemphigoid. Rev Prat. 2005;55(11):1165-1168.

79. Lai YC, Yew YW, Lambert WC. Bullous pemphigoid and its association with neurological diseases: a systematic review and meta-analysis. J Eur Acad Dermatol Venereol. 2016;30(12):2007-2015.

80. Chevalier V, Barbe C, Reguiai Z. Impact of neurological diseases on the prognosis of bullous pemphigoid: A retrospective study of 178 patients. Ann Dermatol Venereol. 2016;143(3):179-186.

81. Lynge Pedersen AM, Nauntofte B, Smidt D, et al. Oral mucosal lesions in older people: relation to salivary secretion, systemic diseases and medications. Oral Dis. 2015;21(6):721-729.

82. Bakker MH, Vissink A, de Baat C, et al. Medicaments and oral healthcare. Oral side effects of -medications commonly used by older people. Ned Tijdschr Tandheelkd. 2017;124(12):645-652.

83. Farage MA, Maibach HI. Morphology and physiological changes of genital skin and mucosa. Curr Probl Dermatol. 2011;40:9-19.

84. Murdan S. Nail disorders in older people, and aspects of their pharmaceutical treatment. Int J Pharm. 2016;512(2):405-411.

85. Van de Kerkhof PC, Pasch MC, Scher RK, et al. Brittle nail syndrome: a pathogenesis-based approach with a proposed grading system. J Am Acad Dermatol 2005;53(4):644-651.

86. Goodier M, Hordinsky M. Normal and aging hair biology and structure 'aging and hair'. Curr Probl Dermatol. 2015;47:1-9.

87. Tobin DJ. Age-related hair pigment loss. Curr Probl Dermatol. 2015;47:128-138.

88. Kaya G, Saurat JH. Dermatoporosis: a chronic cutaneous insufficiency/fragility syndrome. Clinicopathological features, mechanisms, prevention and potential treatments. Dermatology. 2007;215(4):284-294.

89. Colomb D, Pincon JA, Lartaud J. Individualisation anatomo-clinique d'une forme méconnue de la peau sénile: les pseudo-cicatrices stellaires spontanées. Leurs rapports avec le purpura de Bateman. Ann Dermatol Syphiligr (Paris) 1967;94: 273–286.

90. Colomb D. The triad: diffuse senile atrophy, Bateman's purpura, spontaneous stellar pseudo-cicatrices. Association frequently encountered in cutaneous senescence. Maroc Med. 1972;52(558):344-347.

91. Piérard-Franchimont C, Hermanns JF, Hermanns-Lê T, et al. Dermatoporosis, a vintage for atrophoderma and transparent skin. Rev Med Liege. 2014;69(4):210-213.

92. Kaya G, Jacobs F, Prins C, et al. Deep dissecting hematoma: an emerging severe complication of dermatoporosis. Arch Dermatol. 2008;144(10):1303-1308.

93. Kaya G. New therapeutic targets in dermatoporosis. J Nutr Health Aging. 2012;16(4):285-288.

94. Kluger N, Impivaara S. Prevalence of and risk factors for dermatoporosis: a prospective observational study of dermatology outpatients in a Finnish tertiary care hospital. J Eur Acad Dermatol Venereol. 2018. doi: 10.1111/jdv.15240.

95. Bernstein EF, Underhill CB, Lakkakorpi J, et al. Citric acid increases viable epidermal thickness and glycosaminoglycan content of sun-damaged skin. Dermatol Surg. 1997;23(8):689–694.

96. Humbert P, Fanian F, Lihoreau T, et al. Bateman purpura (dermatoporosis): a localized scurvy treated by topical vitamin C - double-blind randomized placebo-controlled clinical trial. J Eur Acad Dermatol Venereol. 2018;32(2):323-328.

97. Kluger N. Dermatoporosis and vitamin C deficiency. J Eur Acad Dermatol Venereol. 2018;32(10):e383.

98. Nouveau S, Bastien P, Baldo F, et al. Effects of topical DHEA on aging skin: a pilot study. Maturitas. 2008;59(2):174–181.

99. McKnight B, Seidel R, Moy R. Topical human epidermal growth factor in the treatment of senile purpura and the prevention of dermatoporosis. J Drugs Dermatol. 2015;14(10):1147–1150.

https://doi.org/10.55453/rjmm.2026.129.6.2

Review

AI in Drug Discovery and Precision Medicine

Richa Sharma[1,*], Richa Saxena[2], Rakshith Maneshwar Hoskeri[3], Ekadashi Rajni[1], Teju Lal Chaurasia[4]

[1] Department of Microbiology, Mahatma Gandhi University of Medical Sciences & Technology, Jaipur, Rajasthan, India
[2] Department of Biotechnology, Invertis University, Bareilly- 243001, U.P., India
[3] Department of Clinical Psychology, Mahatma Gandhi University of Medical Sciences & Technology, Jaipur, Rajasthan, India
[4] School of Allied Health Sciences, Jaipur National University, Jaipur, Rajasthan, India
*Correspondence: Dr. Richa Sharma, email: richa.phd.15@gmail.com

Abstract: Biological data have grown exponentially due to single-cell multi-omics, high-content imaging, and large-scale clinical records; this has transformed modern biology. The landscape has shifted to one of data abundance, and the current approaches to computational analysis are not up to the task of dealing with the scale and complexity of this change. The information in big biological data can be characterized by the volume it occupies, velocity, variety, veracity, and value, and each of these features presents its own challenges to the researcher. Artificial intelligence (AI), including machine learning (ML), deep learning (DL), and natural language processing (NLP), has progressively turned into a requirement in tackling these issues. This chapter discusses how AI can be used to curate, represent, learn, and model the analysis of big biological data. Questions include data curation via methods to compress, represent, and outline big biological data, how to learn representations, how to model with big biological data, and how to translate into clinical problems. Using the conversation of genomics, proteomics, transcriptomics, structural biology, imaging, and electronic health records, this chapter reveals how AI is transformative in bioinformatics. In conclusion, the chapter points to enduring challenges, namely interpretability, data governance, and reproducibility, and provides a step into the future of explainable, trustworthy, and reproducible AI in biology.

Keywords: artificial intelligence; machine learning; bioinformatics; clinical genomics; reproducibility; benchmarking

INTRODUCTION

Biology is a field that has been submerged in a major change in the last several decades. No longer characterized by hypothesis-based investigations that involved small-scale experiments, it is now influenced by the flood of data that high-throughput technologies and large-scale biomedical projects are generating. Experiments such as whole-genome sequencing projects of entire populations, single-cell atlases, mapping millions of cells, multi-modal imaging of tissues and organisms, and the digitization of clinical and health records mean that data measurement has to be in terms of terabytes to petabytes. This paradigm requires not only different analytical methods but a totally different way of thinking about the issues at hand (artificial intelligence (AI)) in which the means of finding meaning in complexity is created [1]. The real meaning of this challenge can be summed up in a term coined as big biological data. The amount of data being handled is enormous, and in most cases, it surpasses the capacity of customary data storage and processing environments. The frequency of data creation- whether it be a continuous drive of sequencing reads or streaming clinical notes- necessitates real-time or near-real-time processing. The diversity of biological modalities, encompassing DNA and RNA sequences, protein structure, matrices of expression, clinical time series, and even unstructured biomedical prose, is the source of diversity [2]. Making this even more difficult is veracity, since biological data is erratic and/or incomplete and inconsistent, with batch effects, missing values, and annotation errors. The utility of these data rests on the capacity to coordinate, combine, and transform this data into knowledge that may be used to move fundamental science and translational medicine. However, these challenges have a unique solution in AI, which can learn complicated patterns, generalize across domains, and adapt to a new task. The importance of AI in bioinformatics can only be appreciated in terms of the analyses that it facilitates. Traditional pipelines were also highly dependent upon manually designed heuristics, hard-coded thresholds,

Citation: Sharma R, Saxena R, Hoskeri RM, Rajni E, Chaurasia TL. *AI in Drug Discovery and Precision Medicine.* R. J. Mil. Med. 2026, CXXIX(6): 600-609. https://doi.org/10.55453/rjmm.2026.129.6.2

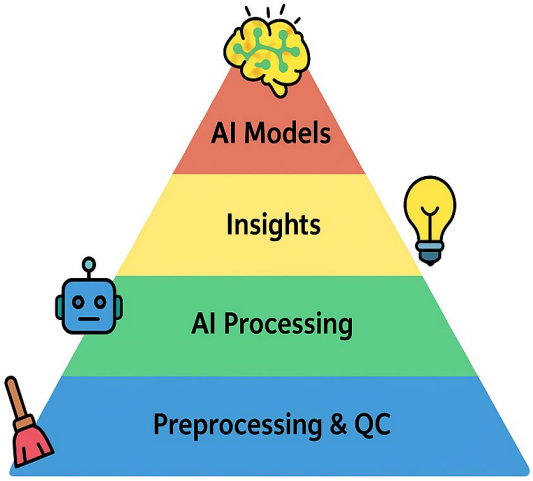
Academic Editor: Dan Spinu

Received: 06 October 2025
Revised: 22 July 2026
Accepted: 28 August 2026

and statistical models of limited scope that were unable to keep up with the sophistication of contemporary data.

AI can make discoveries about the underlying structures and relationships directly based on the data, forming representations that reflect these relationships. In genomics, AI has been used to produce precise variant calling and prediction of pathogenicity, and in transcriptomics, deep learning models have helped to reveal latent states in cells and developmental processes [3]. AlphaFold models, such as the first RCSB PDB-equipped protein of a flexible type, transformed the field of structural biology by demonstrating that AI-directed protein-folding prediction was possible with higher accuracy compared to previous methods. In clinical practice, AI is useful in patient stratification, risk modeling, and individualized treatment plans with the incorporation of genomic, phenotypic, and electronic health records. Significantly, AI is not just about prediction but also about scale and integration. Modern AI systems have a layered structure: data layers that support the findability, accessibility, interoperability and reusability (FAIR principles) of data; engineering layers that deal with data management, onto which data is ingested, how to handle data quality, reconciliation, and how to manage the data; computational layers that rely on both distributed training and high-performance computing infrastructures and modeling layers that focus on predictive, generative and multi-modal learning. The bio-AI stack: this hierarchical reasoning, commonly called the bio-AI stack, acknowledges the fact that biological insights are achieved through synergistic interactions of data engineering, complex modeling, and systems-level reasoning (Fig.1). Lastly, there are substantial ethical, legal, and social concerns regarding the incorporation of AI in bioinformatics. With human-derived data, issues of privacy, consent, algorithmic bias, or the fair distribution of any resulting benefits are of the essence. New strategies like federated learning and differential privacy are trying to develop a compromise between AI utility and protection of sensitive data [4]. To prevent the arrival of a world in which AI is used to play God, we must have governance frameworks, clear reporting practices, and explicable models that ensure that AI does not just move the field of biological discovery forward but does so responsibly and sustainably [5].

Figure 1: Workflow of AI in Bioinformatics



MATERIALS AND METHODS

This study is a narrative review that synthesizes recent advances in artificial intelligence applications in drug discovery and precision medicine. A comprehensive literature search was conducted to identify relevant studies on the application of artificial intelligence in drug discovery and precision medicine.

Databases Searched: The search was performed across four electronic databases: PubMed, Scopus, Web of Science and Google Scholar. The search was conducted across four electronic databases to ensure broad, multidisciplinary coverage. PubMed was selected as the primary source for biomedical and life sciences literature, ensuring access to foundational research in medicine and pharmacology. Scopus and Web of Science were included as large, interdisciplinary databases covering the intersection of computer science, engineering, and biomedical research, providing high-impact, peer-reviewed sources. Google Scholar was incorporated to capture cutting-edge developments in artificial intelligence and machine learning, including preprints and conference papers that may not yet be indexed in traditional databases but represent the latest methodological advancements.

Timeframe for Review Study: The timeframe was limited to articles published between January 2021 and December 2025 to capture the most recent advancements in this rapidly evolving field in the last 5 years. This five-year window was strategically

chosen to focus on the most recent advancements in this rapidly evolving field, capturing the emergence of transformative technologies such as deep learning, generative models, and large language models, while ensuring the findings remain current and relevant.

Keywords for Search: The search strategy utilized a combination of keywords, including Artificial Intelligence, Virtual Screening, Bioinformatics, Drug Discovery, Protein Structure, Precision Medicine, Personalized Medicine, and Target drug interaction. These were employed for a review of the literature at the intersection of AI methodologies and their biomedical applications.

Selection Approach: The selection process prioritized peer-reviewed original research articles, conference papers, and relevant preprints that focused on the application of AI methodologies within drug discovery and precision medicine. Peer-reviewed articles and conference papers were included to ensure a foundation of validated, high-quality research, while preprints were incorporated to reflect the latest innovations and emerging trends in AI development. Studies were included if they demonstrated a clear focus on AI applications, such as target identification, drug design, patient stratification, or biomarker discovery. Articles were excluded if they were opinion pieces, editorials, or lacked a substantive connection to the specified domains.

Evidence Synthesis: Evidence from the included studies was synthesized using a thematic narrative approach. Major themes, technological advancements, clinical applications, limitations, and future directions were systematically identified and organized.

RESULTS

Data Management and Engineering Foundations

Bioinformatics and the effective use of artificial intelligence lie in the efficient processing of big biological data prior to getting into the modeling process. Data management in this scenario cannot be merely reduced to storage: it is much more about the systematic intake, strict quality monitoring and assurance, harmonization of various modalities, and reproducibility of the work by means of standard workflows [5]. Biological data can be extremely heterogeneous, and genomics, transcriptomics, proteomics, metabolomics, imaging, and clinical information may be collected using different platforms and standards. The non-uniformity may cause biases, impair integration, and make downstream analysis more complicated. Hence, data management and data engineering are the basis of bioinformatics with AI [6]. The first challenge is data ingestion, in which raw results of high-throughput technologies are transformed into structured data. Such a process usually entails the derivation of relevant metadata, their compatibility with other existing schemas, and storing them in repositories that comply with the FAIR principles of data, which in this case are Findable, Accessible, Interoperable, and Reusable. The ingestion pipelines should also be able to cope with this velocity to support real-time sequencing results or a patient whose electronic health records are constantly being updated [7]. To meet these demands, cloud-based infrastructures and distributed file systems have been gaining popularity recently because they are scalable solutions to large volumes of data and are collaboratively accessible.

Following ingestion, intense quality control (QC) is required. Biological measurements may be burdened with batch effects, sequencing errors, incomplete values and annotation inconsistencies [8]. Unless provided with systematic QC, AI models will suffer spurious learning or deliver unreliable results. Outlier detection, statistical normalization and missing values imputation are regularly deployed, whereas mounting AI techniques like autoencoders and generative adversarial networks can be successfully utilized to resolve noise and repair data. Vetting truth at this level has a direct bearing on the accuracy of subsequent modeling. Another basis of data management is harmonization and integration. Multi-omics studies such as those that combine genomic, transcriptomic and proteomic data into a single analysis require the combination of disparate data sets of different modalities into a common data environment [9]. This integration is hampered by the fact that measurement scales, noise profiles, and metadata conventions differ. Ontologies and controlled vocabularies - e.g., the Gene Ontology (GO), or Human Phenotype Ontology (HPO) - are crucial to the alignment of heterogeneous data. More imminently, graph-based models and knowledge graphs have been used to model biological entities and relations, and provide more sound data integration. Reproducibility is also of essence. With the advent of big data, workflows may include tens of computational steps, and without thorough documentation, websites creating results may be very difficult to recreate [10]. This is one of the reasons why workflow management systems like Nextflow, Snakemake and Galaxy have become popular; such systems can automate pipelines, ensure version control, and are portable across different computational environments. Such reproducibility is further ensured through the use of containerization tools such as Docker and Singularity, since they can be used to confine software dependencies and help to standardize analyses to make them easy to reproduce across systems.

Machine Learning and Deep Learning in Bioinformatics Applications

ML and DL have become essential in the new bioinformatics, providing highly sophisticated computational options to handle, process and understand the increasing and multi-layered complexity of biological data. The classical statistical tools have the power to analyze big data; however, they are generally unable to cope with vast dimensionality, heterogeneity, and non-linear shapes of omics data, imaging information, and molecular structures [11]. DL and ML can help dissect these difficulties through learning patterns directly from data, which would allow the implementation of predictive modeling, feature extraction, and novelty discovery of unknown relationships between biological entities. Random forests, support vector machines, and gradient

boosting ML algorithms find wide use in genomics, where they can be used to predict the expression of genes, call genetic variants, and identify disease-related mutations. The convolutional neural networks (CNNs) have been shown to be particularly effective in the analysis of next-generation sequencing (NGS) data and in genome-wide association studies (GWAS) [12]. As one example, CNNs are applied to the prediction of transcription factor binding sites, enhancers, and epigenetic modifications on raw DNA sequences. The potential associated with such capabilities is to transform gene regulation and functional genomics studies. In proteomics and structural biology, AlphaFold has become an important tool in protein structure prediction and has reached accuracy resolution near that of experimental results. This paradigm shift not only helps understand the protein folding mechanism better, but also helps expedite drug discovery and protein engineering [13]. Learned models such as recurrent neural networks (RNNs) and transformers have also demonstrated improvements in sequence-based prediction of protein-protein interactions, post-translational modifications, and enzyme-substrate specificities, the basis of systems biology and drug design.

The second broad use case is in biomedical imaging: ML and DL models can be used to analyze large numbers of microscopy images, histopathological slides, and medical scans. Computer-assisted image recognition techniques are fast approaching the level of accuracy in classifying cell types, measuring morphological characteristics of tissues, and even in the diagnosis of diseases like cancer as accurate as a human pathologist [14]. A combination of imaging data and the omics profile adds more dimensions to personalized medicine by detecting the disease mechanism more comprehensively. However, with these successes, there are impediments to the use of ML and DL in bioinformatics. Biological datasets are usually noisy, imbalanced, and even small compared to typical computer vision or natural language processing datasets. This poses a question of overfitting, reproducibility, and generalizability of the models. Moreover, many DL algorithms have a black box, which makes biological interpretation difficult, and solutions are needed to create explainable AI (XAI) methods. To overcome these drawbacks, hybrid models that allow domain knowledge to marry with data-driven learning are being actively explored. To conclude, ML and DL make bioinformatics transformational as they allow finding predictive, scalable, and interpretable models of large bioinformatics data. Through these techniques, we get to know much more about basic biological processes, and they also lead to new innovations in the field of diagnosing illness, pharmaceuticals, and precision medicine [14]. With coming computational sophistication as well as hardware and software capabilities, machine learning and deep learning are poised to make even greater inroads into the world of bioinformatics, bringing the data of biology closer to productive biomedical uses.

AI in Omics Data Analysis

Omics, including genomics, transcriptomics, proteomics, metabolomics, and epigenomics, produce huge and complex datasets that are at center stage in modern biology and medicine. Artificial intelligence (AI) has become an effective method of analyzing this high-dimensional data as it provides methods that extend beyond traditional statistics. With its capacity to integrate different data types and learn patterns in them, AI allows novel biomarker discovery, disease signatures and therapeutic targets [7]. In the genomic world, the use of AI-related applications has incredibly enhanced the processing of next-generation sequencing (NGS) information. Machine learning and deep learning algorithms can be used in alignment of sequencing reads, calling of variants, and predicting functional effect of mutations using their high speed. As an example, AI models are also employed to differentiate pathogenic variants and non-pathogenic variants that can help to diagnose hereditary disorders. What is more, the AI is utilized in genome-wide association studies (GWAS) to compute genetic variants that are related to complex traits and can provide new insights into susceptibility to diseases. AI applications also have immense benefits in transcriptomics. The large amounts of data generated using RNA sequencing reflect dynamic patterns of gene expression, frequently at time-point snapshots, in tissues or disease conditions [15]. I models can cluster expression profiles efficiently, predict gene regulatory networks, and identify differentially expressed genes that can be linked to disease progression. NLP-based models are also being used to learn rules that define the likelihood of RNA splicing events, microRNA targets, and novel non-coding RNAs with functional roles in disease, just as they have been used with sequences such as text (Table 1).

In proteomics, the incorporation of AI has given a new form of studying protein expression and interactions. Much higher sensitivity and specificity can be achieved as a result of analyzing mass spectrometry data using technology based on AI [16-17]. Transformers Deep learning techniques are granting predictions for protein structure, post-translational modifications, and the structure of protein-protein interactions. These observations are vital insights in cell signaling networks, pathogen interactions and disease mechanisms. Metabolomics is difficult because metabolites are diverse and chemically complex [18]. The most frequently applied AI models, particularly those based on neural networks, are currently used to categorize metabolite spectra, identify unknown compounds, and integrate metabolomic data with genomic and proteomic data. The integrated analysis has also contributed to a better detection of metabolic biomarkers of diseases like cancer/diabetes as well as cardiovascular disorders. One of the main advantages of AI in omics is that it allows combining multi-omics data and provides a systems-level analysis of biological processes [19]. Conventional methods tended to study each of these omics layers independently, whereas AI enables the combination of them into a unified framework. Such an integrative analysis can illustrate cross-talk among biological layers, e.g., how genetic variants generate changes to the transcriptome, which produces protein expression and metabolite changes. Such insights are vital in conceiving precision medicine and in the field of systems biology. Despite these, there are still some challenges in using AI in omics. Analysis can be problematic due to data heterogeneity, batch effects, and missing data. The interpretability of the AI models is an issue because in biology, one needs to be able to justify biological

conclusions with transparent reasoning that can be experimentally tested [20]. Further, both the noise and scale, as well as the different data structures used by different omics, are vital components of multi-omics integration. Nonetheless, explainable AI research, powerful data harmonization techniques, and high-volume and collaborative initiatives are most likely to resolve these limitations.

Table 1: Applications of AI in Omics Data Analysis

Omics Field	AI Application	Example Tools/Models
Genomics	Variant calling, mutation prediction, genome annotation	DeepVariant, AlphaFold
Transcriptomics	Gene expression profiling, splicing event prediction	Random Forest, CNN models
Proteomics	Protein structure prediction, biomarker discovery	AlphaFold, DeepCNF
Metabolomics	Pattern recognition, disease classification	SVM, Neural Networks
Epigenomics	Methylation pattern analysis, chromatin accessibility prediction	Gradient Boosting, Deep Learning

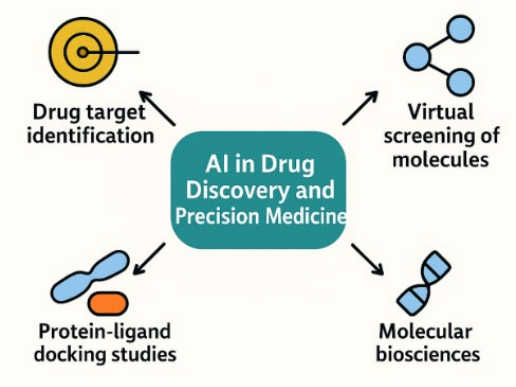
AI in Drug Discovery and Precision Medicine

Artificial intelligence (AI) has demonstrated a transformative potential in two areas: drug discovery and precision medicine. The conventional drug discovery method is lengthy, wastes many resources, and has poor rates due to only a small percentage of potential drugs making it to clinical application. With the emerging AI-based methodologies, this process has already started to be revolutionized, shortening drug target identification, predicting drug and compound interactions, and leveraging lead molecules with better efficacy and safety profiles [21]. The prediction of drug-target interactions and protein structures is one of the great contributions of AI to drug discovery. AI has enabled deep learning models to make significant advances, such as AlphaFold, which predicts protein 3D conformations with extraordinary accuracy [22]. Such structural predictions can give important hints to the possible binding pockets, allowing rational design of small molecules or biologics. Also, AI algorithms are capable of filtering immense chemical databases to find the ones that match the desired chemical structure, which is quite faster and cheaper than carrying out high-throughput screening in wet labs. The sorting of candidate molecules expected to interact best with target proteins using AI-powered screening leads to reduced drug development pipeline efficiency [23]. Other than identifying targets and predicting whether they will bind, AI has also been successful in lead optimization. With the modeling of the pharmacokinetic and pharmacodynamic (PK/PD) attributes, AI algorithms can predetermine the absorption, distribution, metabolism, excretion, and toxicity (ADMET) of compounds. This is useful in the elimination of molecules that possess undesired properties at initial stages, minimizing late-stage failures. With the development of generative models, including generative adversarial networks (GANs) and reinforcement learning systems, novel chemical entities are being generated with a view to not only meeting efficacy requirements but also safety and manufacturability constraints.

In precision medicine, AI is enabling an increasingly personalized approach in which therapies are individually selected on the basis of their genetic, molecular, and clinical characteristics [24]. With the multi-omics data combined with clinical histories and real-life evidence, AI can divide patients into subpopulations with differing reactions to treatments. AI models will enable investigators to determine which immunotherapies or targeted therapies are likely to work for cancer patients, thereby limiting trial-and-error approaches to treatment selection [23]. This stratification not only enhances patient outcomes but also reduces healthcare costs from unnecessary side effects. It is also being used to determine biomarker discovery, which is key to precision medicine. By analyzing large genomic and proteomic data sets, AI systems are able to discover biomarkers predictive of drug response, disease progression, or risk of relapse. These biomarkers are essential to making clinical judgments and to the creation of companion diagnostics that match treatment to patient-specific traits. Although it has a positive future, the integration of AI into drug discovery and precision medicine is not without difficulties. Annotated data is the key to training successful models, but it is usually hindered by privacy implications, proprietary policies, and differences in data standards [25]. Additionally, the explanation of AI models is a topical concern, where clinicians and regulators demand clear and understandable decision-making to keep patients safe (Fig.2). Ethical concerns, including data privacy, algorithmic unfairness, and fair access to AI-enabled treatment, also have to be accommodated. AI is transforming pharmaceutical research and precision medicine to make development in therapeutics faster, more affordable, and more personalized. Ranging between structural biology and virtual

screening, all the way to new biomarker discovery and patient stratification, AI-driven advancements are opening the doors toward the next age of healthcare.

Figure 2: AI in Drug Discovery and Precision Medicine



AI in Medical Imaging and Diagnostics

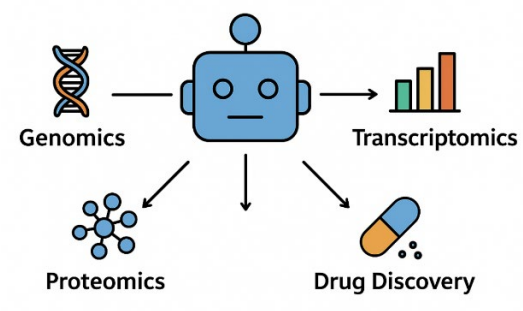
The diagnostic healthcare industry is one of the most pronounced and influential areas of artificial intelligence (AI) in the medical field today. Radiology, pathology, and clinical diagnostics collect image data, patient data, and other data every day in vast amounts, and AI-driven technologies have shown great promise in interpreting this data quickly and efficiently. In contrast to traditional manual data analysis, which is time-consuming and prone to human error, AI models based on deep learning are much faster, providing the ability to analyze thousands of images and identify trends that could not be noticed even by a skilled clinician [26]. In radiology, the use of AI algorithms is at its peak, where they are used to identify and categorize anomalies in X-rays, computed tomography (CT), magnetic resonance imaging (MRI), and ultrasonic images. As an example, CNNs have been trained to detect early symptoms of cardiovascular abnormalities, brain tumors, and lung cancer with accuracy levels superior to or equal to those of professional radiologists. In addition to marking suspicious areas, such systems also give quantitative measures that help clinicians make more assured decisions more swiftly. In pursuit of the same goals, AI is also being used in mammography to screen for breast cancer; this is particularly important because early and proper screening results in a high chance of patient survival [27]. There has also been a paradigm shift in pathology with the emergence of AI. Histological samples on slides can be scanned in high resolution using whole-slide imaging/digital pathology systems, generating terabytes of data that can be amenable to computational analysis. Pathway prediction: Neuro AI-powered pathology applications can categorize tissue type, identify malignant cells, and measure biomarkers within the tumor microenvironment at a very high degree of precision [28]. These capabilities are essential in the field of oncology, where precise staging and grading have a direct impact on treatment design and prognosis. By eliminating time-consuming steps, AI liberates pathologists to work on challenging diagnostic cases and decreases inter-observer variance.

In addition to imaging applications, AI is now transforming laboratory testing through interpretation of the rich data produced in genomics, proteomics, and clinical laboratory assays (Fig.3). Machine learning algorithms can be used to capture a multitude of patient information—such as lab results, medical history, and lifestyle data—and piece it together in order to make a complete diagnostic picture [29]. One particularly useful application is the fact that AI tools are now being used to help predict the risk of sepsis presenting in inpatient services by constantly monitoring electronic health record (EHR)-available data and intervening at the appropriate time, potentially saving lives. Some of the additional contributions that AI makes to precision diagnostics are that AI provides like-and-like comparisons. Diagnostic algorithms can also stratify patients by minute phenotypic dissimilarity, and this can facilitate targeted therapies. As another example, neurodegeneration, including Alzheimer's, comes at a time when MRI and PET scans using AI models can reveal early biomarkers before clinical symptoms come through.

The possibility of chain reaction prevention exists with early detection that will lead to the prevention of intervention and better management of the patient. Even though AI is successful in medical imaging and diagnostics, there are challenges related to its adoption. Data confidentiality, normalization of imaging models and incorporation of AI systems into actual clinical processes are among the topical issues [30]. Further, surveillance of diagnostic AI tools by regulatory bodies needs to have stringent validation as a means of ensuring accuracy, reproducibility, and fairness. Black-box models are vulnerable to scrutiny of interpretation, which makes clinicians reluctant to accept the outputs of the algorithms without any intervention by a human. Ethical aspects such as potential bias in algorithms that can result in healthcare inequality, based on demographic groups, must also be considered. In summary, AI has become a game-changer in the field of medical imaging and diagnostics to advance accuracy,

efficiency, and personalization of health [31]. Applications include radiology and pathology, laboratory diagnostics, and predictive models. Clinical applications: In radiology and pathology, AI is used to aid the detection of diseases earlier and in monitoring progression more accurately, with AI-driven systems also being used in laboratory diagnostics and predictive modeling to deliver specifically targeted interventions.

Figure 3: AI in Omics and Bioinformatics



Ethical Imperatives and Emerging Directions for AI in Bioinformatics

On the one hand, the emergence of artificial intelligence in bioinformatics and healthcare systems has provided new and outstanding prospects in the regulation and analysis of biological big data (Table 2). On the other hand, however, there is indeed a complicated array of challenges in such assimilation. Such obstacles cut across the technical, ethical, and socio-regulatory dimensions and require comprehensive solutions until AI can reach mass and reliable use. An awareness of such concerns is essential to determining the course to be taken by AI in life sciences. Among the biggest obstacles are data quality and heterogeneity. Biological data are produced by a variety of sources, which include genomic sequencing, transcriptomics, proteomics, electronic health record systems, and imaging platforms [32]. These data are usually not homogeneous, do not scale up well, and have inconsistent reliability. Missing values, noise, and biases that occur during sample collection or sequencing methods can adversely affect the performance of the model. The need to provide common data exchange formats and standardized exchange across platforms is a critical means of ensuring that data-driven analysis using AI can be maximized. The other obstacle is algorithm transparency and interpretability. Some of the most effective AI models, especially deep learning neural networks, are so powerful and opaque that little is understood about their decision-making mechanisms. In healthcare, where the actions of clinicians may have a direct effect on patient well-being, this unpredictability in the absence of explainability erodes trust [33]. There is a need to develop interpretable AI models and integrate explainable AI (XAI) frameworks, whereby clinicians and researchers know not only that a particular decision is predicted, but why it is predicted. The issues of moral inclinations also make the landscape more tricky. The privacy and security of data are paramount, especially because genomic and medical information is sensitive in nature.

Ensuring that the global regulations, including GDPR (General Data Protection Regulation) or HIPAA (Health Insurance Portability and Accountability Act), are adhered to is not a trivial task in the case of large-scale datasets that are being processed across borders [34]. In addition, an algorithm can be biased, i.e., it can reinforce unfair treatment in healthcare due to the underrepresentation of certain ethnic, gender, or socioeconomic groups in the training set. As an example, an AI may be developed based on mostly European genomic data and perform poorly when used in underrepresented groups, resulting in errors in diagnosis. There is still a major hurdle in terms of regulatory implications involved in the validation and approval of AI tools to be used in the clinical setting. Regulatory agencies require evidence of reproducibility, generalizability, and safety at a high level before algorithms can be included in the flow of diagnostics or treatment [35]. Such a high degree of validation would demand large and disparate datasets, multinational cooperation between industry and science, and universities, and hospitals. Looking into the future, it is anticipated that AI in bioinformatics is going to shift from predictive analytics to prescriptive and generative AI. The rise of new paradigms like federated learning could help alleviate privacy issues since it means that AI models can be trained using decentralized data without data being shared between organizations. In the same way, the combination of quantum computing with artificial intelligence has the potential to make the analysis of ultra-large biological data, e.g., generated by single-cell sequencing, faster. A second emerging opportunity is the bringing of AI to systems biology, in which global models of biological networks can promise a richer understanding of disease processes and drug targets [36]. What is also significant is the creation of ethical frameworks and governance models that will bring balance between innovation and responsibility. Cross-sector partnerships (with biologists, clinicians, data scientists, ethicists, and policymakers) will be paramount to ensure that the merits of AI-based bioinformatics are equally distributed among all world populations. Training of researchers and clinicians in the use of AI tools will also be instrumental in how they will be effectively and usefully adopted (Table 3).

Table 2: AI Techniques and Their Role in Bioinformatics

AI Technique	Role in Bioinformatics
Machine Learning (ML)	Classification of gene expression data, biomarker discovery
Deep Learning (DL)	Protein structure prediction, drug-target interaction
Natural Language Processing (NLP)	Mining biomedical literature, gene–disease association prediction
Reinforcement Learning (RL)	Optimization in drug design and molecular docking simulations
Graph Neural Networks (GNN)	Modeling biological networks and pathway interactions

Table 3: Comparison of Traditional and AI-Driven Approaches in Bioinformatics

Aspect	Traditional Methods	AI-Driven Approaches
Data Processing	Manual, rule-based	Automated, data-driven
Pattern Detection	Limited statistical models	Deep learning & ML
Scalability	Low	High
Multi-omics Integration	Difficult	Efficient
Drug Discovery Speed	Slow	Accelerated
Predictive Accuracy	Moderate	High

CONCLUSIONS

Artificial intelligence incorporated into bioinformatics sets a paradigm shift in the manner in which large and intricate biological information is handled, inspected, and interpreted. Predictive modeling and multi-omics integration powered by high-throughput data mining have allowed the deployment of AI to transform traditional biological studies into a data-driven scientific approach that can solve previously untenable problems. The applications include genome annotation, protein structure prediction, personalized medicine, and drug discovery, forming just a few features of the central role of AI in fast-tracking scientific discovery and clinical translation.

The potential of AI may not be realized without addressing the issues of information bias, computer program intelligibility, moral standards, and control. Genomic and medical data require care regarding privacy protection and the mitigation of bias. Similarly, transparent interpretability, support for reproducible solutions, and equitable access to solutions across populations are also critical to the successful development of trust in bioinformatics applications powered by AI systems.

There is enormous promise in more disruptive potential, like federated learning, explainable AI, and quantum-enhanced computing, to accelerate and enhance the potential of biological data analysis. To make this vision a reality, however, multidisciplinary cooperation is needed, combining know-how from computational science, biology, medicine, and ethics. Alongside this is a need to create resilient governance and global networks that can coordinate technological advances in accordance with the needs of societies. Despite rapid progress, several research gaps remain. The need for interpretable AI models, standardized benchmarking datasets, cross-population validation, and integration of multi-modal biological data

continues to challenge large-scale clinical translation. Future research should prioritize trustworthy AI frameworks, equitable data representation, and regulatory-ready validation pipelines.

AI in bioinformatics is not the simple processing of big data, in other words, but rather an enabler, rewriting the threshold of biological discovery and healthcare innovation. By taking responsibility for exploiting its opportunities and dealing proactively with its constraints, the scientific community can use AI to unravel the complexity of life, propel sustainable medical breakthroughs, and eventually support the health of people on a global scale.

Conflicts of interest and sources of funding

The authors declare no conflict of interest.

This research received no external funding.

Acknowledgments

The authors used AI-assisted tools for language editing and grammatical refinement. The authors independently developed all scientific content, conceptualization, analysis, and interpretations.

Authors' contribution

Conceptualization, R.S. and R.S.; methodology, R.S.; validation, E.R.; resources, R.S.; data curation, R.S.; writing—original draft preparation, R.S.; writing—review and editing,

H.M.R.; visualization, T.L.C.; supervision, R.S. All authors have read and agreed to the published version of the manuscript.

Ethics approval and consent to participate

Not applicable.

Patient consent for publication

Not applicable.

References

1. Xu Y, Liu X, Cao X, Huang C, Liu E, Qian S, Zhang J. et al. Artificial intelligence: A powerful paradigm for scientific research. The Innovation. 2021; 2(4): 100179. doi:10.1016/j.xinn.2021.100179

2. Lilhore UK, Kumar A, Vyas N, Simaiya S, Dutt V. (Eds.). (2025). Multimodal Data Fusion for Bioinformatics Artificial Intelligence. John Wiley & Sons. 2025; ISBN: 978-1-394-26993-8

3. Chandrashekar K, Niranjan V, Vishal A, Setlur AS. Integration of artificial intelligence, machine learning and deep learning techniques in genomics: review on computational perspectives for NGS analysis of DNA and RNA seq data. Current Bioinformatics.2024; 19(9): 825-844. doi: https://doi.org/10.2174/0115748936284044240108074937

4. Nguyen D, Le T, Le B. Explainability graph neural networks with nearest neighbor estimate interpretations. Neural Computing and Applications. 2025; 37(20): 15891-15922.doi:10.1007/s00521-025-11339-7

5. Cooper DR, Grabowski M, Zimmerman MD, Porebski PJ, Shabalin IG, Woinska M, Minor W. State-of-the-Art data management: improving the reproducibility, consistency, and traceability of structural biology and in vitro biochemical experiments. Structural Genomics: General Applications. 2021; 2199: 209-236. doi: 10.1007/978-1-0716-0892-0_13

6. Bayer JM, Thompson PM, Ching CR, Liu M, Chen A, Panzenhagen AC, Sämann PG. Site effects how-to and when: An overview of retrospective techniques to accommodate site effects in multi-site neuroimaging analyses. Frontiers in Neurology. 2022; 13: 923988. doi: https://doi.org/10.3389/fneur.2022.923988

7. Marques L, Costa B, Pereira M, Silva A, Santos J, Saldanha L, Vale N. Advancing precision medicine: A review of innovative in silico approaches for drug development, clinical pharmacology and personalized healthcare. Pharmaceutics. 2024; 16(3): 332. doi:10.3390/pharmaceutics16030332

8. Yu Y, Mai Y, Zheng Y, Shi L. Assessing and mitigating batch effects in large-scale omics studies. Genome Biology. 2024; 25(1): 254. doi:10.1186/s13059-024-03401-9

9. Hayes CN, Nakahara H, Ono A, Tsuge M, Oka S. (2024). From omics to multi-omics: a review of advantages and tradeoffs. Genes. 2024; 15(12): 1551.

doi:10.3390/genes15121551

10. van Kampen AH, Mahamune U, Jongejan A, van Schaik BD, Balashova D, Lashgari D, Moerland PD. ENCORE: a practical implementation to improve reproducibility and transparency of computational research. Nature Communications. 2024; 15(1): 8117. doi: 10.1038/s41467-024-52446-8

11. Mukherjee A, Abraham S, Singh A, Balaji S, Mukunthan KS. From data to cure: A comprehensive exploration of multi-omics data analysis for targeted therapies. Molecular biotechnology. 2025; 67(4): 1269-1289. doi: 10.1007/s12033-024-01133-6

12. Pimpalkar A, Gandhewar N, Shelke N, Patil S, Chhabria S. An efficient deep convolutional neural networks model for genomic sequence classification. Genomics at the Nexus of AI, Computer Vision, and Machine Learning. 2024; 345-375. doi:10.1002/9781394268832.ch16

13. Gupta U, Pranav A, Kohli A, Ghosh S, Singh D. The contribution of artificial intelligence to drug discovery: Current progress and prospects for the future. Microbial Data Intelligence and Computational Techniques for Sustainable Computing. 2024; 1-23. doi:10.1007/978-981-99-9621-6_1

14. Mezei T, Kolcsár M, Joó A, Gurzu S. Image analysis in histopathology and cytopathology: from early days to current perspectives. Journal of Imaging. 2024; 10(10): 252. doi:10.3390/jimaging10100252

15. Kumar A. AI-driven precision oncology: predictive biomarker discovery and personalized treatment optimization using genomic data. Int J Adv Res Publ Rev. 2024; 1(3): 21-38.

16. Zhang Z, Sun Y, Peng Q, Li T, Zhou P. Integrating dynamical systems modeling with spatiotemporal scRNA-Seq Data Analysis. Entropy. 2025; 27(5): 453. https://doi.org/10.3390/e27050453.

17. Son A, Kim W, Park J, Park Y, Lee W, Lee S, Kim H. Mass spectrometry advancements and applications for biomarker discovery, diagnostic innovations, and personalized medicine. International Journal of Molecular Sciences. 2024; 25(18): 9880. doi:10.3390/ijms25189880

18. Prashar DB, Sharma M, Sharma D, Mir Z, Sood H, Sharma M. Exploring the complexity of plant stress response: role of metabolomics and signalling pathways in metabolic diversification. Journal of Plant Biochemistry and Biotechnology. 2025; 1-14. doi:10.1007/s13562-025-00986-5

19. Savitha S, Keerthana R, Logeswaran K, Keerthika P, Sharmila V, Sangeetha M. Integration of Multi-Omics Data: Genomics, Proteomics, Metabolomics. Harnessing AI and Machine Learning for Precision Wellness. IGI Global Scientific Publishing. 2025; 149-184. doi:10.4018/979-8-3693-9521-9.ch006.

20. Hassija V, Chamola V, Mahapatra A, Singal A, Goel D, Huang K, Hussain A. Interpreting black-box models: a review on explainable artificial intelligence. Cognitive Computation. 2024; 16(1): 45-74. doi:10.1007/s12559-023-10179-8

21. Serrano DR, Luciano FC, Anaya BJ, Ongoren B, Kara A, Molina G, Lalatsa A. Artificial intelligence (AI) applications in drug discovery and drug delivery: Revolutionizing personalized medicine. Pharmaceutics. 2024; 16(10): 1328. doi:10.3390/pharmaceutics16101328

22. Chen L, Li Q, Nasif KFA, Xie Y, Deng B, Niu S, Xie CY. AI-driven deep learning techniques in protein structure prediction. International journal of molecular sciences. 2024; 25(15): 8426. doi:10.3390/ijms25158426

23. Zhang K, Yang X, Wang Y, Yu Y, Huang N, Li G, Yang S. Artificial intelligence in drug development. Nature medicine. 2025; 31(1): 45-59. doi: 10.1038/s41591-024-03434-4

24. Ahmad S, Shah SNA, Parveen R, Raza K. Machine Learning for Genomic Profiling and Drug Discovery in Personalised Lung Cancer Therapeutics. Journal of Drug Targeting. 2025; 1-20. doi: 10.1080/1061186X.2025.2530656

25. Karim MM, Khan S, Van DH, Liu X, Wang C, Qu Q. Transforming Data Annotation with AI Agents: A Review of Architectures, Reasoning, Applications, and Impact. Future Internet. 2025; 17(8): 353. https://doi.org/10.3390/fi17080353

26. Hanna MG, Pantanowitz L, Dash R, Harrison JH, Deebajah M, Pantanowitz J, Rashidi HH. Future of artificial intelligence (AI)-machine learning (ML) trends in pathology and medicine. Modern Pathology. 2025; 36(4): 100705. https://doi.org/10.1016/j.modpat.2025.100705

27. Lauritzen AD, Lillholm M, Lynge E, Nielsen M, Karssemeijer N, Vejborg I. Early indicators of the impact of using AI in mammography screening for breast cancer. Radiology. 2024; 311(3): e232479. https://doi.org/10.1148/radiol.232479

28. Khalighi S, Reddy K, Midya A, Pandav KB, Madabhushi A, Abedalthagafi M. Artificial intelligence in neuro-oncology: advances and challenges in brain tumor diagnosis, prognosis, and precision treatment. NPJ Precision Oncology. 2024; 8(1): 80. doi: 10.1038/s41698-024-00575-0

29. Sathyavathi S, Kavitha RK, Mary GPA, Baskaran KR. Machine Learning-Based Techniques for Predictive Diagnostics in Healthcare. In Cybersecurity and Data Science Innovations for Sustainable Development of HEICC. 2025; 47-61. doi:10.1201/9781032711300-4

30. Obuchowicz R, Strzelecki M, Piórkowski A. Clinical applications of Artificial Intelligence in Medical Imaging and Image Processing—A Review. Cancers. 2024; 16(10): 1870. https://doi.org/10.3390/cancers16101870

31. Zhou J, Park S, Dong S, Tang X, Wei X. Artificial intelligence-driven transformative applications in disease diagnosis technology. Medical Review. 2025; https://doi.org/10.1515/mr-2024-0097

32. Chaudhari JK, Pant S, Jha R, Pathak RK, Singh DB. Biological big-data sources, problems of storage, computational issues, and applications: a comprehensive review. Knowledge and Information Systems. 2024; 66(6): 3159-3209. doi:10.1007/s10115-023-02049-4

33. Rosenbacke R, Melhus Å, McKee M, Stuckler D. How Explainable Artificial Intelligence Can Increase or Decrease Clinicians' Trust in AI Applications in Health Care: Systematic Review. JMIR AI 3. 2024; e53207. doi:10.2196/53207

34. Ike JE, Kessie JD, Popoola R, Azeez MA, Onibokun T. A Novel Approach to Cloud Data Encryption using Homomorphic Encryption. 2024; 5(6): 19-27. doi: https://doi.org/10.54660/.IJFMR.2024.5.6.19-27

35. Caminero A, Tropini C, Valles-Colomer M, Shung DL, Gibbons SM, Surette MG, Verdu EF. Credible inferences in microbiome research: ensuring rigour, reproducibility and relevance in the era of AI. Nature Reviews Gastroenterology & Hepatology. 2025; doi: 10.1038/s41575-025-01100-9

36. Saraf S, De A, Tripathy BK. Effective use of computational biology and artificial intelligence in the domain of medical oncology. In Computational Intelligence for Oncology and Neurological Disorders. 2024; 228-252. doi:10.1201/9781003450153-17

https://doi.org/10.55453/rjmm.2026.129.6.3

Review

Artificial Intelligence for Radiographic Assessment of Peri-Implant Marginal Bone Loss: Current Evidence, Clinical Interpretation, and Limitations

Vladimir Năstasie[1], Ioan Sîrbu[2], Andreea Mihaela Custură[3,*], Elisei Adelin Radu[3,*], Dragoș Epistatu[4], Alexandra Tuță[2], Valentin Daniel Sîrbu[2]

[1] Doctoral School, Faculty of Dentistry, "Carol Davila" University of Medicine and Pharmacy, 050474 Bucharest, Romania
[2] Discipline of Implanto-Prosthesis Therapy, Faculty of Dentistry, "Carol Davila" University of Medicine and Pharmacy, 37 Dionisie Lupu Street, District 2, 020021 Bucharest, Romania
[3] Discipline of Dental Prostheses Technology, Faculty of Dentistry, "Carol Davila" University of Medicine and Pharmacy, 37 Dionisie Lupu Street, District 2, 020021 Bucharest, Romania
[4] Department of Dental Radiology, Faculty of Dentistry, "Carol Davila" University of Medicine and Pharmacy, 020021, Bucharest, Romania
*Correspondence: A.M.C - andreea-mihaela.custura@drd.umfcd.ro; A.E.R – elisei-adelin.radu@drd.umfcd.ro; Tel: +40743907259.

Abstract: Background: Artificial intelligence (AI) is increasingly investigated for radiographic assessment of peri-implant bone conditions, although radiographic marginal bone loss does not alone establish a clinical diagnosis of peri-implantitis. This narrative review aimed to critically synthesize current evidence on AI-assisted radiographic assessment of peri-implant marginal bone levels and bone loss. Methods: A structured literature search was conducted in PubMed/MEDLINE and Scopus. Eligible original studies applying AI or machine-learning methods to human dental radiographs for peri-implant bone assessment were included in a qualitative synthesis. Results: Seventeen studies were included. Periapical radiographs were the predominant imaging modality, while panoramic radiographs and CBCT were less frequently investigated. AI applications included implant and landmark localization, marginal bone-level measurement and quantification, bone-loss severity and defect-morphology classification, and prediction using imaging-derived features. Reported performance was generally promising, although substantial heterogeneity was observed in datasets, target tasks, reference standards, validation strategies, and performance metrics. Conclusions: Current radiograph-based AI systems show potential for image analysis, quantitative assessment, and clinical decision support. However, radiographic AI performance should not be interpreted as autonomous diagnostic accuracy for peri-implantitis. External validation, longitudinal assessment, and integration with relevant clinical parameters remain priorities for future research.

Keywords: artificial intelligence; convolutional neural network; peri-implant marginal bone loss; dental radiography

INTRODUCTION

Long-term implant maintenance requires surveillance of peri-implant soft tissues and supporting bone. Radiography is an essential objective method for identifying and longitudinally measuring peri-implant bone-level changes, but it does not directly demonstrate inflammation or disease activity. Periapical radiographs are generally preferred for standardized marginal bone-level assessment; panoramic radiographs may provide broader screening information, whereas cone-beam computed tomography (CBCT) is reserved for selected indications in which three-dimensional assessment is clinically justified [1].

Citation: Năstase V, Sîrbu I, Custură AM, Radu EA, Epistatu D, Tuță A, Sîrbu VD. *Artificial Intelligence for Radiographic Assessment of Peri-Implant Marginal Bone Loss: Current Evidence, Clinical Interpretation, and Limitations.* R. J. Mil. Med. 2026, CXXIX(6): 610-623.https://doi.org/10.55453/rjmm.2026.129.6.3

Academic Editor: Octavian Vasiliu

Received: 12 September 2026
Revised: 26 October 2026
Accepted: 30 October 2026

Peri-implant health is characterized by the absence of clinical signs of inflammation. Peri-implant mucositis presents with bleeding and/or suppuration on gentle probing without bone loss beyond initial crestal remodeling. Peri-implantitis is a plaque-associated pathological condition characterized by inflammation of the peri-implant mucosa and subsequent progressive loss of supporting bone [1]. Thus, peri-implantitis is not a radiographic diagnosis alone. Diagnosis should integrate bleeding and/or suppuration on probing, increased probing depth relative to previous examinations, and radiographic bone loss beyond initial remodeling [2]. When previous records are unavailable, the 2017 World Workshop case definition uses

bleeding and/or suppuration, probing depths of at least 6 mm, and bone levels at least 3 mm apical to the most coronal intraosseous portion of the implant [1]. The EFP S3 guideline likewise places radiographic findings within a clinical pathway that includes probing findings, patient- and implant-level risk assessment, and longitudinal comparison where available [3].

Marginal bone loss must therefore be distinguished from peri-implantitis-related bone resorption. Early crestal change may reflect physiological remodeling after implant placement and loading, and a single radiograph cannot determine the biological cause of a bone-level change. Baseline or previous radiographs are essential whenever available, because progression beyond expected remodeling is more informative than an isolated measurement [1, 3]. Consequently, radiographic marginal bone loss is an imaging finding, while peri-implantitis is a clinical diagnosis that cannot be determined solely from radiographic information [1, 3]. When evaluating the effectiveness of artificial intelligence models that have only been trained on radiographic images, this distinction is especially crucial.

Radiographic interpretation can nevertheless be challenging. Accurate measurement requires consistent identification of the implant platform, implant-abutment interface, implant apex, first bone-to-implant contact, and exposed threads. Projection error, overlapping anatomy, prosthetic components, image quality and implant design can obscure landmarks. Moreover, two-dimensional radiographs cannot fully depict buccal and lingual bone morphology. These challenges motivate automated methods that can reliably recognize anatomical and implant-related landmarks and measure changes at the peri-implant bone level [4, 5].

Artificial intelligence encompasses computational methods that perform tasks commonly associated with human reasoning or perception. Machine learning is a subset of AI in which algorithms learn patterns from data; deep learning is a subset of machine learning that uses multilayer neural networks. In dento-maxillofacial radiology, these approaches have been investigated to improve consistency, reduce repetitive measurement burden, and support image-based detection and classification [6, 7]. In peri-implant radiographic assessment, convolutional neural networks (CNNs) and related deep-learning architectures have been applied to several tasks, such as implant and tissue localization, landmark detection, bone-level measurement, radiographic severity grading, and defect-pattern classification [4, 5, 8-12]. These image-analysis tasks should not be conflated with the clinical diagnosis of peri-implantitis.

Recent systematic reviews and a meta-analysis have already summarized the performance of AI models applied to peri-implant radiographic assessment [13-15]. However, the available primary studies address heterogeneous imaging tasks, including implant and landmark localization, marginal bone-level measurement, severity grading, and defect-morphology classification. As a result, performance estimates for these specific tasks cannot be consistently interpreted as peri-implantitis diagnostic accuracy. The present review focuses on the precise radiographic task carried out by each AI model and the methodological elements that determine its potential clinical relevance, offering a clinically oriented interpretation of this varied evidence instead of another quantitative synthesis.

Accordingly, this narrative review aims to critically synthesize current evidence on AI-assisted radiographic assessment of peri-implant marginal bone levels and bone loss, with particular emphasis on the specific imaging tasks performed by existing models, their methodological and validation characteristics, and their potential clinical applications and limitations. A further objective is to clarify the distinction between AI-based assessment of radiographic bone changes and the multimodal clinical diagnosis of peri-implantitis.

MATERIALS AND METHODS

Review Design

This study was conceptualized as a narrative review that was complemented by a structured literature search. The objective was to critically synthesize the most recent evidence regarding the radiographic assessment of peri-implant marginal bone levels and bone loss using artificial intelligence (AI). With special attention to the particular imaging tasks carried out by each model, such as implant and peri-implant tissue localization, landmark detection, marginal bone-level measurement, bone-loss detection and severity grading, and defect-morphology classification, the review concentrated on original studies assessing AI-based analysis of dental implant radiographs.

The significant methodological variety across the available studies, especially with regard to imaging modalities, AI architectures, target tasks, reference standards, validation techniques, and reported performance measures, led to a narrative synthesis of the evidence. As a result, neither quantitative pooling nor meta-analysis was carried out.

While consensus reports and clinical practice guidelines established accepted definitions and diagnostic criteria for peri-implant health, peri-implant mucositis, and peri-implantitis, systematic reviews, meta-analyses, and other pertinent evidence syntheses were utilized to contextualize the results from the primary studies. These sources were taken into account independently of the original research that was part of the primary evidence synthesis.

The distinction between the clinical diagnosis of peri-implantitis, which necessitates the integration of radiographic results with clinical and, if available, longitudinal data, and AI-based assessment of radiographic marginal bone alterations was given special attention.

Information Sources and Search Strategy

A structured literature search was conducted in two electronic databases, PubMed/MEDLINE and Scopus, to identify studies investigating artificial intelligence (AI)-based radiographic assessment of peri-implant marginal bone levels and bone loss. The databases were searched between 15th of July and 15th of August 2026. No restrictions regarding publication date, language, or article type were applied at the database-search stage.

The search strategy was developed around three main concepts: (1) artificial intelligence and machine-learning methods; (2) dental implants and peri-implant tissues; and (3) peri-implant marginal bone levels, bone loss, remodeling, and related bone changes. Database-specific search strategies were used to account for differences in indexing systems and search syntax.

For PubMed/MEDLINE, Medical Subject Headings (MeSH) and free-text terms searched within the title and abstract fields were combined using Boolean operators. The final PubMed/MEDLINE search strategy was:

("Artificial Intelligence"[Mesh] OR "artificial intelligence"[Title/Abstract] OR "Machine Learning"[Mesh] OR "machine learning"[Title/Abstract] OR "deep learning"[Title/Abstract] OR "convolutional neural network*"[Title/Abstract] OR CNN[Title/Abstract] OR "object detection"[Title/Abstract]) AND ("Dental Implants"[Mesh] OR "dental implant*"[Title/Abstract] OR "peri-implant"[Title/Abstract] OR "periimplant"[Title/Abstract] OR "peri-implantitis"[Title/Abstract] OR "periimplantitis"[Title/Abstract]) AND ("marginal bone loss"[Title/Abstract] OR "marginal bone level*"[Title/Abstract] OR "peri-implant bone loss"[Title/Abstract] OR "periimplant bone loss"[Title/Abstract] OR "peri-implant bone level*"[Title/Abstract] OR "periimplant bone level*"[Title/Abstract] OR "marginal bone remodeling"[Title/Abstract] OR "marginal bone remodelling"[Title/Abstract] OR "peri-implant bone remodeling"[Title/Abstract] OR "peri-implant bone remodelling"[Title/Abstract] OR "peri-implant bone defect*"[Title/Abstract] OR "periimplant bone defect*"[Title/Abstract] OR "peri-implantitis"[Title/Abstract] OR "periimplantitis"[Title/Abstract]). This search retrieved 80 records.

For Scopus, the search strategy was adapted to the database-specific TITLE-ABS-KEY syntax and was intentionally broader to account for differences in database indexing and terminology. The final Scopus search strategy was: TITLE-ABS-KEY (("artificial intelligence" OR "machine learning" OR "deep learning") AND ("dental implant" OR "peri implant" OR "peri implantitis")). This search retrieved 58 records.

Thus, a total of 138 records were identified through electronic database searching before duplicate removal and eligibility screening. A supplementary targeted search was also performed to identify potentially relevant studies not retrieved by the predefined database search strategies. Additional records identified through this process were assessed according to the same eligibility criteria. Records identified through the database and supplementary searches were subsequently evaluated according to the predefined eligibility criteria described below.

Eligibility Criteria

Studies were considered eligible for the primary evidence synthesis if they met the following criteria: (1) original peer-reviewed research investigating artificial intelligence, machine learning, or deep-learning methods; (2) evaluation of dental implants and/or peri-implant tissues using radiographic images; (3) assessment of at least one imaging task directly related to peri-implant marginal bone status, including peri-implant landmark or tissue detection, marginal bone-level measurement, marginal bone-loss detection or quantification, radiographic bone-loss severity grading, prediction of marginal bone loss using radiographic or imaging-derived features or peri-implant bone-defect morphology classification; (4) use of clinical human radiographic images, including periapical, panoramic, or cone-beam computed tomography (CBCT) images; and (5) availability of the full text in English.

Studies describing AI-based peri-implantitis detection or peri-implantitis classification were considered eligible when the model assessed radiographic bone changes relevant to the scope of this review. However, such studies were classified according to the actual imaging task performed and were not considered to provide evidence of AI-based clinical diagnosis of peri-implantitis unless the reference standard incorporated appropriate clinical diagnostic parameters in addition to radiographic findings.

Studies were excluded if they (1) investigated AI applications exclusively for implant planning or placement, anatomical segmentation for surgical planning, implant identification, implant-brand or implant-system recognition, or prosthetic planning without assessment of peri-implant marginal bone status; (2) evaluated exclusively non-radiographic data; (3) were based exclusively on animal, in vitro, phantom, or synthetic datasets; (4) did not assess an outcome directly related to peri-implant marginal bone level, bone loss, bone remodeling, or peri-implant bone-defect morphology; or (5) were case reports, conference abstracts or proceedings, editorials, letters, commentaries, protocols, or other non-original publications.

Systematic reviews, meta-analyses, scoping reviews, and narrative reviews were excluded from the primary evidence synthesis. Consensus reports and clinical practice guidelines were used to establish clinical definitions and diagnostic criteria but were not considered part of the primary AI evidence set.

Study Selection

All records retrieved from PubMed/MEDLINE and Scopus were screened by title and abstract for potential relevance to the predefined eligibility criteria. The database searches identified a total of 138 records, including 80 records from PubMed/MEDLINE and 58 records from Scopus. After comparison of the records retrieved from the two databases, no duplicates were identified; therefore, all 138 records proceeded to title and abstract screening.

During title and abstract screening, records were excluded when they clearly did not meet the eligibility criteria, including studies based exclusively on non-radiographic clinical or demographic data, large language models applied to simulated clinical scenarios, microbiome or genomic datasets, and other non-imaging approaches to peri-implant disease prediction. Following this screening, 17 articles were considered potentially eligible and underwent full-text assessment.

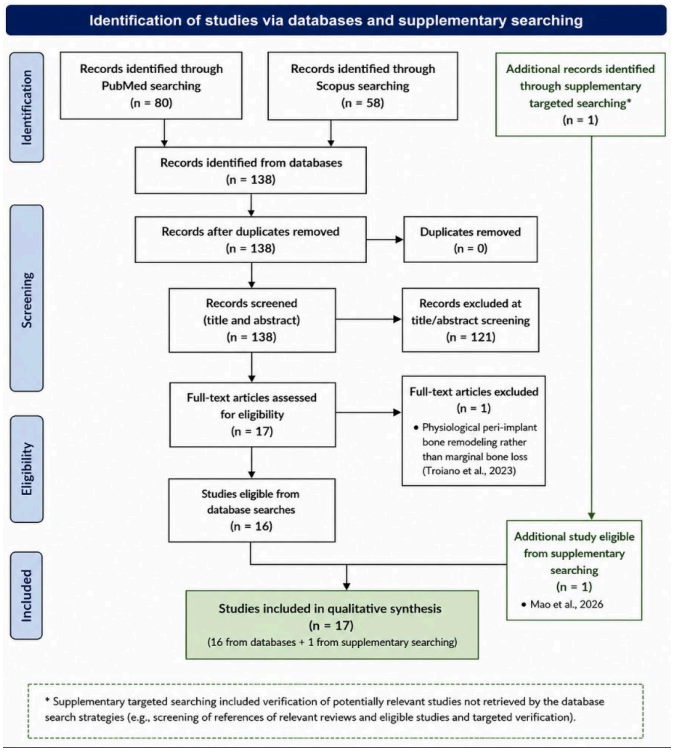
The full texts of these 17 potentially eligible articles were assessed against the predefined inclusion and exclusion criteria. One study was excluded at this stage because the investigated outcome was physiological peri-implant bone remodeling rather than marginal bone loss. Consequently, 16 studies retrieved through the database search fulfilled the eligibility criteria. None of the records retrieved exclusively through the Scopus search met the eligibility criteria for progression to full-text assessment. One additional eligible study was identified through supplementary targeted searching, resulting in a final sample of 17 original studies included in the qualitative synthesis.

Studies describing peri-implantitis detection based on radiographic images were retained when their actual imaging task involved peri-implant marginal bone assessment, bone-defect classification, or related radiographic outcomes. These studies were subsequently categorized according to the specific radiographic task performed rather than being interpreted uniformly as studies of clinical peri-implantitis diagnosis.

Any disagreement regarding eligibility or study classification was resolved through discussion among the authors until consensus was reached.

The study identification, screening, eligibility assessment, and final inclusion process is summarized in Figure 1.

Figure 1: Flow diagram of the literature search and study selection process across PubMed/MEDLINE and Scopus. AI, artificial intelligence; ML, machine learning; DL, deep learning.



Data Extraction and Evidence Synthesis

Data were extracted from each eligible study using a structured framework designed to characterize both the clinical imaging context and the methodological features of the artificial intelligence models. The extracted variables included: first author and year of publication; study design; sample and dataset characteristics; radiographic modality; AI or machine-learning approach; specific radiographic task; reference standard and annotation procedure; training, validation, and test strategy; performance metrics; comparator, when available; and the main findings relevant to peri-implant marginal bone assessment.

Particular attention was given to the specific imaging task performed by each model, rather than relying solely on the diagnostic terminology used by the original authors. Accordingly, eligible studies were categorized according to whether the AI approach was designed for implant or peri-implant landmark localization, marginal bone-level detection or measurement, marginal bone-loss detection or quantification, radiographic severity grading, peri-implant bone-defect morphology classification, or prediction of marginal bone loss using radiographic or imaging-derived features.

For studies using the terms peri-implantitis detection, peri-implantitis diagnosis, or peri-implantitis classification, the reference standard was examined to determine whether peri-implantitis had been defined using radiographic findings alone or a combination of radiographic and clinical parameters. Models based exclusively on radiographic information were interpreted as assessing radiographic manifestations associated with peri-implant disease rather than independently establishing a clinical diagnosis of peri-implantitis.

Because of the heterogeneity of the included studies with respect to imaging modality, AI architecture, dataset characteristics, reference standards, target tasks, and reported performance measures, no quantitative meta-analysis was performed. The findings were therefore synthesized narratively and organized according to the principal radiographic tasks and methodological characteristics of the included models. Performance measures were reported as provided by the original studies and were not pooled across studies when the underlying tasks or reference standards differed.

Methodological and Clinical Appraisal

In addition to descriptive data extraction, the included studies were critically appraised with respect to methodological features that may influence the reliability, generalizability, and clinical interpretation of their findings. The appraisal focused on dataset size and composition, radiographic modality, definition of the target outcome, reference-standard and annotation procedures, data-partitioning strategy, internal and external validation, class distribution, reported performance metrics, and comparison with clinician assessment when available.

Particular attention was paid to the unit of data splitting. When multiple radiographs, implants, image sections, or longitudinal examinations originated from the same patient, the reported training, validation, and test procedures were examined to determine whether partitioning was performed at the patient level or at the image/implant level. The potential for data leakage and overly optimistic performance estimates was considered when independence between training and evaluation datasets could not be established from the reported methodology.

The reference standard used for model development and evaluation was also examined. Studies were assessed according to whether annotations or diagnostic labels were established by one or more clinicians, whether examiner expertise was reported, whether consensus procedures or repeated assessments were used, and whether clinical information was incorporated into the reference standard. Particular caution was applied to studies in which radiographic bone loss or defect morphology alone was labelled as peri-implantitis, because radiographic findings in isolation do not establish the clinical diagnosis of peri-implantitis.

Model validation was categorized according to whether performance was evaluated using an internal test set or an independent external dataset. The presence of clinician comparison, multicenter data, heterogeneous imaging sources, and inclusion of different implant systems was additionally considered when assessing the potential generalizability of each model. Studies relying on single-center datasets, limited implant systems, or internally derived test sets were interpreted cautiously with respect to clinical transferability.

Because the included studies investigated heterogeneous AI tasks and reported different performance measures, model performance was interpreted within the context of the specific task and reference standard used in each study. Accuracy, sensitivity, specificity, precision, recall, F1-score, intersection over union, Dice coefficient, average precision, and other reported metrics were therefore not considered directly interchangeable across studies. High numerical performance was not interpreted as evidence of clinical diagnostic accuracy unless the model outcome and reference standard supported such an interpretation.

The appraisal was used to support the narrative interpretation of the evidence rather than to generate a numerical methodological quality score. No studies were excluded solely on the basis of methodological limitations identified during this appraisal; instead, these limitations were considered when evaluating the strength and clinical applicability of the available evidence. A structured risk-of-bias instrument, such as QUADAS-2 or PROBAST, was not applied, because the included studies addressed heterogeneous AI tasks (localization, measurement, severity classification, and prediction) with correspondingly

different reference standards and validation designs, limiting the applicability of a single standardized tool across all studies. Instead, the domains most relevant to these instruments — reference-standard adequacy, patient-level data partitioning, and validation strategy — were appraised narratively for each study within the context of its specific task.

RESULTS

Study Characteristics

Seventeen original studies met the predefined eligibility criteria and were included in the qualitative synthesis. The included studies were published between 2020 and 2026, reflecting the relatively recent application of artificial intelligence and machine-learning methods to radiographic assessment of peri-implant marginal bone conditions. The studies differed substantially in terms of imaging modality, dataset size, AI architecture, target task, reference standard, and reported performance measures.

Most studies used two-dimensional dental radiographs, particularly periapical radiographs, either alone or in combination with bitewing or panoramic images. For example, Cha et al. evaluated a modified region-based convolutional neural network (R-CNN) on 708 periapical radiographs for detection of the marginal bone level and implant landmarks, subsequent calculation of the peri-implant bone-loss ratio, and classification of bone-resorption severity [4]. Liu et al. used 1,670 periapical radiographs to train and evaluate a Faster R-CNN model for detecting marginal bone loss around dental implants [8]. Vera et al. investigated a combined deep-learning and image-processing approach using 2,920 intraoral periapical and bitewing radiographs to localize implant-related structures and automatically determine peri-implant bone loss [5].

The scope of the included AI applications extended beyond direct marginal bone-loss detection. Some models were developed to identify implants, peri-implant tissues, or radiographic landmarks required for subsequent measurements, whereas others quantified marginal bone levels, classified the severity of radiographic bone loss, characterized peri-implant bone-defect morphology, or distinguished radiographic patterns labelled by the original investigators as peri-implantitis. More recent studies also investigated three-dimensional CBCT-based assessment and prediction of marginal bone loss using imaging-derived features. Consequently, the included studies represented several related but methodologically distinct AI tasks rather than a homogeneous group of diagnostic models.

Convolutional neural networks and related deep-learning architectures predominated among the included studies. The investigated approaches included region-based CNNs, Faster R-CNN, YOLO variants, U-Net-based segmentation, conventional CNN classifiers, and combined object-detection and image-processing pipelines. A smaller subset used conventional machine-learning algorithms applied to quantitative imaging-derived features. This methodological diversity was accompanied by substantial variation in model outputs and evaluation metrics, ranging from landmark localization and segmentation measures to sensitivity, specificity, precision, recall, F1-score, accuracy, and agreement with clinician assessments.

An important source of heterogeneity concerned the definition of the target condition. While some studies explicitly evaluated marginal bone level or marginal bone loss as a radiographic outcome, others described their models as detecting or diagnosing peri-implantitis on radiographs. These studies were retained when their actual AI task fulfilled the eligibility criteria but were interpreted according to the radiographic feature assessed and the reference standard used. Therefore, the use of the term peri-implantitis by the original authors was not considered, by itself, evidence that the model established a clinical diagnosis of peri-implantitis.

The principal characteristics of the 17 included studies, including imaging modality, dataset characteristics, AI approach, radiographic task, reference standard, and principal outcomes are summarized in Table 1, and their methodological and validation features in Table 2.

Table 1: Main characteristics of the studies included in the qualitative synthesis

Study	Imaging modality / dataset	AI approach	Primary radiographic task	Reference standard / annotation	Main reported outcome
Su et al., 2026 [16]	Periapical radiographs; 708 images; 3i and Xive implants	YOLOv8 + custom segmentation + alveolar crest detection + EfficientNet-B3	Implant localization and classification of peri-implant bone-loss severity	Expert/manual radiographic assessment	YOLOv8 precision 99.39%, sensitivity 98.63%; 12-class accuracy 97.42%
Efeoglu et al., 2026 [17]	Panoramic radiographs; 144 patients	Mask R-CNN (ResNet-50) + radiomics/ML	Detection of radiographic peri-implant abnormalities	Regions segmented by two dentomaxillofacial radiology residents; ICC 0.97	Mask R-CNN F1-score 0.84; AUC 0.86
Adnan et al., 2026	Sequential periapical radiographs; 2,960	Six-model DL cascade	Implant/ROI detection and automated MBL	Specialist-established reference standard	MBL model mAP 75.0%, precision 73.0%, recall 69.8%

[18]	retained images		quantification		
Madani et al., 2026 [19]	CBCT; 699 2D sections	YOLOv8	MBL detection and severity grading	Four radiographic classes according to percentage of implant length affected	Accuracy, precision, recall and F1 ≈ 0.90; mAP@0.5 = 0.889
Gao et al., 2025 [20]	Periapical radiographs	YOLOv8-pose	Landmark/keypoint detection, MBL quantification and severity prediction	Radiographic keypoints associated with peri-implant bone loss	Keypoint precision >98%; severity accuracy 0.906 and 0.844 for the two implant sides
Khan et al., 2025 [21]	CBCT; 150 patients, 212 implants	CNN-based system	Implant classification and peri-implant bone-defect/disease detection	Clinical and radiographic assessment validated by two oral radiologists	Sensitivity 91.8%, specificity 93.4%, AUC 0.94
Lee et al., 2025 [12]	Panoramic; 1,075 radiographs, 2,250 implant sites	Ensemble YOLOv8	Bone-defect morphology and severity classification	Expert annotations; comparison with periodontal surgeons	AI overall accuracy 85.33% vs 75.6% mean surgeon accuracy
Kibcak et al., 2025 [22]	Orthopantomographs; 7,696 images	U-Net + CNN	Implant segmentation and radiographic peri-implantitis classification	Clinical identification/assessment by medical professionals	Segmentation DSC 0.986; classification F1-score 0.835
Lee et al., 2024 [10]	Periapical radiographs; 800 images	YOLOv7	Detection and classification of MBL severity	Radiographically defined severity classes	Specificity 100%, precision 100%, recall 94.44%, F1-score 97.10%
Vera et al., 2023 [5]	Periapical and bitewing radiographs; 2,920 images	YOLOv3 + image-processing pipeline	Implant/prosthesis localization, landmark detection and MBL measurement	Dentist-defined reference landmarks	mAP@0.5 varied according to detected structure; automated bone-loss measurements obtained
Chen et al., 2023 [23]	Periapical radiographs	CNN-based system	Implant localization and grading of peri-implant bone damage	Radiographic assessment according to implant thread involvement	Implant localization accuracy 89.31%; damage-grading accuracy 90.45%
Zhang et al., 2023 [24]	529 periapical + 551 panoramic images; 248 patients	Deep CNN/hybrid imaging model	Implant-outcome classification incorporating MBL	Radiographic classification of failure with MBL, failure without MBL, and success	Combined-image accuracy 87%; AUC 0.972 for failure with MBL
Jang et al., 2022 [9]	Periapical radiographs; 300 images	Faster R-CNN with transfer learning	Implant and peri-implant tissue localization	Manually labelled implant/peri-implant tissue regions	Precision 0.977, recall 0.992, F1-score 0.984, mean IoU 0.907
Liu et al., 2022 [8]	Periapical radiographs; 1,670 images	Faster R-CNN	Direct detection of peri-implant MBL	Clinician annotation with expert confirmation	Agreement with expert: κ=0.547 for bone-loss sites and κ=0.568 for implants with bone loss
Cha et al., 2021 [4]	Periapical radiographs; 708 images	Modified region-based CNN	Implant landmark detection, MBL measurement and severity classification	Clinician-defined implant top, apex and marginal bone landmarks	No significant difference between AI and clinician landmark localization; automated bone-loss ratio calculated
Zhang et al., 2020 [25]	CBCT; 81 patients	SVM, ANN, logistic regression and random forest	Prediction of severe MBL from CBCT-derived trabecular features	Severe-MBL versus control classification	Best SVM: AUC 0.967, sensitivity 91.67%, specificity 100%
Mao et al., 2026 [11]	Periapical radiographs; 780 images (1,210 dental implants)	YOLO-based deep learning + image processing	Peri-implant region detection and radiographic bone-loss severity assessment	Radiographic peri-implant bone-loss severity (three grades)	Automated bone-loss severity assessment; performance varied by severity category

Radiographic Modalities and Dataset Characteristics

Two-dimensional dental radiographs represented the predominant imaging source among the included studies. Periapical radiographs were the most frequently investigated modality and were used for implant and peri-implant landmark localization, marginal bone-level measurement, bone-loss detection and quantification, and radiographic severity classification [4,8–11, 16, 18, 20, 23].

Panoramic radiographs were evaluated either independently or in combination with intraoral images. Kibcak et al. used orthopantomographs for implant segmentation and classification of peri-implant conditions [22], whereas Lee et al. investigated

panoramic images for automated classification of peri-implant bone-defect morphology and severity [12]. Efeoglu et al. combined deep-learning-based segmentation with radiomic analysis of panoramic radiographs [17]. Zhang et al. incorporated both periapical and panoramic radiographs into a deep-learning framework for implant-outcome prediction involving marginal bone loss [24]. Vera et al. included both periapical and bitewing radiographs in an automated pipeline for implant-related landmark detection and marginal bone assessment [5].

Three-dimensional imaging was less frequently represented. Madani and Bashizadeh Fakhar applied a YOLOv8-based approach to two-dimensional sections derived from CBCT datasets for detection and grading of peri-implant marginal bone loss [19]. Khan et al. investigated a CNN-based approach using CBCT data for implant classification and peri-implant disease assessment [21]. Zhang et al. used CBCT-derived trabecular microstructural parameters as input variables for machine-learning models designed to predict severe marginal bone loss [25].

Dataset size varied substantially among the included studies. Zhang et al. evaluated CBCT-derived features in 81 patients [25], Jang et al. used 300 periapical radiographs [9], and Cha et al. and Su et al. each evaluated 708 periapical radiographs [4,16]. Liu et al. used 1,670 periapical radiographs [8]. Larger image datasets included 2,920 intraoral radiographs in the study by Vera et al. [5], 2,960 retained periapical images in the study by Adnan et al. [18], and 7,696 orthopantomographs in the study by Kibcak et al. [22]. The unit of analysis also varied across studies, with datasets reported according to patients, implants, radiographs, implant sites, or image sections.

AI Tasks in Peri-Implant Marginal Bone Assessment

The included studies addressed different radiographic tasks, including implant and peri-implant structure localization, landmark detection, marginal bone-level measurement, bone-loss detection and quantification, severity grading, bone-defect classification, and prediction based on imaging-derived features. The studies were therefore grouped according to the principal AI-assisted radiographic task investigated.

Implant, Tissue, and Landmark Localization

Several studies incorporated automated localization or landmark detection either as the primary task or as an initial component of a multi-stage bone-assessment workflow. Jang et al. developed a Faster R-CNN model using 300 periapical radiographs for automated detection of dental implants and peri-implant tissues. The model achieved a precision of 0.977, recall of 0.992, F1-score of 0.984, and mean intersection over union of 0.907 [9]. Cha et al. used a modified region-based CNN to identify the implant top, implant apex, and marginal bone level on periapical radiographs. These landmarks were subsequently used to calculate the ratio of marginal bone loss to implant length. The study reported no significant differences between model- and clinician-derived landmark localization measurements [4]. Vera et al. combined deep learning and image-processing techniques for automatic identification of implants, prosthetic components, and reference landmarks on periapical and bitewing radiographs. The detected landmarks were subsequently used for automated assessment of peri-implant marginal bone changes [5]. Localization was also incorporated into more recent multi-stage approaches. Adnan et al. developed a six-model deep-learning cascade that included image alignment, region-of-interest detection, implant-related structure identification, and subsequent marginal bone-loss estimation from sequential periapical radiographs [18]. Gao et al. used a YOLOv8-pose model for detection of radiographic keypoints required for automated MBL measurement, reporting keypoint-detection precision above 98% [20]. Su et al. combined YOLOv8-based implant localization with segmentation, alveolar crest detection, and subsequent classification of peri-implant bone-loss levels [16].

Marginal Bone-Level Measurement and Bone-Loss Quantification

Several studies investigated automated detection, measurement, or quantification of peri-implant marginal bone loss using two-dimensional radiographic images [4, 5, 8, 18, 20]. Cha et al. developed a region-based CNN approach for peri-implant bone-loss measurement on periapical radiographs. Following identification of the implant top, apex, and marginal bone level, the system calculated marginal bone loss relative to implant length [4]. Vera et al. combined deep learning with image-processing techniques to identify implants, prosthetic structures, and relevant reference points on periapical and bitewing radiographs. These landmarks were subsequently used to determine peri-implant marginal bone-level measurements [5]. Liu et al. evaluated a Faster R-CNN model using 1,670 periapical radiographs for automated detection of marginal bone loss around dental implants. Agreement between the model and expert assessment was reported with κ values of 0.547 for bone-loss sites and 0.568 for implants presenting bone loss [8]. Adnan et al. developed a multi-stage deep-learning cascade for automated marginal bone-loss assessment from sequential periapical radiographs. Following image alignment and localization steps, the MBL component achieved a mean average precision of 75.0%, precision of 73.0%, and recall of 69.8% [18]. Gao et al. applied a YOLOv8-pose architecture to detect key radiographic landmarks and calculate peri-implant marginal bone loss from periapical radiographs. Keypoint-detection precision exceeded 98%, while the subsequent severity assessment achieved accuracies of 0.906 and 0.844 for the two implant sides [20].

Bone-Loss Severity and Defect-Morphology Classification

Several studies applied deep-learning models to classify the severity or morphological characteristics of peri-implant bone loss [10–12, 16, 19, 21–23]. Lee et al. developed a YOLOv7-based model using 800 periapical radiographs for classification of radiographic peri-implant bone-loss severity. The model achieved a specificity and precision of 100%, recall of 94.44%, and F1-score of 97.10% [10]. Because these figures were obtained on a 100-image internal test set, the near-ceiling specificity and precision should be interpreted with caution. Mao et al. combined deep learning and image-processing methods for automated assessment of peri-implant disease severity on periapical radiographs. The workflow included localization of peri-implant regions followed by classification according to predefined radiographic severity categories [11]. Su et al. combined implant localization, alveolar crest detection, segmentation, and classification components for automated assessment of peri-implant marginal bone-loss levels on periapical radiographs. The multiclass classification component achieved an accuracy of 97.42% [16]. Madani and Bashizadeh Fakhar applied YOLOv8 to 699 two-dimensional sections derived from CBCT datasets. Marginal bone loss was classified into four categories according to the proportion of implant length affected. Accuracy, precision, recall, and F1-score were approximately 0.90, with an mAP@0.5 of 0.889 [19]. Lee et al. evaluated an ensemble YOLOv8 model using panoramic radiographs for classification of peri-implant bone-defect morphology and severity. The model achieved an overall accuracy of 85.33%, compared with a mean accuracy of 75.6% among the periodontal surgeons included as comparators [12]. Kibcak et al. combined U-Net-based implant segmentation with CNN-based classification on orthopantomographs. The segmentation model achieved a Dice similarity coefficient of 0.986, whereas the classification component showed a precision of 0.777, recall of 0.903, and F1-score of 0.835 [22]. Khan et al. evaluated a CNN-based approach using CBCT data for dental implant classification and peri-implant disease detection. The reported sensitivity was 91.8%, specificity 93.4%, and AUC 0.94 [21]. Chen et al. used a CNN-based system for implant localization and grading of peri-implant bone damage on periapical radiographs, reporting accuracies of 89.31% for implant localization and 90.45% for grading of peri-implant damage [23].

Prediction Models Using Imaging-Derived Features

A smaller subset of the included studies investigated predictive applications of artificial intelligence using radiographic images or quantitative imaging-derived features rather than direct detection or measurement of marginal bone loss [24, 25]. Zhang et al. developed a deep-learning approach for dental implant outcome prediction using periapical and panoramic radiographs obtained from 248 patients. The dataset included 529 periapical and 551 panoramic images, and implant outcomes were categorized as failure with marginal bone loss, failure without marginal bone loss, or success. Models were developed using periapical and panoramic images separately and in combination. The combined-image approach achieved an overall prediction accuracy of 87%, while an AUC of 0.972 was reported for the classification of implant failure associated with marginal bone loss [24]. In a different predictive approach, Zhang et al. investigated whether trabecular microstructural parameters extracted from CBCT images could predict severe marginal bone loss around mandibular dental implants. The study included 81 patients, comprising 41 cases with severe marginal bone loss and 40 controls. Several machine-learning algorithms were evaluated, including support vector machine, artificial neural network, logistic regression, and random forest models. The support vector machine achieved the highest reported performance, with an AUC of 0.967, sensitivity of 91.67%, and specificity of 100% [25]. Thus, among the included studies, predictive approaches comprised both direct analysis of radiographic images for implant-outcome classification and machine-learning analysis of quantitative features extracted from CBCT datasets [24, 25]. Notably, neither predictive study was prospective or longitudinal: Zhang et al. [24] performed cross-sectional classification of implant outcomes, and Zhang et al. [25] used a 41-versus-40 case–control design, so the reported 100% specificity [25] most plausibly reflects the small, balanced internal sample rather than an ability to forecast future bone loss from a baseline radiograph. This reinforces that progression over time, rather than a single image, is the clinically decisive signal.

Model Performance and Validation Characteristics

The included studies used heterogeneous performance measures according to the specific AI task investigated. Object-detection and localization models were commonly evaluated using precision, recall, F1-score, intersection over union (IoU), and mean average precision (mAP), whereas classification models more frequently reported accuracy, sensitivity, specificity, F1-score, and area under the receiver operating characteristic curve (AUC) [8–12, 16–25]. Studies involving quantitative bone-level assessment additionally reported agreement with expert measurements or comparisons between automated and manually derived values [4, 5, 8, 18, 20].

Validation strategies also varied across studies. Several investigations divided available datasets into training, validation, and/or test subsets. Cha et al. used 508 periapical radiographs for training, 100 for validation, and 100 for testing [4]. Lee et al. divided 800 periapical radiographs into 600 training, 100 validation, and 100 test images [10], whereas Madani and Bashizadeh Fakhar used an 80:10:10 allocation for training, testing, and validation datasets [19]. Kibcak et al. used a 70:15:15 distribution for training, validation, and testing [22].

Other studies used different internal evaluation strategies. Jang et al. allocated 80% of 300 periapical radiographs to training and 20% to testing [9], while Lee et al. used 80% of their panoramic dataset for training and 20% for testing [12]. Vera et al. reported a 50:50 division for the deep-learning component of their image-analysis workflow [5]. Adnan et al. evaluated individual

components of their multi-model cascade and additionally compared automated marginal bone-loss severity scores with specialist-derived reference assessments [18].

Comparison with human observers was incorporated into several studies. Cha et al. compared AI-derived landmark localization with clinician measurements [4], while Lee et al. compared the performance of their AI model for peri-implant bone-defect classification with that of periodontal surgeons [12]. Liu et al. assessed agreement between model predictions and expert interpretation using Cohen's kappa [8].

Reference-standard and annotation procedures differed among the included investigations. Depending on the study, radiographic regions, landmarks, bone-loss measurements, or severity categories were established by dentists, dental specialists, oral and maxillofacial radiologists, periodontal specialists, or combinations of expert assessors [4, 5, 8, 12, 18, 21]. Some studies reported interobserver or agreement measures as part of the reference-standard procedure, whereas others provided more limited information regarding annotation reproducibility.

When these methodological features are tabulated across the 17 included studies (Table 2), several patterns become quantifiable. The reference standard was derived from radiographic information alone in 16 of the 17 studies; only Khan et al. [21] reported incorporating clinical assessment. No study reported independent external validation on a separate dataset, and none explicitly described patient-level data partitioning; where the partition was specified, data were divided at the image or radiograph level. A direct comparison against clinician performance was reported in four studies [4, 8, 12, 18]. Near-ceiling performance on small internal test sets was observed in several reports, including 100% specificity and precision in Lee et al. [10] (100-image test set) and 100% specificity in Zhang et al. [25] (41 cases, 40 controls). These counts substantiate the central caution of this review: with a single exception, current radiograph-based models are trained and evaluated against radiographic reference standards, so their reported performance reflects reproduction of radiographic labels rather than a validated clinical diagnosis of peri-implantitis.

Table 2: Methodological and clinical appraisal of the 17 included studies, derived from the characteristics reported in each primary study.

Study	Reference standard	Data split (unit)	External validation	Clinician comparison	Interpretive flag
Cha et al., 2021 [4]	Radiographic-only	Image-level (508/100/100)	No	Yes	—
Vera et al., 2023 [5]	Radiographic-only	Image-level (50:50)	No	No	—
Liu et al., 2022 [8]	Radiographic-only	NR	No	Yes	Moderate agreement (κ 0.55–0.57)
Jang et al., 2022 [9]	Radiographic-only	Image-level (80/20)	No	No	Near-ceiling F1 0.984
Lee et al., 2024 [10]	Radiographic-only	Image-level (600/100/100)	No	No	100% specificity/precision; test n=100
Mao et al., 2026 [11]	Radiographic-only	NR	No	No	—
Lee et al., 2025 [12]	Radiographic-only	Image-level (80/20)	No	Yes	vs periodontal surgeons
Su et al., 2026 [16]	Radiographic-only	NR	No	No	Near-ceiling precision 99.4%; accuracy 97.4%
Efeoglu et al., 2026 [17]	Radiographic-only	NR	No	No	—
Adnan et al., 2026 [18]	Radiographic-only	NR	No	Yes	vs specialist reference
Madani & Bashizadeh Fakhar, 2026 [19]	Radiographic-only (CBCT 2D sections)	Image-level (80:10:10)	No	No	—
Gao et al., 2025 [20]	Radiographic-only	NR	No	No	—
Khan et al., 2025 [21]	Radiographic + clinical	NR	No	No	Only study incorporating clinical data
Kibcak et al., 2025 [22]	Radiographic-only†	Image-level (70:15:15)	No	No	†label termed clinical but applied to radiographs
Chen et al., 2023 [23]	Radiographic-only	NR	No	No	—
Zhang et al., 2023 [24]	Radiographic-only	NR (248 patients)	No	No	Prediction but cross-sectional
Zhang et al., 2020 [25]	Radiographic-only	NR (81 patients)	No	No	Prediction but case–control; 100% specificity

Entries for external validation and data-partitioning unit reflect what was reported; cells marked NR were not explicitly reported and were not independently verified against the source datasets. RS, reference standard; NR, not reported; κ, Cohen kappa.

DISCUSSION

The present review identified 17 original studies investigating artificial intelligence for radiographic assessment of peri-implant bone conditions. The available evidence demonstrates a rapid expansion of AI applications in this field, particularly during the most recent years, but also reveals substantial heterogeneity in imaging modalities, dataset characteristics, model architectures, target tasks, reference standards, and performance metrics. Most studies relied on two-dimensional radiographs, particularly periapical images, while panoramic radiographs and CBCT-based approaches were less frequently investigated. Importantly, the reviewed models did not address a single diagnostic task. Their applications ranged from implant and landmark localization to marginal bone-level measurement, detection and quantification of bone loss, severity grading, defect-morphology classification, and prediction based on imaging-derived features [4,5,8–12,16–25].

This distinction between AI tasks is clinically important when interpreting the available evidence. Localization models can identify implants, peri-implant tissues, or anatomical landmarks with high technical performance, as demonstrated by Jang et al. [9] and by the localization components incorporated into several multi-stage workflows [4, 5, 16, 18, 20]. Such tasks provide the technical basis for subsequent automated measurements but do not themselves represent disease detection. Similarly, models developed for quantitative assessment provide estimates of marginal bone levels or the extent of bone loss [4,5,8,18,20], whereas classification models assign images to predefined radiographic severity or defect categories [10–12, 16, 19, 21–23]. Consequently, performance values reported for these different tasks should not be interpreted as measures of the same clinical outcome.

A central issue emerging from the reviewed literature is the distinction between radiographically detected marginal bone loss and clinically diagnosed peri-implantitis. According to the 2017 World Workshop, peri-implantitis is a plaque-associated pathological condition characterized by inflammation of the peri-implant mucosa and progressive loss of supporting bone [1]. Diagnostic assessment therefore requires integration of clinical inflammatory findings, probing information, and radiographic bone-level changes rather than radiographic evidence alone [1, 3]. Marginal bone loss identified on an image is consequently an imaging finding whose clinical significance depends on its magnitude, progression, timing, and association with clinical signs of disease. Early crestal remodeling after implant placement and loading must also be distinguished from progressive pathological bone loss.

This distinction is particularly relevant because several studies included in the present review use terms such as peri-implantitis detection, peri-implant disease detection, or peri-implantitis severity for models whose principal input consists of radiographic images [10–12, 21–23]. These studies provide valuable evidence regarding automated recognition of peri-implant bone alterations, but terminology should reflect the actual information available to the algorithm. When a model receives only a radiograph and no information regarding bleeding or suppuration on probing, probing depth, previous bone levels, or other clinical findings, its output is more appropriately interpreted as detection or classification of radiographic features associated with peri-implant bone loss rather than an autonomous clinical diagnosis of peri-implantitis. This distinction is especially important when previous radiographs are unavailable, because a single image cannot establish whether an observed bone level represents stable remodeling or progressive disease [1, 3].

The reported performance of the investigated models was generally promising, although direct numerical comparisons should be approached cautiously. Localization models reported high precision and recall, with Jang et al. achieving an F1-score of 0.984 [9], while several severity-classification systems reported accuracies or F1-scores approaching or exceeding 90% [10, 16, 19, 23]. Lee et al. reported an overall accuracy of 85.33% for AI-based classification of peri-implant bone-defect morphology and severity, compared with a mean accuracy of 75.6% among periodontal surgeons [12]. In contrast, Liu et al. reported only moderate agreement between their Faster R-CNN model and expert assessment, with κ values of 0.547 for bone-loss sites and 0.568 for implants presenting bone loss [8]. Adnan et al. reported a mean average precision of 75.0%, precision of 73.0%, and recall of 69.8% for the marginal bone-loss component of their multi-stage system [18]. These differences illustrate that apparently high performance in one technical task cannot be directly compared with performance obtained using another endpoint or metric.

Heterogeneity in reference standards represents another important consideration. Ground truth across the included studies was established using different approaches, including clinician-defined landmarks, manually annotated bone levels, study-specific severity thresholds, expert radiographic classifications, and, in some cases, combinations of clinical and radiographic findings [4, 5, 8, 12, 18, 21]. The expertise and number of annotators also varied. This is particularly relevant for supervised learning, because model performance is inherently linked to the labels used during training and evaluation. An algorithm trained to reproduce a radiographic severity classification can, at best, reproduce that classification with a certain degree of accuracy; its performance cannot automatically be extrapolated to a broader clinical diagnosis that was not represented in the reference standard.

Dataset characteristics and validation strategies further influence interpretation of the reported results. Dataset sizes ranged from relatively small patient cohorts to collections containing several thousand radiographs [4, 5, 8, 9, 16,18,22,25]. However, the number of images does not necessarily represent the number of statistically independent clinical observations, as individual

patients may contribute multiple implants, bilateral measurements, sequential examinations, or several images. In AI research, the level at which data are separated into training, validation, and test sets is therefore important. If images originating from the same patient or implant are distributed across different subsets, similarities between related observations may contribute to optimistic estimates of model performance. Clear reporting of patient-level data partitioning is consequently desirable in future investigations.

Another limitation of the current evidence is the predominance of internal validation. Most studies developed and evaluated their algorithms within datasets originating from a limited number of institutions, imaging systems, or patient populations [4, 5, 8–12, 16–25]. Models may therefore learn characteristics related not only to peri-implant bone morphology but also to acquisition protocols, image quality, implant design, or dataset-specific patterns. Independent external validation using images acquired in different clinical environments is necessary to establish whether reported performance can be reproduced across populations, radiographic systems, implant brands, and operators. This requirement is particularly relevant for peri-implant imaging because implant geometry, thread design, prosthetic components, image projection, and superimposition can substantially alter radiographic appearance.

The predominance of periapical radiographs among the included studies is clinically understandable because these images are routinely obtained during implant follow-up and provide relatively detailed visualization of mesial and distal marginal bone levels [4,8–11, 16, 18, 20, 23]. Nevertheless, two-dimensional imaging has intrinsic anatomical limitations. Buccal and lingual bone morphology cannot be directly represented, and projection geometry may influence the apparent relationship between the implant and marginal bone. CBCT-based AI approaches may provide additional three-dimensional information [19, 21, 25], but their role should be interpreted within established principles of radiological justification, since CBCT is not indicated as a routine substitute for intraoral radiography solely for peri-implant surveillance.

An especially relevant potential application of AI may therefore be measurement support and longitudinal monitoring rather than autonomous diagnosis. Automated identification of the implant platform, apex, marginal bone contact, and other reference landmarks could reduce the time required for repeated measurements and improve consistency between follow-up examinations [4, 5, 18, 20]. Systems capable of aligning sequential radiographs and quantifying changes over time, such as the approach investigated by Adnan et al. [18], may be particularly valuable because progression of bone loss provides more clinically meaningful information than an isolated radiographic measurement. AI-generated measurements could therefore function as decision-support information to be integrated with probing findings, inflammatory signs, risk factors, and previous examinations.

The present findings are broadly consistent with previous evidence syntheses reporting promising performance of AI methods for peri-implant radiographic analysis [13–15]. However, systematic reviews that aggregate diagnostic-performance estimates face an important conceptual challenge when the underlying studies evaluate different target tasks. Localization, segmentation, marginal bone-level measurement, severity classification, defect-morphology recognition, and prediction are technically and clinically distinct endpoints. Pooling or comparing performance estimates without accounting for these differences may obscure what an algorithm has actually been validated to accomplish. The present review therefore emphasizes task-specific interpretation of the available evidence rather than treating all radiographic AI models as diagnostic systems for peri-implantitis.

A practical consequence of this task-based reading is a figure that pooled-accuracy syntheses [13–15] do not surface: 16 of the 17 studies established their reference standard from radiographic information alone (Table 2), so a single summary estimate of diagnostic accuracy risks describing agreement with radiographic labels rather than detection of clinical disease. The review itself has several limitations. Only PubMed and Scopus were used for the structured database search, and one additional eligible study was identified through supplementary targeted searching. Although the search strategy was designed around AI, dental implants, and peri-implant bone outcomes, relevant studies using different terminology may not have been retrieved. The heterogeneity of the included studies precluded meaningful quantitative pooling and supported a narrative synthesis. Furthermore, differences in study design, imaging modality, reference standards, dataset composition, model architecture, and reported performance measures limited direct comparisons between individual algorithms. The rapidly evolving nature of AI research should also be considered, as recently developed models may not yet have undergone independent replication or external clinical validation.

Future research should prioritize transparent reporting of dataset composition, patient-level separation of training and test data, clearly defined annotation protocols, interobserver agreement where appropriate, and independent external validation. Multicenter datasets incorporating different radiographic systems and implant designs would improve assessment of model generalizability. Longitudinal datasets are particularly important for distinguishing stable peri-implant bone levels from progressive changes. Finally, future systems intended specifically to support peri-implantitis diagnosis should integrate radiographic analysis with relevant clinical variables, including bleeding and/or suppuration on probing, probing depth, previous bone-level measurements, and patient- and implant-level risk information. Such multimodal approaches would more closely correspond to the clinical definition of peri-implantitis than models based solely on radiographic appearance [1, 3].

CONCLUSION

Artificial intelligence shows promising potential for supporting the radiographic assessment of peri-implant marginal bone conditions. Current applications include implant and landmark localization, marginal bone-level measurement and quantification, radiographic severity and defect-morphology classification, and prediction based on imaging-derived features. However, the available evidence remains heterogeneous with respect to imaging modalities, datasets, reference standards, AI architectures, validation strategies, and reported performance metrics.

Importantly, AI performance in detecting or classifying radiographic bone alterations should not be interpreted as equivalent to diagnostic accuracy for peri-implantitis. Marginal bone loss is a radiographic finding, whereas peri-implantitis is a clinical condition whose diagnosis requires integration of inflammatory signs, probing findings, and progressive bone loss [1, 3]. Accordingly, current radiograph-based AI systems are better regarded as tools for image analysis, quantitative assessment, and clinical decision support rather than autonomous diagnostic systems.

Future studies should prioritize standardized outcome definitions, transparent annotation and validation procedures, patient-level data partitioning, independent external validation, and multicenter datasets. Longitudinal and multimodal models integrating radiographic changes with relevant clinical parameters may provide a more appropriate basis for the development of AI-assisted systems for peri-implant disease assessment.

Conflicts of interest and sources of funding

The authors declare no conflict of interest.

This research received no external funding.

Authors' contribution

Conceptualization, A.M.C., V.N. and I.S.; methodology, A.M.C. and E.A.R.; literature search and data curation, A.M.C., E.A.R. and A.T.; formal analysis, A.M.C., V.N. and D.E.; visualization, A.M.C. and E.A.R.; writing—original draft preparation, A.M.C.; writing—review and editing, V.N., I.S., E.A.R., D.E., A.T. and V.D.S.; supervision, V.N., I.S. and V.D.S.; project administration, A.M.C. All authors have read and agreed to the published version of the manuscript.

Ethics approval and consent to participate

Not applicable.

References

1. Berglundh, T.; Armitage, G.; Araujo, M.G.; Avila-Ortiz, G.; Blanco, J.; Camargo, P.M.; Chen, S.; Cochran, D.; Derks, J.; Figuero, E.; et al. Peri-implant diseases and conditions: Consensus report of workgroup 4 of the 2017 World Workshop on the Classification of Periodontal and Peri-Implant Diseases and Conditions. J. Clin. Periodontol. 2018, 45 (Suppl. 20), S286-S291. https://doi.org/10.1111/jcpe.12957.

2. Renvert, S.; Hirooka, H.; Polyzois, I.; Kelekis-Cholakis, A.; Wang, H.L.; Working Group 3. Diagnosis and non-surgical treatment of peri-implant diseases and maintenance care of patients with dental implants—Consensus report of Working Group 3. Int. Dent. J. 2019, 69 (Suppl. 2), 12–17. https://doi.org/10.1111/idj.12490.

3. Herrera, D.; Berglundh, T.; Schwarz, F.; Chapple, I.; Jepsen, S.; Sculean, A.; Kebschull, M.; Papapanou, P.N.; Tonetti, M.S.; Sanz, M.; EFP workshop participants and methodological consultant. Prevention and treatment of peri-implant diseases-The EFP S3 level clinical practice guideline. J. Clin. Periodontol. 2023, 50 (Suppl. 26), 4-76. https://doi.org/10.1111/jcpe.13823.

4. Cha, J.Y.; Yoon, H.I.; Yeo, I.S.; Huh, K.H.; Han, J.S. Peri-implant bone loss measurement using a region-based convolutional neural network on dental periapical radiographs. J. Clin. Med. 2021, 10, 1009. https://doi.org/10.3390/jcm10051009.

5. Vera, M.; Gómez-Silva, M.J.; Vera, V.; López-González, C.I.; Aliaga, I.; Gascó, E.; Vera-González, V.; Pedrera-Canal, M.; Besada-Portas, E.; Pajares, G. Artificial intelligence techniques for automatic detection of peri-implant marginal bone remodeling in intraoral radiographs. J. Digit. Imaging 2023, 36, 2259-2277. https://doi.org/10.1007/s10278-023-00880-3.

6. Hung, K.F.; Ai, Q.Y.H.; Leung, Y.Y.; Yeung, A.W.K. Potential and impact of artificial intelligence algorithms in dento-maxillofacial radiology. Clin. Oral Investig. 2022, 26, 5535-5555. https://doi.org/10.1007/s00784-022-04477-y.

7. Farajollahi, M.; Safarian, M.S.; Hatami, M.; Esmaeil Nejad, A.; Peters, O.A. Applying artificial intelligence to detect and analyse oral and maxillofacial bone loss: A scoping review. Aust. Endod. J. 2023, 49, 720-734. https://doi.org/10.1111/aej.12775.

8. Liu, M.; Wang, S.; Chen, H.; Liu, Y. A pilot study of a deep learning approach to detect marginal bone loss around implants. BMC Oral Health 2022, 22, 11. https://doi.org/10.1186/s12903-021-02035-8.

9. Jang, W.S.; Kim, S.; Yun, P.S.; Jang, H.S.; Seong, Y.W.; Yang, H.S.; Chang, J.S. Accurate detection for dental implant and peri-implant tissue by transfer learning of Faster R-CNN: A diagnostic accuracy study. BMC Oral Health 2022, 22, 591. https://doi.org/10.1186/s12903-022-02539-x.

10. Lee, W.F.; Day, M.Y.; Fang, C.Y.; Nataraj, V.; Wen, S.C.; Chang, W.J.; Teng, N.C. Establishing a novel deep learning model for detecting peri-implantitis. J. Dent. Sci. 2024, 19, 1165-1173. https://doi.org/10.1016/j.jds.2023.11.017.

11. Mao, Y.C.; Chen, C.A.; Lin, Y.J.; Chang, Y.J.; Wei, S.T.; Chen, S.L.; Chen, T.Y.; Li, K.C.; Tu, W.C.; Abu, P.A.R. Automated assessment of peri-implant disease severity by deep learning and image processing in periapical radiographs. J. Dent. Sci. 2026, 21, 963-972. https://doi.org/10.1016/j.jds.2025.08.015.

12. Lee, J.H.; Kim, Y.T.; Schwendicke, F. Performance of artificial intelligence-based diagnosis and classification of peri-implantitis compared with

periodontal surgeon assessment: A pilot study of panoramic radiograph analysis. J. Periodontal Implant Sci. 2025, 55, 436-446. https://doi.org/10.5051/jpis.2500280014.

13. Bonfanti-Gris, M.; Ruales, E.; Salido, M.P.; Martinez-Rus, F.; Özcan, M.; Pradies, G. Artificial intelligence for dental implant classification and peri-implant pathology identification in 2D radiographs: A systematic review. J. Dent. 2025, 153, 105533. https://doi.org/10.1016/j.jdent.2024.105533.

14. Mugri, M.H. Accuracy of artificial intelligence models in detecting peri-implant bone loss: A systematic review. Diagnostics 2025, 15, 655. https://doi.org/10.3390/diagnostics15060655.

15. Atieh, M.A.; Shah, M.; Hakam, A.; AlAli, F.; AlSayed, S.; Tawse-Smith, A.; Alsabeeha, N.H.M. Diagnostic accuracy of deep learning models in detecting peri-implant marginal bone loss: A systematic review and meta-analysis. Clin. Oral Implants Res. 2026, 37, 385-401. https://doi.org/10.1111/clr.70090.

16. Su, Y.S.; Chen, C.A.; Chang, L.H.; Su, H.K.; Sung, C.Y.; Lin, Y.J.; Chen, S.L. Automated detection of marginal bone loss levels in implant brands using deep learning on periapical radiographs. J. Formos. Med. Assoc. 2026, ahead of print. https://doi.org/10.1016/j.jfma.2026.06.011.

17. Efeoglu, S.; Karahan, E.; Gokdeniz, S.T.; Incebeyaz, B.; Gonuldas, F.; Aksoy, S.; et al. Radiomics analysis of panoramic radiographs using machine learning for the detection of peri-implantitis. BMC Oral Health 2026, 26, 964. https://doi.org/10.1186/s12903-026-08190-0.

18. Adnan, N.; Ahmed, S.M.F.; Nooruddin, A.; Sadiq, A.; Khalid, A.; Haseeb, M.; Ghori, M.H.; Umer, F. A web-based deep learning cascade for automated detection and quantification of marginal bone loss. BMC Oral Health 2026, 26, 590. https://doi.org/10.1186/s12903-026-07962-y.

19. Madani, Z.; Bashizadeh Fakhar, H. Detection and classification of peri-implant marginal bone loss in cone-beam computed tomography using a deep learning approach. Clin. Exp. Dent. Res. 2026, 12, e70308. https://doi.org/10.1002/cre2.70308.

20. Gao, T.; Tan, R.; Tian, S.K.; Chen, H.; Wang, H.R.; Xu, J.G. An auxiliary measurement method for marginal bone loss around dental implants based on periapical radiographs. Chin. J. Dent. Res. 2025, 28, 261–276. https://doi.org/10.3290/j.cjdr.b6745502.

21. Khan, G.S.; Aaliyah, S.; Pal, S.; Tiwari, R.; M, S.; Dixit, H.; M C, P.; Ali, T. Artificial intelligence for dental implant classification and peri-implant disease detection: A clinical study. Bioinformation 2025, 21, 2361–2364. https://doi.org/10.6026/973206300212361.

22. Kibcak, E.; Buhara, O.; Temelci, A.; Akkaya, N.; Ünsal, G.; Minervini, G. Deep learning-driven segmentation of dental implants and peri-implantitis detection in orthopantomographs: A novel diagnostic tool. J. Evid. Based Dent. Pract. 2025, 25, 102058. https://doi.org/10.1016/j.jebdp.2024.102058.

23. Chen, Y.C.; Chen, M.Y.; Chen, T.Y.; Chan, M.L.; Huang, Y.Y.; Liu, Y.L.; Lee, P.T.; Lin, G.J.; Li, T.F.; Chen, C.A.; et al. Improving dental implant outcomes: CNN-based system accurately measures degree of peri-implantitis damage on periapical film. Bioengineering 2023, 10, 640. https://doi.org/10.3390/bioengineering10060640.

24. Zhang, C.; Fan, L.; Zhang, S.; Zhao, J.; Gu, Y. Deep learning based dental implant failure prediction from periapical and panoramic films. Quant. Imaging Med. Surg. 2023, 13, 935–945. https://doi.org/10.21037/qims-22-457.

25. Zhang, H.; Shan, J.; Zhang, P.; Chen, X.; Jiang, H. Trabeculae microstructure parameters serve as effective predictors for marginal bone loss of dental implant in the mandible. Sci. Rep. 2020, 10, 18437. https://doi.org/10.1038/s41598-020-75563-y.

https://doi.org/10.55453/rjmm.2026.129.6.4

Original Article

Association of [18F]FDG PET/CT radiomic features with Ki-67 in untreated primary breast carcinoma

Alexandru Mitoi[1], Raluca-Mihaela Mititelu[2,3,*], Cosmin Medar[4,5,*], Vlad-Octavian Bolocan[4], Ciprian Constantin[6], Ioan-Nicolae Mateș[7]

[1] Doctoral Program Studies, Carol Davila University of Medicine and Pharmacy, 050474 Bucharest, Romania; alexandru.mitoi@drd.umfcd.ro, https://orcid.org/0009-0008-4491-0491
[2] Department of Nuclear Medicine, Carol Davila University of Medicine and Pharmacy, 010825 Bucharest, Romania; raluca.mititelu@umfcd.ro, https://orcid.org/0000-0002-5398-3210;
[3] Clinic of Nuclear Medicine, Dr. Carol Davila Central Military Emergency University Hospital, 010825 Bucharest, Romania
[4] Department of Fundamental Sciences, Faculty of Midwifery and Nursing, Carol Davila University of Medicine and Pharmacy, 050474 Bucharest, Romania; cosmin.medar@umfcd.ro, https://orcid.org/0000-0001-8341-1769; and vlad-octavian.bolocan@drd.umfcd.ro;
[5] Clinical Laboratory of Radiology and Medical Imaging, Clinical Hospital "Prof. Dr. Theodor Burghele", 050664 Bucharest, Romania
[6] Department of Diabetes and Nutrition, Faculty of Medicine, Titu Maiorescu University, Bucharest, Romania; ciprian_constantin@yahoo.com, https://orcid.org/0000-0003-3355-5048;
[7] General and Esophageal Surgery Clinic, "Sfanta Maria" Clinical Hospital, Carol Davila University of Medicine and Pharmacy, 020021 Bucharest, Romania; ioan.mates@umfcd.ro, https://orcid.org/0000-0001-7210-0615;
* Correspondence: RMM, raluca.mititelu@umfcd.ro; CM, cosmin.medar@umfcd.ro

Abstract: Whether [18F]FDG PET/CT radiomic features provide information on tumor proliferation beyond conventional PET parameters remains uncertain. We investigated their associations with Ki-67 in untreated primary breast carcinoma using a predefined panel of technically reproducible features. This retrospective, single-center study included 42 women and 19 radiomic features previously selected based on interobserver reproducibility and redundancy, independently of Ki-67. Associations with continuous Ki-67 were evaluated using Spearman correlations, permutation tests, bootstrap confidence intervals, and false discovery rate (FDR) correction, alongside four conventional PET parameters. Five radiomic features showed significant associations with Ki-67 after FDR correction. The strongest association was observed for firstorder_90Percentile (ρ = 0.556; 95% CI, 0.279–0.745; q = 0.002), comparable to that of SUVmax (ρ = 0.565). However, none of these five associations remained significant after adjustment for metabolic tumor volume (MTV), SUVmax, or both, followed by FDR correction. Excluding six small lesions attenuated the correlations for both SUVmax (ρ = 0.440) and firstorder_90Percentile (ρ = 0.427). Although several radiomic features were associated with Ki-67, an independent contribution beyond conventional PET parameters was not demonstrated. These findings require confirmation in independent cohorts.

Keywords: [18F]FDG; PET/CT; breast carcinoma; radiomics; Ki-67; tumor proliferation; feature stability.

INTRODUCTION

Ki-67 indicates tumor proliferative activity and, in breast carcinoma, is interpreted alongside histological grade, hormone receptor (HR) status, HER2 status, and other clinicopathological data. Higher Ki-67 levels are associated with more aggressive tumors and may contribute to prognostic assessment and characterization of the tumor phenotype, particularly in hormone receptor-positive, HER2-negative cancers [1]. Tumor size and estrogen receptor status have also been investigated as correlates of additional axillary nodal involvement in patients with a positive sentinel lymph node [2].

Ki-67 is affected by preanalytical variability, intratumoral heterogeneity, cutoff selection, and interobserver and interlaboratory variability. The International Ki67 in

Citation: Mitoi A, Mititelu RM, Medar C, Bolocan VO, Constantin C, Mateș IN. *Association of [18F]FDG PET/CT radiomic features with Ki-67 in untreated primary breast carcinoma.* R. J. Mil. Med. 2026, CXXIX(6): 624-635. https://doi.org/10.55453/rjmm.2026.129.6.4

Academic Editor: Octavian Vasiliu

Received: 11 October 2026
Revised: 29 October 2026
Accepted: 01 November 2026

Breast Cancer Working Group recommends standardized assessment and cautious interpretation, particularly for intermediate values [1].

Hybrid [18F]FDG PET/CT imaging assesses tumor metabolism and contributes to breast cancer staging. Its sensitivity and specificity vary with tumor size; in subcentimeter lesions, sensitivity is below 50% because of limited spatial resolution [3,4]. Safety considerations related to radiopharmaceuticals in nuclear medicine have also been reviewed [5].

Prior studies link FDG uptake with proliferation. A meta-analysis of 32 PET studies in breast cancer, including 25 using [18F]FDG, identified a moderate positive association between SUVmax and Ki-67 in the FDG subgroup [6]. Another meta-analysis confirmed that [18F]FDG uptake varies with hormone receptor expression, HER2 status, Ki-67, and tumor subtype [7].

Radiomics is an advanced method of medical image analysis that converts images into quantitative data intended to characterize the tumor phenotype and underlying pathophysiological processes [8,9]. Radiomic descriptors include tumor intensity, shape, volume, and heterogeneity, with potential diagnostic and predictive applications [10]. [18F]FDG PET/CT radiomics has been investigated in relation to histopathological features, treatment response, hormone receptor status, and Ki-67 [11–13]. Interpretation of these features requires comparison with conventional PET parameters: maximum and mean standardized uptake values (SUVmax and SUVmean), metabolic tumor volume (MTV), and total lesion glycolysis (TLG).

Soussan et al. [14], Groheux et al. [15], and Lemarignier et al. [16] evaluated relationships between PET texture and histopathological or immunohistochemical characteristics, with variable findings and an important contribution of tumor volume. Moscoso et al. [17] reported associations on dedicated breast PET images, whereas Aide et al. [18] demonstrated the influence of reconstruction on tumor characterization. Other approaches, such as the pilot study by Li et al., integrated radiomic and clinical features to predict Ki-67 [19].

The literature shows substantial variation in methods for feature filtering and dimensionality reduction. Some studies include reproducibility-based filtering [20], univariate filtering, removal of correlated variables, or penalized selection within the same cohort in which the clinical endpoint is analyzed [12,13,19].

These filtering strategies are subsequently used to develop radiomic models, but the results depend on the selection process and characteristics of the study cohort. Radiomic feature values also vary with segmentation, reconstruction, voxel size, and intensity discretization, making reproducibility assessment necessary before biological interpretation. To standardize reporting, the Image Biomarker Standardization Initiative (IBSI) provides standardized definitions of radiomic features [21], while the CLEAR guideline recommends explicit reporting of the radiomics workflow and the sequence of feature selection steps [22].

A systematic review of the literature suggests considerable variation in the intraclass correlation coefficient thresholds used to define stable features [23]. Technical stability is therefore necessary for subsequent biological analysis, but does not establish biological relevance [24].

In our previous study of the same cohort of 42 women, we assessed the interobserver reproducibility of 107 original radiomic features extracted from [18F]FDG PET/CT images. Ninety features had an intraclass correlation coefficient of at least 0.75. Subsequent removal of redundancy based on Spearman correlations reduced this set to 19 features that met the technical selection criteria [20].

The present study aimed to evaluate the association between this set of 19 radiomic features and Ki-67 in untreated primary breast carcinoma, in the context of conventional PET parameters. Ki-67 was analyzed as a continuous variable in the primary analysis and using a 30% cutoff in a secondary comparison. This study is a secondary analysis of the previously published cohort [20].

MATERIALS AND METHODS

This retrospective, single-center observational study included the same cohort of patients as the previous interobserver reproducibility study [20]. Patients underwent PET/CT at the Dr. Carol Davila Central Military Emergency University Hospital, Bucharest, Romania, between 1 January 2022 and 15 March 2026. The initial cohort comprised 52 women with biopsy-confirmed primary breast carcinoma. Availability of both Ki-67 and histological grade was required when the original cohort was assembled to provide complete clinicopathological data for subsequent analyses. Ten women were excluded because of incomplete clinicopathological data: six lacked Ki-67 only, one lacked histological grade only, and three lacked both. The resulting cohort of 42 women was retained for the present secondary analysis (Figure 1). Feature selection was based exclusively on reproducibility and redundancy, independently of Ki-67 values [20].

The inclusion criteria were biopsy-confirmed primary breast carcinoma, a primary breast lesion visible on [18F]FDG PET/CT, and PET/CT performed before surgery, systemic therapy, or radiotherapy. Patients were excluded if they had received endocrine therapy or chemotherapy before PET/CT, if the lesion had previously been operated on (other than biopsy), if the primary tumor could not be delineated on PET/CT, or if image quality was inadequate. One lesion was analyzed per patient. In multifocal or

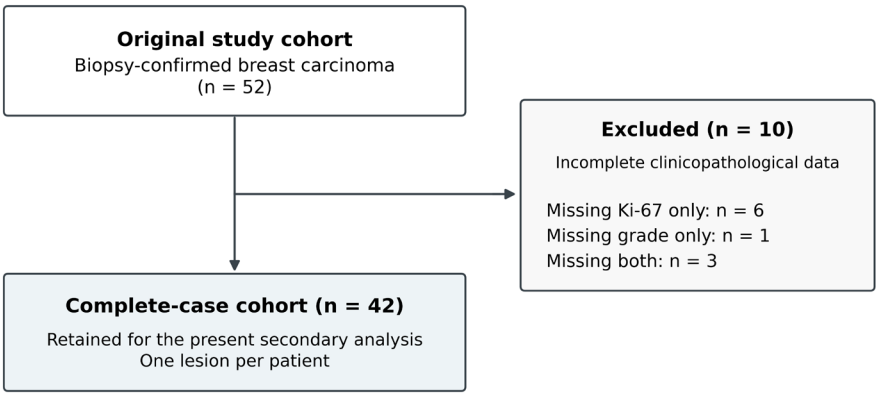
multicentric disease, the dominant lesion was defined as the largest lesion and/or the lesion with the highest FDG uptake. Confluent foci without a clear boundary were segmented as a single lesion complex. In the single case of bilateral lesions, the metabolically dominant lesion was selected [20].

Ki-67 was obtained from the biopsy pathology report and recorded as a percentage. Hormone receptor and HER2 status were obtained from the same reports.

A Ki-67 cutoff of 30% was used for an exploratory secondary comparison between groups with higher (≥30%) and lower proliferation (<30%). This cutoff is consistent with the recommendations of the International Ki67 in Breast Cancer Working Group, which supports the prognostic use of extreme values (≤5% and ≥30%) in specific clinical contexts [1]. The cutoff was not used in radiomic feature selection.

Informed consent was obtained from all participants. The study was approved by the Local Ethics Committee (approval no. 763) and conducted in accordance with the Declaration of Helsinki. PET/CT examinations were performed as part of routine clinical care. The analysis retrospectively used data from the previously published cohort [20].

Figure 1: Patient selection for the analysis



PET/CT acquisition, segmentation, and radiomic features

All patients were imaged on the same PET/CT scanner, a Discovery MI Digital Ready PET/CT system (GE HealthCare, Waukesha, WI, USA), using the same imaging and preparation protocol. Patients were instructed to follow a low-carbohydrate diet for 24 h and to fast for at least 6 h, with water permitted. Capillary blood glucose was measured before radiotracer administration; the maximum accepted value was 200 mg/dL. [18F]FDG was administered at 2.5 MBq/kg. Image acquisition began 60 ± 10 min after injection, with patients supine and their arms raised above the head, using a whole-body acquisition protocol from the vertex or tentorium to the upper third of the thighs. PET reconstruction used ordered-subset expectation maximization (OSEM) with GE VUE Point FX and SharpIR, including time-of-flight (TOF) and point-spread-function modeling, a 256 × 256 matrix, and native voxel dimensions of 2.734 × 2.734 × 3.269 mm. Intensities expressed in Bq/mL were converted to body-weight-normalized SUV, as described in the previous article [20].

Breast lesions were independently segmented by two nuclear medicine physicians [20] using 3D Slicer version 5.10.0 (Slicer Community, Boston, MA, USA) [25]. An initial mask was generated using automatic Otsu thresholding [26], applied to the PET volume without a preselected local region. The mask was then manually corrected using the attenuation-corrected CT as an anatomical reference [20]. Regional lymph nodes, physiological uptake, and uptake outside the lesion were excluded. The observers were blinded to each other's segmentation and to the histopathological and immunohistochemical findings [20].

Radiomic features were extracted using PyRadiomics version 3.1.0 (AIM-Harvard, Boston, MA, USA) [27], with original images, a fixed discretization bin width of 0.25 SUV, and the native PET grid. This was the reference configuration in the previous study. No wavelet or Laplacian-of-Gaussian filters were applied, and no isotropic resampling was performed. Feature definitions follow the PyRadiomics implementation, which differs from the IBSI reference standard in documented respects [21,28].

For the PET analysis, SUVmax and SUVmean represented the maximum and mean uptake within the lesion, normalized to body weight. MTV was calculated from the manually corrected Otsu mask aligned to the PET grid, and TLG was calculated as SUVmean × MTV for each observer before averaging. The descriptive volume in Table 1 was derived from the original masks, as in the previous article [20].

Our previous analysis yielded a final panel of 19 radiomic features selected on technical grounds, based on interobserver reproducibility and redundancy reduction [20]. This predefined panel was used unchanged in the present study; no feature was added or removed on the basis of its relationship with Ki-67.

The redundancy filter included radiomic features only.

Statistical analysis

Analyses used the mean of the two observers' measurements for each patient. Continuous variables were summarized as the median, interquartile range, and minimum–maximum range. Spearman correlation was used to assess the associations of continuous Ki-67 with the 19 radiomic features and with SUVmax, SUVmean, MTV, and TLG, as well as the relationships between radiomic features and conventional parameters. Two-sided p-values were estimated using 99,999 permutations, and 95% confidence intervals (CIs) were obtained from 2000 patient-level bootstrap samples. Benjamini–Hochberg false discovery rate (FDR) correction was applied separately to the 19 radiomic tests and the four conventional tests, with $q < 0.05$ indicating statistical significance.

Sensitivity analyses included rank-based partial correlations adjusted for MTV, SUVmax, or both, and repetition of the continuous analysis after exclusion of lesions with a mean native voxel count across observers <100, corresponding to approximately 2.44 cm^3 on the native PET grid. The continuous analysis was also repeated separately for each observer. In the secondary comparison of Ki-67 ≥30% versus <30%, effect size was expressed as the rank-biserial correlation (RBC), derived from the Mann–Whitney U statistic. Two-sided p values were estimated by permuting group membership while preserving group sizes. CIs were obtained by non-stratified patient-level bootstrap resampling. Sensitivity and binary analyses were exploratory. FDR correction was applied within each analysis and observer, retaining the families of 19 radiomic tests and four conventional tests. Analyses were performed in Python 3.12.14.

RESULTS

1. Cohort and predefined feature set

The final cohort included 42 patients. The median age was 68 years (interquartile range, 50.5–73.5; range, 36–84), the median maximum tumor diameter was 25 mm (16–38; 8–100), and the median segmented tumor volume, averaged across the two observers, was 10.629 cm^3 (5.111–23.287; 0.793–220.073).

The median Ki-67 value was 35% (15–57.5; 2–80); 22 patients had Ki-67 ≥30% and 20 had Ki-67 <30%. Tumor grade was G1 in 5 patients, G2 in 27, and G3 in 10. Hormone receptors were positive in 36 patients, HER2 was positive in 8, and invasive carcinoma of no special type was present in 37 (Table 1).

Table 1: Cohort characteristics.

Characteristic	Value
Sex	Female, 42 (100%)
Age, years	68 (50.5–73.5; 36–84)
Maximum tumor diameter, mm	25 (16–38; 8–100)
Segmented tumor volume, mean across observers, cm^3	10.629 (5.111–23.287; 0.793–220.073)
Lesions with mean native voxels <100	6 (14.3%)
Ki-67, %	35 (15–57.5; 2–80)
Ki-67 ≥30%	22 (52.4%)
Tumor grade, G1/G2/G3	5 / 27 / 10
ER-positive	35 (83.3%)
PR-positive	28 (66.7%)
Hormone receptor-positive	36 (85.7%)
HER2-positive	8 (19.0%)
Invasive carcinoma of no special type	37 (88.1%)

Continuous variables are reported as median (interquartile range; range), and categorical variables as number (percentage). The segmented volume was measured from the original masks and averaged across observers, as in the previous study [20].

2. Associations with Ki-67 as a continuous variable

Of the 19 predefined features, five correlated with continuous Ki-67 after FDR correction (Table 2 and Figure 2). The remaining 14 features did not meet the q < 0.05 criterion.

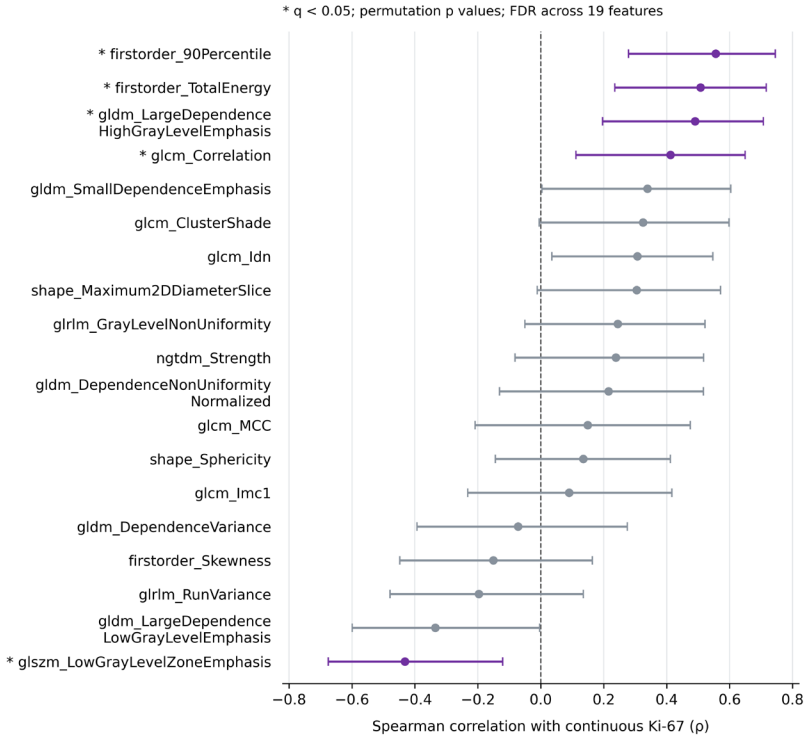
firstorder_90Percentile showed the strongest positive association. Positive correlations were also observed for firstorder_TotalEnergy, gldm_LargeDependenceHighGrayLevelEmphasis, and glcm_Correlation. glszm_LowGrayLevelZoneEmphasis correlated inversely with Ki-67.

Table 2: Associations of the five significant radiomic features and four conventional PET parameters with continuous Ki-67.

Feature / parameter	Spearman ρ	95% CI	p	q
firstorder_90Percentile	0.556	[0.279; 0.745]	<0.001	0.002
firstorder_TotalEnergy	0.507	[0.236; 0.717]	<0.001	0.007
gldm_LargeDependenceHighGrayLevelEmphasis	0.490	[0.196; 0.707]	0.001	0.008
glszm_LowGrayLevelZoneEmphasis	−0.432	[−0.675; −0.121]	0.005	0.022
glcm_Correlation	0.412	[0.112; 0.649]	0.007	0.026
SUVmax	0.565	[0.302; 0.750]	<0.001	<0.001
SUVmean	0.562	[0.310; 0.754]	<0.001	<0.001
MTV	0.442	[0.160; 0.662]	0.004	0.004
TLG	0.479	[0.198; 0.690]	0.002	0.002

CI: 95% bootstrap confidence interval, unadjusted for multiple testing. p values were obtained from two-sided permutation tests. FDR correction was applied separately to the 19 radiomic features and the four PET parameters.

Figure 2: Associations between the 19 predefined radiomic features and continuous Ki-67.



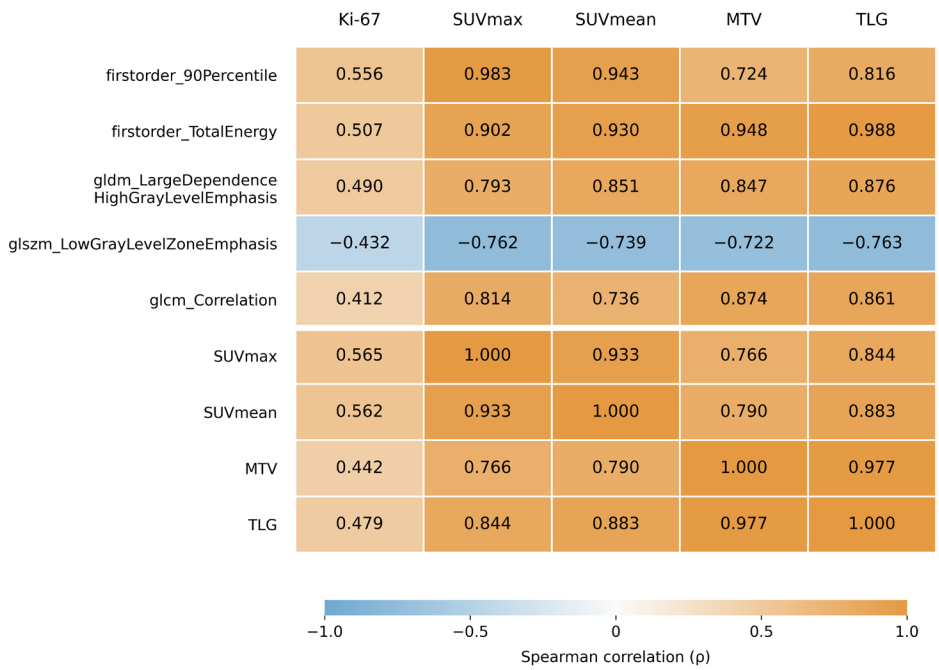
Points represent Spearman correlation coefficients (ρ), and horizontal bars indicate 95% bootstrap CIs, unadjusted for multiple testing. The dashed line marks ρ = 0. An asterisk (*) and purple coloring indicate q < 0.05 after Benjamini–Hochberg correction for the 19 tests. Statistical significance is defined by q, not by whether an individual CI excludes zero.

3. Conventional PET parameters and secondary comparison

All four conventional PET parameters correlated positively with continuous Ki-67, with associations remaining significant after FDR correction (Table 2). SUVmax and SUVmean had the highest Spearman coefficients, at 0.565 and 0.562, respectively.

The radiomic features associated with Ki-67 also correlated with conventional PET parameters (Figure 3). firstorder_90Percentile correlated with SUVmax at ρ = 0.983 and with SUVmean at ρ = 0.943, whereas firstorder_TotalEnergy correlated with MTV at ρ = 0.948 and with TLG at ρ = 0.988. The SUVmax–MTV correlation was ρ = 0.766.

Figure 3: Spearman correlations of the five radiomic features significant in the primary continuous Ki-67 analysis and the four conventional PET parameters.



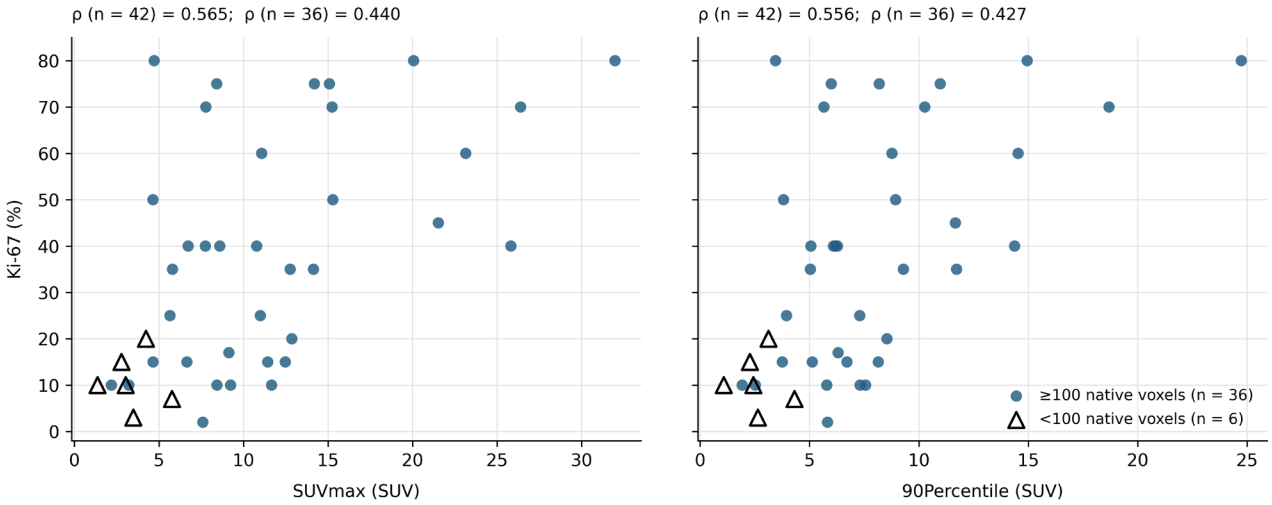
Columns show Ki-67 and the conventional PET parameters. Rows show the five selected radiomic features followed by SUVmax, SUVmean, MTV, and TLG. Cell values are Spearman correlation coefficients (ρ).

In the secondary comparison of Ki-67 ≥30% versus <30%, six radiomic features met the FDR criterion, four of which were also significant in the continuous analysis. All four conventional PET parameters differed between groups after FDR correction.

4. Sensitivity analyses

None of the five features associated with continuous Ki-67 remained significant after adjustment for MTV, SUVmax, or both and FDR correction (Table 3). Across the full 19-feature panel, shape_Sphericity met the FDR criterion only after adjustment for MTV (partial ρ = 0.481; 95% CI, 0.176–0.719; q = 0.030), but not in the unadjusted analysis or after adjustment for SUVmax or both. Exclusion of the six lesions with a mean native voxel count <100 reduced the sample to 36 patients, including 22 with Ki-67 ≥30% and 14 with Ki-67 <30%. All six excluded lesions belonged to the Ki-67 <30% group. The coefficients decreased similarly for SUVmax (ρ = 0.440) and firstorder_90Percentile (ρ = 0.427). No radiomic feature met the FDR criterion in this subset (Figure 4). In the observer-specific continuous analyses, four of the five main associations remained significant for both observers.

Figure 4: Relationships of Ki-67 with SUVmax and firstorder_90Percentile.



Triangles represent the six lesions with a mean native voxel count <100. Circles represent the remaining 36 lesions. Coefficients were calculated separately for the full cohort (n = 42) and the subset excluding small lesions (n = 36).

Table 3: Rank-based partial correlations between radiomic features and Ki-67 after adjustment for MTV, SUVmax, or both (n = 42).

Feature	Adjusted for MTV	Adjusted for SUVmax	Adjusted for MTV + SUVmax
firstorder_TotalEnergy	0.310 [−0.013; 0.594] p = 0.047; q = 0.230	−0.007 [−0.271; 0.321] p = 0.967; q = 0.992	−0.058 [−0.347; 0.382] p = 0.722; q = 0.914
firstorder_90Percentile	0.382 [0.064; 0.631] p = 0.013; q = 0.126	0.003 [−0.318; 0.375] p = 0.987; q = 0.992	0.007 [−0.312; 0.379] p = 0.966; q = 0.980
glcm_ClusterShade	0.185 [−0.164; 0.504] p = 0.247; q = 0.445	−0.100 [−0.355; 0.271] p = 0.532; q = 0.843	−0.100 [−0.359; 0.279] p = 0.541; q = 0.808
glrlm_GrayLevelNonUniformity	−0.253 [−0.543; 0.158] p = 0.109; q = 0.399	0.048 [−0.236; 0.344] p = 0.767; q = 0.992	0.086 [−0.309; 0.411] p = 0.595; q = 0.808
ngtdm_Strength	0.200 [−0.125; 0.497] p = 0.208; q = 0.445	−0.215 [−0.457; 0.077] p = 0.177; q = 0.820	−0.310 [−0.536; 0.060] p = 0.051; q = 0.334
shape_Maximum2DDiameterSlice	−0.310 [−0.547; 0.013] p = 0.048; q = 0.230	−0.105 [−0.375; 0.194] p = 0.514; q = 0.843	−0.247 [−0.500; 0.046] p = 0.127; q = 0.481
glcm_Imc1	−0.141 [−0.445; 0.209] p = 0.378; q = 0.599	0.175 [−0.128; 0.466] p = 0.271; q = 0.820	0.289 [−0.065; 0.549] p = 0.070; q = 0.334
shape_Sphericity	0.481 [0.176; 0.719] p = 0.002; q = 0.030	0.226 [−0.062; 0.510] p = 0.155; q = 0.820	0.339 [0.035; 0.618] p = 0.031; q = 0.334
glcm_Idn	−0.084 [−0.368; 0.235] p = 0.603; q = 0.674	0.028 [−0.242; 0.320] p = 0.861; q = 0.992	0.024 [−0.299; 0.321] p = 0.885; q = 0.980
glcm_Correlation	0.060 [−0.313; 0.427] p = 0.708; q = 0.708	−0.100 [−0.311; 0.184] p = 0.532; q = 0.843	−0.150 [−0.409; 0.181] p = 0.356; q = 0.615
gldm_DependenceVariance	−0.086 [−0.391; 0.245] p = 0.589; q = 0.674	0.150 [−0.167; 0.418] p = 0.348; q = 0.820	0.159 [−0.133; 0.408] p = 0.326; q = 0.615

Feature	Adjusted for MTV	Adjusted for SUVmax	Adjusted for MTV + SUVmax
gldm_SmallDependenceEmphasis	0.195 [−0.140; 0.504] p = 0.219; q = 0.445	−0.257 [−0.523; 0.093] p = 0.105; q = 0.820	−0.307 [−0.570; 0.119] p = 0.054; q = 0.334
glszm_LowGrayLevelZoneEmphasis	−0.181 [−0.493; 0.184] p = 0.257; q = 0.445	−0.002 [−0.327; 0.348] p = 0.992; q = 0.992	0.004 [−0.348; 0.408] p = 0.980; q = 0.980
gldm_LargeDependenceLowGrayLevel Emphasis	−0.133 [−0.469; 0.241] p = 0.410; q = 0.599	−0.017 [−0.359; 0.310] p = 0.914; q = 0.992	−0.015 [−0.367; 0.334] p = 0.928; q = 0.980
gldm_LargeDependenceHighGrayLevel Emphasis	0.244 [−0.110; 0.544] p = 0.126; q = 0.399	0.084 [−0.212; 0.371] p = 0.602; q = 0.880	0.093 [−0.273; 0.426] p = 0.568; q = 0.808
gldm_DependenceNonUniformityNormalized	0.197 [−0.136; 0.484] p = 0.215; q = 0.445	−0.138 [−0.415; 0.191] p = 0.389; q = 0.820	−0.163 [−0.421; 0.206] p = 0.313; q = 0.615
glcm_MCC	0.069 [−0.268; 0.394] p = 0.665; q = 0.702	−0.197 [−0.482; 0.137] p = 0.216; q = 0.820	−0.204 [−0.460; 0.108] p = 0.208; q = 0.564
glrlm_RunVariance	−0.099 [−0.404; 0.224] p = 0.538; q = 0.674	0.203 [−0.112; 0.462] p = 0.202; q = 0.820	0.213 [−0.118; 0.475] p = 0.187; q = 0.564
firstorder_Skewness	−0.085 [−0.388; 0.233] p = 0.600; q = 0.674	−0.155 [−0.452; 0.164] p = 0.333; q = 0.820	−0.155 [−0.467; 0.180] p = 0.338; q = 0.615

DISCUSSION

In this cohort, five of the 19 predefined radiomic features correlated with continuous Ki-67 after FDR correction. Interpretation of these associations depends on their overlap with uptake intensity and tumor volume, the influence of lesion size, and the limitations of a small cohort. Prior selection based on technical criteria enabled biological evaluation of a panel defined independently of Ki-67.

1. Comparison with the breast cancer literature

Surov et al. [6] included 32 studies comprising 1802 patients in their meta-analysis. The [18F]FDG PET/CT analysis included 25 studies with 1624 patients and estimated an SUVmax–Ki-67 correlation of 0.40 (95% CI, 0.34–0.46). In our study, the coefficients were 0.565 for SUVmax and 0.562 for SUVmean. Our values were numerically higher, but showed the same direction and support a relationship between FDG uptake intensity and proliferation. The difference between the correlations does not establish a statistically stronger association in our cohort, given the substantial differences in populations, imaging protocols, and Ki-67 assessment methods.

In a cohort of 114 patients, Li et al. [19] used a Ki-67 cutoff of ≥20% and reported higher SUVmax, SUVmean, and MTV in the high-proliferation group. In our cohort, using a 30% cutoff, rank-biserial effect sizes were 0.614 for SUVmax, 0.623 for SUVmean, 0.364 for MTV, and 0.450 for TLG. For firstorder_90Percentile, the corresponding effect size was RBC = 0.623 (q = 0.008). These results place this feature within the same range of association with proliferation as the conventional parameters. Different Ki-67 cutoffs limit direct comparison between studies.

Studies by de Mooij et al. [7], Groheux et al. [29], and Heudel et al. [30] documented correlations between tracer uptake and histopathological or immunohistochemical characteristics. In our cohort, 36 of the 42 patients had hormone receptor-positive tumors, and eight were HER2-positive. The predominance of hormone receptor-positive tumors and the distribution of tumor grades require PET–Ki-67 associations to be interpreted in the context of tumor phenotype.

Ha et al. [11] analyzed 109 radiomic features in 73 patients with locally advanced breast cancer. Unsupervised clustering identified three radiomic patterns that differed in Ki-67 expression, using a cutoff of >30% to define high proliferation. In our study, the 19 features were evaluated individually, yielding five associations after FDR correction. The strongest association was observed for firstorder_90Percentile (ρ = 0.556; q = 0.002). Both studies support a relationship between the PET phenotype and proliferation, but differences in populations and methods preclude direct validation of our features by the patterns identified by Ha et al.

In 171 patients with ER-positive tumors, Lemarignier et al. [16] found strong correlations between the four texture features evaluated and MTV, as well as associations with histological type, but no significant associations with the immunohistochemical characteristics examined. This observation reinforces the volume dependence also observed in our cohort. In addition, findings from dedicated breast PET studies, such as that of Moscoso et al. [17], should be interpreted separately from the whole-body acquisitions used in our study.

In a cohort of 153 patients, Araz et al. [31] did not identify radiomic features significantly associated with hormone receptor status, whereas the conventional parameters SUV and TLG showed significant associations. Radiomic associations with Ki-67 were

observed in our cohort, but the different biological endpoint prevents direct comparison of the results. The studies by Antunovic et al. [32], Liu et al. [33], and Gelardi et al. [34] addressed treatment response or molecular classification. Their findings cannot be extrapolated to the clinical performance of the panel evaluated here.

2. Overlap with conventional PET parameters

Across three tumor types, including 54 breast lesions, Orlhac et al. [35] found that three histogram indices were strongly correlated with SUV ($|r| \geq 0.84$), while four texture indices were dependent on MTV. In our study, firstorder_90Percentile correlated with SUVmax at $\rho = 0.983$, whereas firstorder_TotalEnergy correlated with TLG at $\rho = 0.988$. These findings are consistent with substantial overlap between radiomic information and conventional PET parameters. However, the Pearson coefficients reported by Orlhac et al. and the Spearman coefficients used here are not interchangeable estimates, and the features and preprocessing were not identical.

Adjustment for SUVmax and/or MTV attenuated the five main radiomic associations, and an independent contribution was not demonstrated. The adjusted results should be interpreted as an assessment of information shared within the same image, without establishing a causal relationship. Sphericity was significantly associated with Ki-67 after FDR correction only in the MTV-adjusted analysis. This finding should be considered exploratory.

Feature definitions help explain this overlap [27,28]. firstorder_90Percentile describes the upper levels of uptake, whereas TotalEnergy depends on the sum of squared intensities and voxel volume. Texture features describe other properties: gldm_LargeDependenceHighGrayLevelEmphasis emphasizes large dependencies with high gray levels, glszm_LowGrayLevelZoneEmphasis emphasizes zones with low gray levels, and glcm_Correlation describes relationships between neighboring gray levels. The directions observed in our study are compatible with a different uptake distribution in tumors with greater proliferation, but do not by themselves identify a biological mechanism. Redundancy filtering among radiomic features does not ensure their independence from intensity or volume. With fixed-bin-width discretization, features that weight gray levels remain linked to the SUV scale. 90Percentile and TotalEnergy are calculated from the original, non-discretized intensities and are therefore unaffected by the discretization setting [28].

3. Influence of lesion size and technical parameters

After analyzing 555 PET/CT examinations across several cancer types, Hatt et al. [36] concluded that the relationship between texture and volume varied with tumor size, with the information becoming relevant above approximately 10 cm^3 and increasing with volume. In our cohort, the median segmented volume was 10.629 cm^3, with a minimum of 0.793 cm^3. After exclusion of the six small lesions (mean native voxel count <100), the SUVmax and 90th percentile correlations were similarly attenuated to 0.440 and 0.427. This attenuation cannot be attributed solely to technical factors, because exclusion reduced both the sample size and the range of volumes. Moreover, all six excluded lesions had Ki-67 <30%, which also changed the distribution of proliferation.

Brooks and Grigsby [37] and Soret et al. [38] described the influence of lesion size and the partial-volume effect on PET quantification and heterogeneity. Araz et al. [31] excluded tumors with fewer than 64 voxels. We retained small lesions in the primary analysis and separately tested exclusion of those with a mean native voxel count <100. Thresholds expressed as voxel counts are not directly comparable across studies, because physical voxel volume and image resolution affect the amount of information available.

Pfaehler et al. [39], Altazi et al. [40], and Galavis et al. [41] showed that some PET radiomic features are sensitive to reconstruction, discretization, noise, or segmentation. Aide et al. [18] also demonstrated the influence of reconstruction on breast tumor characterization. In our study, the use of a single scanner and a common protocol limited technical variation, but the Ki-67 analysis used only one extraction configuration. The previous interobserver assessment [20] does not establish that the association with Ki-67 persists after changes in preprocessing.

4. Reproducibility and the contribution of Ki-67 independent selection

In our previous study, we defined the radiomic feature panel on the basis of reproducibility and redundancy [20]. The present analysis evaluates a distinct property: the association of radiomic features with Ki-67. A feature can be measured reproducibly without having a demonstrable association with a biological marker. Oliveira et al. [42] showed, in a different tumor setting (lung cancer), that preselection of robust PET features did not improve clinical outcome modeling. This distinction between technical robustness and biological relevance is also supported by the methodological literature [23,24].

The strength of our design lies in defining the panel before the Ki-67 analysis, without adding or removing features on the basis of the biological endpoint. However, technical selection and the present evaluation were performed in the same cohort, whose inclusion depended on the availability of clinicopathological data. A predefined panel therefore does not constitute independent validation. Reporting all 19 coefficients and their confidence intervals allows the magnitude and uncertainty of the associations, including nonsignificant findings, to be assessed.

Separate analyses for the two observers supported the internal consistency of the main continuous associations: 90Percentile, TotalEnergy, LargeDepend-enceHighGrayLevelEmphasis, and LowGrayLevelZoneEmphasis remained significant after FDR correction for both segmentations. glcm_Correlation showed the same direction but was significant only for the first observer. These findings indicate differential sensitivity of the features to segmentation and relate to the same patients and images, without validation across centers or scanners.

5. Study limitations

This study is limited by the small cohort, retrospective single-center design, and lack of independent validation. The inherent requirement for complete clinicopathological data, including histological grade, may introduce selection bias, and analysis of a single dominant lesion does not capture the full heterogeneity of the disease. Collinearity with SUV and MTV, small lesions, and segmentation variability limit biological interpretation. Ki-67 values were obtained from routine pathology reports, without standardization of the antibody clone or scoring within this study, both of which are relevant to marker variability [1,43–45]. The biopsy-to-PET interval and the influence of clinical stage, blood glucose, and individual uptake time were not evaluated. The imbalanced distributions of tumor grades and subtypes, together with use of a single extraction configuration, limit generalizability. The results describe exploratory associations and do not establish the predictive performance or clinical utility of the panel. As in other fields of quantitative imaging, translation of such associations into clinical practice requires external validation and standardized reporting [46,47].

CONCLUSION

In this single-center cohort of 42 women with untreated primary breast carcinoma, five of the 19 PET/CT radiomic features predefined exclusively on the basis of reproducibility and redundancy were associated with continuous Ki-67 after FDR correction.

The five primary radiomic associations were similar in magnitude to those of conventional PET parameters, but did not remain significant after adjustment for MTV, SUVmax, or both parameters.

Our findings suggest a relationship between stable radiomic features and tumor proliferation, but do not demonstrate an independent contribution beyond conventional PET parameters. Confirmation in independent cohorts should account for lesion volume, segmentation, and standardized Ki-67 assessment.

Conflicts of interest and sources of funding

The authors declare no conflict of interest. This research received no external funding.

Acknowledgments

All figures and tables are original.

Authors' contribution

Conceptualization, A.M.; methodology, A.M. and R.-M.M.; validation, R.-M.M., V.-O.B. and C.C.; formal analysis, A.M., C.M. and I.-N.M.; writing—original draft preparation, A.M.; writing—review and editing, A.M., I.-N.M., R.-M.M., V.-O.B.; visualization, C.M., I.-N.M.; supervision, I.-N.M. All authors have read and approved the submitted version of the manuscript.

Ethics approval and consent to participate

The study was conducted in accordance with the Declaration of Helsinki and approved by the Local Ethics Committee of the "Dr. Carol Davila" Central Military Emergency University Hospital, Bucharest, Romania, approval number 763/11.03.2025. Informed consent was obtained from all participants involved in the study.

Patient consent for publication

Informed consent was obtained from all participants involved in the study.

References

1. Nielsen TO, Leung SCY, Rimm DL, Dodson A, Acs B, et al. Assessment of Ki67 in Breast Cancer: Updated Recommendations From the International Ki67 in Breast Cancer Working Group. J Natl Cancer Inst. 2021;113:808-819. doi: 10.1093/jnci/djaa201.

2. al Moushaly R, Păduraru DN, Andronic O, Nechita S, Bolocan A, et al. Sentinel node biopsy positivity: is axillary dissection always necessary? A retrospective analysis. Rom J Mil Med. 2024;127(3):228-236. doi: 10.55453/rjmm.2024.127.3.8.

3. Hadebe B, Harry L, Ebrahim T, Pillay V, Vorster M. The Role of PET/CT in Breast Cancer. Diagnostics (Basel). 2023;13:597. doi: 10.3390/diagnostics13040597.

4. Vaz SC, Woll JPP, Cardoso F, Groheux D, Cook GJR, et al. Joint EANM-SNMMI guideline on the role of 2-[18F]FDG PET/CT in no special type breast cancer (endorsed by the ACR, ESSO, ESTRO, EUSOBI/ESR, and EUSOMA). Eur J Nucl Med Mol Imaging. 2024;51:2706-2732. doi: 10.1007/s00259-024-06696-9.

5. Mititelu MR, Stanulovic V, Mitoi A, Bucurica S, Hodolic M, et al. Overview of Adverse Reactions of Radiopharmaceuticals. Clin Oncol (R Coll Radiol). 2025;43:103857. doi: 10.1016/j.clon.2025.103857.

6. Surov A, Meyer HJ, Wienke A. Associations Between PET Parameters and Expression of Ki-67 in Breast Cancer. Transl Oncol. 2019;12:375-380. doi: 10.1016/j.tranon.2018.11.005.

7. de Mooij CM, Ploumen RAW, Nelemans PJ, Mottaghy FM, Smidt ML, et al. The influence of receptor expression and clinical subtypes on baseline [18F]FDG uptake in breast cancer: systematic review and meta-analysis. EJNMMI Res. 2023;13:5. doi: 10.1186/s13550-023-00953-y.

8. Lambin P, Rios-Velazquez E, Leijenaar R, Carvalho S, van Stiphout RGPM, et al. Radiomics: extracting more information from medical images using advanced feature analysis. Eur J Cancer. 2012;48:441-446. doi: 10.1016/j.ejca.2011.11.036.

9. Gillies RJ, Kinahan PE, Hricak H. Radiomics: Images Are More than Pictures, They Are Data. Radiology. 2016;278:563-577. doi: 10.1148/radiol.2015151169.

10. Cuzino D, Capisizu AS. The transformative role of artificial intelligence in the future of radiology. Rom J Mil Med. 2025;128(6):528-535. doi: 10.55453/rjmm.2025.128.6.6.

11. Ha S, Park S, Bang JI, Kim EK, Lee HY. Metabolic radiomics for pretreatment [18F]FDG PET/CT to characterize locally advanced breast cancer: histopathologic characteristics, response to neoadjuvant chemotherapy, and prognosis. Sci Rep. 2017;7:1556. doi: 10.1038/s41598-017-01524-7.

12. Urso L, Manco L, Castello A, Evangelista L, Guidi G, et al. PET-Derived Radiomics and Artificial Intelligence in Breast Cancer: A Systematic Review. Int J Mol Sci. 2022;23:13409. doi: 10.3390/ijms232113409.

13. Mitoi A, Mititelu RM, Medar C, Constantin C, Bolocan VO, et al. [18F]FDG PET/CT Radiomics in Untreated Breast Carcinoma: A Review of the Current State and Future Directions. Diagnostics (Basel). 2025;15:2231. doi: 10.3390/diagnostics15172231.

14. Soussan M, Orlhac F, Boubaya M, Zelek L, Ziol M, et al. Relationship between Tumor Heterogeneity Measured on FDG-PET/CT and Pathological Prognostic Factors in Invasive Breast Cancer. PLoS One. 2014;9:e94017. doi: 10.1371/journal.pone.0094017.

15. Groheux D, Majdoub M, Tixier F, Cheze Le Rest C, Martineau A, et al. Do clinical, histological or immunohistochemical primary tumour characteristics translate into different 18F-FDG PET/CT volumetric and heterogeneity features in stage II/III breast cancer? Eur J Nucl Med Mol Imaging. 2015;42:1682-1691. doi: 10.1007/s00259-015-3110-x.

16. Lemarignier C, Martineau A, Teixeira L, Vercellino L, Espié M, et al. Correlation between tumour characteristics, SUV measurements, metabolic tumour volume, TLG and textural features assessed with 18F-FDG PET in a large cohort of oestrogen receptor-positive breast cancer patients. Eur J Nucl Med Mol Imaging. 2017;44:1145-1154. doi: 10.1007/s00259-017-3641-4.

17. Moscoso A, Ruibal Á, Domínguez-Prado I, Fernández-Ferreiro A, Herranz M, et al. Texture analysis of high-resolution dedicated breast 18F-FDG PET images correlates with immunohistochemical factors and subtype of breast cancer. Eur J Nucl Med Mol Imaging. 2018;45:196-206. doi: 10.1007/s00259-017-3830-1.

18. Aide N, Salomon T, Blanc-Fournier C, Grellard JM, Levy C, et al. Implications of reconstruction protocol for histo-biological characterisation of breast cancers using FDG-PET radiomics. EJNMMI Res. 2018;8:114. doi: 10.1186/s13550-018-0466-5.

19. Li D, Ding H, Liao Y, Yu X, Guo Y, et al. PET/CT Radiomics Integrated with Clinical Indexes as a Tool to Predict Ki67 in Breast Cancer: a Pilot Study. Nucl Med Mol Imaging. 2025;59:164-173. doi: 10.1007/s13139-024-00896-9.

20. Mitoi A, Mititelu R, Medar C, Bolocan VO, Ciprian C, et al. Inter-Observer Reproducibility of [18F]FDG PET/CT Radiomic Features in Primary Breast Carcinoma. J Imaging. 2026;12:300. doi: 10.3390/jimaging12070300.

21. Zwanenburg A, Vallières M, Abdalah MA, Aerts HJWL, Andrearczyk V, et al. The Image Biomarker Standardization Initiative: Standardized Quantitative Radiomics for High-Throughput Image-based Phenotyping. Radiology. 2020;295:328-338. doi: 10.1148/radiol.2020191145.

22. Kocak B, Baessler B, Bakas S, Cuocolo R, Fedorov A, et al. CheckList for EvaluAtion of Radiomics research (CLEAR): a step-by-step reporting guideline for authors and reviewers endorsed by ESR and EuSoMII. Insights Imaging. 2023;14:75. doi: 10.1186/s13244-023-01415-8.

23. Xue C, Yuan J, Lo GG, Chang ATY, Poon DMC, et al. Radiomics feature reliability assessed by intraclass correlation coefficient: a systematic review. Quant Imaging Med Surg. 2021;11:4431-4460. doi: 10.21037/qims-21-86.

24. van Timmeren JE, Cester D, Tanadini-Lang S, Alkadhi H, Baessler B. Radiomics in medical imaging-how-to guide and critical reflection. Insights Imaging. 2020;11:91. doi: 10.1186/s13244-020-00887-2.

25. Fedorov A, Beichel R, Kalpathy-Cramer J, Finet J, Fillion-Robin JC, et al. 3D Slicer as an image computing platform for the Quantitative Imaging Network. Magn Reson Imaging. 2012;30:1323-1341. doi: 10.1016/j.mri.2012.05.001.

26. Otsu N. A threshold selection method from gray-level histograms. IEEE Trans Syst Man Cybern. 1979;9:62-66. doi: 10.1109/TSMC.1979.4310076.

27. van Griethuysen JJM, Fedorov A, Parmar C, Hosny A, Aucoin N, et al. Computational Radiomics System to Decode the Radiographic Phenotype. Cancer Res. 2017;77:e104-e107. doi: 10.1158/0008-5472.CAN-17-0339.

28. PyRadiomics. Radiomic features [Internet]. Version 3.1.0 [cited 2026 Oct 3]. Available from: https://pyradiomics.readthedocs.io/en/stable/features.html.

29. Groheux D, Giacchetti S, Moretti JL, Porcher R, Espié M, et al. Correlation of High 18F-FDG Uptake to Clinical, Pathological and Biological Prognostic Factors in Breast Cancer. Eur J Nucl Med Mol Imaging. 2011;38:426-435. doi: 10.1007/s00259-010-1640-9.

30. Heudel P, Cimarelli S, Montella A, Bouteille C, Mognetti T. Value of PET-FDG in Primary Breast Cancer Based on Histopathological and Immunohistochemical Prognostic Factors. Int J Clin Oncol. 2010;15:588-593. doi: 10.1007/s10147-010-0120-3.

31. Araz M, Soydal C, Gündüz P, Kırmızı A, Bakırarar B, et al. Can Radiomics Analyses in 18F-FDG PET/CT Images of Primary Breast Carcinoma Predict Hormone Receptor Status? Mol Imaging Radionucl Ther. 2022;31:49-56. doi: 10.4274/mirt.galenos.2022.59140.

32. Antunovic L, De Sanctis R, Cozzi L, Kirienko M, Sagona A, et al. PET/CT Radiomics in Breast Cancer: Promising Tool for Prediction of Pathological Response to Neoadjuvant Chemotherapy. Eur J Nucl Med Mol Imaging. 2019;46:1468-1477. doi: 10.1007/s00259-019-04313-8.

33. Liu J, Bian H, Zhang Y, Gao Y, Yin G, et al. Molecular Subtype Classification of Breast Cancer Using Established Radiomic Signature Models Based on 18F-FDG PET/CT Images. Front Biosci (Landmark Ed). 2021;26:475-484. doi: 10.52586/4960.

34. Gelardi F, Cavinato L, De Sanctis R, Ninatti G, Tiberio P, et al. The Predictive Role of Radiomics in Breast Cancer Patients Imaged by [18F]FDG PET: Preliminary Results from a Prospective Cohort. Diagnostics (Basel). 2024;14:2312. doi: 10.3390/diagnostics14202312.

35. Orlhac F, Soussan M, Maisonobe JA, Garcia CA, Vanderlinden B, et al. Tumor texture analysis in [18F]FDG PET: relationships between texture parameters, histogram indices, standardized uptake values, metabolic volumes, and total lesion glycolysis. J Nucl Med. 2014;55:414-422. doi: 10.2967/jnumed.113.129858.

36. Hatt M, Majdoub M, Vallières M, Tixier F, Cheze Le Rest C, et al. 18F-FDG PET Uptake Characterization through Texture Analysis: Investigating the Complementary Nature of Heterogeneity and Functional Tumor Volume in a Multi-Cancer Site Patient Cohort. J Nucl Med. 2015;56:38-44. doi: 10.2967/jnumed.114.144055.

37. Brooks FJ, Grigsby PW. The Effect of Small Tumor Volumes on Studies of Intratumoral Heterogeneity of Tracer Uptake. J Nucl Med. 2014;55:37-42. doi: 10.2967/jnumed.112.116715.

38. Soret M, Bacharach SL, Buvat I. Partial-Volume Effect in PET Tumor Imaging. J Nucl Med. 2007;48:932-945. doi: 10.2967/jnumed.106.035774.

39. Pfaehler E, Beukinga RJ, de Jong JR, Slart RHJA, Slump CH, et al. Repeatability of [18F]FDG PET radiomic features: A phantom study to explore sensitivity to image reconstruction settings, noise, and delineation method. Med Phys. 2019;46:665-678. doi: 10.1002/mp.13322.

40. Altazi BA, Zhang GG, Fernandez DC, Montejo ME, Hunt D, et al. Reproducibility of [18F]FDG PET radiomic features for different cervical tumor segmentation methods, gray-level discretization, and reconstruction algorithms. J Appl Clin Med Phys. 2017;18:32-48. doi: 10.1002/acm2.12170.

41. Galavis PE, Hollensen C, Jallow N, Paliwal B, Jeraj R. Variability of Textural Features in FDG PET Images Due to Different Acquisition Modes and Reconstruction Parameters. Acta Oncol. 2010;49:1012-1016. doi: 10.3109/0284186X.2010.498437.

42. Oliveira C, Amstutz F, Vuong D, Bogowicz M, Hüllner M, et al. Preselection of robust radiomic features does not improve outcome modelling in non-small cell lung cancer based on clinical routine FDG-PET imaging. EJNMMI Res. 2021;11:79. doi: 10.1186/s13550-021-00809-3.

43. Dowsett M, Nielsen TO, A'Hern R, Bartlett J, Coombes RC, et al. Assessment of Ki67 in Breast Cancer: Recommendations from the International Ki67 in Breast Cancer Working Group. J Natl Cancer Inst. 2011;103:1656-1664. doi: 10.1093/jnci/djr393.

44. Polley MYC, Leung SCY, McShane LM, Gao D, Hugh JC, et al. An International Ki67 Reproducibility Study. J Natl Cancer Inst. 2013;105:1897-1906. doi: 10.1093/jnci/djt306.

45. Rimm DL, Leung SCY, McShane LM, Bai Y, Bane AL, et al. An International Multicenter Study to Evaluate Reproducibility of Automated Scoring for Assessment of Ki67 in Breast Cancer. Mod Pathol. 2019;32:59-69. doi: 10.1038/s41379-018-0109-4.

46. Lambin P, Leijenaar RTH, Deist TM, Peerlings J, de Jong EEC, et al. Radiomics: The Bridge between Medical Imaging and Personalized Medicine. Nat Rev Clin Oncol. 2017;14:749-762. doi: 10.1038/nrclinonc.2017.141.

47. Bolocan VO, Mitoi A, Nicu-Canareica O, Baean ML, Medar C, et al. Artificial Intelligence in Prostate MRI: Current Evidence and Clinical Translation Challenges—A Narrative Review. J Imaging. 2025;11:335. doi: 10.3390/jimaging11100335.

https://doi.org/10.55453/rjmm.2026.129.6.5

Review

Deep Brain Stimulation for Parkinson's Disease: Current state and perspectives – a narrative review

Gabriel-Sebastian Donea[1], Miruna-Cătălina Maftei[1], Andreea-Ramona Treteanu[2,3,*], Octavian Andronic[2,3], Octavian Mihai Sîrbu[4,5], Maria Mirabela Manea[2,6]

[1] Faculty of Medicine, Grigore T. Popa University of Medicine and Pharmacy, 16 Universitatii Street, 700115 Iasi, Romania
[2] Faculty of Medicine, Carol Davila University of Medicine and Pharmacy, 37 Dionisie Lupu Street, 020021 Bucharest, Romania
[3] Center of Innovation and eHealth, Carol Davila University of Medicine and Pharmacy, 37 Dionisie Lupu Street, 020021 Bucharest, Romania
[4] Department of Neurosurgery, 'Dr. Carol Davila' Central Military Emergency University Hospital, 010825 Bucharest, Romania
[5] Clinical Neurosciences Department, University of Medicine and Pharmacy "Carol Davila", Bucharest, 050474 Bucharest, Romania
[6] Neurology Clinic, National Institute of Neurology and Neurovascular Diseases, 041915 Bucharest, Romania
*Correspondence: andreea-ramona.treteanu0720@stud.umfcd.ro

Abstract: Deep brain stimulation (DBS) remains one of the most effective advanced therapies for Parkinson's disease (PD), yet considerable heterogeneity persists in clinical outcomes, patient selection, and long-term neuropsychiatric effects. This narrative review synthesizes recent evidence on the mechanisms, efficacy, and evolving applications of DBS, integrating findings from neurophysiology, neuroimaging, genetics, and computational modeling. Current data indicate that stimulation of the subthalamic nucleus (STN) and globus pallidus internus (GPi) reliably improves cardinal motor symptoms and reduces dopaminergic medication requirements, with sustained benefits over time. However, axial symptoms, including gait disturbance, postural instability, and speech, demonstrate variable or limited responsiveness, underscoring the complexity of the underlying neural circuits. Non-motor outcomes also show substantial variability: sleep and gastrointestinal functions often improve, whereas apathy, impulsivity, and speech disturbances may emerge or worsen in selected patients. Emerging biomarkers, including evoked cortical responses, oscillatory signatures, radiomic features, and gray matter morphometry, show promise in refining patient-specific predictions, although external validation remains limited. Genetic variants, particularly in GBA and LRRK2, further modulate cognitive trajectories and long-term outcomes. Advances in imaging-guided "asleep" DBS, directional leads, and personalized programming strategies have improved precision and safety. Concurrently, machine learning and adaptive DBS paradigms represent major future directions, enabling real-time, biomarker-driven modulation tailored to disease dynamics. By integrating multidomain evidence, this review highlights both the established therapeutic value and the persistent challenges of DBS, emphasizing the need for mechanistically informed, precision-based approaches. These developments collectively outline a path toward more individualized and circuit-specific neuromodulation strategies in PD.

Keywords: deep brain stimulation; Parkinson disease; subthalamic nucleus; globus pallidus internus

INTRODUCTION

Parkinson's disease (PD) is a neurodegenerative disorder that affects quality of life (QoL) through a range of motor and non-motor symptoms [1]. It is usually associated with motor symptoms [2] such as tremor, bradykinesia, and postural instability [3,4]. These motor dysfunctions result from the progressive loss of dopaminergic neurons in the substantia nigra (SN) [5–7], leading to reduced dopamine levels in the striatum. Beyond dopaminergic neuronal loss, oxidative stress and mitochondrial dysfunction are increasingly recognized as important contributors to the complex neurodegenerative processes underlying PD [8]. Evidence indicates that PD patients may also exhibit non-motor symptoms: psychiatric, cognitive, autonomic, and other, which tend to become more pronounced as the disease progresses [9].

Deep brain stimulation (DBS) is a neurosurgical procedure known for alleviating motor symptoms and improving QoL in many PD patients [10]. It involves implanting

Citation: Donea GS, Maftei MC, Treteanu AR, Andronic O, Sîrbu OM, Manea MM. *Deep Brain Stimulation for Parkinson's Disease: Current State and Perspectives – a narrative review*. R. J. Mil. Med. 2026, CXXIX(6): 636-651. https://doi.org/10.55453/rjmm.2026.129.6.5

Academic Editor: Octavian Vasiliu

Received: 30 August 2026
Revised: 19 October 2026
Accepted: 22 October 2026

electrodes into specific brain regions, usually the subthalamic nucleus (STN) or globus pallidus internus (GPi) [1,11]. Despite its numerous benefits, DBS has several limitations and challenges. Being a symptomatic treatment [7], it does not halt neurodegeneration or cure PD. Outcomes vary among patients [11] and some symptoms, such as speech, postural instability and gait, may be resistant to DBS or even worsen after surgery [12].

The aim of this narrative review is to provide a comprehensive synthesis of current knowledge on DBS in PD patients, summarizing the current state of the procedure, including its mechanisms, clinical outcomes, predictive factors, selection criteria, risks, and future directions.

MATERIALS AND METHODS

The research was conducted using PubMed, Scopus, and Web of Science, using the following search formula: ("DBS" OR "deep brain stimulation") AND ("PD" OR "Parkinson's Disease") AND "outcome". Titles and abstracts were screened for relevance. We selected articles published in English within the last 5 years to ensure recent and accessible data. Eligible studies included adult and elderly PD patients who received DBS and reported clinical outcomes or predictive factors. We excluded case reports, ongoing trials, and studies based solely on animal models. A total of 129 articles were included in the final analysis and organized thematically according to clinical domain.

RESULTS AND DISCUSSION

1. Deep brain stimulation

Before the widespread use of levodopa in the late 1960s, PD was primarily considered a surgical disease, treated by making lesions in the thalamus (thalamotomy) or globus pallidus (pallidotomy) to improve symptoms [7]. After the introduction of levodopa, these surgeries became less common until the 1980s, when pallidotomy regained attention for its benefits. In 1987, Benabid and Pollak offered a reversible alternative to lesions by introducing thalamic DBS [7,13]. This expanded to the GPi (1994) and STN (1993–95), with STN DBS uniquely reducing medication needs [7]. Following a multicenter trial in 2001, STN and GPi DBS gained FDA approval and became the global standard of care [7].

The DBS procedure involves two steps. First, electrodes are implanted into specific brain targets and connected to an Implantable Pulse Generator (IPG), a small device, typically placed under the skin of the chest during the same surgery or in a separate procedure [1,12]. The IPG modulates abnormal neural activity by generating continuous, high-frequency electrical pulses to the targeted brain regions [1,14,15]. Unlike older surgical methods involving permanent brain lesions, such as pallidotomy [7], DBS is reversible and adjustable through modification of stimulation [7,16].

1.1. Mechanism of action

The exact mechanisms of action of DBS are still not fully understood; however, it is believed to work by modulating complex neural networks and reestablishing more normal movement patterns [17–19]. In PD, specific brain regions, particularly the STN and GPi, become overactive, leading to an imbalance in brain circuitry that contributes to motor symptoms like rigidity and akinesia [7]. DBS is thought to "silence" or disrupt this pathological, excessive neuronal activity, thereby restoring better control over movement [7,13,20]. This modulation involves direct effects on local cell bodies, perturbation of axons (nerve fibers), and interactions with oscillatory brain rhythms [20–22]. For example, in the STN, excessive beta-band oscillatory activity (12–30 Hz) within the cortico-basal ganglia network is considered a well-established pathophysiological biomarker associated with motor impairment in PD, particularly bradykinesia and rigidity [21,23]. Elevated beta synchronization is thought to reflect an "anti-kinetic" state that interferes with normal motor processing and movement initiation. Conventional high-frequency DBS suppresses pathological beta activity and reduces abnormal neuronal synchrony, which correlates with clinical motor improvement [20,21,23]. The relevance of beta oscillations has become even more important with the development of adaptive DBS (aDBS), in which beta power recorded from implanted electrodes is used as a real-time feedback biomarker to dynamically adjust stimulation delivery according to the patient's clinical state (20). Compared with conventional continuous stimulation, aDBS may reduce unnecessary stimulation, improve energy efficiency, and potentially decrease stimulation-related adverse effects while maintaining motor benefit.

1.2. Awake vs Asleep DBS

Traditionally, DBS surgery is performed while the patient is awake under local anesthesia because it allows surgeons to test the stimulation during the operation and monitor side effects [24–26]. However, advances in imaging and intraoperative MRI have supported the growing adoption of asleep surgery under general anesthesia. Microelectrode recording (MER) remains reliable in this setting and is crucial for accurate placement [27]. Combining MER with deep learning may help predict clinical improvement [28]. Many patients prefer asleep surgery because it is perceived as more tolerable than awake surgery and, on average, 26 minutes shorter than awake surgery [29].

Multiple studies have reported no significant differences in motor outcomes between the two approaches [24,27,30]. In 2021, Holewijn et al. [29] conducted a randomized clinical trial which showed no significant difference in the improvement of off-medication Movement Disorders Society Unified Parkinson's Disease Rating Scale (MDS-UPDRS) Motor Examination scores between groups (awake: −27.3 points or 52% improvement; asleep: −25.3 points or 50% improvement). The subscores for tremor, rigidity, bradykinesia, and gait and balance were also similar [29]. This study also showed no significant differences in cognition, mood, and behavior. Izzo et al. [27] reported in a 2024 meta-analysis that complication rates were similar between awake and asleep surgery. Later, in 2025, Roldán et al. [31] observed a low complication rate for asleep surgery of 1 event among 89 patients. Holewijn et al. [29] noted one case of symptomatic intracranial hemorrhage after awake surgery and four after asleep surgery, but classified this as a "random finding" with no statistical differences in incidence between the two approaches.

1.3. DBS Programming Parameters

The key stimulation parameters used in DBS are frequency, pulse width, and amplitude/voltage [32–37]. Frequency represents the delivery rate of the electrical pulses. It is usually 130 Hz, but can range from 125 Hz to 180 Hz [7,20,27,38–40]. High-frequency stimulation is commonly used to suppress pathological network activity and improve motor symptoms in PD [41]. In parallel, oscillatory activity in the gamma range has attracted growing interest as a neurophysiological biomarker. Excessive narrow-band gamma activity, particularly around 60–90 Hz, has been associated with levodopa-induced dyskinesia and may reflect hyperkinetic motor states [24,42–44]. Recent studies suggest that gamma oscillations could help guide adaptive DBS strategies aimed at balancing motor improvement while minimizing dyskinesias. Gamma-related modulation has also been linked to cognitive and speech effects. Increased gamma stimulation may contribute to declines in verbal fluency, unlike theta frequencies (4–10 Hz), which show episodic improvement in verbal fluency but less robust motor benefits [45]. Despite this, combined theta-gamma frequencies improved verbal fluency without affecting motor benefits, with improvements observed in both non-episodic ($p = 0.038$) and episodic ($p = 0.030$) verbal fluency scores after one month of STN-DBS [46]. For specific symptoms such as gait disturbances or dyskinesia, low-frequency stimulation is sometimes used [24,42–44]. Low-frequency paradigms have also been explored for memory modulation during NREM sleep and for speech improvement [40,41].

Pulse width, the duration of each electrical pulse, is usually 60 µs, but can range from 40 µs to 90 µs [7,21,27,38–40,47]. Short pulse widths have been shown to improve speech intelligibility and reduce dyskinesia and pyramidal side effects [24,40].

Amplitude, the strength of the electrical current, varies between 1 and 4 mA or 1.5 to 4.0 V, adjusted based on clinical response and side effects [7,21,27,38–40,47]. Monopolar stimulation (IPG as anode, optimal contact as cathode) is common, but bipolar or double monopolar configurations are also used [7,25,39,48,49].

Recent advances in DBS technology include the development of directional leads, which allow current steering toward specific neural regions while avoiding adjacent structures associated with adverse effects [24,40]. Unlike conventional ring-shaped electrodes that deliver stimulation circumferentially, directional segmented contacts provide greater spatial selectivity and may enlarge the therapeutic window by improving motor benefit at lower stimulation thresholds [24]. Directional stimulation is increasingly used in contemporary DBS practice because it can reduce stimulation-induced side effects, including dysarthria, capsular effects, and sensory disturbances, particularly when electrode placement is suboptimal or located near eloquent pathways [24,40]. This approach also facilitates more individualized programming strategies and may improve overall tolerability and energy efficiency.

Precise DBS electrode placement is crucial for maximizing motor benefit and minimizing side effects [36,50,51]. Suboptimal placement occurs in up to 17% of cases, leading to reduced efficacy and higher side effect rates [50]. In one study, the electrode reached the planned target within 2 mm in only 42.9% of cases, meaning that more than half of the surgeries required depth or track adjustments [27]. Lead location also plays a critical role. One study pointed out that anterior sensorimotor STN placement improved voice outcomes, whereas posterior contacts worsened them [38].

1.4. Targets

The subthalamic nucleus (STN) and globus pallidus internus (GPi) are the most well-known and established targets for DBS (Figure 1) [13,26,35,52]. Their extensive benefits and differences in outcomes have created a vast debate regarding their selection [7,12,52]. Understanding their strengths and differences will help personalize the treatment based on the patient's needs.

STN

The STN is the most frequently targeted site for DBS in the treatment of PD [5,53,54]. It is neuronally dense, highly vascularized [55], measuring approximately 6–8 mm anterior-posterior, 9–11 mm mediolateral, and 3–5 mm dorsoventral [24]. Between the cerebral peduncle and the zona incerta [55], its location is referenced using the anterior commissure–posterior commissure (AC-PC) line coordinates [53]. The dorsolateral STN is believed to be a sweet spot [33,56,57] due to slower motor progression [33] and improvement of gait after DBS [57]. Stimulating this target helps alleviate a range of motor symptoms, such as tremor, akinesia, and rigidity [7,44,58], while also significantly reducing levodopa dosage, thereby avoiding drug-induced motor complications [59,60].

GPi

The GPi is another commonly targeted structure for DBS in PD. It is larger than STN, measuring approximately 10-12 mm anterior-posterior, 15-18 mm mediolateral, and 4-6 mm dorsoventral [24]. It is a primary output nucleus of the basal ganglia [7], and it is separated from the globus pallidus externus (GPe) by the internal medullary lamina [24]. GPi-DBS is particularly effective for controlling dyskinesias [7,8,25,60,61]. It offers greater flexibility in medication adjustments, even if it leads to less overall drug reduction compared to STN-DBS [8,25,61]. Moreover, GPi is associated with fewer neuropsychiatric issues [26] and less harsh on cognition than STN [12]. Bucur and Papagno's meta-analysis [4] suggests that GPi-DBS may cause fewer side effects, including cognitive impairment, than STN-DBS. Supporting this point, França et al. [12] and Murcia Carretero et al. [26], who cite Boogers and Fasano, believe that GPi should be considered the main target for frail older patients with cognitive and neuropsychiatric problems. In contrast, Tröster et al. [62] suggest caution when interpreting meta-analyses comparing the cognitive effects of the two targets, as subject selection bias is likely to occur. Due to GPi being perceived as safer for cognitive effects, patients with poor cognition may be assigned to GPi-DBS, resulting in different sample characteristics –demographic and disease traits– between the two groups pre-surgery [62]. They believe that STN and GPi may be more similar, with GPi only having slightly milder effects on verbal fluency and processing speed [62].

1.5. Emerging/Experimental Targets

While STN and GPi are the primary targets, research is exploring alternative regions to address DBS-resistant symptoms, particularly axial symptoms and cognitive impairment.

The ventral intermediate nucleus (VIM) of the thalamus was the first modern DBS target and is mainly used for treating tremors in PD and essential tremor when medications do not work. VIM DBS reliably reduces tremors over the long term, but it does not help much with other movement problems like slowness or balance issues. Side effects, especially when both sides are stimulated, can include speech difficulties, imbalance, reduced effectiveness over time, and, rarely, problems with coordination. For these reasons, VIM DBS is usually chosen for people with tremor-dominant Parkinson’s disease, rather than those with more widespread movement symptoms [7].

Caudal Zona Incerta (cZi), below the thalamus, has shown excellent effects on both Parkinsonian and essential tremor, possibly with fewer side effects than VIM DBS [7,16,24].

Substantia Nigra Pars Reticulata (SNr), ventrolateral to the STN, has shown a favorable response for axial motor symptoms, including gait impairment and postural instability [16]. Combined STN and SNr stimulation has shown significant improvement in freezing of gait in a pilot trial, though not consistently for other axial symptoms [12,16,42]. This combination might also improve intonation and maximum phonation time [63].

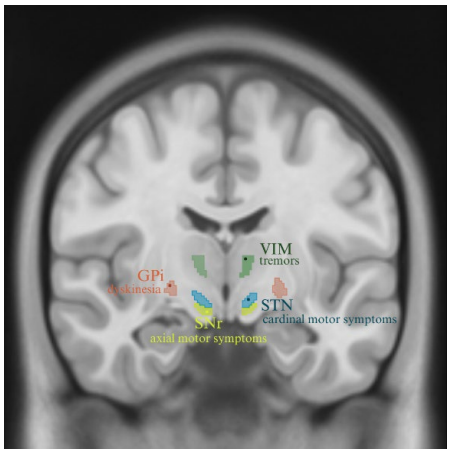
The Pedunculopontine Nucleus (PPN), part of the brainstem locomotor area, has been investigated for therapy-resistant gait and balance disturbances [16,24]. It was suggested that PPN stimulation improves gait freezing and falls, but results remain conflicting [7,24]. Having undefined boundaries, precise targeting is challenging [24].

Nucleus Basalis of Meynert (NBM) provides the primary cholinergic input to the cortex, and it atrophies in PD dementia [7,64]. It’s been hypothesized that NBM may slow cognitive decline, but no significant cognitive outcomes have been reported [7,12].

1.6. Unilateral vs Bilateral Stimulation

Advanced PD patients mostly undergo bilateral, symmetric lead placement surgery, due to often showing motor symptoms on both sides of the body [43]. However, studies have also analyzed the unilateral effects. When the affected site is targeted, the first lead is often the most beneficial [65,66], potentially postponing or canceling the second surgery for the other side [66]. The left-side stimulation may contribute to slower gait velocity than the right-side [67], but better outcomes of rightward visually-guided saccades [47]. Bilateral stimulation also improves these saccades, but doesn’t always outperform left, suggesting that unilateral stimulation may be enough in some cases [47].

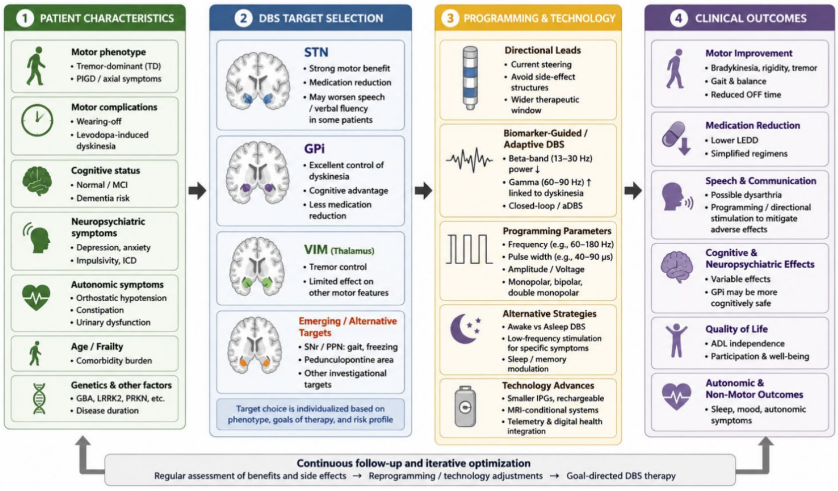
Figure 1: Anatomical localization of DBS targets in Parkinson's disease.



Coronal section (MNI ICBM152 [68,69] template) showing key DBS targets and their principal clinical domains. VIM (green, Morel [70] atlas), GPi (red), STN (blue), and SNr (yellow; CIT168 atlas) are depicted with their predominant therapeutic effects: tremor control (VIM), dyskinesia reduction (GPi), amelioration of cardinal motor symptoms (STN), and modulation of axial motor function (SNr).

Given the heterogeneity of Parkinson's disease manifestations and DBS outcomes, contemporary DBS management increasingly relies on personalized approaches integrating patient characteristics, target selection, programming strategies, and expected clinical outcomes (Figure 2).

Figure 2: Personalized DBS framework in Parkinson's disease.



Schematic overview of individualized DBS management integrating patient characteristics, target selection, programming strategies, emerging technologies, and expected clinical outcomes. The framework highlights the interaction between motor and non-motor features, DBS target choice, adaptive programming approaches, and longitudinal optimization of therapy. Abbreviations: aDBS, adaptive deep brain stimulation; DBS, deep brain stimulation; GPi, globus pallidus internus; LEDD, levodopa equivalent daily dose; MCI, mild cognitive impairment; PD, Parkinson's disease; PIGD, postural instability and gait difficulty; PPN, pedunculopontine nucleus; SNr, substantia nigra pars reticulata; STN, subthalamic nucleus; TD, tremor-dominant; VIM, ventral intermediate nucleus.

2. Selection criteria

Choosing the right patients for DBS in Parkinson's Disease is key to getting the best results and reducing risks [24,71]. Since outcomes differ from person to person, careful selection helps avoid poor results, extra costs, or complications.

In 1999, the Core Assessment Program for Surgical Interventional Therapies in Parkinson's Disease (CAPSIT-PD) was published, becoming the first set of selection criteria that specialists relied on [14,71]. However, the current knowledge on PD evolution and genotyping led to the opinion that CAPSIT-PD is often restrictive and outdated [14,71]. Barbosa et al. [71] reported that CAPSIT-PD initially limited selection eligibility to 1.6% of PD patients, while flexible criteria limited it to 4.5%.

Patients must have a confirmed diagnosis of idiopathic PD based on criteria such as the UK Parkinson's Disease Society Brain Bank criteria [72–74]. In diagnostically uncertain cases, functional neuroimaging may provide complementary information, with brain [^{18}F]FDG PET/CT demonstrating characteristic metabolic patterns that can support the differential diagnosis of PD and atypical parkinsonian syndromes (75). Atypical Parkinsonism does not benefit from DBS [12,14,71]. DBS is mainly indicated in advanced PD when medication can't control disabling motor complications, such as wearing-off, levodopa-induced dyskinesias, or painful dystonia [7,12,22,26,29].

Levodopa responsiveness is supposed to improve by at least 30% in the Unified Parkinson's Disease Rating Scale Part III (UPDRS-III) during a levodopa challenge test (LCT) [24,36,53,55,73,76,77]. Improvement exceeding 50% may indicate a greater likelihood of benefit [24,76,78]. To exclude atypical Parkinsonism, the disease duration should be at least four years [14,71,77]. Patients must be able to attend regular follow-up appointments for device programming and ongoing care [71,79].

2.1. Expanding Criteria and Special Populations

The European Academy of Neurology/Movement Disorder Society (EAN-MDS) 2022 Guideline suggests DBS for patients with "early fluctuations" (less than three years of onset) who meet other criteria [71]. Early-stage surgeries may offer greater long-term medication reduction [80]. Younger age at the time of DBS surgery is generally associated with longer-lasting and more robust motor outcomes and a better cognitive status [7,62,81]. While traditionally, older patients (e.g., over 69-70 years) might have been considered less suitable due to less improvement and more side effects, recent data suggest DBS can be effective and safe in elderly patients, though they may face higher risks of surgical complications [81–83].

Genetic factors were not part of the original CAPSIT-PD criteria. The increased accessibility to genetic testing made these factors considered when deciding on DBS surgery and as possible predictors of outcomes [42].

Glucocerebrosidase (GBA) mutations are a frequent genetic risk factor for PD [84]. GBA carriers are often younger at disease onset and surgery, with stronger levodopa responsiveness and earlier motor complications [85]. Motor outcomes after DBS are generally similar between GBA and non-GBA patients, with sustained improvements in motor symptoms, dyskinesias, fluctuations, and reduced medication burden [85]. However, cognitive outcomes remain the main concern. GBA-PD is linked to faster cognitive decline, and several long-term studies suggest accelerated deterioration after DBS, with higher dementia rates at 5 years (25% vs. 11% in non-GBA PD) [85]. Still, most GBA carriers continue to benefit motorically, and DBS remains a valid option [85,86].

Leucine-Rich Repeat Kinase 2 (LRRK2) is another mutation that can be present in PD. LRRK2 mutation carriers generally show excellent levodopa responsiveness, and their good outcomes from DBS are often long-lasting [7,13]. The G2019S mutation has demonstrated an excellent response to STN-DBS in over 85% of subjects, unlike the R1441G variant, which has shown more unsatisfactory outcomes [24].

Patients with parkin (PRKN) and PINK1 gene mutations often respond very well to dopamine [7]. PRKN-associated PD may present with foot dystonia and depression [71]. Barbosa et al. [71] reported good and sustained motor outcomes (46–84% improvement), with no significant decline in cognitive function generally reported. Other gene variants, like SNCA RS356220, may also be associated with positive QoL outcomes [87].

3. Predictors and biomarkers

As mentioned in the "Selection criteria" section, an improvement greater than 50% in LCT may predict meaningful results from DBS [24,76,78]. However, the LCT's ability to accurately predict individual patient improvement is debated, and its long-term predictive value may be limited, especially for non-motor or axial symptoms [24,71].

The optimal contact orientation is linked to strong evoked cortical responses leading to smoother movement. This leads to the idea that the magnitude is correlated with motor benefits, making the DBS-evoked cortical responses a possible physiological biomarker [88].

Gray Matter Volume (GMV) has potential as a predictive factor, yet its results are debatable for now. Some authors believe that GMV may influence DBS outcomes. For example, Koivu et al. [58] and Yim et al. [19] noted that lower GMV or higher GMV in certain regions may predict medication reduction and greater UPDRS-III scores. Wang et al. [64] reported that less motor improvement is linked to low GMV in the motor cortex and thalamus and to declined cognition linked to low volume in the hippocampus. However, Peter et al. [89] point out that GMV is not predictive of axial symptom improvement. The discrepancies highlight the need for larger, more diverse cohorts to validate GMV as a predictive factor.

The investigation of gender differences in DBS outcomes is important for personalized medicine, but it can also give us insight into women's participation in trials [90]. Kübler et al. [90] pointed out that women are underrepresented in trials, with 30% of participants being women. This percentage is also present in another cohort, with 21 females out of the 70 participants (30%) [91]. A higher percentage of women, with 17 out of 43 (39.5%) was present in Somma et al. [92], a retrospective study, and in Mori et al. [93] with 28 out of 57 (49%), the first study that analyzes gender outcomes of PD in Japan. While both sexes showed

similar motor improvements, only women showed improvements in cognition and only men in depression and impulsivity scores [90]. In the Japanese cohort, women had greater short-term improvements, with 66.3% improvement in women vs. 53.9% in men ($p = 0.028$), when no medication was active [93]. However, these differences disappeared five years post-DBS [93].

The preoperative motor and non-motor symptoms may influence the outcome of DBS. Sauerbier et al. [94] reported that severe impulsive and compulsive behaviors (ICB) and lower doses of dopamine agonists before DBS lead to favorable ICB results after STN-DBS. On the other hand, severe attention or memory deficits pre-DBS are linked to worse ICB after the surgery [94]. Preexisting cognition problems might also influence the amount of benefits after DBS. Patients with mild cognitive impairment have lower motor improvements than those with normal cognition off medication (−41.4% vs −52.2%, $p = 0.013$) [95]. However, mild cognitive impairment isn't linked to dementia development after the procedure [96,97].

Voruz et al. [98] analyzed how motor symptom asymmetry may predict the non-motor outcomes following DBS. The results show that patients with right-sided motor symptoms have great QoL improvements and preserve their cognition, unlike left-sided ones, who have modest QoL improvements and are vulnerable to cognitive decline [98].

4. Clinical outcomes of DBS in PD

Comorbidities complicate DBS. Patients with additional health issues have higher risks of complications and readmissions, though DBS usually results in lower readmission rates than other neurosurgical procedures [71]. Managing patient expectations is also important. Unrealistic hopes for a cure or major improvement can lead to disappointment. Clinicians should discuss the main symptoms patients want to address [24], as perceived symptom severity often shapes expectations [99].

4.1. Motor symptoms

Multiple studies have consistently demonstrated the efficacy of DBS in improving motor symptoms [100]. A meta-analysis reported that the UPDRS-III scores improved by 50.5% after STN-DBS and by 29.8% after GPi-DBS [52]. The cardinal motor symptoms (tremor, rigidity and bradykinesia) have shown significant improvements [101]. One study reported that tremors improved by a mean of 74%, rigidity by 57%, and bradykinesia by 49% [12]. These motor benefits are sustained as noted by De Noordhout et al. [102], after a 12-year comparative study of STN-DBS and best medical therapy in PD patients.

While DBS is associated with good motor outcomes, its effects on axial functions such as speech may be less consistent or even adverse. Postural abnormalities may improve after DBS [103], with one study having 67.8% of Camptocormia and 72.2% of Pisa patients with PD exhibiting positive responses after DBS [104]. Another study noted better scores of axial symptoms such as neck rigidity ($p < 0.0001$), freezing of gait ($p = 0.0031$) and postural stability ($p = 0.0220$), except speech, which did not improve [91]. In patients predisposed to dystonia, STN-DBS may have an additive boost, one study reporting that 74.4% of post-DBS on-dystonia cases were new-onset [105]. Despite better scores on objective scales, some PD patients under DBS perceived speech tasks as more effortful than hand movements, especially in dual treatment states [106]. This highlights the fact that clinical improvement is not always the same as subjective improvement, making patient-perceived effort useful when assessing DBS effectiveness.

Based on motor subtype [(tremor-dominant (TD), akinetic-rigid, postural instability/gait difficulty (PIGD)], DBS outcomes may differ [25,61,71]. After STN-DBS, TD patients often exhibit better short-term motor outcomes [71], but fewer non-motor benefits than PIGD patients [73]. PIGD patients may also demonstrate a greater decline in temporal asymmetry and dyscoordination of walking than TD patients [107].

4.2. Non-motor symptoms (NMS)

Speech outcomes are heterogeneous. Castillo-Triana et al. [108] found no consistent group-level changes, though individual variability was high. However, another study noted that 15% of patients developed dysarthria at 1 year after STN-DBS [109]. GPi-DBS also worsened speech, potentially inducing several types of dysarthria or stuttering [110].

Olfaction, a non-motor symptom affecting over 70% of PD patients and impacting quality of life, appears to be negatively influenced by STN-DBS. A prospective pilot study, utilizing the objective University of Pennsylvania Smell Identification Test (UPSIT), observed a statistically significant worsening of olfaction following bilateral STN-DBS. The mean UPSIT scores declined from 20.0 ± 6.6 (severe hyposmia) before surgery to 17.5 ± 5.7 (total hyposmia) after three months ($p = 0.03$). This objective decline contrasts with some earlier subjective reports, suggesting a potential direct effect of DBS or the natural progression of the disease, rather than changes in mood, as anxiety and depression scores remained stable [111].

Conversely, gastrointestinal symptoms, particularly constipation, which affects up to 70% of PD patients, showed objective improvements after STN-DBS. In the pilot study, 63% (5 of 8) of patients with baseline constipation, as defined by Rome III criteria, experienced resolution of the condition three months post-DBS ($p = 0.03$). Significant improvements were noted in several objective measures: the number of complete spontaneous bowel movements (CSBM) per week increased from 2.2 ± 1.9 to 4.7 ± 2.4 ($p = 0.04$), and the proportion of bowel movements associated with straining decreased from 28% ± 12% to 7% ± 4% ($p = 0.09$). Patient satisfaction with constipation treatment improved from 44 ± 27 mm to 64 ± 25 mm on a visual analog scale ($p = 0.02$). These benefits were not associated with changes in laxative use, dopaminergic medication dosage, or mood, suggesting a

direct effect of DBS, possibly through improved motor function and rectoanal coordination, or modulation of autonomic centers [111].

Despite PD being associated with weight loss, one study found that after DBS patients gained weight, which was positively linked to survival ($R2 = 0.14$, $p < 0.001$) [112]. The patients who had bilateral STN-DBS showed the most weight gain compared to bilateral GPi-DBS (3.03 ± 0.45% vs 1.89 ± 0.31%, $p < 0.01$) [112].

Sleep disturbances are among the most debilitating non-motor symptoms in PD, heavily influencing quality of life. A prospective, controlled, 36-month observational study compared bilateral STN-DBS with standard-of-care medical therapy (MED) in propensity score-matched cohorts (n=40 per group). STN-DBS led to significantly better overall Parkinson's Disease Sleep Scale-1 (PDSS) scores ($p < 0.001$) at 36-month follow-up, indicating substantial improvement in sleep quality. Specific domains demonstrating significant improvement in the STN-DBS group included overall quality of night's sleep, sleep onset and maintenance insomnia, nocturnal restlessness, and nocturnal motor symptoms. In contrast, the MED group experienced a significant worsening in nocturia and nocturnal motor symptoms. STN-DBS was observed to stabilize nocturia and sleep refreshment, while these aspects worsened in the MED group ($P = 0.027$ and $P = 0.032$, respectively). These sleep improvements were significantly correlated with enhanced quality of life ($rs = –0.40$, $p < 0.001$) and motor symptom amelioration ($rs = –0.35$, $p = 0.002$), and remarkably, were independent of changes in depression, anxiety, or dopaminergic medication requirements. Potential mechanisms for improved sleep include enhanced motor function, modulation of brain regions adjacent to the STN, like the pedunculopontine nucleus and improved sensory processing [72].

4.3. Neuropsychiatric symptoms

The influence of DBS on the diverse spectrum of neuropsychiatric symptoms associated with PD is equally significant, albeit more complex and variable, profoundly affecting patients' overall quality of life. These non-motor disturbances, including mood disorders, apathy, impulsivity, and changes in personality and perception, can manifest either as improvements or, in some cases, as exacerbations or de novo occurrences following DBS [4,74,113,114].

A comprehensive meta-analysis of long-term (1–3 years) neuropsychological outcomes indicated a mild, statistically significant improvement in anxiety and depression scores for STN-DBS patients, with a Hedges' g of 0.34 ($p = 0.02$) for STN stimulation. Similarly, GPi-DBS showed a small, significant improvement in depression, with a standardized mean difference (SMD) of 0.11 ($p = 0.03$). This meta-analysis further noted an anxiety improvement with an SMD of 0.30 ($p = 0.01$) [4].

In contrast, other studies reported no significant long-term changes in anxiety and depression levels after STN-DBS when compared to standard medical therapy [72,111].

Changes in depression and anxiety scores are predictive of QoL after STN-DBS. However, apathy and depression were more frequent in the DBS group after 12 years compared to the drug-treated group [102].

Apathy, characterized by a loss of motivation and reduced initiative, represents a frequently reported and often challenging neuropsychiatric symptom in PD that can significantly impact QoL [114–116]. The effects of STN-DBS on apathy are notably controversial. A meta-analysis of 33 articles involving 1,286 patients revealed that apathy scores were significantly higher after STN-DBS compared to both the pre-operative state (Hedges' $g = 0.34$, 95% CI = 0.19–0.48, $p < 0.001$) and control groups receiving only medication (Hedges' $g = 0.36$, 95% CI = 0.03–0.65; $p = 0.004$) [115]. This increase in apathy appeared independent of the reduction in dopaminergic medication, and was even greater if patients with baseline apathy were excluded (Hedges' $g = 0.79$, $P < 0.001$) [115]. Factors such as inaccurate electrode placement within the STN, particularly in associative or limbic areas, rather than the motor portion, have been implicated in inducing or exacerbating apathy [116]. This study suggests a correlation between apathy and more dorsolateral stimulation of the left STN [116]. Apathy scores (AES) showed a slight, non-significant decrease after STN-DBS (54.00 ± 10.30 to 52.69 ± 8.88) at 6 months post-DBS, attributed to a conservative and gradual reduction of dopaminergic drugs [116]. In contrast to STN-DBS, GPi-DBS has been associated with no significant changes in apathy scores postoperatively, possibly due to less pronounced reductions in LEDD [116].

ICB are important considerations given their prevalence in PD and their association with dopaminergic therapy [94]. STN-DBS can lead to complex and variable effects on ICB. While ICB often improves post-DBS, particularly due to the typical reduction in dopaminergic medication, de novo ICB can also emerge [74,94]. 6 months post-DBS, patients with preoperative ICB showed significant improvement in scores on the Questionnaire for Impulsive-Compulsive Disorders in PD-Rating Scale (QUIP-RS). However, there was considerable interindividual variability, with 27.3% experiencing worsening and 29.1% showing improvement [94]. Another study investigating personality traits noted that STN-DBS might have effects on impulsivity, especially a decline in persistence. This was observed even with lowered medication doses, suggesting an effect of DBS beyond pharmacological changes [117]. Impulsivity, as evaluated by scales like the Barratt Impulsiveness Scale 11 (BIS11) and Behavioral Inhibition System/Behavioral Activation System (BIS/BAS), has also been significantly associated with postoperative quality of life at different follow-up points after STN-DBS [114].

Personality and self-perception can be affected following DBS, although early reports raising concerns about unwanted identity or personality changes were often based on retrospective data or case reports with methodological limitations. A recent prospective, patient-centered cohort study specifically investigated changes in characteristics that patients with PD themselves identified as personally meaningful and feared losing. This study found that, at a group level, DBS did not result in negative changes in these valued personal characteristics. Instead, participants often reported greater (more positive) manifestations of these traits 6- and 12-months post-DBS. While negative changes were observed in 4 out of 49 patients, the majority reported no change or increased manifestation across domains such as prosociality, cognition, self-regulation, and positive emotionality. These changes were observed to be unrelated to improvements in motor scores, and behaviors related to positive emotions were among the characteristics patients most feared losing [113].

Regarding perceptual problems and hallucinations, a long-term follow-up study reported that hallucinations were present in 58% of PD patients after at least ten years of DBS treatment [4]. However, a more recent prospective, observational multicenter study indicated improved perceptual problems and hallucinations specifically in patients with the PIGD motor subtype, while outcomes remained stable in tremor-dominant patients after 6 months of DBS [73]. This improvement was partly attributed to the postoperative reduction of dopaminergic medication [73].

4.4. Quality of Life

DBS has presented benefits in QoL in multiple studies. For example, one study noted that 80.8% of the cohort reported “much or very much improvement” in Health-Related Quality of Life (HRQoL) [118]. Tandra et al. reported an improvement in the Parkinson’s Disease Questionnaire (PDQ-39) by 49% [18]. These results are sustained even after 5 years post-DBS, unlike the patients just on medication who exhibit QoL deterioration [119]. Combining scalp nerve block with intercostal nerve block improves the quality of recovery after DBS [120].

Medication usage is also decreasing. One study shows a 47% reduction in the LEDD at one year post-surgery [121]. Furthermore, another study noted that 10 years after the STN-DBS, mean LEDD was 600 mg in DBS patients vs. 1316 mg in controls ($p < 0.001$), sustaining the initial benefits [122]. When implemented in earlier stages of PD, DBS has been shown to lower medication costs by a factor of 2.4 over a five-year period compared to standard medical therapy alone [123].

Degirmenci et al. [17] analyzed STN-DBS from the caregivers’ perspective via telephone interviews. Caregivers noted improvements in both motor symptoms (tremor 58.1%, dyskinesia 59.6%, gait/ataxia 59.6%) and non-motor symptoms (depression 46.8%, sleep 43.6%, pain 41.9%). Notably, 80.6% of patients showed better daily life functioning post-DBS, reducing caregivers’ burden [17].

5. Complications

As with any surgical procedure, DBS is associated with a spectrum of potential complications and limitations that must be comprehensively addressed during the preoperative informed consent process. These encompass acute neurological disturbances, such as delirium, to diverse surgical and hardware-related problems, as well as other specific postoperative concerns [30,124].

A notable neurocognitive adverse event observed is postoperative delirium (POD), which manifests as an acute disruption of attention and awareness, coupled with cognitive alterations. Its fluctuating symptoms often include hallucinations, confusion, and disorientation. While incidence ranges from 5.8% to 42.6%, it is often insufficiently studied in the context of DBS. Different diagnostic criteria and detection methods may contribute to this variation. A prospective study focusing on POD showed that in 21 out of 57 (36.8%) of PD patients after the procedure. These cases generally presented with mild severity. The typical onset was rapid, approximately 1.7 ± 2.0 days after surgery, and lasted for an average of 7.5 ± 6.4 days, even up to 21 days in some cases. The clinical significance of POD is underscored because it is linked to worse prognoses, elevated mortality, and accelerated PD progression [124].

Beyond postoperative delirium, individuals undergoing DBS are vulnerable to various surgical and hardware-related complications. An investigation involving 800 PD patients who received STN-DBS reported that 8.4% encountered intracranial complications resulting in neurological deficits; of these, 7.4% were temporary, while 1.0% led to lasting impairment. The most critical acute complication observed was ICH, manifesting symptomatically in 2.8% (22 patients) of this patient group. Out of these, 0.6% (5 patients) sustained permanent neurological deficits, encompassing conditions like hemiparesis, severe cognitive impairment, hemiplegia, persistent diplopia, dysarthria, and balance disorders. The other 16 patients experienced transient deficits, such as aphasia, dysarthria, central facial palsy, frontal lobe syndrome, delirium, and cognitive decline, which typically resolved within six months to a year. Although previous research has suggested various risk factors for ICH, including the quantity of MER trajectories, age, anesthesia technique, hypertension, and sex, this extensive retrospective study did not establish a statistically significant impact for these factors across the entire cohort. However, a higher risk was noted for patients who did not undergo MER compared to those with a single MER trajectory. Strategies to mitigate ICH include precise preoperative trajectory planning to bypass blood vessels, positioning the trajectory entry over a sulcus, and applying fibrin glue in the burr hole to minimize brain shift [30].

The necessity for revision surgeries constitutes a notable limitation, with 18.4% of patients in a particular cohort undergoing an additional surgical procedure after their initial DBS system implantation. Notably, this rate significantly diminished over time, falling from 27.3% among the first 300 cases to 13.0% in the following 500 cases ($p < 0.001$), highlighting an evident learning curve and improvements in surgical methodologies. Frequent causes for revision included infection (3.4% overall), which also saw a reduction from 5.3% to 2.2% over the study period and often mandated complete hardware extraction, antibiotic therapy, and later reimplantation. Lead migration also represented a reason for revision, impacting 2.1% of patients. However, the prevalence of lead migration was substantially lowered using lead anchoring devices (1.1% of electrodes) when contrasted with previous miniplate fixation techniques (6.3% of electrodes; OR: 0.15, 95% CI: 0.05–0.32, $p < 0.001$). Other triggers for revision included skin erosion, hardware malfunctions, and pain, with pain emerging as the most common reason in this study [30].

Delayed-onset edema localized around the DBS leads was noted in 1.6% (13 patients). This condition typically manifests with temporary symptoms such as cognitive decline, dysarthria, apathy, and confusion, with only a single patient experiencing persistent mild cognitive impairment. This form of edema was more commonly observed with segmented leads (3.1% of 390 patients with segmented leads) when contrasted with traditional ring electrodes, though enhanced awareness and reporting in more recent years might contribute to this perceived difference. The overall incidence of delirium documented within this cohort was 4.3%, a figure recognized as being lower than in some other studies, potentially attributable to underreporting in a retrospective study design without standardized delirium assessment. Fatalities directly associated with DBS electrode implantation were infrequent, with one instance of cardiac arrest following IPG replacement and another death due to a hip fracture, neither of which was deemed directly caused by the electrode placement itself [30].

It is crucial to acknowledge the inherent limitations of the studies themselves. The retrospective design of some analyses, particularly the extensive cohort study, inherently carries a risk of incomplete data or the underreporting of milder, transient complications. The lengthy observational periods, spanning over two decades in the retrospective study of surgical complications, introduce heterogeneity resulting from ongoing advancements in surgical techniques, imaging, and hardware. This makes direct comparisons across the entire cohort challenging [30]. Moreover, the comparatively small sample size in certain prospective studies, such as the one investigating POD severity (n=57), restricts the statistical power to identify all significant predictors, especially when numerous potential factors are explored. Although the predictive models developed for POD severity showed performance better than random chance, they might not yet offer clinically meaningful predictive capabilities, underscoring the necessity for validation through larger, international multicenter trials. Finally, distinguishing acute delirium symptoms from pre-existing PD symptoms, such as fluctuating hallucinations or attention deficits, can present a diagnostic difficulty [124].

6. Future directions

The increasing integration of digital technologies, artificial intelligence, and wearable devices into neurological practice may further facilitate objective and longitudinal monitoring of patients [125]. Machine learning (ML) is paving the way for personalized care, being used in various stages such as patient selection, outcome prediction, and parameter management [20]. To predict clinical outcomes, Chang et al. [126] used a DLRad model, which combines multi-instance learning (MIL) and radiomics features. It achieved the highest discriminative ability with an Area Under the Curve (AUC) of 0.871 in the test cohort, higher than radiomics (AUC 0.825) and MIL models (AUC 0.846) alone. When age was added to the combined model, a decrease in AUC 0.858 appeared. This suggests that age didn't add predictive value, underlining the need for careful feature selection [126].

In another study, ML found predictors of QoL after DBS. It was found that the PDQ-39 scores and upper beta band activity (>20 Hz) in the left STN can influence QoL. Lower initial QoL burden predicted worsening, while higher beta activity was linked to improvement [127].

Deep learning combined with microelectrode recording (MER) was used to predict motor improvements after bilateral STN-DBS. The learning model presented 80.21% maximal accuracy and an AUC of 0.88, proving deep learning's capabilities to predict clinical improvements [28].

Vision-based machine learning models were also tried for analyzing changes in gait in PD patients. While the model couldn't predict gait scores with accuracy, it could detect weak but real improvements in walking after medication and DBS use. For now, they are hard to apply universally, due to differences in gait and camera angles. Large, diverse datasets are needed to improve the current state of this technique [128].

The future is adaptive. Despite being a great option for PD patients, conventional DBS (cDBS) lacks the ability to adjust to the patient's changing needs [129]. Adaptive DBS (aDBS) aims to overcome the limitations of cDBS by using real-time detection of brain signals to automatically adjust stimulation parameters in response to patients' needs [129]. A study showed that aDBS is effective, providing more energy when needed and less when it's not, works well with medication, and is safe [129]. Above that, ML is explored as a way to identify electrophysiological biomarkers for aDBS [20].

Robot-Assisted DBS (RAS-DBS) can be a reliable and safe approach for PD patients. It offers greater accuracy than traditional methods, with a pooled vector error of 1.09 mm versus 1.11 to 3.70 mm. However, RAS-DBS shows similar improvements in motor symptoms and reduction of medication, compared to the standard procedure [130].

CONCLUSION

DBS is an effective therapy for PD, offering sustained symptom benefits, medication reduction, and better QoL. However, outcomes may be heterogeneous: while tremor and rigidity show sustained improvements, axial symptoms like speech remain challenging to treat. Future advances in adaptive stimulation and machine learning promise more personalized and precise DBS, expanding its therapeutic reach while minimizing risks.

Conflicts of interest and sources of funding

The authors declare no conflict of interest.

This research received no external funding.

Acknowledgments

This article was written as part of the "Tech-Review Summer School: academic writing summer camp for young researchers" organized by the Center of Innovation and e-Health, Carol Davila University of Medicine and Pharmacy in Bucharest.

Authors' contribution

Conceptualization, G.-S.D., M.-C.M., A.-R.T. and O.A; methodology, G.-S.D., M.-C.M. and A.-R.T.; validation, A.-R.T., O.A., O.M.S., M.M.M.; formal analysis, G.-S.D. and M.-C.M.; investigation, G.-S.D., M.-C.M. and A.-R.T.; resources, O.A., O.M.S and M.M.M.; data curation, G.-S.D., M.-C.M. and A.-R.T.; writing—original draft preparation, G.-S.D. and M.-C.M.; writing—review and editing, A.-R.T., O.A., O.M.S. and M.M.M; visualization, G.-S.D., M.-C.M. and A.-R.T.; supervision, A.-R.T. O.M.S and O.A.; project administration, A.-R.T. O.A, and M.M.M. All authors have read and agreed to the published version of the manuscript.

Ethics approval and consent to participate

Not applicable.

Patient consent for publication

Not applicable.

References

1. Moshayedi, A.J.; Mokhtari, T.; Emadi Andani, M. Brain Stimulation Techniques in Research and Clinical Practice: A Comprehensive Review of Applications and Therapeutic Potential in Parkinson's Disease. Brain Sci. 2025, 15, 20, doi:10.3390/brainsci15010020.
2. Andrews, L.; Keller, S.S.; Bhojak, M.; Osman-Farah, J.; Macerollo, A. Investigating the Neural Correlates of Subjective Sleep Changes Following Subthalamic Nucleus Deep Brain Stimulation for Parkinson's Disease. Parkinsonism Relat. Disord. 2025, 136, 107887, doi:10.1016/j.parkreldis.2025.107887.
3. Canesi, M.; Lippi, L.; Rivaroli, S.; Vavassori, D.; Trenti, M.; Sartorio, F.; Meucci, N.; de Sire, A.; Siri, C.; Invernizzi, M. Long-Term Impact of Deep Brain Stimulation in Parkinson's Disease: Does It Affect Rehabilitation Outcomes? Medicina 2024, 60, 927, doi:10.3390/medicina60060927.
4. Bucur, M.; Papagno, C. Deep Brain Stimulation in Parkinson Disease: A Meta-Analysis of the Long-Term Neuropsychological Outcomes. Neuropsychol. Rev. 2023, 33, 307–346, doi:10.1007/s11065-022-09540-9.
5. Yuzkan, S.; Hasimoglu, O.; Balsak, S.; Mutlu, S.; Karagulle, M.; Kose, F.; Altinkaya, A.; Tugcu, B.; Kocak, B. Utility of Diffusion Tensor Imaging and Generalized Q-Sampling Imaging for Predicting Short-Term Clinical Effect of Deep Brain Stimulation in Parkinson's Disease. Acta Neurochir. 2024, 166, 217, doi:10.1007/s00701-024-06096-w.
6. Chen, W.; Wang, M.; Wang, N.; Du, C.; Ma, X.; Li, Q. The Impacts of Subthalamic Nucleus-Deep Brain Stimulation (STN-DBS) on the Neuropsychiatric Function of Patients with Parkinson's Disease Using Image Features of Magnetic Resonance Imaging under the Artificial Intelligence Algorithms. Contrast Media Mol. Imaging 2021, 2021, 9915206, doi:10.1155/2021/9915206.
7. Hariz, M.; Blomstedt, P. Deep Brain Stimulation for Parkinson's Disease. J. Intern. Med. 2022, 292, 764–778, doi:10.1111/joim.13541.
8. Enache, I.I.; Dragos, D.; Stoican, C.; et al. Oxidative Stress and Nutritional Antioxidants in Neurological Diseases. Rom. J. Mil. Med. 2025, 128, 215–224, doi:10.55453/rjmm.2025.128.3.5.
9. Peña-Zelayeta, L.; Delgado-Minjares, K.M.; Villegas-Rojas, M.M.; León-Arcia, K.; Santiago-Balmaseda, A.; Andrade-Guerrero, J.; Pérez-Segura, I.; Ortega-Robles, E.; Soto-Rojas, L.O.; Arias-Carrión, O. Redefining Non-Motor Symptoms in Parkinson's Disease. J. Pers. Med. 2025, 15, 172, doi:10.3390/jpm15050172.
10. Lee, J.M.; Pak, K. Comparison of UPDRS III Score between Young and Late Onset Parkinson Disease after Deep Brain Stimulation: A Meta-Analysis. Medicine 2023, 102, e35861, doi:10.1097/MD.0000000000035861.
11. Schoen, D.; Deutsch, S.; Mehta, J.; Wang, S.; Kornak, J.; Starr, P.A.; Wang, D.D.; Ostrem, J.L.; Bledsoe, I.O.; Morrison, M.A. Boundary Complexity of Cortical and Subcortical Areas Predicts Deep Brain Stimulation Outcomes in Parkinson's Disease. Nat. Commun. 2025, 16, 5590, doi:10.1038/s41467-025-60695-4.
12. França, C.; Carra, R.B.; Diniz, J.M.; Munhoz, R.P.; Cury, R.G. Deep Brain Stimulation in Parkinson's Disease: State of the Art and Future Perspectives. Arq. Neuropsiquiatr. 2022, 80, 105–115, doi:10.1590/0004-282X-ANP-2022-S133.
13. Mahlknecht, P.; Foltynie, T.; Limousin, P.; Poewe, W. How Does Deep Brain Stimulation Change the Course of Parkinson's Disease? Mov. Disord. 2022, 37, 1581–1592, doi:10.1002/mds.29052.
14. Artusi, C.A.; Lopiano, L.; Morgante, F. Deep Brain Stimulation Selection Criteria for Parkinson's Disease: Time to Go beyond CAPSIT-PD. J. Clin. Med. 2020, 9, 3931, doi:10.3390/jcm9123931.
15. Yao, L.; Chen, R.; Zheng, Z.; Hatami, M.; Koc, S.; Wang, X.; Bai, Y.; Yao, C.; Lu, G.; Skutella, T. Translational Evaluation of Metabolic Risk Factors Impacting DBS Efficacy for PD-Related Sleep and Depressive Disorders: Preclinical, Prospective and Cohort Studies. Int. J. Surg. 2025, 111, 543–566, doi:10.1097/JS9.0000000000002081.
16. Doshi, P.K.; Das, D. Deep Brain Stimulation for Parkinson's Disease: Currents Status and Emerging Concepts. Neurol. India 2020, 68, S179–S186, doi:10.4103/0028-3886.302466.

17. Degirmenci, Y.; Tezcan, S.; Savas, A.; Akbostanci, M.C. Caregivers' Impression About the Effect of Subthalamic Nucleus Deep Brain Stimulation in the Treatment of Parkinson's Disease. Turk. Neurosurg. 2023, 33, 393–397, doi:10.5137/1019-5149.JTN.40367-22.2.
18. Tandra, S.; Ramavath, B.; Kandadai, R.M.; Jabeen, S.A.; Kannan, M.A.; Borgohain, R. Functional Outcome of Bilateral Subthalamic Nucleus-Deep Brain Stimulation in Advanced Parkinson's Disease Patients: A Prospective Study. Ann. Indian Acad. Neurol. 2020, 23, 54–58, doi:10.4103/aian.AIAN_357_18.
19. Yim, Y.; Kim, S.J.; Jung, S.C.; Kim, H.S.; Choi, C.G.; Lee, J.K.; Lee, C.S.; Lee, S.H.; Shim, W.H.; Cheong, E.-N.; et al. Pretreatment Brain Volumes Can Affect the Effectiveness of Deep Brain Stimulation in Parkinson's Disease Patients. Sci. Rep. 2020, 10, 22065, doi:10.1038/s41598-020-79138-9.
20. Oliveira, A.M.; Coelho, L.; Carvalho, E.; Ferreira-Pinto, M.J.; Vaz, R.; Aguiar, P. Machine Learning for Adaptive Deep Brain Stimulation in Parkinson's Disease: Closing the Loop. J. Neurol. 2023, 270, 5313–5326, doi:10.1007/s00415-023-11873-1.
21. Ozturk, M.; Viswanathan, A.; Sheth, S.A.; Ince, N.F. Electroceutically Induced Subthalamic High-Frequency Oscillations and Evoked Compound Activity May Explain the Mechanism of Therapeutic Stimulation in Parkinson's Disease. Commun. Biol. 2021, 4, 393, doi:10.1038/s42003-021-01915-7.
22. Sun, J.; Ma, S.; Li, Z.; Jia, J.; Wu, Q.; Hou, Y.; Wang, H.; Wang, Q.; Zhang, G.; Zhao, Z.; et al. The Reduction of LEDD Leads to Visual Dysfunction in Patients with PD after STN-DBS: A Randomized Clinical Trial. Int. J. Surg. 2025, 111, 650–660, doi:10.1097/JS9.0000000000002018.
23. Boon, L.I.; Hillebrand, A.; Potters, W.V.; de Bie, R.M.A.; Prent, N.; Bot, M.; Schuurman, P.R.; Stam, C.J.; van Rootselaar, A.-F.; Berendse, H.W. Motor Effects of Deep Brain Stimulation Correlate with Increased Functional Connectivity in Parkinson's Disease: An MEG Study. Neuroimage Clin. 2020, 26, 102225, doi:10.1016/j.nicl.2020.102225.
24. Wagle Shukla, A.; Bange, M.; Muthuraman, M. Patient, Target, Device, and Program Selection for DBS in Parkinson's Disease: Advancing toward Precision Care. NPJ Parkinsons Dis. 2025, 11, 195, doi:10.1038/s41531-025-01015-x.
25. Fan, S.; Liu, D.; Shi, L.; Meng, F.; Fang, H.; Liu, H.; Zhang, H.; Yang, A.; Zhang, J. Differential Effects of Subthalamic Nucleus and Globus Pallidus Internus Deep Brain Stimulation on Motor Subtypes in Parkinson's Disease. World Neurosurg. 2022, 164, e245–e255, doi:10.1016/j.wneu.2022.04.084.
26. Murcia Carretero, S.; Petermann, K.; Debove, I.; Amstutz, D.; Sousa, M.; Waskönig, J.; Diamantaras, A.A.; Tinkhauser, G.; Nowacki, A.; Pollo, C.; et al. Quality of Life after Deep Brain Stimulation in Parkinson's Disease: Does the Target Matter? Mov. Disord. Clin. Pract. 2024, 11, 1379–1387, doi:10.1002/mdc3.14199.
27. Izzo, A.; Piano, C.; D'Ercole, M.; D'Alessandris, Q.G.; Tufo, T.; Fuggetta, M.F.; Figà, F.; Martinelli, R.; Obersnel, M.; Pambianco, F.; et al. Intraoperative Microelectrode Recording during Asleep Deep Brain Stimulation of Subthalamic Nucleus for Parkinson Disease. A Case Series with Systematic Review of the Literature. Neurosurg. Rev. 2024, 47, 342, doi:10.1007/s10143-024-02563-1.
28. Park, K.H.; Sun, S.; Lim, Y.H.; Park, H.R.; Lee, J.M.; Park, K.; Jeon, B.; Park, H.-P.; Kim, H.C.; Paek, S.H. Clinical Outcome Prediction from Analysis of Microelectrode Recordings Using Deep Learning in Subthalamic Deep Brain Stimulation for Parkinson's Disease. PLoS ONE 2021, 16, e0244133, doi:10.1371/journal.pone.0244133.
29. Holewijn, R.A.; Verbaan, D.; van den Munckhof, P.M.; Bot, M.; Geurtsen, G.J.; Dijk, J.M.; Odekerken, V.J.; Beudel, M.; de Bie, R.M.A.; Schuurman, P.R. General Anesthesia vs Local Anesthesia in Microelectrode Recording-Guided Deep-Brain Stimulation for Parkinson Disease: The GALAXY Randomized Clinical Trial. JAMA Neurol. 2021, 78, 1212–1219, doi:10.1001/jamaneurol.2021.2979.
30. Holewijn, R.A.; Wiggerts, Y.; Bot, M.; Verbaan, D.; de Bie, R.M.A.; Schuurman, R.; van den Munckhof, P. Surgical Complications in Subthalamic Nucleus Deep Brain Stimulation for Parkinson's Disease: Experience in 800 Patients. Stereotact. Funct. Neurosurg. 2024, 102, 275–283, doi:10.1159/000539483.
31. Roldán, P.; Mosteiro, A.; Rumià Arboix, J.; Asín, D.; Sánchez-Gómez, A.; Valldeoriola, F.; García-Orellana, M.; de Riva, N.; Valero, R. Subthalamic Deep Brain Stimulation under General Anaesthesia for Parkinson's Disease: Institutional Experience and Outcomes. Stereotact. Funct. Neurosurg. 2025, 103, 102–110, doi:10.1159/000542791.
32. Louie, K.H.; Petrucci, M.N.; Grado, L.L.; Lu, C.; Tuite, P.J.; Lamperski, A.G.; MacKinnon, C.D.; Cooper, S.E.; Netoff, T.I. Semi-Automated Approaches to Optimize Deep Brain Stimulation Parameters in Parkinson's Disease. J. Neuroeng. Rehabil. 2021, 18, 83, doi:10.1186/s12984-021-00873-9.
33. Hacker, M.L.; Isaacs, D.A.; Rajamani, N.; Pazira, K.; Abdou, E.; Sharp, S.; Davis, T.L.; Hedera, P.; Phibbs, F.T.; Charles, D.; et al. Evaluating a Motor Progression Connectivity Model across Parkinson's Disease Stages. J. Neurol. 2024, 271, 7309–7315, doi:10.1007/s00415-024-12703-8.
34. Nazan, Ş.E.; Gökçe, G.G.Y.; Tanju, U.; Sehur, Ö.S. Effects of the Combined Treatment of Bilateral Subthalamic Nucleus Stimulation and Levodopa on Balance and Mobility in Parkinson's Disease. Ideggyogy. Sz. 2023, 76, 173–179, doi:10.18071/isz.76.0173.
35. Tsuboi, T.; Lemos Melo Lobo Jofili Lopes, J.; Moore, K.; Patel, B.; Legacy, J.; Ratajska, A.M.; Bowers, D.; Eisinger, R.S.; Almeida, L.; Foote, K.D.; et al. Long-Term Clinical Outcomes of Bilateral GPi Deep Brain Stimulation in Advanced Parkinson's Disease: 5 Years and Beyond. J. Neurosurg. 2021, 135, 601–610, doi:10.3171/2020.6.JNS20617.
36. Zhang, F.; Wang, F.; Li, W.; Wang, N.; Han, C.; Fan, S.; Li, P.; Xu, L.; Zhang, J.; Meng, F. Relationship between Electrode Position of Deep Brain Stimulation and Motor Symptoms of Parkinson's Disease. BMC Neurol. 2021, 21, 122, doi:10.1186/s12883-021-02148-1.
37. Wu, S.; Cen, Z.; Zheng, X.; Xie, F.; Luo, W. Investigation of the Impact of Deep Brain Stimulation of the Subthalamic Nucleus on Parkinson Disease Patients with Genetic Risk Factors/Causes. World Neurosurg. 2025, 198, 124021, doi:10.1016/j.wneu.2025.124021.
38. Jorge, A.; Dastolfo-Hromack, C.; Lipski, W.J.; Kratter, I.H.; Smith, L.J.; Gartner-Schmidt, J.L.; Richardson, R.M. Anterior Sensorimotor Subthalamic Nucleus Stimulation Is Associated With Improved Voice Function. Neurosurgery 2020, 87, 788–795, doi:10.1093/neuros/nyaa024.
39. Jiang, L.; Chen, W.; Guo, Q.; Yang, C.; Gu, J.; Xian, W.; Liu, Y.; Zheng, Y.; Ye, J.; Xu, S.; et al. Eight-Year Follow-up Outcome of Subthalamic Deep Brain Stimulation for Parkinson's Disease: Maintenance of Therapeutic Efficacy with a Relatively Low Levodopa Dosage and Stimulation Intensity. CNS Neurosci. Ther. 2021, 27, 1366–1373, doi:10.1111/cns.13713.
40. Swinnen, B.E.K.S.; Lotfalla, V.; Scholten, M.N.; Prins, R.H.N.; Goes, K.M.; de Vries, S.; Geytenbeek, J.J.M.; Dijk, J.M.; Odekerken, V.J.; Bot, M.; et al. Programming Algorithm for the Management of Speech Impairment in Subthalamic Nucleus Deep Brain Stimulation for Parkinson's Disease. Neuromodulation 2024, 27, 528–537, doi:10.1016/j.neurom.2023.05.002.
41. Herz, D.M.; Blech, J.; Winter, Y.; Gonzalez-Escamilla, G.; Groppa, S. Low-Frequency Deep Brain Stimulation in Non-Rapid Eye Movement Sleep Modifies Memory Retention in Parkinson's Disease. Mov. Disord. 2025, 40, 285–291, doi:10.1002/mds.30064.
42. Artusi, C.A.; Ledda, C.; Gallo, S.; Rinaldi, D.; Campisi, C.; Rousseau, V.; Thalamas, C.; Barbosa, R.; Ory-Magne, F.; Brefel-Courbon, C.; et al.

Subthalamic and Nigral Stimulation for Freezing of Gait in Parkinson's Disease: Randomized Pilot Trial. J. Parkinsons Dis. 2024, 14, 1602–1613, doi:10.1177/1877718X241292315.
43. Lin, Z.; Zhang, C.; Li, D.; Sun, B. Lateralized Effects of Deep Brain Stimulation in Parkinson's Disease: Evidence and Controversies. NPJ Parkinsons Dis. 2021, 7, 64, doi:10.1038/s41531-021-00209-3.
44. Rajamani, N.; Friedrich, H.; Butenko, K.; Dembek, T.; Lange, F.; Navrátil, P.; Zvarova, P.; Hollunder, B.; de Bie, R.M.A.; Odekerken, V.J.J.; et al. Deep Brain Stimulation of Symptom-Specific Networks in Parkinson's Disease. Nat. Commun. 2024, 15, 4662, doi:10.1038/s41467-024-48731-1.
45. Lam, J.; Lee, J.; Williams, M.; Cohn, M.; Wilson, M.; Mark, C.; Esnaashari, N.; Petkus, A.; Hui, J.; Feigenbaum, D.; et al. Cognitive Effects of Theta Frequency Bilateral Subthalamic Nucleus Stimulation in Parkinson's Disease: A Pilot Study. Brain Stimul. 2021, 14, 230–240, doi:10.1016/j.brs.2020.12.014.
46. Imbalzano, G.; Montanaro, E.; Ledda, C.; Donetto, F.; D'Angelo, F.; Campisi, C.; Artusi, C.A.; Romagnolo, A.; Rizzone, M.G.; Bozzali, M.; et al. Theta-Gamma Subthalamic Stimulation for Verbal Fluency in Parkinson's Disease: A Randomized, Crossover Trial. Mov. Disord. 2025, 40, 1189–1194, doi:10.1002/mds.30218.
47. Munoz, M.J.; Reilly, J.L.; Pal, G.D.; Verhagen Metman, L.; Sani, S.B.; Rosenow, J.M.; Rivera, Y.M.; Drane, Q.H.; Goelz, L.C.; Corcos, D.M.; et al. Benefits of Subthalamic Nucleus Deep Brain Stimulation on Visually-Guided Saccades Depend on Stimulation Side and Classic Paradigm in Parkinson's Disease. Clin. Neurophysiol. 2024, 162, 41–52, doi:10.1016/j.clinph.2024.03.010.
48. Tamir, I.; Wang, D.; Chen, W.; Ostrem, J.L.; Starr, P.A.; de Hemptinne, C. Eight Cylindrical Contact Lead Recordings in the Subthalamic Region Localize Beta Oscillations Source to the Dorsal STN. Neurobiol. Dis. 2020, 146, 105090, doi:10.1016/j.nbd.2020.105090.
49. Antenucci, P.; Colucci, F.; Gozzi, A.; Scerrati, A.; Cavallo, M.A.; Capone, J.G.; Pugliatti, M.; Sensi, M. Global Improvement after Deep Brain Stimulation in Parkinson's Disease: Comparison between Patient and Clinician Perspectives. J. Clin. Neurosci. 2025, 137, 111323, doi:10.1016/j.jocn.2025.111323.
50. Andrews, J.C.; Roy, F.D.; Ba, F.; Sankar, T. Intraoperative Changes in the H-Reflex Pathway during Deep Brain Stimulation Surgery for Parkinson's Disease: A Potential Biomarker for Optimal Electrode Placement. Brain Stimul. 2020, 13, 1765–1773, doi:10.1016/j.brs.2020.09.024.
51. Ricciuti, R.A.; Ottaviani, M.M.; Mancini, F.; Marano, M.; Marruzzo, D.; Barbieri, F.; Paracino, R.; De Domenico, P.; Pagano, S.; Di Lazzaro, V.; et al. Deep Brain Stimulation in Parkinson's Disease: A Comparison of Accuracy and Clinical Outcomes of Frame-Based, Frameless and Frameless Fiducial-Less Techniques. Neurol. Sci. 2025, 46, 2675–2685, doi:10.1007/s10072-025-08102-0.
52. Lachenmayer, M.L.; Mürset, M.; Antih, N.; Debove, I.; Muellner, J.; Bompart, M.; Schlaeppi, J.-A.; Nowacki, A.; You, H.; Michelis, J.P.; et al. Subthalamic and Pallidal Deep Brain Stimulation for Parkinson's Disease—Meta-Analysis of Outcomes. NPJ Parkinsons Dis. 2021, 7, 77, doi:10.1038/s41531-021-00223-5.
53. Hasimoglu, O.; Karaçoban, T.Ö.; Hanoglu, T.; Geylan, N.B.; Altinkaya, A.; Erkan, B.; Postalci, L.Ş.; Tugcu, B. Anatomical Determinants of STN Coordinate Shift in Idiopathic Parkinson's Disease DBS Surgery. CNS Neurosci. Ther. 2025, 31, e70307, doi:10.1111/cns.70307.
54. Pham, T.A.; Luong, C.M.; Dao, P.D.; Vo, N.T.; Tran, T.N.; Diem Nguyen, T.A. How Do Craniometric Measurements and Skull Morphology Influence Subthalamic Nucleus Target Coordinations in Deep Brain Stimulation Surgery for Parkinson Disease? World Neurosurg. 2025, 194, 123366, doi:10.1016/j.wneu.2024.10.095.
55. Li, Z.; Sun, J.; Lin, H.; Wu, Q.; Jia, J.; Guo, X.; Li, W. Predicting Motor Function Improvement Following Deep Brain Stimulation of the Subthalamic Nucleus for Parkinson's Disease Based on STN-T2MRI Radiomics. J. Parkinsons Dis. 2025, 15, 561–572, doi:10.1177/1877718X251319697.
56. Dong, J.; Peschke, S.; Kirschner, A.; Palleis, C.; Mehrkens, J.H.; Scherer, M.; Kaufmann, E.; Koeglsperger, T. Subjective Patient Rating as a Novel Feedback Signal for DBS Programming in Parkinson's Disease. Brain Stimul. 2025, 18, 770–779, doi:10.1016/j.brs.2025.03.008.
57. Nickl, R.C.; Eldebakey, H.; Grossmann, J.A.; Roothans, J.; Navrátil, P.; Isaias, I.U.; Lange, F.; Fricke, P.; Capetian, P.; Matthies, C.; et al. Probabilistic Mapping of Gait Changes after STN-DBS for Parkinson's Disease. Parkinsonism Relat. Disord. 2025, 136, 107871, doi:10.1016/j.parkreldis.2025.107871.
58. Koivu, M.; Sihvonen, A.J.; Eerola-Rautio, J.; Pauls, K.A.M.; Resendiz-Nieves, J.; Vartiainen, N.; Kivisaari, R.; Scheperjans, F.; Pekkonen, E. Clinical and Brain Morphometry Predictors of Deep Brain Stimulation Outcome in Parkinson's Disease. Brain Topogr. 2024, 37, 1186–1194, doi:10.1007/s10548-024-01054-2.
59. Cai, Y.Z.; Zheng, Y.; Li, W.; Saffari, S.E.; Ng, H.L.; Zhan, A.; Xu, Z.; Tay, K.Y.; Au, W.L.; Ng, W.H.; et al. Long-Term Outcomes of Subthalamic Nucleus Deep Brain Stimulation for Parkinson's Disease in Singapore. Ann. Acad. Med. Singap. 2024, 53, 481–489, doi:10.47102/annals-acadmedsg.2023374.
60. Dafsari, H.S.; Dos Santos Ghilardi, M.G.; Visser-Vandewalle, V.; Rizos, A.; Ashkan, K.; Silverdale, M.; Evans, J.; Martinez, R.C.R.; Cury, R.G.; Jost, S.T.; et al. Beneficial Nonmotor Effects of Subthalamic and Pallidal Neurostimulation in Parkinson's Disease. Brain Stimul. 2020, 13, 1697–1705, doi:10.1016/j.brs.2020.09.019.
61. Tsuboi, T.; Lemos Melo Lobo Jofili Lopes, J.; Patel, B.; Legacy, J.; Moore, K.; Eisinger, R.S.; Almeida, L.; Foote, K.D.; Okun, M.S.; Ramirez-Zamora, A. Parkinson's Disease Motor Subtypes and Bilateral GPi Deep Brain Stimulation: One-Year Outcomes. Parkinsonism Relat. Disord. 2020, 75, 7–13, doi:10.1016/j.parkreldis.2020.05.004.
62. Tröster, A.I. Developments in the Prediction of Cognitive Changes Following Deep Brain Stimulation in Persons with Parkinson's Disease. Expert Rev. Neurother. 2024, 24, 643–659, doi:10.1080/14737175.2024.2360121.
63. Müller, F.; Nienstedt, J.C.; Buhmann, C.; Hidding, U.; Gulberti, A.; Pötter-Nerger, M.; Pflug, C. Effect of Subthalamic and Nigral Deep Brain Stimulation on Speech and Voice in Parkinson's Patients. J. Neural Transm. 2025, 132, 419–429, doi:10.1007/s00702-024-02860-5.
64. Wang, F.; Lai, Y.; Pan, Y.; Li, H.; Liu, Q.; Sun, B. A Systematic Review of Brain Morphometry Related to Deep Brain Stimulation Outcome in Parkinson's Disease. NPJ Parkinsons Dis. 2022, 8, 130, doi:10.1038/s41531-022-00403-x.
65. Cernera, S.; Eisinger, R.S.; Wong, J.K.; Ho, K.W.D.; Lopes, J.L.; To, K.; Carbunaru, S.; Ramirez-Zamora, A.; Almeida, L.; Foote, K.D.; et al. Long-Term Parkinson's Disease Quality of Life after Staged DBS: STN vs GPi and First vs Second Lead. NPJ Parkinsons Dis. 2020, 6, 13, doi:10.1038/s41531-020-0115-3.
66. Sarmento, F.; Daga, A.; Wang, A.; Srikar Lavu, V.; de Araújo, T.; Aghili Mehrizi, S.; Hilliard, J.D.; Forghani, R.; Okun, M.S.; Wong, J.K. Motor Outcomes in Unilateral, Bilateral Rapid, and Bilateral Delayed Staging Deep Brain Stimulation for Parkinson's Disease. J. Parkinsons Dis. 2024, 14, 1614–1622, doi:10.1177/1877718X241296014.
67. Lizarraga, K.J.; Gnanamanogaran, B.; Al-Ozzi, T.M.; Cohn, M.; Tomlinson, G.; Boutet, A.; Elias, G.J.B.; Germann, J.; Soh, D.; Kalia, S.K.; et al.

Lateralized Subthalamic Stimulation for Axial Dysfunction in Parkinson's Disease: Exploratory Outcomes and Open-Label Extension. Mov. Disord. Clin. Pract. 2024, 11, 1421–1426, doi:10.1002/mdc3.14188.
68. Fonov, V.; Evans, A.C.; Botteron, K.; Almli, C.R.; McKinstry, R.C.; Collins, D.L. Unbiased Average Age-Appropriate Atlases for Pediatric Studies. NeuroImage 2011, 54, 313–327, doi:10.1016/j.neuroimage.2010.07.033.
69. Fonov, V.; Evans, A.; McKinstry, R.; Almli, C.; Collins, D. Unbiased Nonlinear Average Age-Appropriate Brain Templates from Birth to Adulthood. NeuroImage 2009, 47, S102, doi:10.1016/S1053-8119(09)70884-5.
70. Grabner, G.; Janke, A.L.; Budge, M.M.; Smith, D.; Pruessner, J.; Collins, D.L. Symmetric Atlasing and Model Based Segmentation: An Application to the Hippocampus in Older Adults. Med. Image Comput. Comput. Assist. Interv. 2006, 9, 58–66, doi:10.1007/11866763_8.
71. Barbosa, R.M.G.; Soares, M.C.; Portela, D.M.M.C.; Guimarães, T.G.; Cury, R.G. New Perspectives of Deep Brain Stimulation Indications for Parkinson's Disease: A Critical Review. Brain Sci. 2024, 14, 638, doi:10.3390/brainsci14070638.
72. Jost, S.T.; Ray Chaudhuri, K.; Ashkan, K.; Loehrer, P.A.; Silverdale, M.; Rizos, A.; Evans, J.; Petry-Schmelzer, J.N.; Barbe, M.T.; Sauerbier, A.; et al. Subthalamic Stimulation Improves Quality of Sleep in Parkinson Disease: A 36-Month Controlled Study. J. Parkinsons Dis. 2021, 11, 323–335, doi:10.3233/JPD-202278.
73. Jost, S.T.; Konitsioti, A.; Loehrer, P.A.; Ashkan, K.; Rizos, A.; Sauerbier, A.; Dos Santos Ghilardi, M.G.; Rosenkranz, F.; Strobel, L.; Gronostay, A.; et al. Non-Motor Effects of Deep Brain Stimulation in Parkinson's Disease Motor Subtypes. Parkinsonism Relat. Disord. 2023, 109, 105318, doi:10.1016/j.parkreldis.2023.105318.
74. Meyer, G.M.; Sahin, I.A.; Hollunder, B.; Butenko, K.; Rajamani, N.; Neudorfer, C.; Hart, L.A.; Petry-Schmelzer, J.N.; Dafsari, H.S.; Barbe, M.T.; et al. Subthalamic Deep Brain Stimulation: Mapping Non-Motor Outcomes to Structural Connections. Hum. Brain Mapp. 2025, 46, e70207, doi:10.1002/hbm.70207.
75. Mititelu, R.; Prisacariu, G.S.; Bajenaru, A.I.; et al. Brain [^{18}F]FDG PET/CT in Clinical Practice: Indications, Methodological Considerations and Metabolic Patterns. Rom. J. Mil. Med. 2026, 129, 30–37, doi:10.55453/rjmm.2026.129.1.3.
76. Ni, Y.; Xiao, Y.; Shen, B.; Sun, Y.-M.; Zhao, J.; Wu, B.; Tang, Y.-L.; Liu, F.-T.; Wang, J.; Wu, J.-J. Impact of Deep Brain Stimulation on Cognitive Impairment in Parkinson's Disease: A Retrospective Longitudinal Study. Neurotherapeutics 2025, 22, e00561, doi:10.1016/j.neurot.2025.e00561.
77. Hurt, C.P.; Kuhman, D.J.; Moll, A.; Guthrie, B.L.; Olson, J.W.; Nakhmani, A.; Wade, M.; Brinkerhoff, S.A.; Holland, M.T.; Walker, H.C. Pointing in the Right Direction: Greater Motor Improvements with Directional versus Circular Subthalamic Nucleus Deep Brain Stimulation for Parkinson's Disease. J. Parkinsons Dis. 2025, 15, 202–213, doi:10.1177/1877718X241301071.
78. Zheng, Z.; Yin, Z.; Zhang, B.; Fan, H.; Liu, D.; Zhou, Y.; Duan, J.; Zhou, D.; Wu, X.; Lu, G. Levodopa Challenge Test Predicts STN-DBS Outcomes in Various Parkinson's Disease Motor Subtypes: A More Accurate Judgment. Neural Plast. 2021, 2021, 4762027, doi:10.1155/2021/4762027.
79. Duffley, G.; Lutz, B.J.; Szabo, A.; Wright, A.; Hess, C.W.; Ramirez-Zamora, A.; Zeilman, P.; Chiu, S.; Foote, K.D.; Okun, M.S.; et al. Home Health Management of Parkinson Disease Deep Brain Stimulation: A Randomized Clinical Trial. JAMA Neurol. 2021, 78, 972–981, doi:10.1001/jamaneurol.2021.1910.
80. Hacker, M.L.; Turchan, M.; Heusinkveld, L.E.; Currie, A.D.; Millan, S.H.; Molinari, A.L.; Konrad, P.E.; Davis, T.L.; Phibbs, F.T.; Hedera, P.; et al. Deep Brain Stimulation in Early-Stage Parkinson Disease: Five-Year Outcomes. Neurology 2020, 95, e393–e401, doi:10.1212/WNL.0000000000009946.
81. Wang, X.; Wang, J.; Li, N.; Wen, Y.; Wang, B.; Kou, H.; Fu, J.; Qu, H.; Qiu, C.; Jing, Z.; et al. Deep Brain Stimulation in Parkinson's Disease Patients Over 75 Years of Age: A Single-Institution Retrospective Analysis. CNS Neurosci. Ther. 2025, 31, e70397, doi:10.1111/cns.70397.
82. Wu, W.; Gong, S.; Wang, S.; Lei, W.; Yuan, L.; Wu, W.; Qiu, J.; Sun, W.; Luan, G.; Zhu, M.; et al. Safety and Efficiency of Deep Brain Stimulation in the Elderly Patients with Parkinson's Disease. CNS Neurosci. Ther. 2024, 30, e14899, doi:10.1111/cns.14899.
83. Mitchell, K.T.; Younce, J.R.; Norris, S.A.; Tabbal, S.D.; Dowling, J.L.; Rich, K.M.; Perlmutter, J.S.; Ushe, M. Bilateral Subthalamic Nucleus Deep Brain Stimulation in Elderly Patients With Parkinson Disease: A Case-Control Study. Oper. Neurosurg. 2020, 19, 234–240, doi:10.1093/ons/opaa049.
84. Dy Closas, A.M.F.; Tan, A.H.; Tay, Y.W.; Hor, J.W.; Toh, T.S.; Lim, J.L.; Lew, C.Y.; Cham, C.Y.; Yim, C.C.W.; Chee, K.Y.; et al. New Insights from a Malaysian Real-World Deep Brain Stimulation Cohort. J. Parkinsons Dis. 2025, 15, 189–201, doi:10.1177/1877718X241297715.
85. Avenali, M.; Zangaglia, R.; Cuconato, G.; Palmieri, I.; Albanese, A.; Artusi, C.A.; Bozzali, M.; Calandra-Buonaura, G.; Cavallieri, F.; Cilia, R.; et al. Are Patients with GBA-Parkinson Disease Good Candidates for Deep Brain Stimulation? A Longitudinal Multicentric Study on a Large Italian Cohort. J. Neurol. Neurosurg. Psychiatry 2024, 95, 309–315, doi:10.1136/jnnp-2023-332387.
86. Pal, G.; Corcos, D.M.; Metman, L.V.; Israel, Z.; Bergman, H.; Arkadir, D. Gaps and Controversies: Cognitive Effects of STN-DBS in Parkinson's Disease with GBA1 Pathogenic Variants. Mov. Disord. 2023, 38, 2155–2162, doi:10.1002/mds.29647.
87. Weiss, D.; Landoulsi, Z.; May, P.; Sharma, M.; Schüpbach, M.; You, H.; Corvol, J.C.; Paschen, S.; Helmers, A.-K.; Barbe, M.; et al. Genetic Stratification of Motor and QoL Outcomes in Parkinson's Disease in the EARLYSTIM Study. Parkinsonism Relat. Disord. 2022, 103, 169–174, doi:10.1016/j.parkreldis.2022.08.025.
88. Spooner, R.K.; Bahners, B.H.; Schnitzler, A.; Florin, E. DBS-Evoked Cortical Responses Index Optimal Contact Orientations and Motor Outcomes in Parkinson's Disease. NPJ Parkinsons Dis. 2023, 9, 37, doi:10.1038/s41531-023-00474-4.
89. Peter, A.; Petersen, M.; Wrobel, P.; Schott, F.; Gulberti, A.; Magnus, T.; Thomalla, G.; Cheng, B.; Pötter-Nerger, M. Regional Gray Matter Volumes Are Not Predictive of Axial Symptom Response to Subthalamic Deep Brain Stimulation in Parkinsonian Patients. Parkinsonism Relat. Disord. 2025, 130, 107193, doi:10.1016/j.parkreldis.2024.107193.
90. Kübler, D.; Astalosch, M.; Gaus, V.; Krause, P.; de Almeida Marcelino, A.L.; Schneider, G.-H.; Kühn, A. Gender-Specific Outcomes of Deep Brain Stimulation for Parkinson's Disease—Results from a Single Movement Disorder Center. Neurol. Sci. 2023, 44, 1625–1631, doi:10.1007/s10072-023-06598-y.
91. Butler, M.; Askari, A.; Zhu, B.; Wyant, K.; Leventhal, D.; Patil, P.G.; Chou, K.L. Ventral STN Stimulation Is Associated with Improved Axial Motor Outcomes in Parkinson's Disease. J. Neural Transm. 2025, 132, 1031–1040, doi:10.1007/s00702-025-02931-1.
92. Somma, T.; Bove, I.; Vitulli, F.; Solari, D.; Bocchino, A.; Palmiero, C.; Scala, M.R.; Zoia, C.; Cappabianca, P.; Esposito, F. Gender Gap in Deep Brain Stimulation for Parkinson's Disease: Preliminary Results of a Retrospective Study. Neurosurg. Rev. 2024, 47, 63, doi:10.1007/s10143-024-02290-7.
93. Mori, F.; Fukaya, C.; Watanabe, M.; Sumi, K.; Ikeda, T.; Oshima, H.; Yoshino, A. Gender Difference in Outcome of Subthalamic Nucleus-Deep Brain Stimulation in Japan. Neurol. Med. Chir. (Tokyo) 2025, 65, 126–132, doi:10.2176/jns-nmc.2024-0108.

94. Sauerbier, A.; Loehrer, P.; Jost, S.T.; Heil, S.; Petry-Schmelzer, J.N.; Herberg, J.; Bachon, P.; Aloui, S.; Gronostay, A.; Klingelhoefer, L.; et al. Predictors of Short-Term Impulsive and Compulsive Behaviour after Subthalamic Stimulation in Parkinson Disease. J. Neurol. Neurosurg. Psychiatry 2021, 92, 1313–1318, doi:10.1136/jnnp-2021-326131.
95. Sisodia, V.; Ursinus, R.; Geurtsen, G.J.; Wiggerts, Y.; Schuurman, P.R.; Beudel, M.; de Bie, R.M.A.; Swinnen, B.E.K.S. Impact of Preoperative Cognition on Motor Improvement in Bilateral Subthalamic Nucleus-Deep Brain Stimulation for Parkinson's Disease. Neuromodulation 2025, 28, 484–491, doi:10.1016/j.neurom.2024.07.011.
96. Fjeldhøj, S.; Thomsen, B.L.C.; Pedersen, P.M.; Jensen, S.R.; Clausen, A.; Karlsborg, M.; Jespersen, B.; Bergdal, O.K.; Løkkegaard, A. Mild Cognitive Impairment Is Not Predictive of Dementia up to 15 Years after Subthalamic Deep Brain Stimulation in Parkinson's Disease. J. Parkinsons Dis. 2025, 15, 879–891, doi:10.1177/1877718X251334049.
97. Park, K.W.; Jo, S.; Kim, M.S.; Choi, N.; Jeon, S.R.; Park, H.K.; Kwon, K.-Y.; Lee, C.S.; Chung, S.J. Cognitive Profile as a Predictor of the Long-Term Outcome after Deep Brain Stimulation in Parkinson's Disease. J. Neurol. Sci. 2020, 417, 117063, doi:10.1016/j.jns.2020.117063.
98. Voruz, P.; Pierce, J.; Ahrweiller, K.; Haegelen, C.; Sauleau, P.; Drapier, S.; Drapier, D.; Vérin, M.; Péron, J. Motor Symptom Asymmetry Predicts Non-Motor Outcome and Quality of Life Following STN DBS in Parkinson's Disease. Sci. Rep. 2022, 12, 3007, doi:10.1038/s41598-022-07026-5.
99. Loftus, A.M.; Nielsen, C.; Corti, E.J.; Starkstein, S.; Gasson, N.; Egan, S.J. Measuring General Expectations of Advanced Stage Treatment Outcomes in Parkinson's Disease. J. Parkinsons Dis. 2021, 11, 2017–2026, doi:10.3233/JPD-212777.
100.Szlufik, S.; Duszynska-Lysak, K.; Przybyszewski, A.; Laskowska-Levy, I.; Drzewinska, A.; Dutkiewicz, J.; Mandat, T.; Habela, P.; Koziorowski, D. The Potential Neuromodulatory Impact of Subthalamic Nucleus Deep Brain Stimulation on Parkinson's Disease Progression. J. Clin. Neurosci. 2020, 73, 150–154, doi:10.1016/j.jocn.2019.12.059.
101.Rosenfeldt, A.B.; Davidson, S.; Kaya, R.D.; West, E.; Liao, J.Y.; Walter, B.L.; Fernandez, H.; Alberts, J.L. Including Individuals with Parkinson's Disease and Deep Brain Stimulation in Rehabilitation Trials: Feasibility, Challenges, and Preliminary Gait and Postural Stability Results. Parkinsonism Relat. Disord. 2025, 137, 107920, doi:10.1016/j.parkreldis.2025.107920.
102.de Noordhout, A.M.; Mouchamps, M.; Remacle, J.-M.; Delstanche, S.; Bonhomme, V.; Gonce, M. Subthalamic Deep Brain Stimulation versus Best Medical Treatment: A 12-Year Follow-Up. Acta Neurol. Belg. 2022, 122, 197–202, doi:10.1007/s13760-022-01874-8.
103.Lai, Y.; Song, Y.; Huang, P.; Wang, T.; Wang, L.; Pan, Y.; Sun, Q.; Sun, B.; Zhang, C.; Li, D. Subthalamic Stimulation for Camptocormia in Parkinson's Disease: Association of Volume of Tissue Activated and Structural Connectivity with Clinical Effectiveness. J. Parkinsons Dis. 2021, 11, 199–210, doi:10.3233/JPD-202259.
104.Spindler, P.; Alzoobi, Y.; Kühn, A.A.; Faust, K.; Schneider, G.-H.; Vajkoczy, P. Deep Brain Stimulation for Parkinson's Disease-Related Postural Abnormalities: A Systematic Review and Meta-Analysis. Neurosurg. Rev. 2022, 45, 3083–3092, doi:10.1007/s10143-022-01830-3.
105.Lo Faso, V.; Schisano, L.; Remore, L.G.; Tariciotti, L.; Fiore, G.; Valcamonica, G.; Borellini, L.; Cogiamanian, F.; D'Ammando, A.; Pirola, E.; et al. Deep Brain Stimulation in Parkinson Disease: A Switch for On/Off Dystonia. World Neurosurg. 2025, 194, 123438, doi:10.1016/j.wneu.2024.11.021.
106.Atkinson-Clement, C.; Cavazzini, É.; Zénon, A.; Legou, T.; Witjas, T.; Fluchère, F.; Azulay, J.-P.; Baunez, C.; Pinto, S.; Eusebio, A. Subthalamic Stimulation Breaks the Balance between Distal and Axial Signs in Parkinson's Disease. Sci. Rep. 2021, 11, 21810, doi:10.1038/s41598-021-01386-0.
107.Ravi, D.K.; Baumann, C.R.; Bernasconi, E.; Gwerder, M.; Ignasiak, N.K.; Uhl, M.; Stieglitz, L.; Taylor, W.R.; Singh, N.B. Does Subthalamic Deep Brain Stimulation Impact Asymmetry and Dyscoordination of Gait in Parkinson's Disease? Neurorehabil. Neural Repair 2021, 35, 1020–1029, doi:10.1177/15459683211041309.
108.Castillo-Triana, N.; Camargo-Mendoza, M.; Bernal-Pacheco, Ó. Effects of Subthalamic Nucleus Deep Brain Stimulation on the Speech of Spanish-Speaking Parkinson's Disease Patients during the First Year of Treatment. CoDAS 2024, 36, e20230194, doi:10.1590/2317-1782/20242023194en.
109.Ollivier, T.; Pinto, S.; Rolland, A.-S.; Cailliau, E.; Touzet, G.; Thobois, S.; Eusebio, A.; Hainque, E.; Rouaud, T.; Drapier, S.; et al. Parkinson's Disease, Speech and Neurosurgery. Brain Behav. 2025, 15, e70101, doi:10.1002/brb3.70101.
110.Chiu, S.Y.; Tsuboi, T.; Hegland, K.W.; Herndon, N.E.; Shukla, A.W.; Patterson, A.; Almeida, L.; Foote, K.D.; Okun, M.S.; Ramirez-Zamora, A. Dysarthria and Speech Intelligibility Following Parkinson's Disease Globus Pallidus Internus Deep Brain Stimulation. J. Parkinsons Dis. 2020, 10, 1493–1502, doi:10.3233/JPD-202246.
111.Kola, S.; Prichard, D.O.; Bharucha, A.E.; Hassan, A. A Prospective Pilot Study of the Effects of Deep Brain Stimulation on Olfaction and Constipation in Parkinson's Disease. Clin. Neurol. Neurosurg. 2021, 207, 106774, doi:10.1016/j.clineuro.2021.106774.
112.Eisinger, R.S.; Okun, M.S.; Cernera, S.; Cagle, J.; Beke, M.; Ramirez-Zamora, A.; Kim, B.H.; Barbosa, D.A.N.; Qiu, L.; Vaswani, P.; et al. Weight and Survival after Deep Brain Stimulation for Parkinson's Disease. Parkinsonism Relat. Disord. 2023, 115, 105810, doi:10.1016/j.parkreldis.2023.105810.
113.Merner, A.R.; Frazier, T.W.; Ford, P.J.; Lapin, B.; Wilt, J.; Racine, E.; Gase, N.; Leslie, E.; Machado, A.; Vitek, J.L.; et al. A Patient-Centered Perspective on Changes in Personal Characteristics After Deep Brain Stimulation. JAMA Netw. Open 2024, 7, e2434255, doi:10.1001/jamanetworkopen.2024.34255.
114.Liu, W.; Yamamoto, T.; Yamanaka, Y.; Asahina, M.; Uchiyama, T.; Hirano, S.; Shimizu, K.; Higuchi, Y.; Kuwabara, S. Neuropsychiatric Symptoms in Parkinson's Disease After Subthalamic Nucleus Deep Brain Stimulation. Front. Neurol. 2021, 12, 656041, doi:10.3389/fneur.2021.656041.
115.Zoon, T.J.C.; van Rooijen, G.; Balm, G.M.F.C.; Bergfeld, I.O.; Daams, J.G.; Krack, P.; Denys, D.A.J.P.; de Bie, R.M.A. Apathy Induced by Subthalamic Nucleus Deep Brain Stimulation in Parkinson's Disease: A Meta-Analysis. Mov. Disord. 2021, 36, 317–326, doi:10.1002/mds.28390.
116.Oner, O.G.; Jafarova, S.; Ozden, H.; Seker, A.; Gunal, D.I. The Impact of Subthalamic Deep Brain Stimulation on Apathy in Parkinson's Disease Patients. Turk. Neurosurg. 2024, 34, 672–677, doi:10.5137/1019-5149.JTN.43415-23.3.
117.Pham, U.; Skogseid, I.M.; Pripp, A.H.; Bøen, E.; Toft, M. Impulsivity in Parkinson's Disease Patients Treated with Subthalamic Nucleus Deep Brain Stimulation—An Exploratory Study. PLoS ONE 2021, 16, e0248568, doi:10.1371/journal.pone.0248568.
118.Martinez-Martin, P.; Deuschl, G.; Tonder, L.; Schnitzler, A.; Houeto, J.-L.; Timmermann, L.; Rau, J.; Schade-Brittinger, C.; Stoker, V.; Vidailhet, M.; et al. Interpretation of Health-Related Quality of Life Outcomes in Parkinson's Disease from the EARLYSTIM Study. PLoS ONE 2020, 15, e0237498, doi:10.1371/journal.pone.0237498.
119.Jost, S.T.; Aloui, S.; Evans, J.; Ashkan, K.; Sauerbier, A.; Rizos, A.; Petry-Schmelzer, J.N.; Gronostay, A.; Fink, G.R.; Visser-Vandewalle, V.; et al. Neurostimulation for Advanced Parkinson Disease and Quality of Life at 5 Years: A Nonrandomized Controlled Trial. JAMA Netw. Open 2024, 7,

e2352177, doi:10.1001/jamanetworkopen.2023.52177.
120.Lu, W.; Chang, X.; Wu, W.; Jin, P.; Lin, S.; Xiong, L.; Yu, X. The Scalp Nerve Block Combined with Intercostal Nerve Block Improves Recovery After Deep Brain Stimulation in Patients with Parkinson's Disease: A Prospective, Randomized Controlled Trial. Clin. Interv. Aging 2024, 19, 1881–1889, doi:10.2147/CIA.S473421.
121.Kocabicak, E.; Yildiz, O.; Aygun, D.; Temel, Y. Effects of Deep Brain Stimulation of the Subthalamic Nucleus on the Postoperative Levodopa Response: One Year Follow Up. Turk. Neurosurg. 2021, 31, 88–92, doi:10.5137/1019-5149.JTN.30065-20.1.
122.Theyer, C.; Beliveau, V.; Krismer, F.; Peball, M.; Mair, K.; Heim, B.; Djamshidian, A.; Kiechl, S.; Eisner, W.; Eschlböck, S.; et al. Long-Term Medication Profiles in Parkinson's Disease under Subthalamic Deep Brain Stimulation: A Controlled Study. Mov. Disord. Clin. Pract. 2024, 11, 855–860, doi:10.1002/mdc3.14065.
123.Hacker, M.; Cannard, G.; Turchan, M.; Meystedt, J.; Davis, T.; Phibbs, F.; Hedera, P.; Konrad, P.; Charles, D. Early Subthalamic Nucleus Deep Brain Stimulation in Parkinson's Disease Reduces Long-Term Medication Costs. Clin. Neurol. Neurosurg. 2021, 210, 106976, doi:10.1016/j.clineuro.2021.106976.
124.Astalosch, M.; Mousavi, M.; Ribeiro, L.M.; Schneider, G.-H.; Stuke, H.; Haufe, S.; Borchers, F.; Spies, C.; von Hofen-Hohloch, J.; Al-Fatly, B.; et al. Risk Factors for Postoperative Delirium Severity After Deep Brain Stimulation Surgery in Parkinson's Disease. J. Parkinsons Dis. 2024, 14, 1175–1192, doi:10.3233/JPD-230276.
125.Sîrbu, C.A.; Mihai, A.C.; Pleșa, F.C.; Vasile, T.M.; Caloianu, I.; Manole, A.M.; Tuță, S. Is Still Neurology Desirable as a Specialty for Aspiring Physicians? Rom. J. Mil. Med. 2023, 126, 144–148, doi:10.55453/rjmm.2023.126.2.3.
126.Chang, B.; Geng, Z.; Mei, J.; Wang, Z.; Chen, P.; Jiang, Y.; Niu, C. Application of Multimodal Deep Learning and Multi-Instance Learning Fusion Techniques in Predicting STN-DBS Outcomes for Parkinson's Disease Patients. Neurotherapeutics 2024, 21, e00471, doi:10.1016/j.neurot.2024.e00471.
127.Ferrea, E.; Negahbani, F.; Cebi, I.; Weiss, D.; Gharabaghi, A. Machine Learning Explains Response Variability of Deep Brain Stimulation on Parkinson's Disease Quality of Life. NPJ Digit. Med. 2024, 7, 269, doi:10.1038/s41746-024-01253-y.
128.Sabo, A.; Iaboni, A.; Taati, B.; Fasano, A.; Gorodetsky, C. Evaluating the Ability of a Predictive Vision-Based Machine Learning Model to Measure Changes in Gait in Response to Medication and DBS within Individuals with Parkinson's Disease. Biomed. Eng. Online 2023, 22, 120, doi:10.1186/s12938-023-01175-y.
129.Oehrn, C.R.; Cernera, S.; Hammer, L.H.; Shcherbakova, M.; Yao, J.; Hahn, A.; Wang, S.; Ostrem, J.L.; Little, S.; Starr, P.A. Chronic Adaptive Deep Brain Stimulation versus Conventional Stimulation in Parkinson's Disease: A Blinded Randomized Feasibility Trial. Nat. Med. 2024, 30, 3345–3356, doi:10.1038/s41591-024-03196-z.
130.Huang, Z.; Meng, L.; Bi, X.; Xie, Z.; Liang, W.; Huang, J. Efficacy and Safety of Robot-Assisted Deep Brain Stimulation for Parkinson's Disease: A Meta-Analysis. Front. Aging Neurosci. 2024, 16, 1419152, doi:10.3389/fnagi.2024.1419152.

https://doi.org/10.55453/rjmm.2026.129.6.6

Article

Design and validation of a questionnaire regarding the occupational risk of cancer for clinical practice in Romania

Cristina Mandanach[1,2], Alice Elena Munteanu[3,4], Alexandru Ștefan Cătălin Rașcu[5,6], Ștefan Dumitrache-Rujinski[7,8], Mihai Teodor Georgescu[9,10], Andreea Maftei[1], Claudia Lucia Toma[7,8,*], Marina Ruxandra Oțelea[2,11]

1 Doctoral School, "Carol Davila" University of Medicine and Pharmacy, 37 Dionisie Lupu Street, Sector 2, 020021, Bucharest, Romania ; cristina.paraschiv@drd.umfcd.ro (C.M.); andreea.mutu@drd.umfcd.ro (A.M.)
2 Clinical Department 5, "Carol Davila" University of Medicine and Pharmacy, 37 Dionisie Lupu Street, Sector 2, 020021, Bucharest, Romania; dralicepopescu@yahoo.com (A.E.M)
3 Department of Cardiology, Titu Maiorescu University – Faculty of Medicine, 67A Gheorghe Petrașcu Street, Sector 3, 031593, Bucharest, Romania;
4 Carol Davila Central Universitary Emergency Military Hospital, 134 Calea Plevnei Street, Sector 1, 010825, Bucharest, Romania;
5 Clinical Department 3, "Carol Davila" University of Medicine and Pharmacy, 37 Dionisie Lupu Street, Sector 2, 020021, Bucharest, Romania; stefan.rascu@umfcd.ro (A.S.C.R.)
6 Urology Clinic, "Professor Doctor Theodor Burghele" Clinical Hospital, 20 Panduri Street, Sector 5, 050506, Bucharest, Romania;
7 Clinical Department 4, "Carol Davila" University of Medicine and Pharmacy, 37 Dionisie Lupu Street, Sector 2, 020021, Bucharest, Romania; stefan.dumitrache@umfcd.ro (S.D.R), claudia.toma@umfcd.ro (C.L.T.)
8 Pulmonology Department IV, "Marius Nasta" Institute of Pneumology, 90 Viilor Street, Sector 5, 050159, Bucharest, Romania;
9 Clinical Department 8, "Carol Davila" University of Medicine and Pharmacy, 37 Dionisie Lupu Street, Sector 2, 020021, Bucharest, Romania; mihai.georgescu@umfcd.ro (M.T.G.)
10 Radiotherapy Department II, "Prof.Dr.Alexandru Trestioreanu" Institute of Oncology, 252 Fundeni Street, 022328, Bucharest, Romania;
11 Clinic of Occupational Medicine, Colentina Clinical Hospital, 19-21 Stefan cel Mare Street, Sector 2, 020125, Bucharest, Romania; marina.otelea@umfcd.ro (M.R.O.)
*Correspondence: claudia.toma@umfcd.ro

Abstract: Background: Occupational cancer is one of the most common occupational diseases. Identifying exposure to carcinogens is important both for implementing measures to prevent and control the risk of exposure and for the post-exposure medical surveillance of workers. The purpose of this study is to develop and validate a questionnaire that can be used in clinical practice to identify exposure and ultimately facilitate the diagnosis of occupational cancer. Methods: The first step involves designing the questionnaire, which will then be validated in the second step by ensuring it meets all the validation criteria for a questionnaire. Results: Scientific validation, logical validation, and construct validation were completed to ensure that the questionnaire is appropriate both structurally and in terms of content. The questionnaire was evaluated by comparing it to a reference standard, and the results, based on the exposure risk level category, showed good agreement (k = 0.719). The intra-observer and inter-observer reliability tests showed an excellent concordance for exposure risk level category (k = 1.000 and k = 0.945). Conclusions: The questionnaire was developed and validated to identify the risk of occupational cancer, and its systematic use in Romania could make a better selection of subjects who should be included in the post-exposure surveillance.

Keywords: occupational cancers; questionnaire; occupational exposure;

Citation: Mandanach C, Munteanu AE, Rașcu ASC, Dumitrache-Rujinski S, Georgescu MT, Maftei A, et al. *Design and validation of a questionnaire regarding the occupational risk of cancer for clinical practice in Romania.* R. J. Mil. Med. 2026, CXXIX(6): 652-686 https://doi.org/10.55453/rjmm.2026.129.6.6

Academic Editor: Raluca Mititelu

Received: 03 September 2026
Revised: 17 October 2026
Accepted: 22 October 2026

INTRODUCTION

Occupational cancer is one of the most common occupational diseases. The estimated fraction of all cancer incidents that can be attributed to occupational risk factors generally varies between 2 and 8% worldwide [1]. The incidence and mortality rates associated with occupational cancer are, therefore, important. Based on these data, strategies and methods for preventing and controlling risk related to the carcinogens' presence in the workplace were developed. Exposure data are collected directly and systematically only in a few countries; for the worldwide evaluation, they have to be compiled from several indirect sources, such as the

number of people employed in certain high-risk industries or jobs, the prevalence of exposure among these individuals, and the relative risk found in epidemiological studies. The diversity of sources and the differences in methodologies of various studies could lead either to an overestimated or an underestimated risk [2].

Prevention strategies begin with primary prevention, which aims to eliminate or reduce exposure to carcinogens in the workplace and is supplemented by secondary prevention measures implemented by occupational medicine. The crucial point of secondary prevention is early detection, which includes screening and early diagnosis of occupational cancer. There are numerous screening methods, ranging from medical history (personal and family history), physical examination, and medical screening tests (CT, hematologic tests, etc.).The identification of exposure to carcinogens (occupational history, designated questionnaires to identify a possible exposure, registries for workers exposed to carcinogens or for jobs with a high risk of exposure) is currently used to define the workers at risk, for whom postexposure monitoring should be implemented. The effective use of a structured questionnaire is one method to improve the early diagnosis of certain work-related cancers [3].

Using one, two, or three methods—or a combination of them— increases the rate of identification of occupational cancers [4].

The aim of this study is to design and validate a questionnaire to detect the possibility of occupational exposure and, afterward, the possibility of an earlier diagnosis of occupational cancer. Incorporating a structured, easy-to-use, and reliable questionnaire in the medical routine can improve the detection of occupational cancers and facilitate the diagnostic algorithm for cancers in patients who have been exposed to occupational carcinogens.

MATERIALS AND METHODS

1. Study design

This study aims to validate a questionnaire on exposure to occupational carcinogens (Occupational Exposure to Carcinogens Questionnaire) and to develop a risk score based on the intensity and duration of occupational exposure.

This is a multicenter study conducted in several public hospitals and clinics in Bucharest: Colentina Clinical Hospital, Prof. Dr. Theodor Burghele Clinical Hospital, the Marius Nasta Institute of Pneumophysiology in Bucharest, the "Prof. Dr. Alexandru Trestioreanu" Oncology Institute in Bucharest, and the Domina-Sana Clinic. The subjects were recruited intermittently between 2023 and 2026, depending on the center.

The study was conducted in accordance with the principles of the Declaration of Helsinki and Good Clinical Practice Guidelines and was approved by the Ethics Committee of each hospital (20/23.12.2022; 3291/03.04.2023; 23941/25.10.2023; 6571/09.05.2024; 576/19.04.2023).

In addition to administering the questionnaire, various medical data were also collected: age, sex, level of formal education (highest level of education completed), profession, occupation, occupational domain of activity, age at diagnosis, medical history, localization of the cancer, comorbidities, treatment for previous cancer diagnoses. These data were used in the final analysis of the population to which the questionnaire was administered.

2. Population

The target population consisted of 400 patients diagnosed with cancer located in the respiratory system—lung cancer; urinary system—kidney, bladder, and prostate cancer; but also other locations of the cancer: reproductive system—breast, ovarian, and uterine cancer; digestive system—gastric, hepatic and colon cancer; skin, endocrine glands, and lymphoid-related cancers.

The first two types of cancer were the most represented, as they are the most frequent occupational cancers, in general. According to epidemiological data, the annual incidence of lung cancer and bladder cancer in Romania is approximately 12500 and 5000 respectively [5]. From epidemiological research, we know that occupational lung cancers represent 8-15% of all lung cancers [6], with a prevalence of 10% in Romania [7] and sometimes with not very long exposure [8]. A percentage of 4-10% of total bladder cancers are related to occupational exposure [9,10]. Based on this data, the study required a sample of 137 patients with lung cancer and 86 patients with bladder cancer [11]. For cancers in other body locations, there are approximately 81000 new cases in Romania with a 2- 8% occupational etiology [12], and the required sample size is 113 patients with a cancer diagnosis. The final number of 400 patients is the sum of 132 lung cancers, 125 bladder cancers, and 143 other types of cancers.

Inclusion criteria:

- patients, male or female, diagnosed with any type of cancer

- aged 18 or older

- who had worked in their lifetime

- Romanian residents

- willing to complete questionnaires.

Exclusion criteria:

- who had never worked

- non-Romanian residents.

The subjects were clearly informed about the study procedure and its objectives. They were enrolled after signing a written informed consent form and data confidentiality was ensured by registering subjects in the database using a code.

The reasons for refusals to participate were noted.

3. Validation of Occupational Exposure to Carcinogens Questionnaire

3.1. Characteristics of the Questionnaire

The questionnaire was designed specifically for the study after a review of the literature and various similar questionnaires [13-17].

The initial draft of the Occupational Exposure to Carcinogens Questionnaire consisted of 21 questions to cover both occupational and main non-occupational exposures: 14 questions relate to occupational factors, 3 to domestic exposure, and 4 to assess exposure to smoking and second-hand smoke. The questions are closed-ended, with yes-no or multiple-choice answers. The answers to the multiple-choice questions—which covered the list of carcinogens, industrial processes, and occupations with a high risk of exposure—were selected based on information from the scientific literature [18]. Only group I carcinogens selected from the International Agency for Research on Cancer (IARC) lists that might be present in the workplace were included, as they are the only ones recognized as causes of occupational cancer in Romania.

Considering that the three most common types of occupational cancers are mesothelioma, lung cancer, and bladder cancer [19], and that the carcinogenic risk factors have a specificity depending on the cancer's location, three versions of the same questionnaire were drafted: one for lung cancer, one for bladder cancer, and a general one for the others. Mesothelioma is a rare form of cancer, and in fact, all mesotheliomas should be assessed for their occupational exposure to asbestos by an occupational physician. Therefore, only lung and bladder cancer had distinct versions of the questionnaire. There are 2 main differences between the 3 versions of the questionnaire: the list of carcinogens, and the most frequent occupations associated with the different forms of cancers. Thus, for lung and bladder cancer, the list was limited to the ones in the IARC tables targeting these localizations. For all other cancers, the questionnaire included all carcinogens in Group I that might be present in the working environment. The occupations related to lung cancer and bladder cancer were selected based on data from IARC classification by cancer site [20] and other reliable information published by occupational health and safety centers around the world [21-25]. In the questionnaire for patients with lung cancer, 3 other questions related to dermal exposure and exposure to certain carcinogens were removed because they had no association with lung cancer.

This final questionnaire, with all three versions, is available in Supplementary Materials.

3.2. Questionnaire Validation Criteria

3.2.1. Scientific validation

The ability of the questionnaire to measure the dimensions of the construct was evaluated. The group of experts, together with other medical specialists, evaluated its structure and whether the questions in the questionnaire are relevant to what needs to be measured. The draft was discussed with an expert group in occupational medicine and with one expert in lung cancer, in urology, an oncologist, and a radiotherapist. They conducted an assessment of the questionnaire's structure and its relevance to the items being analyzed, as well as its clinical applicability and the time required to administer it.

3.2.2. Logical or face validity

After an interviewer administered the questionnaire, 30 participants evaluated its comprehensibility. The expert committee determined whether the questionnaire measured what it was intended to measure and whether the respondents understood all the questions.

3.2.3. Construct validity

Construct validity was achieved by applying the questionnaire and obtaining a result similar to known clinical or epidemiological data. The result obtained from the administration of the questionnaire is a proportion (in both absolute number and percentage) of subjects diagnosed with cancer that have definite exposure to occupational carcinogens.

The accuracy of identifying occupational exposure can be improved by combining the exposure data with an exposure risk level score.

The score for the level of risk derived from the exposure to carcinogens is based on 4 items— the presence of the hazard in the workplace (the exposure), the duration of this exposure, the actual use of personal protective equipment and the presence of ventilation. Ventilation was chosen as a general protective measure, as most carcinogens have this route of absorption [26]. For dermal absorption, individual protective measures are mostly relevant, but they were assessed with a specific item of the questionnaire. Each item has several response options scored according to their impact on the risk (Table 1). Because personal protective measures are ranked at the top of the pyramid of risk control, we also included in this item the duration of daily exposure. Adding the scores gives a total score ranging from 0 to 13. Exposure risk stratification is performed by calculating intermediate exposure levels, with the maximum score indicating a high level of retrospective exposure risk for the subject in question [27]. There are 4 levels of risk exposure: No risk or very low risk between 0 – 2; low risk between 3 – 6; moderate risk between 7–9; and high risk between 10 – 13.

Table 1: Items for calculating the risk level score

Item	Score	Minimum	Maximum
Exposure			
NO	0		
YES	1		
YES, more than 1 carcinogen	2		
Total score exposure		0	2
Duration of exposure (years)			
0	0		
<10 years	1		
10-19 years	2		
20-29 years	3		
> 30 years	4		
Total score duration		0	4
General protection measures (Ventilation)			
YES	0		
YES, intermittent	1		
NO	2		
Total score general protective measures		0	2
Personal protective equipment			
YES, permanently	0		
NO, for < 2h of the total exposure time	1		
NO, for 2-4h of total exposure time	2		
NO, for 4h of the total exposure time	3		
NO, for 6h of the total exposure time	4		
NO for all day work (8h exposure time)	5		
Total score personal protective equipment/time of exposure		0	5
TOTAL SCORE		0	13

3.2.4. Criterion Validation

The questionnaire was evaluated by comparing it to a gold standard represented by an occupational medical history. The comparison was performed based on the results obtained with the questionnaire filled in by 100 subjects, and a standard occupational medical history which was taken by an occupational physician. The questionnaire and occupational history were afterward reviewed by two different investigators.

3.2.5. Intra-observer Reliability or Test–Retest Reliability

Intra-observer reliability or test–retest reliability was evaluated by administering the questionnaire by the same interviewer, using the same method, to the same patient, at two different times, separated by an interval of 2–3 months. The intra-observer reliability was tested on 30 patients. This longer time interval attempts to eliminate the problem of recall bias. The percentage of different answers was calculated.

3.2.6. Inter-observer Reliability

Inter-observer reliability was assessed by administering the questionnaire to another subgroup of 30 subjects on two different occasions by three independent interviewers. Of note, the second interviewer was also a doctor, but not a certified specialist in occupational medicine. The purpose of administering the questionnaire by different interviewers is to evaluate the level of

correlation among responses and the possible influence of the interviewer on those answers. The percentage of different responses was determined.

4. Statistical Analysis

The data obtained from the questionnaires and the medical data were statistically analyzed using statistical analysis software such as SPSS (IBM SPSS Statistics 20). For the construct validity, analyses related to occupational exposures were performed for the whole group and for the subgroups with lung cancer, bladder cancer, and other types of cancers. The criterion validation and intra-observer and inter-observer reliability were evaluated by calculating Cohen's Kappa index (k); the concordance was considered poor under 0.20, low between 0.21-0.40, moderate between 0.41-0.60, good between 0.61-0.80, and excellent if k was 0.81 and over [28].

RESULTS

1. Sample characteristics

The total number of participants for validating the questionnaire was 400, divided into 132 lung cancers, 125 bladder cancers and 143 other types of cancers. Men accounted for 253 of the total number of participants (63.25%). The average age was 66.48 years (SD=10.64), and the average age at the moment of diagnosis was lower, 63.80 years (SD= 10.86). Smokers outnumbered non-smokers in the overall cohort and in the groups with lung cancer and bladder cancer (66.75%, 78.03% and 74.40%), but they were fewer in number than non-smokers in the group with cancers of other sites (49.65%). A high percentage of smokers were heavy smokers (69.92%), with more than 20 packs/years, the average was 38.47 packs/years (SD=25.66) and more than 20 years of smoking.

The level of education showed that the largest group was undergraduate (73.50%), and among these, the highest percentages were represented by technical school (24.75%) and high school (22.25%). In the graduate category, the highest percentage is represented by participants with university degrees (18%).

The short form of the European Health Literacy Survey Questionnaire was applied to the entire group. The questionnaire, with 16 items, validated in Romanian [29], was applied to assess the patients for the four core competencies of health literacy (find, understand, appraise, and apply health information) in three domains (health care, disease prevention, health promotion). The total score (HLS-EU-Q16) could be 16, and for the total group the average score was 13.71 (SD=2.79). The distribution of health literacy levels showed that the majority of participants had an adequate health literacy level (71.78%), 27 participants had an inadequate score (6.75%), and 86 had a problematic one (21.50%).

Nearly a quarter (25.50%) of all participants had a family history of cancer, and 25 of them (6.25%) had family members with the same type of cancer as the participant.

The characteristics of the study population are presented in Table 2. The differences between the three groups are statistically significant, with Group 3 accounting for the difference, while the other two groups are much more similar.

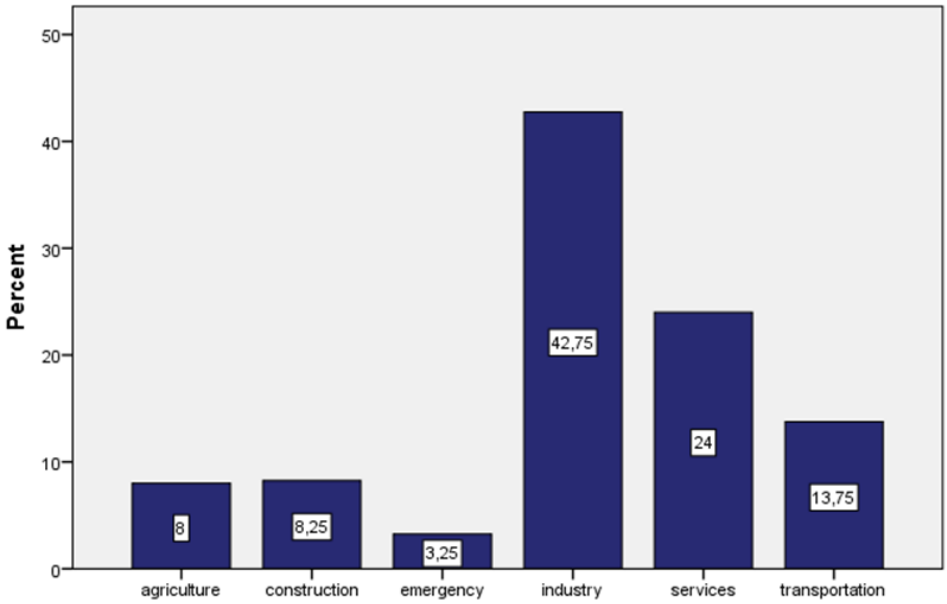
Table 2: General characteristics and comparison of the study groups

	Total	Group 1	Group 2	Group 3	p
Age (mean ± SD)	66.48±10.64	65.20±9.92	69.50±9.47	65.02±11.71	0.001
Age at dg (mean ± SD)	63.80±10.86	63.67±10.08	65.86±9.76	62.12±12.15	0.035
Gender (no of Women, %)	147 (36.75%)	51 (38.64%)	29 (23.20%)	67 (46.85%)	0.000
Smokers (no, %)	267 (66.75%)	103 (78.03%)	93 (74.40%)	71 (49.65%)	0.000
Level of education (no of undergraduate, %)	294 (73.50%)	102 (77.27%)	82 (65.60%)	110 (76.92%)	0.000
HLS-EU-Q16 total score (mean, SD)	13.71±2.79	13.04±2.93	14.39±2.38	13.73±2.85	0.000
Family history of cancer (no, %)	102 (25.50%)	36 (27.27%)	27 (21.60%)	39 (27.27%)	0.000

Group 1 – patients with lung cancer, Group 2- patients with bladder cancer, Group 3 – patients with any other types of cancers

The activity domains of the subjects included in the study were grouped into six broad categories (Figure 1).

Figure 1: The percentage of domains of activity



2. Criteria for validation of the questionnaire

2.1. Scientific validation

The group of experts considered the questionnaire to be adequate from both structural and content perspectives, as it is capable of accurately identifying exposure to carcinogens (i.e., occupational or non-occupational). Three questions were removed from the questionnaire because they did not provide information relevant to the screening or to the calculation of the exposure risk score. The input to separate the industrial processes from IARC into two separate questions, because only some of these industrial processes are included in Romania's table of occupational cancers, was included in the final version. The final version of the questionnaire contains 19 questions, while the version focused on lung cancer contains only 16. Most discussions were to include supplementary details on the exposure (such as daily exposure time and frequency during the week) from the side of the occupational physicians and the length of the questionnaire from the other experts. Finally, the compromise presented above led to 85.71% agreement among all.

Administration time for the questionnaire was also tested and took about 10–15 minutes.

2.2. Logical or face validity

The comprehension and logical reasoning were assessed, and the expert group considered that the majority of the questions were adequate. Only three of them presented difficulty and needed to be revised. The questions were rephrased to eliminate confusion between years of employment and years of actual exposure to carcinogens, work equipment and protective equipment for that exposure, and meals served at work, taking into account the existing hygiene conditions.

2.3. Construct validity

Overall, after administering the questionnaire, 279 patients out of 400 (69.75%) were exposed to at least one possible carcinogenic agent at the workplace, and 192 (48%) were able to designate at least one carcinogenic agent from the list. There were 212 participants (53% of the entire sample) who were exposed both to occupational carcinogenic agents and to non-occupational ones.

We had a higher number of cases of moderate and high levels of occupational exposure in the lung cancer group than in the bladder cancer or cancers in other locations groups, which is to be expected given the high percentage of occupational lung cancers recorded worldwide (Table 3).

Table 3: Occupational exposure

	Total	Group 1	Group 2	Group 3
Occupational exposure related to Romanian table of occupational cancers (no, %)	63 (15.75%)	42 (31.82%)	13 (10.40%)	8 (5.59%)
Occupational exposure related to Romanian table of occupational cancers with moderate and high level of risk (no, %)	44 (11%)	34 (25.75%)	6 (4.80%)	4 (2.79%)
Occupational exposure related to IARC carcinogenic agents with sufficient evidence (no, %)	98 (24.50%)	53 (40.15%)	33 (26.40%)	12 (8.39%)

Group 1 – patients with lung cancer, Group 2- patients with bladder cancer, Group 3 – patients with other types of cancers

2.4. Criterion Validation

For the comparison of the questionnaire with the respondent's occupational history, we used the items included in the exposure risk level score. The comparison was conducted for each item individually, for the final score, and for the exposure risk category (Supplementary Table 1). The result based on Exposure risk level category showed a good concordance (k = 0.719).

2.5. Intra-observer Reliability or Test–Retest Reliability

The intra-observer reliability test was performed for each question in the Occupational Exposure to Carcinogens Questionnaire. Of the 19 questions, 3 have moderate agreement, 1 has good agreement, and the rest are excellent (Supplementary Table 2). Overall, the intra-observer reliability test showed a Cohen's kappa coefficient value of 0,795 for exposure risk level score and a k = 1.000 for exposure risk level category.

2.6. Inter-observer Reliability

The result of the inter-observer test indicates a good level of reliability with a k = 0.790 for exposure risk level score and an excellent one with a k = 0.945 for exposure risk level category. For this test, out of the 19 questions, 3 are rated "moderate agreement," 6 are rated "good agreement," and the rest are rated "excellent" (Supplementary Table 3).

DISCUSSION

This questionnaire was developed to identify patients diagnosed with cancer who have been exposed to carcinogens. The questions focused on IARC Group I occupational carcinogens and high-risk occupations involving exposure to carcinogens. Some of the questions also tried to highlight non-occupational exposure, both from smoking and from the environment. Smoking, a major risk factor for cancer, was considered both as active smoking and as exposure to secondhand smoke. Meanwhile, smoking assessment is important, as occupational cancer risk in smokers is higher [30]. It is also important in terms of interventions, as educational programs should target not only the occupational hazards, but also smoking and the complex, personalized interventions [31].

After the initial pilot testing of the questionnaire on 30 patients and following discussions with the expert group, the structure of the questionnaire was slightly modified. The final version of the questionnaire was deemed to have good acceptability and comprehensibility by participants and scientific validity by experts.

A comparison with the reference standard—the occupational medical history—revealed good agreement with the Questionnaire on Occupational Exposure to Carcinogens. Furthermore, both the intra-observer and inter-observer reliability tests indicated high agreement, suggesting a high degree of repeatability and consistency.

The time required to complete the questionnaire—between 10 and 15 minutes— makes it easier to use in consultations.

All of these factors contribute to the advantage of this questionnaire, which can be used by doctors from various specialties and can even be self-administered by the patient, justifying its use as an effective and user-friendly tool in practice.

Most of the patients included in our study can be considered representative of patients with occupational cancer. The median age at diagnosis was similar to the peak identified in the literature [32]. The median age at diagnosis in the study was slightly

lower than what is reported in the literature, a finding which might be correlated to the fact that more than half of them reported occupational exposure to at least one carcinogen. In a previous analysis of an older Romanian cohort of lung cancer, we identified an earlier onset in some activity domains [33].

There is a disparity in the incidence of occupational cancers between men and women. The number of men is 4 to 5 times higher than the number of women in the workforce [34]. In this study, the number of women with medium and high risk was lower than that of men, but by a smaller proportion than shown in other statistics (36.75%). This could be explained by past employment (during the communist period) of many women in occupations in which, in other countries, the majority of the workforce is represented by men.

The fields of activity of the participants in the study were grouped into six broad categories: agriculture, construction, emergency (police, military), industry (industry, power generation, water distribution), services (education, healthcare, public administration, scientific activities, financial intermediation, hospitality), and transportation (trade, transportation). The largest number of respondents were those who worked in the industrial sector (42.75%), followed by the services and transportation sectors. These data overlap with what we know about work areas with high levels of exposure to carcinogens. Increased exposure to carcinogens was related to the leather and leather products industry, the wood, woodworking and furniture industries, extractive industry, production of electricity, thermal energy, gas, hot water and air conditioning, metal construction industry, metallurgical industry and products from non-metallic materials. Most of these types of industry are included or related to IARC group I carcinogens and studies demonstrated an elevated prevalence of lung cancer [33]. The industry and transportation sectors are also related to increased prevalence of bladder cancer [24].

The questionnaire identified 69.75% of the 400 subjects diagnosed with cancer who reported possible exposure to a known carcinogen. Of these, 63 (15.75%) showed a correlation between the carcinogen and the cancer's location, based on the list of carcinogens included in Romania's Table of Occupational Diseases [35]. Based on the risk score, we identified 44 (11%) subjects who had occupational exposure and a moderate to high risk of exposure to carcinogens, which is concordant with the expected prevalence of occupational cancer. This demonstrates the questionnaire's ability to be relevant in identifying potential occupational cancers; therefore, patients with moderate or high-risk levels should be referred to an occupational physician.

This study has several limitations. The first is a possible selection bias, because those who were more interested in responding to the questionnaire may have had occupational exposure, leading to an overestimation of occupational exposure to carcinogens. The second limitation is a possible recall bias, as some subjects had difficulty recalling information, most commonly due to a lack of knowledge about the products used.

CONCLUSION

As part of this study, a concise and easy-to-apply questionnaire — Occupational Exposure to Carcinogens Questionnaire — was developed and validated for identifying occupational exposure to carcinogens. Its systematic use in Romania could simplify the identification of individuals with occupational cancer. Recognizing these types of cancer could contribute to epidemiological monitoring, the implementation of preventive measures, and the provision of information to workers exposed to carcinogens. Furthermore, the questionnaire can be used in everyday medical practice and can assist physicians in the cancer diagnosis algorithm for patients who have been exposed to occupational carcinogens.

Conflicts of interest and sources of funding

The authors declare no conflict of interest.

Acknowledgments

I would like to express my sincere thanks to everyone who contributed to the successful completion of this study. I would like to thank Dr. Liliana Râpas (Department of Public Health) for her guidance. Her experience in occupational medicine and her valuable insights regarding practical cases were essential in defining the structure of this questionnaire. I would also like to thank Dr. Andrei Popescu (Colentina Clinical Hospital—Oncology Department) for his valuable observations and support throughout the entire project. I am appreciative of Cătălina Elena Coșcleacără for her assistance in conducting the interviews. I am also grateful to the medical support staff at all the hospitals and clinics that facilitated the operations necessary to carry out this research.

Authors' contribution

Conceptualization, C.M., A.S.C.R., S.D.R., M.T.G., C.L.T., and MRO.; methodology, C.M., A.E.M., M.T.G., C.L.T., and M.R.O.; software, C.M.; validation, C.M., A.S.C.R., S.D.R., A.M., and M.R.O.; formal analysis, C.M.; investigation, C.M., and A.M.; resources, C.M., A.S.C.R., and S.D.R.; data curation, A.E.M.; writing—original draft preparation, C.M.; writing—review and editing, A.E.M., M.T.G., C.L.T., and M.R.O.; supervision, C.L.T., and M.R.O. All authors have read and agreed to the published version of the manuscript.

Ethics approval and consent to participate

The study was conducted in accordance with the Declaration of Helsinki, and approved by the Institutional Review Board (or Ethics Committee) of COLENTINA CLINICAL HOSPITAL (protocol no. 20 from 23.12.2022), PROF. DR. THEODOR BURGHELE CLINICAL HOSPITAL (protocol no.3291 from 03.04.2023), THE MARIUS NASTA INSTITUTE OF PNEUMOPHYSIOLOGY IN BUCHAREST (protocol no.23941 from 25.10.2023), THE "PROF. DR. ALEXANDRU TRESTIOREANU" ONCOLOGY INSTITUTE IN BUCHAREST (protocol no. 6571 from 09.05.2024), AND THE DOMINA-SANA CLINIC (protocol no. 576/19.04.2023).

Patient consent for publication

Informed consent was obtained from all subjects involved in the study.

References

1. Purdue MP, Hutchings SJ, Rushton L, Silverman DT. The proportion of cancer attributable to occupational exposures. Annals of Epidemiology. 2015 Mar 1; Causes of Cancer25(3):188–92. doi:10.1016/j.annepidem.2014.11.009

2. Cherrie JW, van Tongeren M, Kromhout H. Estimating occupational disease burden: a way forward. Ann Work Expo Health. 2024 Aug 1;68(7):673–7. doi:10.1093/annweh/wxae040

3. Zellner M, Jungmann OP, Schöps W. [Occupational cancer of the urinary tract-incidence, reporting behavior, and administrative procedures]. Urologie. 2022 Nov;61(11):1179–85. doi:10.1007/s00120-022-01942-0 PubMed PMID: 36280644.

4. Langård S, Lee LJH. Methods to recognize work-related cancer in workplaces, the general population, and by experts in the clinic, a Norwegian experience. J Occup Med Toxicol. 2011 Sep 7; 6:24. doi:10.1186/1745-6673-6-24 PubMed PMID: 21899752; PubMed Central PMCID: PMC3179924.

5. Cancer Today [Internet]. [cited 2026 Aug 12]. Available from: https://gco.iarc.who.int/today/

6. Mandanach C, Maftei A, Țocan OM, Toma CL, Oțelea MR, Mandanach C, et al. Neglected Occupational Risk Factors—A Contributor to Diagnostic Delays in Lung Cancer. Healthcare. 2026 Jan 1;14(1). doi:10.3390/healthcare14010106

7. GHEORGHE AG, NIŢU FM, STANCIU IA, STREBA CT. Association between Risk Factors and the Existence of Lung Malignancies in a Population from the South-West Romania: A Single-Center Study. Curr Health Sci J. 2021;47(4):485–93. doi:10.12865/CHSJ.47.04.02 PubMed PMID: 35444830; PubMed Central PMCID: PMC8987467.

8. Handra CM, Chirila M, Smarandescu RA, Ghita I. Near Missed Case of Occupational Pleural Malignant Mesothelioma, a Case Report and Latest Therapeutic Options. International Journal of Environmental Research and Public Health. 2022 Jan;19(22):14763. doi:10.3390/ijerph192214763

9. Sciannameo V, Carta A, d'Errico A, Giraudo M, Fasanelli F, Arici C, et al. New insights on occupational exposure and bladder cancer risk: a pooled analysis of two Italian case–control studies. International Archives of Occupational and Environmental Health. 2019 Apr 1;92. doi:10.1007/s00420-018-1388-2

10. Risks and causes of bladder cancer. Cancer research UK. [Internet]. Last reviewed 06.08.2026 [cited 2026 Aug 30]. Available from: https://www.cancerresearchuk.org/about-cancer/bladder-cancer/risks-causes

11. Sample Size Calculator [Internet]. [cited 2026 Aug 12]. Available from: https://www.calculator.net/sample-size-calculator.html?type=1&cl=95&ci=5&pp=6&ps=5000&x=Calculate

12. CDC. Cancer (Occupational). [Internet]. 2025 [cited 2026 Feb 18]. Occupational Cancer. Available from: https://www.cdc.gov/niosh/cancer/about/index.html

13. Ferrer J, Granados G, Hernández S, Cruz MJ, Sampol J, Alvarez-Simon D, et al. Validation of an Asbestos Exposure Questionnaire (QEAS-7) for Clinical Practice. International Journal of Environmental Research and Public Health. 2020 Dec 8; 17:9167. doi:10.3390/ijerph17249167

14. Vazquez FL, Silveira HCS, Otero UB, Hosokawa TT, Fregnani JHTG, Longatto-Filho A, et al. The Usefulness of an Online Simplified Screening Questionnaire (SSQ) in Identifying Work-Related Cancers. Healthcare (Basel). 2023 May 26;11(11):1563. doi:10.3390/healthcare11111563 PubMed PMID: 37297703; PubMed Central PMCID: PMC10252760.

15. Pélissier C, Dutertre V, Fournel P, Gendre I, Michel Vergnon J, Kalecinski J, et al. Design and validation of a self-administered questionnaire as an aid to detection of occupational exposure to lung carcinogens. Public Health. 2017 Feb; 143:44–51. doi:10.1016/j.puhe.2016.10.026

16. Inail.it [Internet]. 2021 Oct 11. [cited 2025 Dec 22]. Renaloccam. Il sistema di monitoraggio delle neoplasie a bassa frazione eziologica - Manuale operativo. Available from: https://www.inail.it

17. Bladder Cancer Questionnaire - IfADo [Internet]. [cited 2025 Dec 15]. Available from: https://www.ifado.de/en/transfer-advice/bladder-cancer-questionnaire

18. IARC Monographs – <I>List of Classifications by Cancer Site</I> [Internet]. [cited 2026 Jul 26]. Available from: https://www.iarc.who.int/news-events/iarc-monographs-list-of-classifications-by-cancer-site

19. Occupational diseases statistics - occupational cancers. Statistics explain. 131281.pdf [Internet]. [cited 2026 Jul 22]. Available from: https://ec.europa.eu/eurostat/statistics-explained/SEPDF/cache/131281.pdf

20. IARC Monographs – <I>List of Classifications by Cancer Site</I> [Internet]. [cited 2026 Aug 14]. Available from: https://www.iarc.who.int/news-events/iarc-monographs-list-of-classifications-by-cancer-site

21. Government of Canada CC for OH and S. CCOHS: Cancer Sites Associated with Occupational Exposures [Internet]. 2025 [cited 2026 Aug 14]. Available from: https://www.ccohs.ca/oshanswers/diseases/cancer/carcinogen_site.html

22. Occupational cancer in Australia | Safe Work Australia [Internet]. 2020 Mar 19 [cited 2026 Aug 14]. Available from: https://www.safeworkaustralia.gov.au/resources-and-publications/statistical-reports/occupational-cancer-australia

23. Paris L, Scarselli A, Marinaccio A, Massari S. Assessment of Occupational Carcinogenic Risk by Comparing Data from the Italian Register of Occupational Exposures to Carcinogens (SIREP) with the International Agency for Research on Cancer (IARC) Evidence. International Journal of Environmental Research and Public Health. 2023 May 17; 20:5850. doi:10.3390/ijerph20105850

24. Mandanach C, Handra CM, Rascu A, Hohor S, Gurzu IL, Otelea MR, et al. Occupational hazards and bladder cancer-An umbrella review of the risk in workers exposed over the past 30 years. Front Public Health. 2025; 13:1667873. doi:10.3389/fpubh.2025.1667873 PubMed PMID: 41122539; PubMed Central PMCID: PMC12536731.

25. Reed O, Jubber I, Griffin J, Noon AP, Goodwin L, Hussain S, et al. Occupational bladder cancer: A cross section survey of previous employments, tasks and exposures matched to cancer phenotypes. PLoS One. 2020; 15(10):e0239338. doi:10.1371/journal.pone.0239338 PubMed PMID: 33085669; PubMed Central PMCID: PMC7577448.

26. Loomis D, Guha N, Hall AL, Straif K. Identifying occupational carcinogens: an update from the IARC Monographs. Occup Environ Med. 2018

Aug 1;75(8):593–603. doi:10.1136/oemed-2017-104944 PubMed PMID: 29769352.

27. Darcey E, Carey R, Reid A, Fritschi L, Driscoll T. The Australian Work Exposure Study (AWES): carcinogen exposures in the manufacturing industry. Canberra, Australian Capital Territory: Safe Work Australia; 2016.

28. Landis JR, Koch GG. The measurement of observer agreement for categorical data. Biometrics. 1977 Mar;33(1):159–74. PubMed PMID: 843571.

29. Coman MA, Forray AI, Van den Broucke S, Chereches RM. Measuring Health Literacy in Romania: Validation of the HLS-EU-Q16 Survey Questionnaire. Int J Public Health. 2022; 67:1604272. doi:10.3389/ijph.2022.1604272 PubMed PMID: 35185446; PubMed Central PMCID: PMC8855985.

30. Epistemonikos [Internet]. [cited 2026 Aug 30]. Indirect adjustment of tobacco smoking in occupational studies of lung cancer: A systematic review of the available methods and their applications. Available from: https://www.epistemonikos.org/en/documents/97160e43366862e242e24b3afba4c3ffe85b49ec

31. Chirila M, Ghita I, Handra C, Fulga I. Genetic variants influencing smoking behavior and efficacy of smoking cessation therapies. Romanian Biotechnological Letters. 2014 Sep 1; 19:9727–34.

32. Risk Factors: Age - NCI [cgvArticle] [Internet]. 2015 [cited 2026 Aug 24]. Located at: nciglobal,ncienterprise. Available from: https://www.cancer.gov/about-cancer/causes-prevention/risk/age

33. Mandanach C, Mateș D, Jinga V, Otelea M. Occupational domains and age at onset of lung cancer diagnosis. Romanian Journal of Occupational Medicine. 2024 Dec 20; 75:18–25. doi:10.2478/rjom-2024-0003

34. Olsson A, Kromhout H. Occupational cancer burden: the contribution of exposure to process-generated substances at the workplace. Molecular Oncology. 2021;15(3):753–63. doi:10.1002/1878-0261.12925

35. HOTARARE 259 23/02/2022 - Portal Legislativ [Internet]. [cited 2026 Aug 24]. Available from: https://legislatie.just.ro/Public/DetaliiDocument/252418

Supplementary Materials

Supplementary Table 1. Kappa coefficient between the Questionnaire and the occupational history

	Exposure	Duration of exposure	Personal protective equipment/ time of daily exposure	Ventilation	Exposure risk level score	Exposure risk level category
Cohen's Kappa Index (k)	0.704 (p=0.000)	0.809 (p=0.000)	0.650 (p=0.000)	0.629 (p=0.000)	0.543 (p=0.000)	0.719 (p=0.000)

Supplementary Table 2. Cohen's Kappa Index for each question in the Questionnaire for intra-observer reliability

	Q1	Q2	Q3	Q4	Q5	Q6	Q7	Q8	Q9	Q10
K	1.000	0.582	0.509	1.000	0.904	0.802	1.000	1.000	1.000	0.944

	Q11	Q12	Q13		Q14				Q15	
			1	2	1	2	3	4	1	2
K	1.000	0.946	0.960	0.846	1.000	1.000	0.962	1.000	1.000	0.822

	Q16								Q17	Q18	Q19	
	1	2	3	4	5	6	7	8			1	2
K	1.000	0.857	0.348	0.923	0.933	1.000	1.000	1.000	0.792	0.933	0.959	0.615

Supplementary Table 3. Cohen's Kappa Index for each question in the Questionnaire for inter-observer reliability

	Q1	Q2	Q3	Q4	Q5	Q6	Q7	Q8	Q9	Q10
K	1.000	0.502	0.724	1.000	0.864	1.000	1.000	1.000	0.916	0.928

	Q11	Q12	Q13		Q14				Q15	
			1	2	1	2	3	4	1	2
K	1.000	0.899	0.917	0.838	1.000	0.930	0.870	0.474	1.000	0.778

	Q16								Q17	Q18	Q19	
	1	2	3	4	5	6	7	8			1	2
K	0.864	0.762	0.762	0.831	1.000	1.000	1.000	0.533	1.000	0.772	1.000	0.736

Chestionar

Număr identificare.....

Vârsta.....

Ultima școală absolvită.....

Q1.Ce tip de cancer aveți?

1.	al cavității nazale și al sinusurilor feței	
2.	nazofaringian	
3.	laringian	
4.	bronhopulmonar	
5.	gastric	
6.	hepatic	
7.	osos	
8.	al pielii - melanom	
9.	al pielii	
10.	mezoteliom	
11.	endoteliom (sarcom Kaposi)	
12.	renal	
13.	al vezicii urinare	
14.	ocular	
15.	cerebral și al sistemului nervos central	
16.	tiroidian	
17.	ovarian	
18.	leucemie și/sau limfom	
19.	alte afecțiuni maligne	

Q2.Știți dacă ați fost expus în trecut la următoarele:

		DA	NU
1.	Metale		
2.	Praf sau fibre		
3.	Fumuri, gaze și vapori		
4.	Pesticide		
5.	Solvenți		
6.	Orice alt tip de substanțe chimice		
7.	Radiații		
8.	Agenți biologici		

Q3.Dacă răspunsul este DA, detaliați:

			DA	NU
Metal	1.	Arseniu		
	2.	Beriliu		
	3.	Cadmiu		
	4.	Crom		
	5.	Nichel		
Praf organic si anorganic, fibre	6.	Azbest - fibre (actinolit, amosit, antofilit, crisotil, crocidolit, tremolit)		
	7.	Siliciu – pulbere (cuarț, cristobalit)		
	8.	Lemn - pulbere		
	9.	Piele - fibre și pulbere		
Substanțe chimice	10.	1,3 butadiena		
	11.	1,2 dicloropropan		
	12.	Alcool izopropilic		
	13.	Bis(clorometil)eter, clorometil-metileter		
	14.	Bifenil policlorurat (PCBs)		
	15.	Clorura de vinil monomer		
	16.	Formaldehidă		
	17.	Oxizi de fier		
	18.	Vapori de acizi organici tari		
	19.	Amine aromatice (Xenilamină, Benzidină, 2-naftilamină, MOCA, O-dianisidină, O-toluidină, P-cloro-o-toluidină, auramină)		
	20.	Coloranți derivați din benzidină (CI direct black 38, CI direct blue 6, CI direct brown 95)		
	21.	Hidrocarburi aromatice policiclice din funingine, gudron de cărbune sau smoală de huilă		
	22.	Oxid de etilenă		
Uleiuri	23.	Uleiuri minerale		
	24.	Uleiuri de șist		
Fumuri	25.	Emisii de eșapament motoare Diesel		
	26.	Fumuri de sudură		
	27.	Funingine de cărbune, lemn		
	28.	Fum de țigară pasiv		
Pesticide	29.	Organoclorurate(lindan, pentaclorofenol)		
	30.	Organofosfate (malation)		
	31.	Produse cu arseniu		
Solvenți	32.	Benzen		
	33.	Tricloroetilena		
	34.	Tetracloretilena		

Radiații	35.	UV - artificiale		
	36.	UV - solare		
	37.	Radiații ionizante (X si gamma)		
	38.	Substanțe radioactive (radon, radiu, plutoniu, stroțiu, cesiu, tritiu, iod, toriu, fosfor)		
Agenți biologici	39.	Virus hepatitic B		
	40.	Virus hepatitic C		
	41.	HIV tip1		
	42.	Virus herpetic (HHV8) al sarcomului Kaposi		
	43.	Virus Epstein Barr (HHV 4)		
	44.	Helicobacter pylori		
	45.	Consum de alcool		
	46.	Alți agenți carcinogeni		

Q4.Ați lucrat în vreunul din următoarele procese industriale:

		DA	NU
1.	Fabricarea cauciucului		
2.	Fabricarea carburii de siliciu (proces Acherson)		
3.	Fabricarea aluminiului (proces Sodenberg)		
4.	Fabricarea auraminei		
5.	Fabricarea cocsului		
6.	Gazeificarea si distilarea cărbunelui (gudron de cărbune, smoală de huilă)		
7.	Fabricare magenta		
8.	Fabricarea fontă și oțel		

Q5.Ați lucrat în una din următoarele activități profesionale:

		DA	NU
1.	Șantiere de construcții sau drumuri		
2.	Industria sticlei		
3.	Industria ceramică		
4.	Vopsitorie		
5.	Curățătorii chimice (curățare uscată)		
6.	Tipografie		
7.	Minerit		
8.	Fabricare, prelucrare și asamblare piese metalice		
9.	Metalurgie metale neferoase (cupru, zinc) – turnare		
10.	Prelucrarea și vopsirea fibrelor textile (se exclud fabricile de confecții)		

Q6. Ați folosit echipament de protecție?

DA	NU

Q7. Cât ați folosit echipamentul de protecție?

Tot timpul	Aproape tot timpul	3/4 din timp (aprox.30 ore/lună)	1/2 din timp (aprox.20 ore/lună)	1/4 din timp (aprox.10 ore/lună)	Extrem de puțin timp	Niciodată

Q8. Exista ventilație la locul de muncă?

DA	Cu funcționare intermitentă
NU	

Q9. Ați lucrat în aer liber?

Tot timpul	Aproape tot timpul	3/4 din timp (aprox.30 ore/lună)	1/2 din timp (aprox.20 ore/lună)	1/4 din timp (aprox.10 ore/lună)	Extrem de puțin timp	Niciodată

Q10. Ați folosit creme de protecție (de exemplu: pentru mâini sau față)?

Tot timpul	Aproape tot timpul	3/4 din timp (aprox.30 ore/lună)	1/2 din timp (aprox.20 ore/lună)	1/4 din timp (aprox.10 ore/lună)	Extrem de puțin timp	Niciodată

Q11. De obicei, v-ați spălat mâinile cu solvenți la locul de muncă?

DA	
NU	

Q12. Sunteți fumător?

DA - fumător	NU
DA - fost fumător	

Q13. Dacă răspunsul este DA, detaliați:

Câți ani ați fumat?	
La ce vârstă ați început să fumați?	
Câte țigări ați fumat în medie/zi?	

Q14.	DA	NU
Ați fumat la locul de muncă?		
Ați fumat acasă?		
Erați expus la fumat pasiv la locul de muncă?		
Erați expus la fumat pasiv acasă?		

Q15. Dacă da, câti ani ați fost expus la fumat pasiv?

Câți ani ați fost expus la fumat pasiv la locul de muncă?	
Câți ani ați fost expus la fumat pasiv acasă?	

Q16.	DA	NU
Ați mâncat la locul de muncă?		
Ați mâncat în condiții igienice?		
Locuiți în apropiere de o fabrică, complex comercial sau groapă de gunoi?		
Ați facut renovări în casă?		
Locuința dvs.are sobă/ șemineu cu lemne?		
Locuința dvs.are sobă/șemineu cu gaz?		
Folosiți apa de puț/fântână?		
Folosiți legume de pe teren propriu sau de la producători locali?		

Q17. Folosiți pesticide, insecticide sau erbicide pe lângă casă?

DA	
NU	

Q18. Aveți alte activități frecvente efectuate pe langă casă sau mașină?
(de exemplu: pictură, bricolaj, grădinărit, mecanică)

DA	
NU	

Q19. În ce domeniu ați lucrat/lucrați? (daca ati lucrat în mai multe domenii, bifați cel în care ați fost expus la agenții menționați de dvs; dacă ați fost expus la aceleași condiții de muncă în mai multe domenii, bifați toate domeniile)

	Domeniu ocupațional	Profesia	Perioada
1.	**Agricultură, silvicultură și pescuit**		
2.	**Industria extractivă**		
	Industria prelucrătoare		
3.	*Industria alimentară*		
4.	*Industria textilă*		
5.	*Prelucrare piele*		

6.	*Prelucrare lemn*		
7.	*Fabricare hârtie*		
8.	*Tipărire și reproducere pe diferite suporturi*		
9.	*Fabricare produse cocserie*		
10.	*Fabricarea substanțelor și produselor chimice*		
11.	*Industria farmaceutică*		
12.	*Fabricarea de produse de cauciuc sau mase plastice*		
13.	*Fabricarea produselor din materiale nemetalice*		
14.	*Industria metalurgică*		
15.	*Industria construcțiilor metalice*		
16.	*Fabricare echipamente electronice și optice*		
17.	*Fabricarea echipamentelor electrice*		
18.	*Fabricarea autovehiculelor, mașini și utilaje*		
19.	*Fabricarea altor mijloace de transport*		
20.	*Alte activități industriale*		
21.	**Producția și furnizarea de energie electrică, termică, gaze, apă caldă și aer condiționat**		
22.	**Distribuția apei; salubritate, gestionarea deșeurilor, activități de decontaminare**		
23.	**Constructii**		
24.	**Comert cu ridicata și cu amanuntul; repararea autovehiculelor și motocicletelor**		
25.	**Transport și depozitare**		
26.	**Hoteluri și restaurante**		
27.	**Informații și comunicații**		
28.	**Intermedieri financiare și asigurări**		
29.	**Tranzacții imobiliare**		
30.	**Activități profesionale, științifice și tehnice**		
31.	**Activități de servicii administrative și activități de servicii suport**		
32.	**Administrație publică și apărare; asigurări sociale din sistemul public**		
33.	**Învățământ**		
34.	**Sănătate și asistență socială**		
35.	**Activități de spectacole, culturale și recreative**		
36.	**Alte activități de servicii**		
37.	**Activități ale gospodăriilor private în calitate de angajator de personal casnic**		
38.	**Activități ale organizațiilor și organismelor extrateritoriale**		

Chestionar – versiunea aparat urinar

Număr identificare .....

Vârsta.....

Ultima școală absolvită.....

Q1. Ce tip de cancer aveți?

1)	renal	
2)	al vezicii urinare	

3)	de prostată	
4)	alte afecțiuni maligne	

Q2. Știți dacă ați fost expus în timpul activității profesionale la următoarele:

		DA	NU
1.	Metale		
2.	Praf sau fibre		
3.	Fumuri, gaze și vapori		
4.	Pesticide		
5.	Solvenți		
6.	Orice alt tip de substanțe chimice		
7.	Radiații ionizante		
8.	Agenți biologici		

Q3. Dacă răspunsul este DA, detaliați:

			DA	NU
Metale	1.	Arseniu		
	2.	Cadmiu		
Fumuri	3.	Emisii de eșapament motoare Diesel		
	4.	Fumuri de sudură		
	5.	Fum de țigară pasiv		
Pesticide	6.	Organofosforice (malathion)		
	7.	Produse cu arseniu		
Substanțe chimice	8.	Hidrocarburi aromatice policiclice din funingine, gudron de cărbune sau smoală de huilă		
	9.	Amine aromatice (Xenilamină, Benzidină, 2-naftilamină, MOCA, O-dianisidină, P-cloro-o-toluidină, auramină)		
	10.	Coloranți derivați din benzidină (CI direct black 38, CI direct blue 6, CI direct brown 95)		
	11.	O-toluidină		
	12.	2 mercaptobenzotiazol		
	13.	Acid perfluorooctanoic		
Solvenți	14.	Tetracloroetilena		
	15.	Tricloroetilena		
Radiații	16.	Radiații ionizante (X si gamma)		

Q4.Ați lucrat în vreunul din următoarele procese industriale:

		DA	NU
1.	Fabricarea cauciucului		

2.	Fabricarea carburii de siliciu (proces Acherson)		
3.	Fabricarea aluminiului (proces Sodenberg)		
4.	Fabricarea auraminei		
5.	Fabricarea cocsului		
6.	Gazeificarea si distilarea cărbunelui (gudron de cărbune, smoală de huilă)		
7.	Fabricare magenta		
8.	Fabricarea fontă și oțel		

Q5.Ați lucrat în una din următoarele activități profesionale:

		DA	NU
1.	Șantiere de construcții sau drumuri		
2.	Industria sticlei		
3.	Industria ceramică		
4.	Vopsitorie		
5.	Curățătorii chimice (curățare uscată)		
6.	Tipografie		
7.	Minerit		
8.	Fabricare, prelucrare și asamblare piese metalice		
9.	Metalurgie metale neferoase (cupru, zinc) – turnare		
10.	Prelucrarea și vopsirea fibrelor textile (se exclud fabricile de confecții)		

Q6. Ați folosit echipament de protecție?

DA	NU

Q7. Cât ați folosit echipamentul de protecție?

Tot timpul	Aproape tot timpul	3/4 din timp (aprox.30 ore/lună)	1/2 din timp (aprox.20 ore/lună)	1/4 din timp (aprox.10 ore/lună)	Extrem de puțin timp	Niciodată

Q8. Exista ventilație la locul de muncă?

DA - funcționare bună	NU
DA - funcționare intermitentă	

Q9. Ați lucrat în aer liber?

Tot timpul	Aproape tot timpul	3/4 din timp (aprox.30 ore/lună)	1/2 din timp (aprox.20 ore/lună)	1/4 din timp (aprox.10 ore/lună)	Extrem de puțin timp	Niciodată

Q10. Ați folosit creme de protecție (de exemplu: pentru mâini sau față)?

Tot timpul	Aproape tot timpul	3/4 din timp (aprox.30 ore/lună)	1/2 din timp (aprox.20 ore/lună)	1/4 din timp (aprox.10 ore/lună)	Extrem de puțin timp	Niciodată

Q11. De obicei, v-ați spălat mâinile cu solvenți la locul de muncă?

DA	
NU	

Q12. Sunteți fumător?

DA - fumător	NU
DA - fost fumător	

Q13. Dacă răspunsul este DA, detaliați:

Câți ani ați fumat?	
La ce vârstă ați început să fumați?	
Câte țigări ați fumat în medie/zi?	

Q14.	DA	NU
Ați fumat la locul de muncă?		
Ați fumat acasă?		
Erați expus la fumat pasiv la locul de muncă?		
Erați expus la fumat pasiv acasă?		

Q15. Dacă da, câti ani ați fost expus la fumat pasiv?

Câți ani ați fost expus la fumat pasiv la locul de muncă?	
Câți ani ați fost expus la fumat pasiv acasă?	

Q16.	DA	NU
Ați mâncat la locul de muncă?		
Ați mâncat în condiții igienice?		
Locuiți în apropiere de o fabrică, complex comercial sau groapă de gunoi?		
Ați facut renovări în casă?		
Locuința dvs.are sobă/ șemineu cu lemne?		
Locuința dvs.are sobă/șemineu cu gaz?		
Folosiți apa de puț/fântână?		

Folosiți legume de pe teren propriu sau de la producători locali?		

Q17. Folosiți pesticide, insecticide sau erbicide pe lângă casă?

DA	
NU	

Q18. Aveți alte activități frecvente efectuate pe langă casă sau mașină? (de exemplu: pictură, bricolaj, grădinărit, meșterit, sudură)

DA	
NU	

Q19. În ce domeniu ați lucrat/lucrați? (daca ati lucrat în mai multe domenii, bifați cel în care ați fost expus la agenții menționați de dvs; dacă ați fost expus la aceleași condiții de muncă în mai multe domenii, bifați toate domeniile)

	Domeniu ocupațional		Profesia	Perioada
A	**Agricultură, silvicultură și pescuit**	1.	Agricultor	
		2.	Medic veterinar	
		3.	Tehnician în fermele de animale	
		4.	Altă profesie	
B	**Industria extractivă**	5.	Minerit în aer liber	
		6.	Minerit în subteran	
		7.	Excavatorist	
		8.	Altă profesie	
C	**Industria prelucratoare**	9.	Lucrător în extracția uleiurilor și grăsimilor cu ajutorul solvenților.	
	Industria alimentară			
		10.	Lucrător în producția de ulei de măsline	
		11.	Lucrător în producția de ceai, cafea, infuzii	
		12.	Lucrător în tratamente pentru conservarea produselor alimentare	
		13.	Altă profesie	
	Industria textilă	14.	Prelucrator fibre, fire, țesături	
		15.	Călcătoreasă lenjerie	
		16.	Operator curățitor chimic	
		17.	Finisor textile (vopsitor,imprimeur)	
		18.	Altă profesie	
	Prelucrare lemn	19.	Finisor-lăcuitor produse din lemn.	
		20.	Altă profesie	
	Fabricare hârtie	21.	Lucrător în industria hârtiei	
		22.	Altă profesie	
	Tipărire și reproducere pe diferite suporturi	23.	Lucrător în producția de cerneluri, gumă	

			arabică, adezivi, imprimante	
		24.	Lucrător în producția de matrici pentru imprimare fotomecanică, fotogravură	
		25.	Lucrător în tipografie și imprimerie	
		26.	Altă profesie	
	Fabricarea substanțelor și produselor chimice	27.	Operator chimist la fabricarea substanțelor chimice anorganice	
		28.	Operator chimist la fabricarea substanțelor chimice organice	
		29.	Lucrător în industria produselor toxice și corozive	
		30.	Operator chimist la fabricarea coloranților	
		31.	Operator chimist la fabricarea lacurilor, vopselelor, uleiurilor	
		32.	Operator chimist producere insecticide,pesticide, erbicide	
		33.	Operator chimist fabricare de esențe și parfumuri	
		34.	Biochimist în laborator industrial	
		35.	Altă profesie	
	Industria farmaceutică	36.	Operator chimist fabricare produse farmaceutice	
		37.	Altă profesie	
	Industria cauciucului sau maselor plastice	38.	Lucrător în prelucrarea cauciucului brut	
		39.	Operator la confecționarea industrială articole din cauciuc și textile cauciucate	
		40.	Lucrător în producția de cauciuc sintetic	
		41.	Lucrător în producția de polimeri sintetici și artificiali	
		42.	Lucrător în producția de rășină epoxidică	
		43.	Prelucrător rășini sintetice și materiale polimerice termoplastice și termorezistente	
		44.	Operator la obținerea produselor din spume poliuretanice și latex	
		45.	Altă profesie	
	Fabricarea produselor din materiale nemetalice - Industria sticlei	46.	Tehnician fabricare sticlă, sticlă tehnică	
		47.	Tehnician fabric. sticlă plată	
		48.	Lucrător la fabricarea de vată de sticlă	
		49.	Vopsitor industrial	
		50.	Altă profesie	
	Industria metalurgică	51.	Topitor metale și aliaje	
		52.	Prelucrător țevi pentru instalațiile de încălzire,re-frigerare și aer condiționat	
C		53.	Laminator semifabricate, profiluri tablă, platbandă	

		54.	Laminator tablă subțire	
		55.	Acoperitor-învelitor tablă	
		56.	Mașinist la litografiat și vernisat tablă	
		57.	Mașinist pod rulant	
		58.	Operator tratare combustibili nucleari și eliminare deșeuri radioactive	
		59.	Altă profesie	
	Industria construcțiilor metalice	60.	Prelucrător în emailarea, cromarea și tratamente fizico-chimice ale produselor metalice	
		61.	Lucrător în construcția generatoare de aburi	
		62.	Lucrător în construcția de rezervoare, containere din material metalic	
		63.	Sudor	
		64.	Lucrător în producția de dispozitive explozive, dispozitive explozive pentru extracție; propulsoare.	
		65.	Altă profesie	
	Fabricarea echipamentelor electrice	66.	Confecționer cabluri și arbori de cabluri	
		67.	Confecționer instalații electrice	
		68.	Confecționer echipamente electrice, electronice	
		69.	Altă profesie	
	Fabricarea autovehiculelor	70.	Lucrător în construcție, reparare, întreținere, dezmembrare autovehicule	
		71.	Confecționer cablaje auto	
		72.	Altă profesie	
	Fabricarea altor mijloace de transport	73.	Lucrător în construcție, reparare echipamente mobile pentru căi ferate, tramvaie și cabine pt. schi	
		74.	Lucrător în construcție, echipare, reparare, dezmembrare nave și ambarcațiuni	
		75.	Lucrător în construcție, echipare, conversie, reparare, întreținere, dezafectare, dezmembrare mijloace de transp.aerian	
		76.	Altă profesie	
	Alte activități industriale	77.	Lucrător în construcția de echipamente medico-chirurgicale, instrumente de măsurare și control	
		78.	Lucrător în producția și reparația de piese metalice mici	
		79.	Lucrător în construcția de tâmplărie metalică și lucrări cu material metalic	
		80.	Lucrător în producția de aparate de uz casnic sau gospodăresc	
		81.	Lucrător în construcția de ascensoare	
		82.	Bijutier	

		83.	Vopsitor industrial	
		84.	Lucrător cu pigment cromat	
		85.	Altă profesie	
D	**Producția și furnizarea de energie electrică, termică, gaze, apă caldă și aer condiționat**	86.		
E	**Distribuția apei;** **salubritate, gestionarea deșeurilor, activități de decontaminare**	87.	Instalator apa, canal	
		88.	Instalator retele de distribuție și transport fluide, sub presiune	
		89.	Instalator centrale termice	
		90.	Instalator tehnico-sanitare și gaze	
		91.	Instalator încălzire centrală și gaze	
		92.	Instalator frigotehnist	
		93.	Altă profesie	
F	**Constructii**	94.	Lucrător pe șantier	
		95.	Mașinist pentru utilaje specifice la extracție și execuția tunelurilor	
		96.	Mașinist utilaje grele pt. construcții	
		97.	Altă profesie	
G	**Comert cu ridicata și cu amanuntul; repararea autovehiculelor și motocicletelor**	98.	Lucrător comercial	
		99.	Vopsitor auto	
		100.	Mecanic auto	
		101.	Sudor	
		102.	Tinichigiu carosier	
		103.	Vulcanizator auto	
		104.	Lucrător în atelier mecanic	
		105.	Altă profesie	
H	**Transport și depozitare**	106.		
I	**Hoteluri și restaurante**	107.		
J	**Informații și comunicații**	108.		
K	**Intermedieri financiare și asigurări**	109.		
L	**Tranzacții imobiliare**	110.		
M	**Activități profesionale, științifice și tehnice**	111.		
N	**Activități de servicii administrative și activități de servicii suport**	112.		
O	**Administrație publică și apărare; asigurări sociale din sistemul public**	113.	Pompier	
		114.	Altă profesie	
P	**Învățământ**	115.		
Q	**Sănătate și asistență socială**	116.	Asistent medical de laborator	
		117.	Asistent farmacist	
		118.	Farmacist	
		119.	Medic imagist	

		120.	Altă profesie	
R	**Activități de spectacole, culturale și recreative**	121.		
S	**Alte activități de servicii**	122.	Coafor/ coafeză	
		123.	Frizer	
		124.	Stilist	
		125.	Pictor	
		126.	Pictor ceramică, sticlă	
		127.	Pictor decor	
		128.	Altă profesie	
T	**Activități ale gospodăriilor private cu personal casnic**	129.		
U	**Activități ale organizațiilor și organismelor extrateritoriale**	130.		

Chestionar – varianta aparat respirator

Număr identificare.....

Vârsta.....

Ultima școală absolvită.....

Q1.Ce tip de cancer aveți?

1.	bronhopulmonar	
2.	mezoteliom	
3.	alte afecțiuni maligne	

Q2.Știți dacă ați fost expus în trecut la următoarele:

		DA	NU
1.	Metale		
2.	Praf sau fibre		
3.	Fumuri, gaze și vapori		
4.	Pesticide		
5.	Solvenți		
6.	Orice alt tip de substanțe chimice		
7.	Radiații		
8.	Agenți biologici		

Q3.Dacă răspunsul este DA, detaliați:

		DA	NU

Metal	1.	Arseniu		
	2.	Beriliu		
	3.	Cadmiu		
	4.	Crom		
	5.	Nichel		
Praf organic si anorganic, fibre	6.	Azbest - fibre (actinolit, amosit, antofilit, crisotil, crocidolit, tremolit)		
	7.	Siliciu – pulbere (cuarț, cristobalit)		
	8.	Carbură de siliciu		
Substanțe chimice	9.	Bis(clorometil)eter, clorometil-metileter		
	10.	Oxizi de fier		
	11.	Hidrocarburi aromatice policiclice din funingine, gudron de cărbune sau smoală de huilă (benzopiren)		
	12.	Vapori de acizi organici tari		
	13.	Epiclorohidrina		
	14.	1,3 butadiena		
Uleiuri	15.	Uleiuri minerale (sub formă de vapori)		
Fumuri	16.	Emisii de eșapament motoare Diesel		
	17.	Fumuri de sudură		
	18.	Funingine de cărbune, lemn, uleiuri		
	19.	Fum de țigară pasiv		
Pesticide	20.	Produse cu arseniu		
Radiații	21.	Radiații ionizante (X si gamma)		
	22.	Substanțe radioactive (radon, plutoniu, uraniu)		

Q4.Ați lucrat în vreunul din următoarele procese industriale:

		DA	NU
1.	Fabricarea cauciucului		
2.	Fabricarea carburii de siliciu (proces Acherson)		
3.	Fabricarea aluminiului (proces Sodenberg)		
4.	Fabricarea auraminei		
5.	Fabricarea cocsului		
6.	Gazeificarea si distilarea cărbunelui (gudron de cărbune, smoală de huilă)		
7.	Fabricare magenta		
8.	Fabricarea fontă și oțel		

Q5.Ați lucrat în una din următoarele activități profesionale:

		DA	NU
1.	Șantiere de construcții sau drumuri		

2.	Industria sticlei		
3.	Industria ceramică		
4.	Vopsitorie		
5.	Curățătorii chimice (curățare uscată)		
6.	Tipografie		
7.	Minerit		
8.	Fabricare, prelucrare și asamblare piese metalice		
9.	Metalurgie metale neferoase (cupru, zinc) – turnare		
10.	Prelucrarea și vopsirea fibrelor textile (se exclud fabricile de confecții)		

Q6. Ați folosit echipament de protecție?

DA	NU

Q7. Cât ați folosit echipamentul de protecție?

Tot timpul	Aproape tot timpul	3/4 din timp (aprox.30 ore/lună)	1/2 din timp (aprox.20 ore/lună)	1/4 din timp (aprox.10 ore/lună)	Extrem de puțin timp	Niciodată

Q8. Exista ventilație la locul de muncă?

DA	Cu funcționare intermitentă
NU	

Q9. Sunteți fumător?

DA - fumător	NU
DA - fost fumător	

Q10. Dacă răspunsul este DA, detaliați:

Câți ani ați fumat?	
La ce vârstă ați început să fumați?	
Câte țigări ați fumat în medie/zi?	

Q11.	DA	NU
Ați fumat la locul de muncă?		
Ați fumat acasă?		
Erați expus la fumat pasiv la locul de muncă?		
Erați expus la fumat pasiv acasă?		

Q12. Dacă da, câti ani ați fost expus la fumat pasiv?

Câți ani ați fost expus la fumat pasiv la locul de muncă?	
Câți ani ați fost expus la fumat pasiv acasă?	

Q13.	DA	NU
Ați mâncat la locul de muncă?		
Ați mâncat în condiții igienice?		
Locuiți în apropiere de o fabrică, complex comercial sau groapă de gunoi?		
Ați facut renovări în casă?		
Locuința dvs.are sobă/ șemineu cu lemne?		
Locuința dvs.are sobă/șemineu cu gaz?		
Folosiți apa de puț/fântână?		
Folosiți legume de pe teren propriu sau de la producători locali?		

Q14. Folosiți pesticide, insecticide sau erbicide pe lângă casă?

DA	
NU	

Q15. Aveți alte activități frecvente efectuate pe langă casă sau mașină? (de exemplu: pictură, bricolaj, grădinărit, meșterit, sudură)

DA	
NU	

Q16. În ce domeniu ați lucrat/lucrați? (daca ati lucrat în mai multe domenii, bifați cel în care ați fost expus la agenții menționați de dvs; dacă ați fost expus la aceleași condiții de muncă în mai multe domenii, bifați toate domeniile)

	Domeniu ocupațional		Profesia	Perioada
A	**Agricultură, silvicultură și pescuit**	1.	Agricultor	
		2.	Viticultor	
		3.	Tăietor silvic (drujbist)	
		4.	Gaterist	
		5.	Mașinist motoagregate și mașini	
		6.	Altă profesie	
B	**Industria extractivă**	7.	Miner în aer liber	
		8.	Miner în subteran	
		9.	Excavatorist	
		10.	Concasorist	
		11.	Sondor	
		12.	Altă profesie	

C	**Industria prelucrătoare** *Industria alimentară*	13.	Frigotehnist	
		14.	Morar	
		15.	Brutar	
		16.	Cofetar	
		17.	Lucrător în producția de vin și alcool	
		18.	Lucrător în producția de ceară și produse din ceară	
		19.	Altă profesie	
	Industria textilă	20.	Prelucrător fibre sintetice	
		21.	Țesător	
		22.	Mecanic întreținere utilaje	
		23.	Vopsitor industrial	
		24.	Confecționer textile impregnate cu azbest	
		25.	Altă profesie	
	Prelucrare piele	26.	Tăbăcar /argăsitor	
		27.	Blănar/cojocar	
		28.	Meșteșugar finisor	
		29.	Confecționer produse piele	
		30.	Altă profesie	
	Prelucrare lemn	31.	Vopsitor produse lemn	
		32.	Finisor-lăcuitor produse lemn	
		33.	Altă profesie	
	Fabricare hârtie	34.	Operator în prod. celulozei	
		35.	Operator producere hârtie, carton, fibre celulozice	
		36.	Altă profesie	
	Tipărire și reproducere pe diferite suporturi	37.	Lucrător în producția de cerneluri, pigmenți	
		38.	Lucrător în imprimare magnetică, fotogravură	
		39.	Lucrător în tipografie, litogravură și imprimerie	
		40.	Altă profesie	
	Fabricare produse cocserie	41.	Operator producție de cocs	
		42.	Operator la chimizare gaz de cocs	
		43.	Fochist	
		44.	Altă profesie	
	Fabricarea substanțelor și produselor chimice	45.	Operator chimist fabricare subst. chimice anorganice	
		46.	Operator chimist la fabricarea substanțelor chimice organice	
		47.	Operator în producerea de agenți tensioactivi	
		48.	Operator în producerea de sodiu, potasiu, calciu, bariu, magneziu, litiu și compușii lor	

		49.	Lucrător în industria produselor toxice și corozive	
		50.	Operator chimist la fabricarea coloranților	
		51.	Operator chimist la fabricarea lacurilor, vopselelor, uleiurilor	
		52.	Operator chimist în producția de fitosanitare și îngrășăminte	
		53.	Operator chimist la fabricarea de esențe și parfumuri	
		54.	Operator chimist la fabricarea fibrelor sintetice și artificiale	
		55.	Biochimist în laborator industrial	
		56.	Altă profesie	
	Industria farmaceutică	57.	Operator chimist la fabricarea produselor farmaceutice	
		58.	Altă profesie	
	Fabricarea de produse de cauciuc sau mase plastice	59.	Lucrător în prelucrarea cauciucului brut	
		60.	Operator la confecționarea industrială articole din cauciuc și textile cauciucate	
		61.	Lucrător în producția de cauciuc sintetic	
		62.	Lucrător în producția de polimeri sintetici și artificiali	
		63.	Lucrător în producția de rășină sintetice	
		64.	Prelucrător rășini sintetice și materiale polimerice termoplastice și termorezistente	
		65.	Altă profesie	
	Fabricarea produselor din materiale nemetalice	66.	Tehnician la fabricarea sticlei obișnuite, a sticlei tehnice și speciale	
		67.	Tehnician la fabricarea sticlei plate/mate	
		68.	Vopsitor industrial	
		69.	Lucrător la fabricarea lacurilor și emailurilor vitroase	
		70.	Lucrător la fabricarea de vată de sticlă	
		71.	Operator la fabricarea materialelor și produselor refractare	
		72.	Fochist	
		73.	Operator la fabricarea ceramicii	
		74.	Operator la fabricarea de cărămizi, țigle și alte produse pentru construcții	
		75.	Operator la fabricarea elementelor prefabricate din beton, azbociment, ciment, piatră artificială, conglomerate suflate	
		76.	Operator la fabricarea elementelor din vată de lemn, paie, stuf, zgură aglomerate cu ciment, tencuială sau alte lianți minerali	
		77.	Operator la fabricarea de lianți minerali, argile expandate și perleți	

		78.	Operator la fabricarea produselor din ipsos și gips	
		79.	Operator prelucrare marmură, pietre ornamentale, pietre molare, roci și minerale	
		80.	Operator la fabricarea produselor abrazive.	
		81.	Operator la producția de materiale de frecare și materiale carbonice	
		82.	Altă profesie	
	Industria metalurgică	83.	Topitor metale și aliaje	
		84.	Lucrător în producerea de pulberi metalice	
		85.	Operator la tratarea și prelucrarea materiilor prime pentru producția de metale și aliaje	
		86.	Turnător-formator al produselor din fontă sau oțel.	
		87.	Debavurator, sablator al produselor din fontă sau oțel.	
		88.	Operator producție de piese finite și semifinite metalice	
		89.	Curățitor produse metalice	
		90.	Vopsitor produse metalice	
		91.	Galvanizator	
		92.	Strungar, slefuitor	
		93.	Frezor	
		94.	Forjor matrițer	
		95.	Prelucrător țevi pentru instalațiile de încălzire,re-frigerare și aer condiționat	
C		96.	Laminator semifabricate, profiluri tablă, platbandă	
		97.	Laminator tablă	
		98.	Acoperitor-învelitor de tablă sau placi azbociment	
		99.	Mașinist la litografiat și vernisat tablă	
		100.	Mașinist pod rulant	
		101.	Sudor	
		102.	Altă profesie	
	Industria construcțiilor metalice	103.	Prelucrător în emailarea, cromarea și tratamente fizico-chimice ale produselor metalice	
		104.	Debitator semifabricate	
		105.	Sculer matrițer	
		106.	Lăcătuș	
		107.	Maistru mecanic	
		108.	Lucrător în construcția și repararea containerelor metalice mari și mobilier din material metalic	

		109.	Lucrător în construcția generatoare de aburi	
		110.	Lucrător la fabricarea echipamentelor de încălzire, refrigerare și aer condiționat	
		111.	Lucrător în construcția de rezervoare, containere din material metalic	
		112.	Lucrător în construcția mașinilor de operare și/sau hidraulice	
		113.	Sudor	
		114.	Vopsitor industrial	
		115.	Lucrător în producția de explozivi pentru spargere și aruncare, dispozitive explozive pentru extracție, propulsoare, pirotehnie	
		116.	Altă profesie	
	Fabricarea echipamentelor electronice și optice	117.	Confecționer tuburi cu raze catodice, tuburi de vid, de gaz	
		118.	Confecționer corpuri de iluminat	
		119.	Confecționer instrumente de măsurare și control	
		120.	Confecționer calculatoare și echipamente periferice	
		121.	Confecționer echipamente telecomunicații	
		122.	Confecționer echipamente fotografice	
		123.	Altă profesie	
	Fabricarea echipamentelor electrice	124.	Confecționer cabluri	
		125.	Confecționer instalații electrice	
		126.	Confecționer echipamente electrice, electronice	
		127.	Altă profesie	
	Fabricarea autovehiculelor, mașini, utilaje	128.	Lucrător în construcție, echipare, reparare, întreținere, dezmembrare autovehicule	
		129.	Lucrător în construcția de autovehicule, remorci, betoniere, camioane industriale, motociclete, motorete, biciclete	
		130.	Lucrător în construcția de ascensoare	
		131.	Confecționer cablaje auto	
		132.	Altă profesie	
	Fabricarea altor mijloace de transport	133.	Lucrător în construcție, reparare echipamente mobile pentru căi ferate, tramvaie și cabine pt.schi	
		134.	Lucrător în construcție, reparare, întreținere, dezmembrare nave	
		135.	Lucrător în construcție, reparare, întreținere, dezafectare, dezmembrare mijloace transport aerian	
		136.	Altă profesie	

	Alte activități industriale	137.	Lucrător în construcția de echipamente medico-chirurgicale, instrumente de măsurare și control	
		138.	Lucrător în producția și reparația de piese metalice mici	
		139.	Lucrător în construcția de tâmplărie metalică și lucrări cu material metalic	
		140.	Lucrător în producția de aparate de uz casnic sau gospodăresc	
		141.	Bijutier (aur,argint, pietre prețioase, semiprețioase)	
		142.	Vopsitor industrial	
		143.	Lucrător cu pigment cromat	
		144.	Operator în reactoare nucleare (tratarea combustibililor nucleari și eliminarea deșeurilor radioactive)	
		145.	Lucrător în industria produselor radioactive	
		146.	Altă profesie	
D	**Producția și furnizarea de energie electrică, termică, gaze, apă caldă și aer condiționat**	147.	Lucrător în centrale electrice pentru producerea și transformarea energiei electrice	
		148.	Lucrător în construcția de linii de transport și distribuție a energiei electrice	
		149.	Operator în distilarea lemnului, a combustibililor fosili și a gudronului	
		150.	Lucrător în construcția centrale hidroelectrice	
		151.	Altă profesie	
E	**Distribuția apei;** **salubritate, gestionarea deșeurilor, activități de decontaminare**	152.	Lucrător în construcția de conducte urbane pentru gaz și apă.	
		153.	Instalator apa, canal	
		154.	Instalator retele de distribuție	
		155.	Instalator centrale termice	
		156.	Instalator tehnico-sanitare și gaze	
		157.	Instalator frigotehnist	
		158.	Instalator încălzire centrală și gaze	
		159.	Altă profesie	
F	**Constructii**	160.	Lucrător pe șantier industrial sau civil	
		161.	Mașinist pentru utilaje specifice la extracție și execuția tunelurilor	
		162.	Prelucrator roci asfaltice și/sau bituminoase	
		163.	Lucrător la întreținerea drumului, poduri, ecartamente, șanțuri sau terasamente	
		164.	Lucrător la drumuri sau suprastructură rutieră	
		165.	Lucrător la structura căilor ferate, metrou și tramvaie	
		166.	Lucrător la construirea de aeroport, aerodrom sau heliport	

		167.	Lucrător în finisare, reparare, întreținere construcții	
		168.	Lucrător la demolări	
		169.	Altă profesie	
G	**Comert cu ridicata și cu amanuntul; repararea autovehiculelor și motocicletelor**	170.	Lucrător comercial cu produse pe baza de azbest, azbociment	
		171.	Vopsitor auto	
		172.	Mecanic auto	
		173.	Sudor	
		174.	Tinichigiu carosier	
		175.	Lucrător în atelier mecanic	
		176.	Lucrător la stații de alimentare cu combustibili	
		177.	Lucrător în garaje	
		178.	Electrician auto	
		179.	Altă profesie	
H	**Transport și depozitare**	180.	Șofer în servicii publice urbane și periferie pentru transportul de persoane	
		181.	Șofer în transportul de mărfuri	
		182.	Șofer în transportul poștal cu camioane, vehicule articulate	
		183.	Lucrător în transportul aerian, feroviar și maritim	
		184.	Mecanic	
		185.	Altă profesie	
I	**Hoteluri și restaurante**	186.		
J	**Informații și comunicații**	187.		
K	**Intermedieri financiare și asigurări**	188.		
L	**Tranzacții imobiliare**	189.		
M	**Activități profesionale, științifice și tehnice**	190.	Laborant sau tehnician chimist	
		191.	Altă profesie	
N	**Activități de servicii administrative și activități de servicii suport**	192.		
O	**Administrație publică și apărare; asigurări sociale din sistemul public**	193.	Pompier	
		194.	Altă profesie	
P	**Învățământ**	195.		
Q	**Sănătate și asistență socială**	196.	Asistent medical de laborator	
		197.	Asistent farmacist	
		198.	Farmacist	
		199.	Medic imagist	
		200.	Asistent medical de radiologie	
		201.	Stomatolog	
		202.	Altă profesie	

R	**Activități de spectacole, culturale și recreative**	203.		
S	**Alte activități de servicii**	204.	Sticlar	
		205.	Sticlar decorator	
		206.	Pictor	
		207.	Pictor ceramică, sticlă	
		208.	Pictor decor	
		209.	Altă profesie	
T	**Activități ale gospodăriilor private în calitate de angajator de personal casnic; activități ale gospodăriilor**	210.		
U	**Activități ale organizațiilor și organismelor extrateritoriale**	211.		

https://doi.org/10.55453/rjmm.2026.129.6.7

Article

Discordance between coronary CT angiography and invasive coronary angiography at low Agatston scores: a bicentric cohort of 124 Romanian patients

Andra-Maria Barota-Bebeselea[1,2,*], Doru-Florian Cornel Moga[1,2,*], Ioan Manitiu[1,2]

[1] "Dr. Alexandru Augustin" Military Emergency Clinical Hospital, Sibiu, Romania
[2] Clinical Medical Department, Faculty of Medicine, "Lucian Blaga" University of Sibiu, Romania
*Correspondence: A-M.B-B. andra.bebeselea@gmail.com, D-F.C.M cornel.moga@ulbsibiu.ro

Abstract: Coronary CT angiography (CCTA) is used as a triage test before invasive coronary angiography (ICA). In this study we assessed the level of agreement between the two methods in patients whose CCTA reported severe stenosis in the presence of a low coronary artery calcium (CAC) score. We retrospectively analyzed 124 patients selected from a total of 2,742 examinations who underwent both CCTA and ICA. A discordant group (n=33) had stenosis reported on CCTA together with a low CAC (<400 and <100 AU). Across the whole cohort, obstructive disease (≥50% in the left main coronary artery or ≥70% in the other segments) was present in 44.4% of patients. In the discordant subgroup, agreement between CCTA and ICA was markedly worse: ICA showed obstructive disease in only 6.1% of patients. These results suggest that, although CAC remains a stand-alone predictor of obstructive disease, its predictive value is limited in a population already selected by referral for catheterization. The substantial discrepancy observed in cases where CCTA reports severe disease in the presence of a low CAC score raises the possibility that CCTA overestimates stenosis severity. In patients showing this pattern of discordance, non-invasive functional testing before referral to ICA could therefore be useful.

Keywords: coronary CT angiography; invasive coronary angiography; coronary artery calcium; Agatston score; diagnostic agreement; referral bias; non-calcified plaque

INTRODUCTION

Coronary CT angiography (CCTA) has become established as the first-line non-invasive test for patients with suspected chronic coronary syndrome. This position is supported by a Class I recommendation in both the 2019 and the 2024 European Society of Cardiology guidelines [1, 2]. One essential reason for its clinical usefulness is its high ability to rule out disease. When the test is negative, obstructive coronary disease can be safely excluded. This spares the patient an unnecessary diagnostic cardiac catheterization [3, 4]. Evidence from randomized controlled trials — among them SCOT-HEART, PROMISE and DISCHARGE — also suggests that an approach centered on anatomical assessment is not inferior to a strategy based on functional testing in predicting and subsequently preventing adverse cardiovascular events [5, 6, 7].

CCTA has high diagnostic performance, but it also has a widely known anatomical limitation: it frequently overestimates the severity of some stenoses. Part of this comes from the plaque itself. Non-calcified plaque with positive remodeling, low-attenuation areas, and irregular calcification are graded as more severe on computed tomography than on invasive angiography [8, 9].

Beyond these intrinsic differences, technical factors add to the impression of narrowing. Partial volume averaging, the blooming effect produced by dense microcalcifications, and vessel motion all contribute to additional overestimation of luminal stenosis [10]. As a result, a substantial proportion of the patients referred for catheterization solely on the basis of a CCTA report turn out, in the end, to have non-obstructive disease. This means these patients took on the risks, the contrast exposure, the radiation exposure, and the costs of an invasive procedure without obtaining any therapeutic benefit.

Citation: Barota-Bebeselea AM, Moga DFC, Manitiu I. *Discordance between coronary CT angiography and invasive coronary angiography at low Agatston scores: a bicentric cohort of 124 Romanian patients.* R. J. Mil. Med. 2026, CXXIX(6): 687-695. https://doi.org/10.55453/rjmm.2026.129.6.7

Academic Editor: Octavian Vasiliu

Received: 14 September 2026
Revised: 27 October 2026
Accepted: 29 October 2026

Solid real-world data describing how the two methods correlate remain limited in Romania. An unselected outpatient registry from Cluj-Napoca, for example, reported the frequency of significant lesions on CCTA, but it did not then follow the patients up to obtain invasive confirmation [11]. To our knowledge, no Romanian study has specifically examined the situation in which CCTA describes a severe stenosis in the presence of a low Agatston score. This gap matters because, when the coronary calcium burden is low, assessment of the vessel lumen relies largely on the morphological features of non-calcified plaque. Under these conditions, CCTA is most exposed to the risk of overestimation. Establishing how often such cases are ultimately confirmed is therefore an essential condition for calibrating local referral thresholds.

We carried out a study on a patient cohort from two clinical centers (in Sibiu, Romania). It included 124 patients who underwent coronary CT angiography (CCTA) followed later by invasive coronary angiography. An institutional registry from the same centers was analyzed in a past study in order to characterize referral patterns by age and sex, using a proportionally stratified subsample of 397 examinations [12]. The cohort analyzed here comes from the same registry, but it is designed to answer a different question — invasive confirmation, rather than the characterization of referral patterns. The objectives of the study were: (1) to assess how well the Agatston score can identify obstructive coronary artery disease; (2) to identify the factors that, independently of one another, are associated with the presence of coronary obstruction; and (3) to assess how well the CCTA findings match the other available data in patients who had a low coronary calcium level but in whom CCTA showed a stenosis.

MATERIALS AND METHODS

The study was observational, retrospective, and bicentric. The source population comprised 2,742 consecutive CCTA examinations performed at the Sibiu Pediatric Clinical Hospital between March 2019 and January 2025. This is the public hospital that provides part of the outpatient cardiovascular computed tomography services for Sibiu County. The same patient registry was also used in an earlier study, which analyzed age- and sex-related patterns of referral to CCTA. That study analyzed a subsample of 397 examinations, selected by proportional stratification [12].

Although the two studies are based on the same population, they had different objectives and different selection criteria. The earlier study used a proportionally selected sample, whereas the present study included patients according to whether they subsequently underwent catheterization. The two studies also examined different outcomes. From the source population, we identified the patients who subsequently underwent invasive coronary angiography (ICA) at the Sibiu County Emergency Clinical Hospital. We then included 124 patients for whom both the CCTA and the ICA examinations were available and analyzable. These accounted for 4.5% of the source population (124 of 2,742 examinations).

Referral for ICA was driven by symptoms, by the results of non-invasive risk assessment, or by the identification of an abnormal finding on CCTA. This way of selecting patients may introduce verification bias, because ICA was not performed in the catheterization laboratory of the SCJU for every patient in the initial population who had an indication for invasive investigation. No weighting or statistical adjustment method was applied for the patients who were not referred for catheterization or who underwent this investigation in another center. For inclusion in the study, the CCTA examination had to be clear enough for interpretation and had to allow calculation of the Agatston score [13]. The patient also had to have subsequently undergone a diagnostic ICA, with no revascularization procedure performed between the two examinations. Patients were excluded if severe motion artifacts prevented calculation of the calcium score, if catheterization was performed solely for valvular assessment, or if the available medical data were incomplete. Clinical data were extracted from the electronic medical records using a standardized chart review procedure [14, 15]. The following information was collected for each patient: age, sex, coronary dominance, Agatston calcium score, stenosis severity for each coronary vessel, the presence of previously implanted stents, the existence of diffuse coronary disease, and whether a revascularization procedure was subsequently performed. Stenosis severity in invasive coronary angiography (ICA) was taken from the report of the interventional cardiologist who performed the procedure. The data were extracted by a single researcher, using the same criteria for all patients. Setting these criteria before the results were analyzed reduced the risk that certain data would later be selected according to the results obtained. The data were not independently verified by a second researcher and, consequently, agreement between two raters was not assessed.

The primary outcome of the study, termed CAD_70, was defined as the presence of a stenosis of at least 50% in the left main coronary artery or of at least 70% in one of the main coronary vessels. These included the left anterior descending artery, the circumflex artery and the right coronary artery. Dominant side branches were also included: the diagonal branches, the obtuse marginal branches and the ramus intermedius. Coronary fistulae and myocardial bridges without systolic compression were not considered obstructive coronary artery disease, because these findings are not caused by atherosclerosis. The threshold used in this study is the one used in the studies that compared coronary CT angiography with invasive coronary angiography, without the use of functional testing. This threshold should not be confused with the criteria used by the 2024 European Society of Cardiology guidelines to indicate revascularization. In the guidelines, the revascularization decision is based on functional criteria and requires at least one of the following values: fractional flow reserve ≤0.80, instantaneous wave-free ratio ≤0.89, or quantitative flow ratio ≤0.80. These measurements are used in particular for intermediate lesions and, in routine practice, for stenoses visually estimated at 40–90%, with the exception of stenoses in the left main coronary artery [2].

The secondary outcome, termed CAD_50, was defined as the presence of a stenosis of at least 50% in any epicardial vessel. Thirteen cases had initially been coded ambiguously because they had intermediate lesions. All these cases were re-adjudicated deterministically according to the rule above. Three met the primary threshold, and ten did not. Consistent application of the rule changed other cases as well, in both directions. Two further cases were reclassified as non-obstructive during the final check of the database: one with a 60% diagonal lesion and all major vessels below 30%, whose angiographic conclusion was itself negative, and another for which the only finding above the threshold was an arterio-cavitary fistula, not an atherosclerotic stenosis.

The subgroup with discordant findings (n = 33) was defined on the basis of the reason for referral. It included the patients referred for catheterization because the CCTA report described a severe stenosis even though their calcium score was low or disproportionate to the severity of the stenosis described. To check whether the results depend on the calcium score threshold chosen, sensitivity analyses were planned using two thresholds: CAC <400 AU and CAC <100 AU.

Continuous variables were checked for normality with the Shapiro–Wilk test and are reported as mean with standard deviation or as median with interquartile range. Categorical variables are summarized as frequencies, expressed as absolute numbers alongside the corresponding percentages. When comparing groups, we used the Student t test for suitable continuous variables, the Mann–Whitney U test when a non-parametric approach was needed, and the chi-square test for categorical comparisons, according to the requirements of each analysis. To assess the ability of the Agatston score to distinguish patients by CAD_70 and CAD_50, we applied ROC (receiver operating characteristic) curve analysis. Within this approach, we reported the area under the curve together with 95% confidence intervals obtained by bootstrapping, and we selected the optimal operating point using Youden's J statistic. We then calculated sensitivity, specificity, predictive values and likelihood ratios across the standard Agatston score intervals. Multivariable logistic regression was used to assess whether log10(CAC+1), age measured per decade, and male sex were each independently associated with CAD_70. Goodness of fit was reported using the McFadden pseudo-R^2 and was further assessed by a likelihood ratio test comparing the full model with the null model. Statistical significance was established using two-sided p-values, with values below 0.05 considered significant.

The study was carried out with the approval of four separate institutional bodies. Ethics approval no. 31 / 24.04.2026 was formally issued by the Ethics Council of the Sibiu Military Emergency Clinical Hospital. In addition, the Sibiu Pediatric Clinical Hospital granted administrative and research approval no. 7969 / 07.11.2023 and also provided institutional data use agreement no. 3697 / 07.05.2026. These approvals allowed retrospective access to the anonymized CCTA records. Separate ethics approval, relating specifically to access to the catheterization archive, was granted by the Ethics, Medical Deontology and Discipline Committee of the Sibiu County Emergency Clinical Hospital, through Decision no. 17160 / 29.05.2026. Because the study was retrospective and relied on fully anonymized records, already obtained in the course of routine medical care, the authors did not seek individual written informed consent. This approach complies with Order no. 1502/2016 of the Ministry of Health, with Law no. 46/2003 on patients' rights, and with Article 89 of Regulation (EU) 2016/679. These provisions allow the secondary use of health data for scientific research, subject to appropriate data protection safeguards.

RESULTS

The study cohort included 124 patients, with a mean age of 64.2 ± 8.6 years. The median age of the group was 65 years, with participants aged between 42 and 84 years. There were 76 men, representing 61.3% of the sample, and 48 women, representing 38.7%. The women were significantly older than the men, with a mean age of 66.6 ± 7.4 years against 62.7 ± 8.9 years (p = 0.012). Coronary dominance favored the right coronary circulation in 79.8% of patients. Co-dominant patterns, by contrast, were seen in 9.7% of patients, and left-dominant patterns accounted for the remaining 10.5%. The study found a median Agatston score of 480 AU, with an interquartile range from 176 to 777 and an overall observed range from 0 to 2,749. On comparison by sex, the median score was higher in men than in women, measuring 543 AU against 424 AU (p = 0.032). By the usual Agatston score categories [18], 2 patients (1.6%) had a score of zero, 17 patients (13.7%) had values between 1 and 99 AU, 30 patients (24.2%) between 100 and 399 AU, and 50 patients (40.3%) between 400 and 999 AU. A score of at least 1,000 AU was recorded in 25 patients (20.2%) (Table 1).

Table 1: Baseline demographic, anatomical and angiographic characteristics of the study cohort (n = 124).

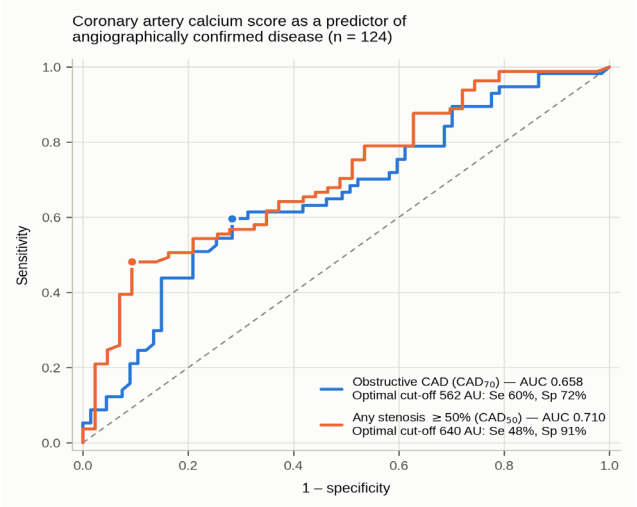
Characteristic	Value
Total patients, n	124
Age, years (mean ± SD)	64.2 ± 8.6
Age, median (IQR), years	65 (58–70)
Age range, years	42–84
Men, n (%)	76 (61.3)

Women, n (%)	48 (38.7)
Right coronary dominance, n (%)	99 (79.8)
Balanced / co-dominant, n (%)	12 (9.7)
Left coronary dominance, n (%)	13 (10.5)
Agatston score, median (IQR), AU	480 (176–777)
Agatston score, range, AU	0–2,749
CAC = 0, n (%)	2 (1.6)
CAC 1–99, n (%)	17 (13.7)
CAC 100–399, n (%)	30 (24.2)
CAC 400–999, n (%)	50 (40.3)
CAC ≥ 1000, n (%)	25 (20.2)
Multivessel disease (≥2 vessels ≥70%), n (%)	21 (16.9)
Diffuse coronary disease, n (%)	72 (58.1)
Significant side-branch disease, n (%)	14 (11.3)
Prior stenting, n (%)	5 (4.0)
CAD_70 confirmed at invasive angiography, n (%)	55 (44.4)
CAD_50 confirmed at invasive angiography, n (%)	81 (65.3)

During catheterization, obstructive stenosis of at least 70% was identified most often in the left anterior descending artery, accounting for 21.0% of cases. It was then seen in the right coronary artery in 18.5% of cases, followed by the circumflex artery, with 15.3%. In addition, a left main stenosis of 50% or more was detected in five patients (4.0%), consistent with the upstream enrichment expected in a catheterization cohort [19]. A dominant side branch showed significant involvement in 14 patients (11.3%). Multivessel disease — defined as involvement of two or more vessels with stenosis of 70% or more — was present in 21 patients (16.9%). Diffuse coronary atherosclerosis was also documented in 72 patients (58.1%). Applying the CAD_70 definition, obstructive disease was confirmed in 55 of the 124 patients (44.4%). Using a broader threshold, any stenosis of at least 50% (CAD_50) was identified in 81 of 124 patients (65.3%).

In this population referred for catheterization, the Agatston score separated the outcomes only modestly (Figure 1). The area under the ROC curve was estimated at 0.653 (95% CI 0.555–0.749) for CAD_70 and was higher, 0.710 (95% CI 0.614–0.801), for CAD_50. For CAD_70, the optimal Youden threshold was 562 AU, corresponding to a sensitivity of 60%, a specificity of 71%, a positive predictive value of 62%, and a negative predictive value of 69%; for CAD_50, the optimal threshold was 640 AU, with a sensitivity of 48% and a specificity of 91%. As the operating thresholds changed, sensitivity fell, and specificity rose, as expected, but at no threshold did the score reach a level of accuracy sufficient to justify a referral decision on its own (Table 2).

Figure 1: ROC (receiver operating characteristic) curves for the coronary calcium (Agatston) score, presented as a predictor of angiographically confirmed disease, for the whole cohort (n = 124).



Two outcome definitions are shown: obstructive coronary artery disease (CAD_70 — defined as a stenosis of at least 50% in the left main coronary artery or of at least 70% in any other major epicardial vessel or dominant side branch) and any stenosis of at least 50% (CAD_50).

Filled circles indicate the optimal Youden threshold for each curve. The dotted diagonal represents the line of no discrimination. AU — Agatston units.

Table 2: Diagnostic accuracy of the coronary calcium score for obstructive coronary artery disease (CAD_70) at the operating thresholds.

CAC threshold (AU)	Se	Sp	PPV	NPV	Accuracy	LR+	LR–
≥ 10	0.98	0.03	0.45	0.67	0.45	1.01	0.63
≥ 100	0.93	0.22	0.49	0.79	0.53	1.18	0.33
≥ 400	0.69	0.46	0.51	0.65	0.56	1.29	0.67
≥ 562 (Youden)	0.60	0.71	0.62	0.69	0.66	2.07	0.56
≥ 1000	0.29	0.87	0.64	0.61	0.61	2.23	0.82

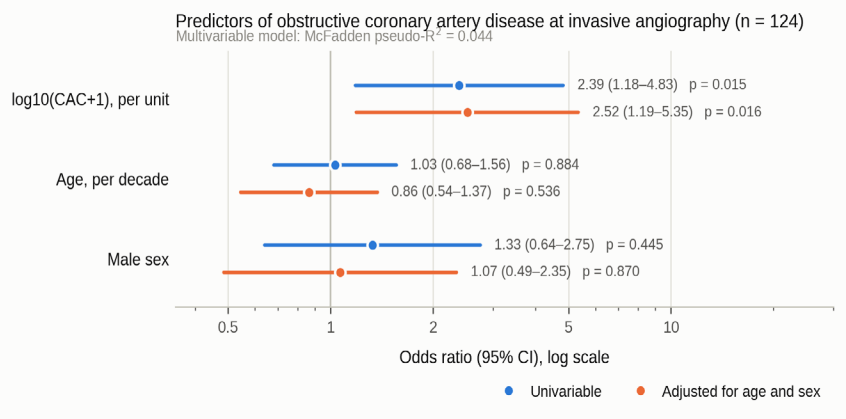
In univariable logistic regression, log10(CAC+1) was significantly associated with the presence of angiographically confirmed CAD_70. For each one-unit increase in log10(CAC+1), the odds of having CAD_70 were 2.28 times higher (OR 2.28; 95% CI: 1.13–4.60; p = 0.021).

Age, expressed per 10-year increase, was not associated with CAD_70 (OR 1.05; 95% CI: 0.69–1.59; p = 0.83). Male sex was not significantly associated with CAD_70 either (OR 1.37; 95% CI: 0.66–2.86; p = 0.40).

In the multivariable model, log10(CAC+1) remained the only independent predictor associated with CAD_70. The adjusted OR was 2.35 (95% CI: 1.11–4.95; p = 0.025; Figure 2). Age (aOR 0.90 per 10 years; 95% CI: 0.57–1.43; p = 0.65) and male sex (aOR 1.14; 95% CI: 0.52–2.50; p = 0.75) were not significantly associated with CAD_70.

The multivariable model explained little of the variation in the outcome. The McFadden pseudo-R^2 was 0.039 and the area under the ROC curve was 0.655. The likelihood ratio test showed no significant difference between the adjusted model and the null model (p = 0.082).

Figure 2: Univariable odds ratios and odds ratios adjusted for age and sex for obstructive coronary artery disease at invasive angiography (n = 124, 55 events).

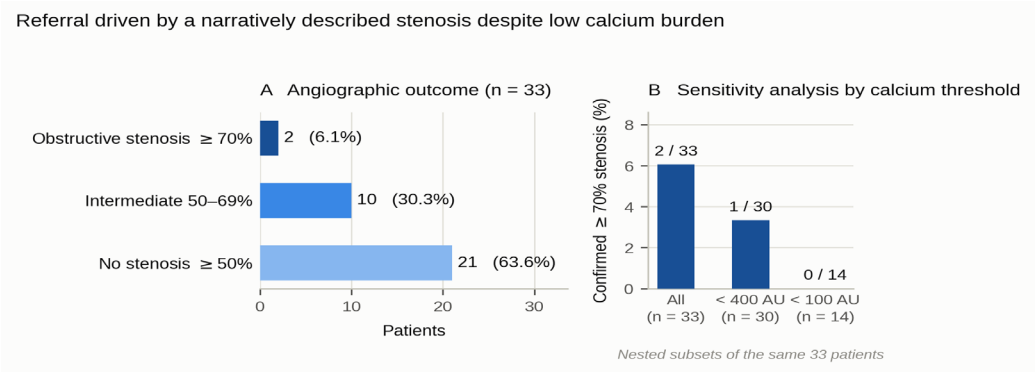


Circles indicate the point estimates and the horizontal lines represent the 95% confidence intervals. The dotted vertical line marks the reference odds ratio of 1. The x axis is logarithmic. The calcium score was the only independent predictor among the three available variables. The multivariable model showed limited explanatory power (McFadden pseudo-R^2 = 0.039). CAC — coronary artery calcium.

The pre-specified subgroup, made up of the patients referred for catheterization on the basis of a stenosis described on CCTA despite a low or disproportionately small calcium burden, included 33 patients (26.6% of the cohort). The median Agatston score in this subgroup was 135 AU (IQR 51–246). Agreement between CCTA and invasive angiography was markedly lower in this subgroup (Figure 3A). Of the 33 patients, two (6.1%) had confirmed obstructive disease; 12 (36.4%) had a stenosis of at least 50% somewhere in the coronary tree, and 21 (63.6%) had no vessel reaching 50%. The sensitivity analyses showed the same pattern at stricter calcium thresholds (Figure 3B): below 400 AU (n = 30), obstructive disease was confirmed in a single patient (3.3%), and in 21 (70.0%) no stenosis reached 50%; below 100 AU (n = 14), confirmation fell to zero, and in 11 patients (78.6%) no stenosis

reached 50%. The three patients in the subgroup whose scores exceeded 400 AU had values of 474, 485, and 2,179 AU, which shows that the discordance is not simply an artifact driven by a few patients with extreme calcium values.

Figure 3: Angiographic findings and sensitivity analyses in the patients referred for invasive angiography on the basis of a stenosis described on CCTA, despite a low calcium burden (n = 33; 26.6% of the cohort).



(A) Angiographic outcome: two patients (6.1%) had confirmed obstructive stenosis (≥70%), while in 21 (63.6%) no vessel reached 50%. (B) Sensitivity analysis narrowing the subgroup by calcium threshold, on nested subsets of the 33 patients. Confirmation of obstructive disease falls from 6.1% in the full subgroup to 3.3% below 400 AU and to zero below 100 AU, showing that the discordance is robust and independent of extreme calcium values. AU — Agatston units.

Post-catheterization management was medical in 77 patients (62.1%), percutaneous intervention was completed in 23 (18.5%), surgical consultation was recommended in 10 (8.1%), staged intervention took place in six patients (4.8%), and additional functional testing was indicated in eight patients (6.5%). Treatment allocation closely reflected the angiographic findings: all the patients who underwent percutaneous coronary intervention had confirmed obstructive disease, and 64 of the 77 treated medically (83.1%) did not (Table 3). In the discordant low-calcium subgroup, management reflected the low disease burden: 31 of the 33 patients (93.9%) received medical treatment, two were referred for functional ischemia testing, and none underwent PCI.

Table 3: Treatment decisions after invasive coronary angiography and their agreement with confirmed obstructive disease (CAD_70).

Treatment decision	n (%)	CAD_70+, n	CAD_70+, %
PCI performed	23 (18.5)	23	100
CABG consultation	10 (8.1)	10	100
Staged PCI	6 (4.8)	5	83
Functional testing recommended	8 (6.5)	4	50
Optimal medical therapy (OMT)	77 (62.1)	13	17
Total	124 (100)	55	44.4

DISCUSSION

This bicentric analysis of 124 Romanian patients who underwent both coronary CT angiography and invasive angiography yields three main findings.

First, the Agatston score was the only one of the three analyzed variables that was independently associated with angiographically confirmed obstructive coronary artery disease. The higher the calcium score, the higher the probability of CAD_70. This association had modest discriminatory power, however. The area under the curve was 0.653 for CAD_70 and 0.710 for CAD_50.

The multivariable regression results show that this association is not sufficient to identify patients with obstructive disease accurately. The model that included calcium score, age, and sex had low explanatory power (McFadden pseudo-R^2 = 0.039), and

the difference from the null model was not statistically significant (p = 0.082). In a population already selected for catheterization, therefore, calcium score, age, and sex provide limited information for distinguishing patients with and without obstructive coronary artery disease.

Second, agreement between CCTA and invasive angiography was lower in the pre-specified subgroup of patients referred for catheterization for a stenosis described on CCTA despite a low calcium burden. Obstructive coronary artery disease was confirmed in only 2 patients (6.1%) of the 33, and in 21 patients (63.6%) no coronary vessel had a stenosis of at least 50%. In the patients with CAC <100 AU, no case of obstructive disease was confirmed.

These results must be interpreted in the context of patient selection. All the patients in this subgroup were referred for catheterization because CCTA had already indicated a possible stenosis. This subgroup therefore has a different profile from that of an unselected outpatient population. The results obtained here should not be extrapolated to all patients assessed by CCTA and do not contradict earlier data on the good ability of CCTA to rule out obstructive disease in unselected populations [4].

Third, the treatment decisions taken after catheterization were consistent with the angiographic findings. All the patients who were revascularized had confirmed obstructive coronary artery disease.

Comparisons with previously published results must be made with caution, because the performance of a test depends both on the characteristics of the test and on the population in which it is evaluated. The multicenter validation studies CORE-320 and NXT reported areas under the curve between 0.85 and 0.93 [3, 20]. These values, however, were obtained for CT angiography used together with myocardial perfusion or with CT-derived fractional flow reserve, and not for the calcium score used on its own. These studies also included patients with different levels of pre-test probability.

In the present study, all the patients had already been selected for catheterization. This selection reduced the variation in predictor values and may therefore reduce the area under the curve, even if the actual performance of the test is no different. For this reason, the AUC values in our study cannot be compared directly with those reported in CORE-320 and NXT.

A similar difference appears with regard to disease prevalence. In the outpatient cohort from Cluj-Napoca, which included unselected patients, CAD_50 was present in 41% of patients [11]. In our study, the proportion was 65.3%, which is to be expected in a population selected for catheterization.

The distribution of coronary disease was similar to that reported in the CONFIRM and PROMISE registries, with the lesions located most often in the left anterior descending artery and the right coronary artery [19, 6].

The low rate of disease confirmation in the low calcium score subgroup also raises the possibility that invasive angiography underestimated stenosis severity in this particular category of patients. This is possible because invasive angiography relies on two-dimensional images, and the assessment of intermediate stenoses can vary between observers. The variability is greater when angiography is not complemented by measurement of fractional flow reserve or by intravascular ultrasound.

This explanation does not appear to be the main cause of the discordance observed, however. Differences in assessment between observers can mean that a stenosis is graded, for example, at 50% instead of 70% or the other way round. They do not explain the situation in which, in 21 patients (63.6%) of the subgroup, no coronary vessel had a stenosis of at least 50%, even though the angiographic assessment was made in several projections.

A more likely explanation is therefore that CCTA overestimated the severity of some stenoses. In patients with little calcium, the suspected lesions are often made up of non-calcified or mixed plaque. These plaques can cause outward remodeling of the arterial wall and can make the lumen border harder to define. CCTA images can also be affected by cardiac motion [8, 9, 10].

These results have important clinical implications. When CCTA overestimates the severity of a stenosis in patients with a low calcium score, the patient may be referred for catheterization unnecessarily. Every catheterization carries a certain procedural risk and additional exposure to contrast agent and radiation. It also involves additional costs.

The 2024 ESC guidelines recommend, with a Class I, Level B indication, the use of functional imaging to assess myocardial ischemia when CCTA shows coronary disease whose functional importance is unclear or when the CCTA examination is non-diagnostic [2]. The NXT study showed that using CT-derived fractional flow reserve can raise diagnostic specificity from 34% to 79% [20]. The ESC guidelines nevertheless recommend caution in using this method and classify it as a Class IIb, Level B option for intermediate stenoses located in the proximal or mid coronary segments [2].

In the Sibiu region, access to non-invasive functional methods is limited. Single photon emission tomography has only very recently become available under contract with the health insurance house (CASS), but with a considerable waiting time; stress cardiac magnetic resonance requires travel to another center, and CT-derived fractional flow reserve is not reimbursed by the state. Under these conditions, when a CCTA report indicates a suspected stenosis, direct referral to invasive angiography often remains the most accessible option.

Wider access to non-invasive functional investigations, and reimbursement of these methods, could therefore reduce the number of patients referred unnecessarily for catheterization. Developing a regional functional assessment capacity could also contribute to better selection of the patients who need invasive angiography.

One particular feature of this study is the availability, for the same patients, of both coronary CT angiography and invasive coronary angiography data. Patients were included on the basis of pre-specified criteria, and this pairing allowed direct comparison of the results of the two methods. Pre-specified sensitivity analyses were also carried out to check whether the results hold at different calcium score thresholds.

The study does have a number of limitations. The cohort of 124 patients was a population selected for invasive investigation and does not reflect the general population assessed by coronary CT angiography. Referral for catheterization was driven by symptoms plus the identification of an abnormality on imaging and was not random. All the accuracy estimates are conditional on this selection and cannot be transferred to an unselected referral population.

CCTA reporting at the institution the patients came from was narrative and did not systematically use the CAD-RADS 2.0 categories. For this reason, automatic re-adjudication of stenoses at the level of each coronary segment was not possible [21]. Introducing a structured reporting system in line with CAD-RADS 2.0, including the use of standardized modifiers, could be a quality improvement measure in regional centers and could reduce subjective overestimation of stenosis severity.

Conventional cardiovascular risk factors were not recorded systematically in the archive and, for this reason, could not be included in the multivariable model. This limitation may contribute to the low explanatory power of the model, reflected in the modest pseudo-R^2 value.

Stenosis severity at invasive angiography was assessed visually, in several projections. Fractional flow reserve measurement and intravascular ultrasound were not used systematically. An independent functional or intravascular assessment of the stenoses was therefore not possible.

The interval between CCTA and catheterization was not recorded systematically in the available documentation. For this reason, we could not analyze whether the length of this interval influenced the agreement between the two methods. A longer interval between the examinations could reduce the agreement between the results.

Finally, the data were extracted by a single researcher and were not independently verified by a second researcher. Agreement between raters was therefore not formally assessed.

CONCLUSION

In a referral-selected cohort of 124 patients from Romania, assessed by both CCTA and invasive coronary angiography, the coronary calcium score was an independent but modest predictor of obstructive coronary artery disease. The discordance between the two methods was evident in the patients referred for catheterization for a suspected stenosis despite a low calcium burden. In this subgroup, only 6.1% of patients had confirmed obstructive disease, and in 63.6% no coronary vessel had a stenosis of at least 50%. This pattern suggests that the overestimation of stenoses on CCTA may be related to the features of non-calcified plaque and to motion artifacts, rather than to a general underestimation of stenosis severity at invasive angiography.

Access to non-invasive functional assessment methods within the public health system could reduce the number of cardiac catheterization assessments performed in patients in whom CCTA raises the suspicion of a stenosis but in whom obstructive disease is not confirmed. In patients with a low calcium score and an equivocal CCTA result, functional assessment performed before catheterization could help establish the ischemic relevance of the lesion and improve the selection of the patients who need invasive angiography.

Conflicts of interest and sources of funding

The authors declare that they have no conflict of interest.

Acknowledgments

The authors thank the Sibiu Pediatric Clinical Hospital, as the source of the coronary CT angiography data, and Dr. Ciprian Radu Sofariu, Medical Director of that institution, for the scientific collaboration on this research. They also thank the Sibiu County Clinical Hospital as the source of the data on the patients assessed by invasive coronary angiography, Assoc. Prof. Dr. Minodora Teodoru, head of the Cardiology Clinic of SCJU Sibiu, and Dr. Cornel Ioan Bitea, head of the Catheterization Laboratory of SCJU Sibiu.

In line with the ICMJE and WAME recommendations on the use of artificial intelligence in academic publishing, the authors declare that the assistance of a large language model was used for the language editing of a manuscript drafted by the authors, for checking the reference list, and for checking the internal consistency of the reported data against the study database. It was not used to generate data, to perform or interpret the statistical analyses, or to formulate the conclusions. The authors have read and verified every sentence of the final text and take full responsibility for the accuracy and integrity of the work.

Authors' contribution

Conceptualization, methodology, validation, A-M.B-B., D-F.C.M and I.M.; investigation, data curation, writing — original draft preparation, A-M.B-B.; writing — review and editing, visualization, A-M.B-B., D-F.C.M and I.M.; supervision, I.M. All authors have read and agreed to the published version of the manuscript.

Ethics approval and consent to participate

The study was covered by four institutional authorizations. Ethics approval no. 31 / 24.04.2026 was issued by the Ethics Council of the Sibiu Military Emergency Clinical Hospital. Administrative and research approval no. 7969 / 07.11.2023 and institutional data use agreement no. 3697 / 07.05.2026 were granted by the Sibiu Pediatric Clinical Hospital for retrospective access to the anonymized CCTA records. Ethics approval for access to the catheterization archive was granted by the Ethics, Medical Deontology and Discipline Committee of the Sibiu County Emergency Clinical Hospital, through Decision no. 17160 / 29.05.2026. Because the analysis was retrospective and used fully anonymized records, already collected in the course of routine medical care, individual written informed consent was not sought; this complies with Order no. 1502/2016 of the Ministry of Health, with Law no. 46/2003 on patients' rights and with Article 89 of Regulation (EU) 2016/679, which allows the secondary use of pseudonymized health data for scientific research purposes, subject to appropriate safeguards.

Patient consent for publication

Individual written informed consent for publication was not required: the analysis was retrospective and used fully anonymized records, and no information allowing individual identification of patients appears in this article. The legal basis is set out above, in the Ethics approval and consent to participate section.

References

1. Knuuti J, Wijns W, Saraste A. 2019 ESC guidelines for the diagnosis and management of chronic coronary syndromes. European Heart Journal. 2020. doi:10.1093/eurheartj/ehz425
2. Vrints C, Andreotti F, Koskinas KC. 2024 ESC guidelines for the management of chronic coronary syndromes. European Heart Journal. 2024. doi:10.1093/eurheartj/ehae177
3. Rochitte CE, George RT, Chen MY. Computed tomography angiography and perfusion to assess coronary artery stenosis causing perfusion defects by single photon emission computed tomography: The CORE320 study. European Heart Journal. 2014. doi:10.1093/eurheartj/eht488
4. Knuuti J, Ballo H, Juarez-Orozco LE. The performance of non-invasive tests to rule-in and rule-out significant coronary artery stenosis in patients with stable angina: A meta-analysis focused on post-test disease probability. European Heart Journal. 2018. doi:10.1093/eurheartj/ehy267
5. Newby DE, Adamson PD, Berry C. Coronary CT angiography and 5-year risk of myocardial infarction. New England Journal of Medicine. 2018. doi:10.1056/NEJMoa1805971
6. Douglas PS, Hoffmann U, Patel MR. Outcomes of anatomical versus functional testing for coronary artery disease. New England Journal of Medicine. 2015. doi:10.1056/NEJMoa1415516
7. Maurovich-Horvat P, Bosserdt M, Kofoed KF. CT or invasive coronary angiography in stable chest pain (DISCHARGE trial). New England Journal of Medicine. 2022. doi:10.1056/NEJMoa2200963
8. Bittencourt MS, Hulten E, Ghoshhajra B. Prognostic value of nonobstructive and obstructive coronary artery disease detected by coronary computed tomography angiography. Circulation: Cardiovascular Imaging. 2014. doi:10.1161/CIRCIMAGING.113.001047
9. Chang HJ, Lin FY, Lee SE. Coronary atherosclerotic precursors of acute coronary syndromes (PROMISE substudy). Journal of the American College of Cardiology. 2018. doi:10.1016/j.jacc.2018.02.079
10. Hou ZH, Lu B, Gao Y. Prognostic value of coronary CT angiography and calcium score for major adverse cardiac events in outpatients. JACC: Cardiovascular Imaging. 2012. doi:10.1016/j.jcmg.2012.06.006
11. Popa LE, Petresc B, Cătană C. Coronary CT angiography prevalence of significant lesions in patients suspected of coronary artery disease — a single-centre experience from cluj-napoca, romania. BMJ Open. 2020. doi:10.1136/bmjopen-2020-040395
12. Barota-Bebeșelea AM, Negrea MO, Neamțu B, Teodoru M, Sofariu CR, Moga DFC, Manițiu I, Cioca AL. Age- and sex-related patterns in coronary CT angiography referrals and coronary atherosclerotic burden: A single-center real-world referral-based analysis. Medicina. 2026;62(7):1416. doi:10.3390/medicina62071416
13. Agatston AS, Janowitz WR, Hildner FJ. Quantification of coronary artery calcium using ultrafast computed tomography. Journal of the American College of Cardiology. 1990. doi:10.1016/0735-1097(90)90282-T
14. Vassar M, Holzmann M. The retrospective chart review: Important methodological considerations. Journal of Educational Evaluation for Health Professions. 2013. doi:10.3352/jeehp.2013.10.12
15. Worster A, Bledsoe RD, Cleve P. Reassessing the methods of medical record review studies in emergency medicine research. Annals of Emergency Medicine. 2005. doi:10.1016/j.annemergmed.2004.11.021
16. Elm E von, Altman DG, Egger M. The strengthening the reporting of observational studies in epidemiology (STROBE) statement: Guidelines for reporting observational studies. Lancet. 2007. doi:10.1016/S0140-6736(07)61602-X
17. Benchimol EI, Smeeth L, Guttmann A. The REporting of studies conducted using observational routinely-collected health data (RECORD) statement. PLoS Medicine. 2015. doi:10.1371/journal.pmed.1001885
18. Greenland P, Bonow RO, Brundage BH. ACCF/AHA 2007 clinical expert consensus document on coronary artery calcium scoring. Journal of the American College of Cardiology. 2007. doi:10.1016/j.jacc.2006.10.001
19. Min JK, Dunning A, Lin FY. Age- and sex-related differences in all-cause mortality risk based on coronary computed tomography angiography findings — CONFIRM registry. Journal of the American College of Cardiology. 2011. doi:10.1016/j.jacc.2011.02.063
20. Nørgaard BL, Leipsic J, Gaur S. Diagnostic performance of noninvasive fractional flow reserve derived from coronary computed tomography angiography in suspected coronary artery disease: The NXT trial. Journal of the American College of Cardiology. 2014. doi:10.1016/j.jacc.2013.11.043
21. Cury RC, Leipsic J, Abbara S. CAD-RADS 2.0 — 2022 coronary artery disease — reporting and data system. Radiology: Cardiothoracic Imaging. 2022. doi:10.1148/ryct.220183

https://doi.org/10.55453/rjmm.2026.129.6.8

Original Article

Psychiatric disorders due to brain tumors: A perspective on diagnostic vigilance and integrated care

Cristian Năstase[1], Bogdan M. Petrescu[2,3,*], Octavian Vasiliu[2,3], Cristian A. Cândea[3], Andrei G. Mangalagiu[2,3]

[1] Department of Neurosurgery, Dr. Carol Davila University Emergency Central Military Hospital, Bucharest, Romania
[2] Discipline of Psychiatry II, Department of Clinical Neurosciences, Carol Davila University of Medicine and Pharmacy, Bucharest, Romania
[3] Department of Psychiatry, Dr. Carol Davila University Emergency Central Military Hospital, Bucharest, Romania
*Correspondence: bogdan.petrescu@umfcd.ro

Abstract: Brain tumors may present themselves initially under the appearance of depression, anxiety, psychosis, apathy, personality change, or cognitive decline, and psychiatric comorbidity remains frequent throughout the course of the neuro-oncological disease. In this Perspective, we argue that psychiatric expertise should be embedded in neuro-oncology care from the patient's first presentation through survivorship and palliation. We draw on the literature and on two cases from our liaison psychiatry service, in which older adults referred for depressive symptoms were found to have intracranial tumors and continued to need psychotropic treatment after successful surgery. We compare how DSM-5-TR and ICD-11 classify psychiatric syndromes secondary to brain disease and propose a four-domain etiological formulation that separates direct tumor effects, treatment-related and endocrine effects, psychological reactions, and pre-existing vulnerability. This article also presents the most relevant red flags that should prompt neuroimaging, the distinction between apathy and depression, the burden of depression, distress, suicide risk, and postoperative delirium, and the psychiatric effects of corticosteroids, antiseizure medications, dopamine agonists, and cranial irradiation. We also address practical psychopharmacology, electroconvulsive therapy, decision-making capacity, cognitive rehabilitation, and mood assessment in aphasia, while highlighting the scarcity of controlled evidence in this population. Finally, a phase-based, multidisciplinary model of care is proposed, and an outline of research priorities is presented.

Keywords: brain tumors; secondary mood syndrome; apathy; liaison psychiatry; neuro-oncology; corticosteroids; antiseizure medication; decision-making capacity

1. INTRODUCTION

Primary brain and other central nervous system (CNS) tumors have an average annual age-adjusted incidence of 26.05 per 100,000 population in the United States, with glioblastoma accounting for 52.2% of malignant tumors and meningioma for 42.6% of all tumors [1]. The five-year relative survival after a malignant CNS tumor remains only 34.8% in the latest report [1], almost unchanged from the 35.7% reported for the 2016-2020 period [2], and malignant primary brain tumors are among the most difficult cancers to treat [3]. Brain metastases add considerably to this burden, developing in an estimated 20% of patients with cancer [4]. The 2021 World Health Organization classification of CNS tumors has made molecular markers central to diagnosis [5], and genomic profiling has revealed recurrent alterations, such as epidermal growth factor receptor rearrangements in glioblastoma [6]. Some of these markers are directly relevant to neuropsychiatric care, since gliomas carrying a mutation in isocitrate dehydrogenase (IDH) present with seizures in 59-74% of patients, compared with 18-34% of IDH-wild-type gliomas, probably because the oncometabolite D-2-hydroxyglutarate, which is structurally similar to glutamate, increases neuronal excitability [7]. Seizure burden, in turn, determines exposure to antiseizure medications and to their psychiatric adverse effects (as highlighted further in Section 5). Meningiomas, in contrast, are mostly benign and often curable by gross total resection [8].

Citation: Năstase C, Petrescu BM, Vasiliu O, Cândea CA, Managalagiu AG. *Psychiatric disorders due to brain tumors: A perspective on diagnostic vigilance and integrated care.* R. J. Mil. Med. 2026, CXXIX(6): 696-708. https://doi.org/10.55453/rjmm.2026.129.6.8

Academic Editor: Clara Ursescu

Received: 01 October 2026
Revised: 28 October 2026
Accepted: 01 November 2026

Behind these figures lies a clinical reality that is less often discussed, i.e., many patients with brain tumors first come into contact with the health system because of changes in mood, behavior, or cognition, and psychiatric symptoms are occasionally the only manifestation of the tumor [9]. Once the diagnosis is established,

depression, anxiety, distress, and cognitive impairment accompany patients through surgery, adjuvant therapy, and survivorship. In this Perspective, we argue that psychiatry should not be an occasional consultant in neuro-oncology but a structural component of care. This view is argued based on the published evidence and on our experience in a liaison psychiatry service working alongside neurosurgery. The focus of this article is on adults, because pediatric neuro-oncology involves different tumor types, developmental considerations, and assessment tools that deserve separate discussion.

2. A NOSOLOGICAL FRAMEWORK: WHEN IS A PSYCHIATRIC DISORDER DUE TO A BRAIN TUMOR?

Both major classifications of psychiatric disorders (Diagnostic and Statistical Manual of Mental Disorders, Fifth Edition, Text Revision—DSM-5-TR, and International Classification of Diseases, Eleventh Revision—ICD-11) [10,11] recognize that a brain tumor can directly cause a mental illness or at least a corresponding syndrome, but they frame this possibility differently (Table 1). The DSM-5-TR places categories such as depressive disorder, bipolar and related disorder, anxiety disorder, obsessive-compulsive and related disorder, psychotic disorder, catatonia, and personality change due to another medical condition within the corresponding diagnostic chapters [10]. Such a diagnosis requires evidence from the history, physical examination, or laboratory findings that the disturbance is the direct pathophysiological consequence of the medical condition, that it is not better explained by another mental disorder, including an adjustment disorder in which the medical illness is the stressor, and that it does not occur exclusively during delirium [10]. The ICD-11 groups the equivalent conditions in a single block of secondary mental or behavioral syndromes associated with disorders or diseases classified elsewhere (6E60-6E6Z), which includes secondary psychotic, mood, anxiety, obsessive-compulsive or related, dissociative, impulse control, neurocognitive, and catatonia syndromes as well as secondary personality change [11]. ICD-11 speaks of syndromes rather than disorders, which highlights that the psychiatric picture is a manifestation of the underlying disease; it asks for the secondary code to be used in addition to the code for that disease, and it states explicitly that the symptoms must not be a psychologically mediated response to a severe medical condition, such as depressive symptoms in reaction to a life-threatening diagnosis [11].

Applying these criteria to patients with brain tumors is less straightforward than the definitions suggest, because the tumor, its treatment, the psychological impact of the diagnosis, and premorbid vulnerability usually act together, and their relative weight changes over the course of the disease. Both classifications also assign syndromes induced by medications, such as corticosteroids or levetiracetam, to separate substance- or medication-induced categories rather than to the secondary categories [10,11], so a single patient may legitimately move between diagnostic labels as treatment evolves. The two cases presented in Section 3 illustrate the complexity of distinguishing organic from psychological factors in assessing psychiatric syndromes with onset in neuro-oncology cases. The depressive syndromes at presentation were attributable to the tumors on clinical grounds, yet the persistence of core depressive symptoms after successful resection raises the possibility of residual network injury, of a primary depressive disorder unmasked by the illness, or of a reaction to the diagnosis and surgery. Rather than forcing a binary choice between primary and secondary disorders, we therefore propose that clinicians formulate each case across four etiological domains (Table 2). This formulation is not equivalent to a new diagnostic category but proposes a practical framework that links the diagnostic label to management, because each active domain points to a different intervention, and it should be revisited at each phase of care.

Table 1: Comparison of the DSM-5-TR and ICD-11 approaches to psychiatric syndromes caused by brain disease, including brain tumors [10,11]

Feature	DSM-5-TR	ICD-11
Terminology	Mental disorder due to another medical condition	Secondary mental or behavioral syndrome associated with disorders or diseases classified elsewhere
Place in the classification	Distributed across the corresponding diagnostic chapters (e.g., depressive, psychotic, and anxiety disorders)	Grouped in a single block (6E60-6E6Z) within the chapter on mental, behavioral or neurodevelopmental disorders
Core requirement	Evidence from history, physical examination, or laboratory findings that the disturbance is the direct pathophysiological consequence of the medical condition	Syndrome judged to be a direct pathophysiological consequence of the health condition, based on history, examination, or laboratory findings
Exclusions	Not better explained by another mental disorder, including adjustment disorder with the illness as stressor, and not occurring exclusively during delirium	Not accounted for by delirium or another mental disorder, and not a psychologically mediated response to a severe medical condition
Categories relevant to brain tumors	Depressive disorder (with depressive features, with major depressive-like episode, or with mixed features), bipolar and related, anxiety, obsessive-compulsive and related, and psychotic disorders, catatonia, personality change (including apathetic and disinhibited types), and neurocognitive disorder due to another medical condition	Secondary psychotic (6E61), mood (6E62, with depressive, manic, or mixed symptoms), anxiety (6E63), obsessive-compulsive or related (6E64), dissociative (6E65), impulse control (6E66), and neurocognitive (6E67) syndromes, secondary personality change (6E68), and secondary catatonia syndrome (6E69)

Feature	DSM-5-TR	ICD-11
Coding	The medical condition is coded first, followed by the mental disorder	The secondary code is used in addition to the code for the underlying disease
Medication effects	Coded as substance/medication-induced disorders	Coded among substance-induced disorders rather than as secondary syndromes

Table 2: A four-domain etiological formulation of psychiatric symptoms in patients with brain tumors

Domain	Clinical clues	Diagnostic correlate	Management implications
Direct tumor effect	Onset or worsening linked to tumor growth, edema, or progression, late or atypical onset, neurological or cognitive signs, apathy or personality change, improvement after resection or edema control	Disorder due to another medical condition (DSM-5-TR) or secondary syndrome (ICD-11)	Tumor-directed and antiedema treatment, psychotropic drugs as adjuncts, vigilance for progression
Treatment-related and endocrine	Onset after starting or increasing corticosteroids, antiseizure drugs, or dopamine agonists; symptoms during steroid taper; late fatigue and low mood after cranial irradiation; abnormal pituitary function	Substance/medication-induced disorder, or secondary syndrome due to an endocrine disorder	Dose reduction or switching, endocrine testing and hormone replacement, joint review with neuro-oncology
Psychological reaction	Content centered on diagnosis, prognosis, disability, or loss, onset after disclosure or a treatment milestone, preserved emotional reactivity	Adjustment disorder, or a primary disorder if full criteria are met	Psycho-oncological support, psychotherapy, involvement of caregivers
Pre-existing vulnerability	Previous episodes, family history, persistence after the other domains have been addressed	Primary mental disorder (e.g., major depressive disorder) co-occurring with the tumor	Standard evidence-based treatment adapted for seizure risk, drug interactions, and cognition

3. WHEN THE TUMOR PRESENTS AS A PSYCHIATRIC DISORDER

3. WHEN THE TUMOR PRESENTS AS A PSYCHIATRIC DISORDER

Neurobehavioral presentations of brain tumors have long been recognized in clinical settings and in medical literature as challenging aspects. In a series of eight patients, frontal tumors presented with abulia, personality change, or depression, whereas temporolimbic tumors presented with hallucinations, mania, panic attacks, or amnesia, and after treatment the syndromes abated or resolved in seven patients [12]. In another series, eight patients with brain lesions, including four meningiomas and two high-grade gliomas, were diagnosed and treated for a significant period as having Alzheimer's disease, schizoaffective disorder, schizophrenia, or depression before neurological signs led to neuroimaging [13]. Meningiomas are particularly prone to such delays because of their slow growth. In a retrospective hospital sample, 15 of 72 patients (21%) with meningioma presented with psychiatric symptoms in the absence of neurological symptoms, most commonly affective disorders [14]. An individual patient data analysis of published meningioma cases confirmed a wide range of presentations, from mood disorders to psychosis and obsessive-compulsive symptoms [15].

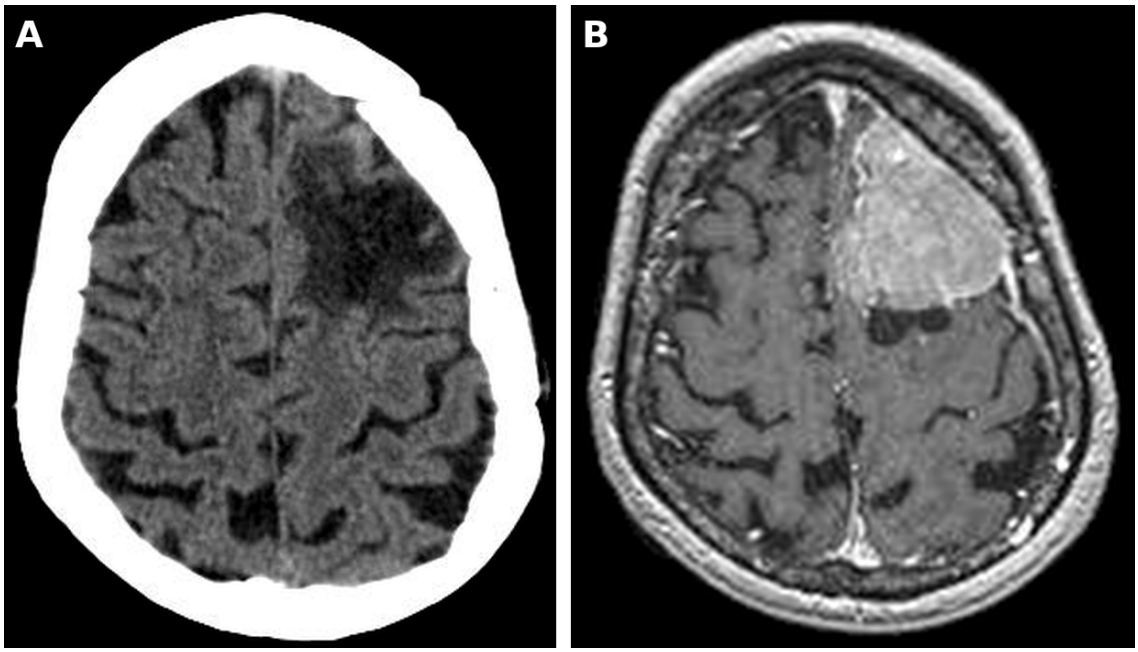
Table 3: Clinical red flags that should prompt neuroimaging or further work-up in adults presenting with psychiatric symptoms [9,12,13,15-19]

Feature	Examples
Onset or course	First psychiatric episode in later life (usually after about 50 years of age), particularly when combined with any other feature in this table, subacute, progressive, or fluctuating course
Atypical presentation	Personality change, apathy without sadness, abulia, or disinhibition, anorexia without body-image concerns, new-onset psychosis or mania without a personal or family history
Treatment response	Poor or paradoxical response to adequate psychotropic treatment, prolonged confusion or new neurological signs after electroconvulsive therapy
Cognitive signs	Memory impairment, disorientation, inattention, or language disturbance (e.g., receptive dysphasia misread as thought disorder)
Neurological signs	Headache, vomiting, papilledema, or other signs of raised intracranial pressure, seizures, focal deficits, urinary incontinence, visual disturbances, anosmia
Endocrine context	Features suggesting a sellar lesion, hyperprolactinemia that is very high, persistent, or not temporally linked to antipsychotic treatment
Systemic context	History of cancer (risk of brain metastases, and of paraneoplastic or immune-mediated encephalitis when imaging is unrevealing), treatment with immune checkpoint inhibitors

Anatomical localization is, however, a weak guide to establish correspondence between the neurological problems and the psychiatric ones. A meta-analysis of published case reports found a statistically significant association only between anorexia and hypothalamic tumors [20]. Lesion network mapping offers a more modern explanation for this inconsistency, since in 461 patients with focal lesions of different etiologies, lesions associated with depression were spread across many regions but mapped onto a common functional circuit centered on the left dorsolateral prefrontal cortex [21]. Thinking in terms of networks rather than lobes may help explain why tumors located far from the prefrontal cortex can still present with depression. Clinicians should therefore rely less on predicting tumor site from symptoms and more on recognizing features that make a primary psychiatric disorder unlikely. These features, summarized in Table 3, include new-onset symptoms in later life, atypical presentations, poor response to standard treatment, and any neurological or cognitive sign [9,12,15]. Late onset is a weak criterion on its own, because depression in later life is common and only rarely caused by a tumor, so the threshold for imaging should fall mainly when late onset coincides with at least one other feature in Table 3 [9]. The question of routine imaging is not settled, but a meta-analysis of first-episode psychosis found a clinically relevant magnetic resonance imaging (MRI) abnormality in 5.9% of patients, meaning that one such finding was detected for every 18 patients scanned [16]. Imaging may also reveal lesions whose relevance to the psychiatric picture is uncertain, such as the multinodular and vacuolating neuronal tumor, a rare, benign neuronal tumor that is frequently asymptomatic and most often discovered incidentally, and that, when it causes no symptoms, is often managed by observation with serial MRI rather than by resection [22]. Finding such a lesion does not by itself establish that the psychiatric syndrome is secondary to it, a conclusion that still requires the evidence of a direct pathophysiological link discussed in Section 2.

In patients with known systemic cancer, a new psychiatric syndrome with unrevealing or nonspecific imaging should also raise the possibility of autoimmune encephalitis. The clinical criteria for possible autoimmune encephalitis require a subacute onset, over less than three months, of working memory deficits, altered mental status, or psychiatric symptoms, together with at least one supportive finding, such as new focal neurological signs, unexplained seizures, cerebrospinal fluid pleocytosis, or suggestive MRI changes, once reasonable alternative causes have been excluded [17]. The updated criteria for paraneoplastic neurological syndromes classify limbic encephalitis as a high-risk phenotype and grade antibodies according to their association with cancer [23]. Because immune checkpoint inhibitors, now widely used in metastatic cancers, can also trigger immune-mediated neurological syndromes, a careful oncological treatment history is part of the differential diagnosis [23].

Figure 1: Case 1. Axial non-contrast computed tomography (CT) (A) showing an area of hypodensity (perilesional edema) in the left frontal lobe, and axial contrast-enhanced T1-weighted MRI (B) showing a homogeneously enhancing, extra-axial, left frontal parasagittal lesion. Images are displayed in radiological convention (patient left on image right) and have been anonymized.



Two cases from our service are further presented to illustrate these points. Both patients were referred by their general practitioners for psychiatric evaluation of depressive symptoms. The first, a 60-year-old patient with obesity and diabetes, presented with memory disturbances, a depressive syndrome, behavioral changes, and non-fluent, effortful speech, and

neuroimaging showed a left frontal parasagittal, extra-axial, contrast-enhancing lesion with perilesional edema (Figure 1). The second, a 67-year-old patient, presented with depressive symptoms and, on closer examination, signs of intracranial hypertension and a receptive dysphasia, which neuroimaging explained as a left temporo-parietal convexity meningioma compressing Wernicke's area (Figure 2). A receptive language deficit can easily be misread as confusion, inattention, or disorganized thinking in a patient labeled as depressed. Both diagnoses were reached through a team-based approach with successive investigations. After surgery, which in the second case was a gross total resection, most neurological and cognitive symptoms remitted significantly. However, core depressive symptoms persisted at follow-up in both patients and required continued psychotropic treatment. These observations are consistent with population data showing that depression often does not resolve after surgery, especially in patients with a history of depression or residual disability [24], and they show that surgical success does not end the need for psychiatric care. Table 4 applies the four-domain formulation proposed in Section 2 to both cases and shows that the direct tumor effect, which dominated the initial presentation, could not fully account for the depressive symptoms that persisted after resection, so residual network injury and the remaining domains had to be reassessed at follow-up.

Figure 2: Case 2. Preoperative axial contrast-enhanced CT (A) and gadolinium-enhanced T1-weighted MRI (B) showing a large, well-circumscribed, homogeneously enhancing left temporo-parietal convexity meningioma, and postoperative axial CT (C) showing the left temporo-parietal resection cavity after gross total resection. Images are displayed in radiological convention (patient left on image right) and have been anonymized.

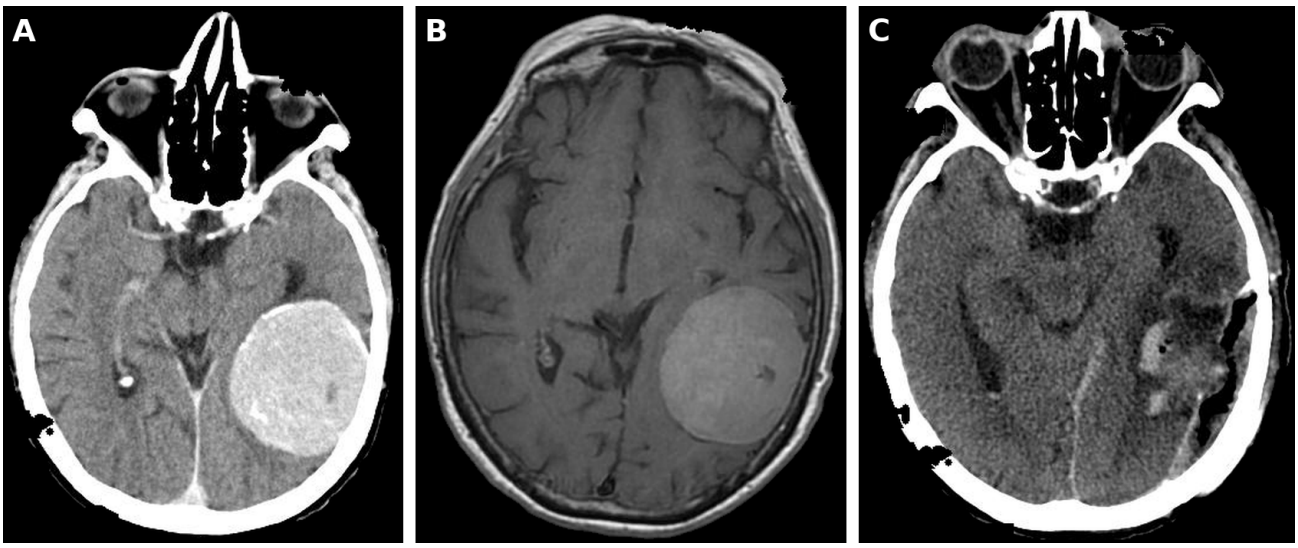


Table 4: Application of the four-domain etiological formulation (Table 2) to the two cases

Domain	Case 1	Case 2
Direct tumor effect	Left frontal parasagittal, extra-axial, contrast-enhancing lesion with perilesional edema. The depressive syndrome was accompanied by memory disturbances, behavioral changes, and non-fluent, effortful speech, and apathy was a plausible contributor given the frontal location. Most neurological and cognitive symptoms remitted after surgery.	Left temporo-parietal convexity meningioma compressing Wernicke's area. The depressive symptoms were accompanied by signs of intracranial hypertension and receptive dysphasia. Most neurological and cognitive symptoms remitted after gross total resection.
Treatment-related and endocrine	Not available in the source documents	Not available in the source documents
Psychological reaction	Depressive cognitions of helplessness and incurability	Receptive dysphasia made self-report unreliable before surgery, which favored observer-rated assessment of mood.
Pre-existing vulnerability	No previous psychiatric episodes, and no family history of psychiatric illnesses. Obesity and diabetes as medical comorbidities.	No previous psychiatric episodes, and no family history of psychiatric illnesses.
Formulation at follow-up	Core depressive symptoms persisted after surgery and	Core depressive symptoms persisted despite gross total

Domain	Case 1	Case 2
	required continued psychotropic treatment, so residual network injury, a reaction to the diagnosis and surgery, and a primary depressive disorder unmasked by the illness remained the hypotheses to be weighed.	resection and required continued psychotropic treatment, with the same three hypotheses to be weighed.

Apathy deserves separate attention, because it is one of the most frequent ways in which a frontal tumor is mistaken for depression. The 2018 international consensus criteria define apathy as a quantitative reduction of goal-directed activity, compared with the patient's previous level of functioning, that persists for at least four weeks, affects at least two of three dimensions (behavior and cognition, emotion, and social interaction), and causes identifiable functional impairment [25]. Unlike depression, apathy is not driven by sadness, guilt, hopelessness, or negative cognitions, and patients often show little concern about their own passivity, which is why informant ratings are more informative than self-report. The Apathy Evaluation Scale, available in self-, informant-, and clinician-rated versions, can quantify the syndrome and follow its course [26]. In the DSM-5-TR paradigm, a persistent apathetic presentation caused by the tumor corresponds to personality change due to another medical condition, apathetic type, and in ICD-11 to secondary personality change [10,11]. The distinction has direct therapeutic consequences, since escalating antidepressant doses is unlikely to help when the core problem is loss of motivation rather than low mood, whereas structured activity, caregiver education, and cognitive rehabilitation are more rational options. Psychostimulants may be considered in selected cases, although the evidence in this population is limited to uncontrolled data and a negative trial of modafinil for fatigue, mood, and cognition [27,28]. In Case 1, the parasagittal frontal location made apathy a plausible contributor to the depressive presentation, and this possibility should be assessed explicitly in similar patients.

4. PSYCHIATRIC COMORBIDITY ACROSS THE DISEASE COURSE

Depression is the best-studied psychiatric complication of brain tumors. A meta-analysis of 37 studies estimated a pooled prevalence of depression or depressive symptoms of 21.7% [29]. Estimates depend heavily on how depression is measured: in a systematic review of glioma studies, the median frequency was 15% by clinical interview but 39% with the Beck Depression Inventory [30]. In the Glioma Outcomes Project, physicians reported depression in 15% of patients early after surgery for high-grade glioma, rising to 22% at 3 and 6 months, whereas 93% of patients reported depressive symptoms, and antidepressants were given to only 60% of those whom physicians recognized as depressed [31]. In a population-based cohort, 35% of patients had depression before surgery, and lower functional status was associated with higher depression scores at 3 months and 1 year [24]. Anxiety is similarly common and frequently coexists with depression, with female sex, lower tumor grade, lower education, and a psychiatric history among its predictors [32]. Shortly after craniotomy, 48.4% of patients report clinically relevant distress, which cannot be predicted from tumor stage or sociodemographic data [33].

These conditions matter beyond quality of life, since they can have devastating consequences at multiple levels of mental health and daily functionality. Depression is consistently associated with reduced physical function, cognitive impairment, and poorer quality of life [30], and it may shorten survival. Preoperative depression was independently associated with reduced survival after resection of malignant astrocytoma [34], and a meta-analysis found a borderline increased risk of death among depressed patients with high-grade glioma [35]. In glioblastoma, depression may also reduce treatment adherence [36]. Suicide risk deserves explicit attention, since the standardized mortality ratio for suicide among patients with cancer is 4.44 compared with the general population [37]. In a population-based analysis of 87,785 patients with brain cancer, the risk of suicide in the first year after diagnosis was three times higher than expected (observed-to-expected ratio 3.05, 95% CI 2.04-4.37), rising to 5.04 in patients older than 64 years, and most of those who died by suicide were men with glioblastoma [38]. Suicide risk assessment therefore belongs to the first months after diagnosis, when patients are also undergoing surgery and adjuvant treatment. Tumors of the sellar region raise specific issues, since depression scores improved after surgery for pituitary adenoma in one cohort [24], but patients cured of Cushing's disease show persistent psychopathology and maladaptive personality traits years after remission, suggesting lasting effects of glucocorticoid excess on the brain [39].

Screening is feasible in this population, and should be applied thoroughly whenever possible. In adults with glioma, the depression subscale of the Hospital Anxiety and Depression Scale at a threshold of 8 or more and the Patient Health Questionnaire-9 at 10 or more performed well, whereas the Distress Thermometer was inferior, although positive screens still require clinical assessment [40]. However, self-report instruments become unreliable when receptive or expressive aphasia is present, as in our second case, and observer-rated tools developed for stroke offer a practical alternative. The Stroke Aphasic Depression Questionnaire is completed by a caregiver or nurse on the basis of observable behaviors and also exists in shorter and hospital versions [41], whereas the Aphasic Depression Rating Scale is rated by clinical staff and was validated in patients with aphasia in the subacute phase of stroke [42]. Neither instrument has been validated in patients with brain tumors, but both are preferable to omitting mood assessment altogether.

Postoperative delirium is another frequent and underrecognized complication. A meta-analysis of patients undergoing intracranial surgery estimated an incidence of 19%, ranging from 12% to 26% according to clinical features and assessment method [43], and a more recent meta-analysis found delirium in 17% of hospitalized patients with brain tumors [44]. After

craniotomy for brain metastases, delirium was associated with postoperative hematoma and with poorer survival [45]. Hypoactive delirium is easily mistaken for depression or apathy, and fluctuating attention can be misread as a new psychiatric disorder, so routine screening with validated instruments, such as the Confusion Assessment Method [46], should be part of perioperative care. An episode of delirium should also prompt closer cognitive follow-up, because delirium and later cognitive decline are distinct but related problems.

5. IATROGENIC AND ENDOCRINE CONTRIBUTORS TO PSYCHIATRIC MORBIDITY

A distinctive feature of psychiatric care in neuro-oncology is that the treatments themselves can cause or worsen psychiatric symptoms. Corticosteroids, usually dexamethasone, remain essential for controlling peritumoral edema [47,48], yet severe psychiatric reactions occur in nearly 6% of patients receiving systemic corticosteroids and mild-to-moderate reactions in about 28%, with short-term therapy most often inducing euphoria or hypomania, long-term therapy tending to cause depression, and delirium or psychosis occurring at higher doses [49]. Steroid-related insomnia, agitation, or mood changes should therefore be considered before a new psychiatric diagnosis is made, and the lowest effective dose should be the goal. The taper deserves equal attention, because steroid withdrawal and secondary adrenal insufficiency can produce fatigue, anorexia, and low mood that closely resemble depression [48].

Seizures are common, affecting 60-75% of patients with low-grade glioma, 20-50% of those with meningioma, and 20-35% of those with brain metastases [50]. Current guidelines, updating the 2000 practice parameter [51], advise against anticonvulsant prophylaxis in patients who have never had a seizure and suggest levetiracetam over older agents when treatment is needed [52]. Levetiracetam, however, has its own psychiatric burden, as 14.1% of patients with epilepsy develop a psychiatric symptom or disorder within 2 years of starting it, and a history of depression or anxiety substantially increases this risk [53]. When irritability, aggression, or depressive symptoms emerge, switching the antiseizure drug is often more effective than adding a psychotropic, and in a retrospective series of patients switched overnight from levetiracetam to brivaracetam, levetiracetam-related neuropsychological adverse events improved in 76% [54]. Valproate has mood-stabilizing properties and may therefore be attractive in patients with comorbid bipolar disorder, but in the European Organization for Research and Treatment of Cancer and National Cancer Institute of Canada (EORTC/NCIC) trial it was associated with more grade 3-4 thrombocytopenia and leukopenia during temozolomide-based chemoradiotherapy, although the same post hoc analysis also suggested longer survival in patients taking valproate alone [55]. This survival signal was not confirmed in a pooled analysis of four prospective trials in newly diagnosed glioblastoma, which found no survival benefit for either valproate or levetiracetam and concluded that these drugs should be used for seizure control rather than to improve survival [56]. Enzyme-inducing antiseizure drugs, in turn, interact with chemotherapeutic agents and should be avoided where possible [50,57].

Endocrine pathways add a further and often overlooked source of psychiatric morbidity. The hypothalamic-pituitary axis is highly radiosensitive, and radiation-induced hypopituitarism develops insidiously over the years after cranial irradiation, is usually irreversible and progressive, and affects growth hormone secretion first, followed by gonadotropin, corticotropin, and thyrotropin deficiencies [58]. Its manifestations, including fatigue, low mood, reduced libido, and cognitive slowing, overlap so extensively with depression that long-term survivors presenting with new depressive symptoms should have pituitary function assessed before an antidepressant is started. Sellar tumors carry their own risks. Prolactinomas are treated with dopamine agonists, which can induce impulse control disorders such as pathological gambling, compulsive shopping, and hypersexuality, and men with dopamine agonist-treated prolactinomas were almost ten times more likely to develop such disorders than men with non-functioning adenomas [59]. Conversely, psychiatrists frequently encounter hyperprolactinemia caused by antipsychotics, and endocrine guidelines recommend pituitary imaging when the drug cannot safely be stopped or replaced and the onset of hyperprolactinemia does not coincide with the start of treatment [19].

Oncological treatments have improved survival, which increases the need for long-term psychiatric care. Radiotherapy plus temozolomide extended median survival in glioblastoma from 12.1 to 14.6 months [60], tumor-treating fields added further benefit [61], and vorasidenib more than doubled progression-free survival in grade 2 IDH-mutant glioma [62]. European guidelines now define multimodal standards for diffuse gliomas [63] and meningiomas, including watch-and-scan strategies for many asymptomatic meningiomas [64]. Cognitive deficits, however, arise from the tumor itself, from surgery, from antiseizure and steroid treatment, and from radiotherapy [65]. In brain metastases, memantine given during whole-brain radiotherapy did not significantly reduce the decline in delayed recall at 24 weeks, the primary endpoint ($p = 0.059$), probably because only 149 patients remained analyzable, but it prolonged the time to cognitive failure (hazard ratio 0.78, 95% CI 0.62-0.99) and lowered the probability of cognitive failure at 24 weeks from 64.9% to 53.8% [66]. Hippocampal avoidance plus memantine reduced the risk of cognitive failure further compared with whole-brain radiotherapy plus memantine (adjusted hazard ratio 0.74, 95% CI 0.58-0.95) [67]. These advances show that neurotoxicity can be modified, and psychiatrists should be involved when treatment options with different cognitive risks are weighed.

6. TREATMENT: WORKING WITH LIMITED EVIDENCE

The most intriguing finding in this field is the absence of controlled trials of antidepressants. The latest Cochrane review found no eligible study of any pharmacological treatment of depression in people with a primary brain tumor [68]. In practice, clinicians extrapolate from other populations and choose agents on the basis of tolerability, seizure risk, and drug interactions, and selective serotonin reuptake inhibitors (SSRIs) are generally favored [9]. Pharmacological pathways shared by depression and glioblastoma, and possible interference of some antidepressants with tumor treatment, add a further layer of uncertainty [36]. These choices should be made jointly with the neuro-oncology team.

Several practical points follow from this approach. Sertraline, citalopram, and escitalopram have a low potential for pharmacokinetic interactions and are reasonable first choices, whereas bupropion, clomipramine, maprotiline, and amoxapine lower the seizure threshold in a dose-dependent manner and are best avoided in patients with tumor-related epilepsy [69]. SSRIs increase the risk of bleeding, with a pooled odds ratio of 1.41 for severe bleeding in a meta-analysis of 42 observational studies [70], which matters in the perioperative period and during temozolomide treatment, when thrombocytopenia is common, so platelet counts should be checked, and mirtazapine may be preferred when bleeding risk is high. All antidepressants except mianserin were associated with hyponatremia in a large register-based study, with the strongest association for citalopram [71], and the risk is compounded by carbamazepine or oxcarbazepine and by the sodium disturbances that frequently follow intracranial surgery, so sodium should be monitored after an antidepressant is started. Mirtazapine can also relieve insomnia, poor appetite, and nausea, which are common during chemoradiotherapy. When a hypnotic is still required, for example for corticosteroid-related insomnia, it should be prescribed at the lowest effective dose and for a short period, because Z-drug hypnotics such as zolpidem, as well as some benzodiazepines, antidepressants, and antipsychotics, can trigger sleep-related eating disorder, a parasomnia that may involve hazardous behaviors during nocturnal eating episodes [72]. For corticosteroid-induced mania or psychosis, dose reduction is the first step, with short-term low-dose antipsychotic treatment when symptoms are severe [49]. When antipsychotics are needed for psychosis due to the tumor, the lowest effective dose should be used with attention to sedation, QTc prolongation, and seizure threshold, and clozapine, which carries a dose-dependent seizure risk, should be reserved for exceptional cases [69]. Cardiac safety also deserves attention, because brain lesions can affect the heart through autonomic pathways, as suggested by the frequent elevation of cardiac enzymes in acute ischemic stroke, particularly when the insula is involved [73], so a baseline electrocardiogram is advisable before an antipsychotic is started.

Electroconvulsive therapy (ECT) poses a particular dilemma. For decades, an intracranial mass was considered an absolute contraindication, a view based largely on early reports of neurological deterioration [74]. A review of 75 patients who received ECT in the presence of a brain tumor over 80 years found that, among the more recently reported cases, meningiomas were the most common lesions and adverse effects occurred in 15%, and it concluded that ECT can be applied safely in patients with small, benign, or otherwise clinically insignificant lesions [18]. Large lesions, multiple metastases, peritumoral edema, mass effect, and raised intracranial pressure nevertheless remain major risk factors, because seizures transiently increase cerebral blood flow and intracranial pressure, so the decision should be taken jointly with neurosurgery and anesthesia, with consideration of premedication such as corticosteroids [18]. Two further implications are relevant for psychiatrists. Neuroimaging is advisable before ECT in patients whose depression has atypical features or late onset, and unexpectedly prolonged confusion or new neurological signs after ECT should prompt imaging rather than a mere change in stimulation parameters.

Evidence for other drugs is also limited. Methylphenidate improved cognition, mood, and function in an early uncontrolled study [27], but modafinil did not outperform placebo for fatigue, mood, or cognition in a randomized crossover trial [28]. Donepezil did not improve the overall cognitive composite score in irradiated survivors but modestly improved memory and motor speed, especially in more impaired patients [75]. Psychological interventions face similar challenges: an internet-based guided self-help program based on problem-solving therapy did not reduce depressive symptoms in glioma patients, although it may have reduced fatigue, and the trial was underpowered [76]. For caregivers, a Cochrane review found only eight small trials and could not draw reliable conclusions [77].

Cognitive rehabilitation has stronger support. In a randomized controlled trial of 140 adults with mostly low-grade glioma in remission, a program of six weekly two-hour sessions combining computer-based attention retraining with compensatory strategy training improved attention and verbal memory at six months and reduced mental fatigue compared with usual care [78]. Because cognitive complaints are often intertwined with low mood, apathy, and fatigue, cognitive rehabilitation should be coordinated with psychiatric treatment rather than offered in parallel.

Cognition deserves a central place in outcome assessment. Verbal memory performance independently predicted survival in recurrent malignant glioma [79], and cognitive deterioration preceded radiographic progression by about 6 weeks [80]. A change in cognition or behavior during follow-up may therefore be an early sign of tumor progression rather than a new psychiatric disorder. Repeated cognitive screening and clear distinction between delirium and progressive cognitive decline are core tasks of the liaison psychiatrist. In advanced disease, palliative care guidelines identify disorders of behavior and mood, fatigue, and caregiver needs as areas with scarce evidence, and recommend an early palliative approach [81].

7. TOWARD AN INTEGRATED MODEL OF CARE

Our experience and the evidence reviewed above support a phase-based model in which psychiatric tasks are defined in advance for each stage of the disease (Table 5). In neuro-oncology, the key milestones are disclosure of the diagnosis, surgery, adjuvant treatment, and the transition to survivorship or palliative care. The core team should include psychiatrists, psychologists, neurologists, neurosurgeons, oncologists, endocrinologists, physical therapists, speech and language therapists, social workers, and specialized nurses, each with clear roles in managing psychiatric and organic symptoms in the short and long term. In the prediagnostic phase, the priority is recognition, which means that psychiatrists and general practitioners should know the red flags in Table 3 and have rapid access to neuroimaging [9,16]. In the perioperative phase, baseline assessment of mood, apathy, cognition, suicide risk, decision-making capacity, and delirium risk allows postoperative changes to be interpreted correctly [31,33,43,82]. During adjuvant therapy, review of corticosteroid and antiseizure regimens is as important as psychotropic prescribing [49,53]. In survivorship and palliative care, the focus shifts to persistent depression and apathy, endocrine late effects, cognitive rehabilitation, caregiver support, and advance care planning [58,77,78,81].

Table 5: Proposed phase-based tasks for psychiatry within the neuro-oncology team [31,33,43,49,53,58,77,80-82]

Phase	Psychiatric tasks	Key considerations
Prediagnostic	Recognize red flags, request neuroimaging (including before ECT in atypical or late-onset depression), avoid premature psychiatric labeling	Close communication with general practitioners and neurology, consider autoimmune encephalitis in patients with known cancer
Perioperative	Baseline assessment of mood, anxiety, apathy, cognition, suicide risk, and decision-making capacity, delirium screening with validated instruments	Distress is high after craniotomy and is not predicted by tumor stage; observer-rated tools are needed in aphasia
Adjuvant treatment	Monitor corticosteroid- and antiseizure drug-related psychiatric effects, treat depression and anxiety, check drug interactions, sodium, and platelet counts	Lowest effective steroid dose and careful taper, preference for non-enzyme-inducing antiseizure drugs, switching rather than adding when levetiracetam causes behavioral effects
Follow-up and survivorship	Repeated screening of mood, apathy, and cognition, psychotherapy, cognitive rehabilitation, endocrine review after cranial irradiation, return-to-work support	New cognitive or behavioral change may signal tumor progression
Palliative and end of life	Management of delirium, agitation, and mood, caregiver support, reassessment of capacity and advance care planning	Early integration of palliative care

Such a model does not require new specialized units. It requires routine screening with validated instruments [40], shared protocols for steroid and antiseizure drug review, and a liaison psychiatrist who follows the patient across departments rather than being called only in a crisis. Our two cases illustrate the value of continuity: without follow-up visits after successful surgery, the persistent depression of both patients would probably have gone untreated. The psychometric evaluation of ClinFIT COVID-19 illustrates standardized measurement of functioning across care settings, although use in neuro-oncology would require adaptation and validation [83].

Decision-making capacity runs through every phase of this model. Soon after diagnosis, patients with malignant glioma performed worse than healthy controls on the understanding, appreciation, and reasoning standards of a structured capacity instrument, and these impairments were explained mainly by deficits in short-term verbal memory, which led the authors to recommend repeated assessment of capacity throughout the disease [82]. Capacity is decision-specific and may fluctuate with edema, seizures, delirium, or steroid effects, and aphasia can make a capable patient appear incapable unless communication is supported with simplified language, written or pictorial aids, and the help of a speech and language therapist. The liaison psychiatrist is well placed to assess capacity for consent to surgery, adjuvant treatment, and trial participation, and to encourage advance care planning while capacity is preserved, so that surrogate decision-makers can later act on the patient's known wishes.

8. RESEARCH PRIORITIES AND LIMITATIONS

Several gaps should be addressed. First, randomized trials of antidepressants and psychotherapies in patients with brain tumors are needed, ideally stratified by tumor type, grade, and phase of treatment [68]. Second, screening thresholds and diagnostic criteria for depression should be validated in patients with aphasia, cognitive impairment, or fatigue, in whom self-report instruments may be unreliable, and observer-rated tools developed for stroke, such as the Stroke Aphasic Depression Questionnaire and the Aphasic Depression Rating Scale, should be tested in neuro-oncology [30,40-42]. Third, prospective studies should clarify whether treating depression improves adherence, functional outcome, and survival, a hypothesis already raised by the Glioma Outcomes Project [31,35]. Fourth, psychiatric and cognitive outcomes, including apathy and decision-making capacity, should be included as endpoints in neuro-oncology trials, alongside survival and imaging response [67,80]. Fifth, the four-domain

formulation proposed here should be tested for inter-rater reliability and for its ability to predict treatment response. Nonlinear dynamics and fractal metrics explored in simulation-based post-COVID respiratory rehabilitation offer another methodological direction, whose usefulness in neuro-oncology would require investigation [84]. Finally, the biological links between tumors, inflammation, glucocorticoid exposure, and mood merit translational research, and lesion network mapping applied to tumor cohorts could clarify why lesions in different locations produce similar psychiatric syndromes [21,36,39].

This Perspective has several limitations. First of all, it is not a systematic review, and the literature was selected to support a clinical argument rather than identified through a predefined search strategy with formal appraisal of study quality, so relevant evidence may have been missed. The two cases come from a single liaison psychiatry service and were chosen because they illustrate diagnostic pitfalls, which means that they cannot establish how often tumors present as depression or how often depression persists after surgery. Much of the evidence on psychiatric comorbidity and treatment derives from patients with glioma, and its applicability to meningioma, brain metastases, and sellar tumors is uncertain. Several recommendations, including the use of observer-rated mood scales in aphasia and of structured capacity assessment, are extrapolated from stroke, dementia, or other populations, and the four-domain formulation and the phase-based model are proposals that have not yet been validated. Finally, our discussion is limited to adults and is shaped by the organization of care in our own setting, which may limit its transferability to health systems with different resources.

9. CONCLUSIONS

Psychiatric symptoms can be the first sign of a brain tumor and remain a common, prognostically relevant, and undertreated problem after diagnosis. Psychiatrists should keep a low threshold for neuroimaging when psychiatric symptoms are atypical, start late in life, or are accompanied by neurological, cognitive, or endocrine signs, and they should distinguish apathy from depression, because the two call for different treatments. Classifying a syndrome as secondary to the tumor is only the first step, and a formulation that also weighs treatment-related and endocrine effects, psychological reactions, and pre-existing vulnerability offers a more useful guide to management, particularly when symptoms persist after successful surgery. After diagnosis, depression, anxiety, distress, delirium, suicide risk, and cognitive impairment should be screened for and treated as part of oncological care, with attention to the psychiatric effects of corticosteroids, antiseizure drugs, dopamine agonists, and cranial irradiation, to the specific risks of psychotropic drugs and electroconvulsive therapy in this population, and to the patient's capacity to take part in decisions. Until controlled evidence becomes available, a multidisciplinary, phase-based model with regular psychiatric follow-up offers the most reasonable way to protect patients' quality of life before, during, and after surgery.

Conflicts of interest and sources of funding

The authors declare no conflicts of interest.

Acknowledgments

The authors declared that generative AI (Claude Opus 5.5, Anthropic) was used for grammar and style revisions of this text. The authors take full responsibility for the final manuscript.

Authors' contribution

Conceptualization, C.N., B.M.P., O.V., C.A.C., and A.G.M.; methodology, C.N., B.M.P., O.V., C.A.C., and A.G.M.; literature search and data curation, C.N., C.A.C., and A.G.M.; formal analysis, C.N., B.M.P., O.V., C.A.C., and A.G.M.; visualization, O.V.; writing—original draft preparation, C.N., B.M.P., O.V., C.A.C., and A.G.M.; writing—review and editing, C.N., B.M.P., O.V., C.A.C., and A.G.M.; supervision, B.M.P. and O.V.; project administration, A.G.M. All authors have read and agreed to the published version of the manuscript.

Ethics approval and consent to participate

The study was conducted in accordance with the Declaration of Helsinki and approved by the Local Ethics Committee of the "Dr. Carol Davila" University Emergency Central Military Hospital, Bucharest, Romania (approval no. 631, 14 September 2023).

Patient consent for publication

Written informed consent was obtained from both patients for the publication of their clinical data and anonymized images.

References

1. Price M, Ballard C, Benedetti J, Kruchko C, Barnholtz-Sloan JS, Ostrom QT. CBTRUS statistical report: primary brain and other central nervous system tumors diagnosed in the United States in 2018-2022. Neuro Oncol. 2025;27(Suppl 4):iv1-iv66. doi:10.1093/neuonc/noaf194

2. Ostrom QT, Price M, Neff C, Cioffi G, Waite KA, Kruchko C, et al. CBTRUS statistical report: primary brain and other central nervous system tumors diagnosed in the United States in 2016-2020. Neuro Oncol. 2023;25(12 Suppl 2):iv1-iv99. doi:10.1093/neuonc/noad149

3. Lapointe S, Perry A, Butowski NA. Primary brain tumours in adults. Lancet. 2018;392(10145):432-46. doi:10.1016/S0140-6736(18)30990-5

4. Achrol AS, Rennert RC, Anders C, Soffietti R, Ahluwalia MS, Nayak L, et al. Brain metastases. Nat Rev Dis Primers. 2019;5(1):5. doi:10.1038/s41572-018-0055-y

5. Louis DN, Perry A, Wesseling P, Brat DJ, Cree IA, Figarella-Branger D, et al. The 2021 WHO Classification of Tumors of the Central Nervous System: a summary. Neuro Oncol. 2021;23(8):1231-51. doi:10.1093/neuonc/noab106

6. Brennan CW, Verhaak RG, McKenna A, Campos B, Noushmehr H, Salama SR, et al. The somatic genomic landscape of glioblastoma. Cell. 2013;155(2):462-77. doi:10.1016/j.cell.2013.09.034

7. Chen H, Judkins J, Thomas C, Wu M, Khoury L, Benjamin CG, et al. Mutant IDH1 and seizures in patients with glioma. Neurology. 2017;88(19):1805-13. doi:10.1212/WNL.0000000000003911

8. Ogasawara C, Philbrick BD, Adamson DC. Meningioma: a review of epidemiology, pathology, diagnosis, treatment, and future directions. Biomedicines. 2021;9(3):319. doi:10.3390/biomedicines9030319

9. Madhusoodanan S, Ting MB, Farah T, Ugur U. Psychiatric aspects of brain tumors: a review. World J Psychiatry. 2015;5(3):273-85. doi:10.5498/wjp.v5.i3.273

10. American Psychiatric Association. Diagnostic and statistical manual of mental disorders. 5th ed., text rev. Washington (DC): American Psychiatric Association Publishing; 2022. doi:10.1176/appi.books.9780890425787

11. World Health Organization. International Classification of Diseases for Mortality and Morbidity Statistics, 11th Revision (ICD-11). Geneva: World Health Organization; 2022. Available from: https://icd.who.int/browse/mms/en

12. Filley CM, Kleinschmidt-DeMasters BK. Neurobehavioral presentations of brain neoplasms. West J Med. 1995;163(1):19-25.

13. Bunevicius A, Deltuva VP, Deltuviene D, Tamasauskas A, Bunevicius R. Brain lesions manifesting as psychiatric disorders: eight cases. CNS Spectr. 2008;13(11):950-8. doi:10.1017/s1092852900014000

14. Gupta RK, Kumar R. Benign brain tumours and psychiatric morbidity: a 5-years retrospective data analysis. Aust N Z J Psychiatry. 2004;38(5):316-9. doi:10.1080/j.1440-1614.2004.01357.x

15. Gyawali S, Sharma P, Mahapatra A. Meningioma and psychiatric symptoms: an individual patient data analysis. Asian J Psychiatr. 2019;42:94-103. doi:10.1016/j.ajp.2019.03.029

16. Blackman G, Neri G, Al-Doori O, Teixeira-Dias M, Mazumder A, Pollak TA, et al. Prevalence of neuroradiological abnormalities in first-episode psychosis: a systematic review and meta-analysis. JAMA Psychiatry. 2023;80(10):1047-54. doi:10.1001/jamapsychiatry.2023.2225

17. Graus F, Titulaer MJ, Balu R, Benseler S, Bien CG, Cellucci T, et al. A clinical approach to diagnosis of autoimmune encephalitis. Lancet Neurol. 2016;15(4):391-404. doi:10.1016/S1474-4422(15)00401-9

18. Buday J, Albrecht J, Mareš T, Podgorná G, Horáčková K, Kališová L, et al. Brain tumors and electroconvulsive therapy: a literature overview of the last 80 years. Front Neurol. 2020;11:723. doi:10.3389/fneur.2020.00723

19. Melmed S, Casanueva FF, Hoffman AR, Kleinberg DL, Montori VM, Schlechte JA, et al. Diagnosis and treatment of hyperprolactinemia: an Endocrine Society clinical practice guideline. J Clin Endocrinol Metab. 2011;96(2):273-88. doi:10.1210/jc.2010-1692

20. Madhusoodanan S, Opler MG, Moise D, Gordon J, Danan DM, Sinha A, et al. Brain tumor location and psychiatric symptoms: is there any association? A meta-analysis of published case studies. Expert Rev Neurother. 2010;10(10):1529-36. doi:10.1586/ern.10.94

21. Padmanabhan JL, Cooke D, Joutsa J, Siddiqi SH, Ferguson M, Darby RR, et al. A human depression circuit derived from focal brain lesions. Biol Psychiatry. 2019;86(10):749-58. doi:10.1016/j.biopsych.2019.07.023

22. Mitrica M, Plesa A, Sirbu OM, Vasiliu O. Multinodular and vacuolating neuronal tumor – challenges and perspectives. Rom J Mil Med. 2025;128(1):10-6. doi:10.55453/rjmm.2025.128.1.2

23. Graus F, Vogrig A, Muñiz-Castrillo S, Antoine JG, Desestret V, Dubey D, et al. Updated diagnostic criteria for paraneoplastic neurologic syndromes. Neurol Neuroimmunol Neuroinflamm. 2021;8(4):e1014. doi:10.1212/NXI.0000000000001014

24. Mainio A, Hakko H, Niemelä A, Koivukangas J, Räsänen P. Depression and functional outcome in patients with brain tumors: a population-based 1-year follow-up study. J Neurosurg. 2005;103(5):841-7. doi:10.3171/jns.2005.103.5.0841

25. Robert P, Lanctôt KL, Agüera-Ortiz L, Aalten P, Bremond F, Defrancesco M, et al. Is it time to revise the diagnostic criteria for apathy in brain disorders? The 2018 international consensus group. Eur Psychiatry. 2018;54:71-6. doi:10.1016/j.eurpsy.2018.07.008

26. Marin RS, Biedrzycki RC, Firinciogullari S. Reliability and validity of the Apathy Evaluation Scale. Psychiatry Res. 1991;38(2):143-62. doi:10.1016/0165-1781(91)90040-v

27. Meyers CA, Weitzner MA, Valentine AD, Levin VA. Methylphenidate therapy improves cognition, mood, and function of brain tumor patients. J Clin Oncol. 1998;16(7):2522-7. doi:10.1200/JCO.1998.16.7.2522

28. Boele FW, Douw L, de Groot M, van Thuijl HF, Cleijne W, Heimans JJ, et al. The effect of modafinil on fatigue, cognitive functioning, and mood in primary brain tumor patients: a multicenter randomized controlled trial. Neuro Oncol. 2013;15(10):1420-8. doi:10.1093/neuonc/not102

29. Huang J, Zeng C, Xiao J, Zhao D, Tang H, Wu H, et al. Association between depression and brain tumor: a systematic review and meta-analysis. Oncotarget. 2017;8(55):94932-43. doi:10.18632/oncotarget.19843

30. Rooney AG, Carson A, Grant R. Depression in cerebral glioma patients: a systematic review of observational studies. J Natl Cancer Inst. 2011;103(1):61-76. doi:10.1093/jnci/djq458

31. Litofsky NS, Farace E, Anderson F, Meyers CA, Huang W, Laws ER, et al. Depression in patients with high-grade glioma: results of the Glioma Outcomes Project. Neurosurgery. 2004;54(2):358-66. doi:10.1227/01.neu.0000103450.94724.a2

32. Arnold SD, Forman LM, Brigidi BD, Carter KE, Schweitzer HA, Quinn HE, et al. Evaluation and characterization of generalized anxiety and depression in patients with primary brain tumors. Neuro Oncol. 2008;10(2):171-81. doi:10.1215/15228517-2007-057

33. Goebel S, Stark AM, Kaup L, von Harscher M, Mehdorn HM. Distress in patients with newly diagnosed brain tumours. Psychooncology. 2011;20(6):623-30. doi:10.1002/pon.1958

34. Gathinji M, McGirt MJ, Attenello FJ, Chaichana KL, Than K, Olivi A, et al. Association of preoperative depression and survival after resection of malignant brain astrocytoma. Surg Neurol. 2009;71(3):299-303. doi:10.1016/j.surneu.2008.07.016

35. Shi C, Lamba N, Zheng LJ, Cote D, Regestein QR, Liu CM, et al. Depression and survival of glioma patients: a systematic review and meta-analysis. Clin Neurol Neurosurg. 2018;172:8-19. doi:10.1016/j.clineuro.2018.06.016

36. Mugge L, Mansour TR, Crippen M, Alam Y, Schroeder J. Depression and glioblastoma, complicated concomitant diseases: a systemic review of published literature. Neurosurg Rev. 2020;43(2):497-511. doi:10.1007/s10143-018-1017-2

37. Zaorsky NG, Zhang Y, Tuanquin L, Bluethmann SM, Park HS, Chinchilli VM. Suicide among cancer patients. Nat Commun. 2019;10(1):207. doi:10.1038/s41467-018-08170-1

38. Saad AM, Elmatboly AM, Gad MM, Al-Husseini MJ, Jazieh KA, Alzuabi MA, et al. Association of brain cancer with risk of suicide. JAMA Netw Open. 2020;3(5):e203862. doi:10.1001/jamanetworkopen.2020.3862

39. Tiemensma J, Biermasz NR, Middelkoop HA, van der Mast RC, Romijn JA, Pereira AM. Increased prevalence of psychopathology and maladaptive personality traits after long-term cure of Cushing's disease. J Clin Endocrinol Metab. 2010;95(10):E129-41. doi:10.1210/jc.2010-0512

40. Rooney AG, McNamara S, Mackinnon M, Fraser M, Rampling R, Carson A, et al. Screening for major depressive disorder in adults with cerebral glioma: an initial validation of 3 self-report instruments. Neuro Oncol. 2013;15(1):122-9. doi:10.1093/neuonc/nos282

41. Sutcliffe LM, Lincoln NB. The assessment of depression in aphasic stroke patients: the development of the Stroke Aphasic Depression Questionnaire. Clin Rehabil. 1998;12(6):506-13. doi:10.1191/026921598672167702

42. Benaim C, Cailly B, Perennou D, Pelissier J. Validation of the aphasic depression rating scale. Stroke. 2004;35(7):1692-6. doi:10.1161/01.STR.0000130591.95710.20

43. Kappen PR, Kakar E, Dirven CMF, van der Jagt M, Klimek M, Osse RJ, et al. Delirium in neurosurgery: a systematic review and meta-analysis. Neurosurg Rev. 2022;45(1):329-41. doi:10.1007/s10143-021-01619-w

44. Tentor Z, Finnemore A, Miller PJ, Davis J, Juarez Martinez E, Lindvall C, et al. Occurrence rates of delirium in brain tumor patients: a systematic review and meta-analysis. Cancers (Basel). 2025;17(12):1998. doi:10.3390/cancers17121998

45. Yoo J, Joo B, Park J, Park HH, Park M, Ahn SJ, et al. Delirium-related factors and their prognostic value in patients undergoing craniotomy for brain metastasis. Front Neurol. 2022;13:988293. doi:10.3389/fneur.2022.988293

46. Inouye SK, van Dyck CH, Alessi CA, Balkin S, Siegal AP, Horwitz RI. Clarifying confusion: the confusion assessment method. A new method for detection of delirium. Ann Intern Med. 1990;113(12):941-8. doi:10.7326/0003-4819-113-12-941

47. Roth P, Wick W, Weller M. Steroids in neurooncology: actions, indications, side-effects. Curr Opin Neurol. 2010;23(6):597-602. doi:10.1097/WCO.0b013e32833e5a5d

48. Dietrich J, Rao K, Pastorino S, Kesari S. Corticosteroids in brain cancer patients: benefits and pitfalls. Expert Rev Clin Pharmacol. 2011;4(2):233-42. doi:10.1586/ecp.11.1

49. Warrington TP, Bostwick JM. Psychiatric adverse effects of corticosteroids. Mayo Clin Proc. 2006;81(10):1361-7. doi:10.4065/81.10.1361

50. Englot DJ, Chang EF, Vecht CJ. Epilepsy and brain tumors. Handb Clin Neurol. 2016;134:267-85. doi:10.1016/B978-0-12-802997-8.00016-5

51. Glantz MJ, Cole BF, Forsyth PA, Recht LD, Wen PY, Chamberlain MC, et al. Practice parameter: anticonvulsant prophylaxis in patients with newly diagnosed brain tumors. Report of the Quality Standards Subcommittee of the American Academy of Neurology. Neurology. 2000;54(10):1886-93. doi:10.1212/wnl.54.10.1886

52. Walbert T, Harrison RA, Schiff D, Avila EK, Chen M, Kandula P, et al. SNO and EANO practice guideline update: anticonvulsant prophylaxis in patients with newly diagnosed brain tumors. Neuro Oncol. 2021;23(11):1835-44. doi:10.1093/neuonc/noab152

53. Josephson CB, Engbers JDT, Jette N, Patten SB, Singh S, Sajobi TT, et al. Prediction tools for psychiatric adverse effects after levetiracetam prescription. JAMA Neurol. 2019;76(4):440-6. doi:10.1001/jamaneurol.2018.4561

54. Abraira L, Salas-Puig J, Quintana M, Seijo-Raposo IM, Santamarina E, Fonseca E, et al. Overnight switch from levetiracetam to brivaracetam. Safety and tolerability. Epilepsy Behav Rep. 2021;16:100504. doi:10.1016/j.ebr.2021.100504

55. Weller M, Gorlia T, Cairncross JG, van den Bent MJ, Mason W, Belanger K, et al. Prolonged survival with valproic acid use in the EORTC/NCIC temozolomide trial for glioblastoma. Neurology. 2011;77(12):1156-64. doi:10.1212/WNL.0b013e31822f02e1

56. Happold C, Gorlia T, Chinot O, Gilbert MR, Nabors LB, Wick W, et al. Does valproic acid or levetiracetam improve survival in glioblastoma? A pooled analysis of prospective clinical trials in newly diagnosed glioblastoma. J Clin Oncol. 2016;34(7):731-9. doi:10.1200/JCO.2015.63.6563

57. Vecht CJ, Wagner GL, Wilms EB. Interactions between antiepileptic and chemotherapeutic drugs. Lancet Neurol. 2003;2(7):404-9. doi:10.1016/s1474-4422(03)00435-6

58. Fernandez A, Brada M, Zabuliene L, Karavitaki N, Wass JA. Radiation-induced hypopituitarism. Endocr Relat Cancer. 2009;16(3):733-72. doi:10.1677/ERC-08-0231

59. Bancos I, Nannenga MR, Bostwick JM, Silber MH, Erickson D, Nippoldt TB. Impulse control disorders in patients with dopamine agonist-treated prolactinomas and nonfunctioning pituitary adenomas: a case-control study. Clin Endocrinol (Oxf). 2014;80(6):863-8. doi:10.1111/cen.12375

60. Stupp R, Mason WP, van den Bent MJ, Weller M, Fisher B, Taphoorn MJ, et al. Radiotherapy plus concomitant and adjuvant temozolomide for glioblastoma. N Engl J Med. 2005;352(10):987-96. doi:10.1056/NEJMoa043330

61. Stupp R, Taillibert S, Kanner A, Read W, Steinberg D, Lhermitte B, et al. Effect of tumor-treating fields plus maintenance temozolomide vs maintenance temozolomide alone on survival in patients with glioblastoma: a randomized clinical trial. JAMA. 2017;318(23):2306-16. doi:10.1001/jama.2017.18718

62. Mellinghoff IK, van den Bent MJ, Blumenthal DT, Touat M, Peters KB, Clarke J, et al. Vorasidenib in IDH1- or IDH2-mutant low-grade glioma. N Engl J Med. 2023;389(7):589-601. doi:10.1056/NEJMoa2304194

63. Weller M, van den Bent M, Preusser M, Le Rhun E, Tonn JC, Minniti G, et al. EANO guidelines on the diagnosis and treatment of diffuse gliomas

of adulthood. Nat Rev Clin Oncol. 2021;18(3):170-86. doi:10.1038/s41571-020-00447-z

64. Goldbrunner R, Stavrinou P, Jenkinson MD, Sahm F, Mawrin C, Weber DC, et al. EANO guideline on the diagnosis and management of meningiomas. Neuro Oncol. 2021;23(11):1821-34. doi:10.1093/neuonc/noab150

65. Taphoorn MJ, Klein M. Cognitive deficits in adult patients with brain tumours. Lancet Neurol. 2004;3(3):159-68. doi:10.1016/S1474-4422(04)00680-5

66. Brown PD, Pugh S, Laack NN, Wefel JS, Khuntia D, Meyers C, et al. Memantine for the prevention of cognitive dysfunction in patients receiving whole-brain radiotherapy: a randomized, double-blind, placebo-controlled trial. Neuro Oncol. 2013;15(10):1429-37. doi:10.1093/neuonc/not114

67. Brown PD, Gondi V, Pugh S, Tome WA, Wefel JS, Armstrong TS, et al. Hippocampal avoidance during whole-brain radiotherapy plus memantine for patients with brain metastases: phase III trial NRG Oncology CC001. J Clin Oncol. 2020;38(10):1019-29. doi:10.1200/JCO.19.02767

68. Beevers Z, Hussain S, Boele FW, Rooney AG. Pharmacological treatment of depression in people with a primary brain tumour. Cochrane Database Syst Rev. 2020;7(7):CD006932. doi:10.1002/14651858.CD006932.pub4

69. Alper K, Schwartz KA, Kolts RL, Khan A. Seizure incidence in psychopharmacological clinical trials: an analysis of Food and Drug Administration (FDA) summary basis of approval reports. Biol Psychiatry. 2007;62(4):345-54. doi:10.1016/j.biopsych.2006.09.023

70. Laporte S, Chapelle C, Caillet P, Beyens MN, Bellet F, Delavenne X, et al. Bleeding risk under selective serotonin reuptake inhibitor (SSRI) antidepressants: a meta-analysis of observational studies. Pharmacol Res. 2017;118:19-32. doi:10.1016/j.phrs.2016.08.017

71. Leth-Møller KB, Hansen AH, Torstensson M, Andersen SE, Ødum L, Gislasson G, et al. Antidepressants and the risk of hyponatremia: a Danish register-based population study. BMJ Open. 2016;6(5):e011200. doi:10.1136/bmjopen-2016-011200

72. Vasiliu O. Current evidence and future perspectives in the exploration of sleep-related eating disorder – a systematic literature review. Front Psychiatry. 2024;15:1393337. doi:10.3389/fpsyt.2024.1393337

73. Manea MM, Dragos D, Ghenu MI, Enache II, Stoican IC, Ciulavu C, et al. The neurocardiogenic impact of ischemic stroke: intricacies of cardiac enzymes and the vegetative system. Rom J Mil Med. 2025;128(1):36-42. doi:10.55453/rjmm.2025.128.1.5

74. Maltbie AA, Wingfield MS, Volow MR, Weiner RD, Sullivan JL, Cavenar JO. Electroconvulsive therapy in the presence of brain tumor. Case reports and an evaluation of risk. J Nerv Ment Dis. 1980;168(7):400-5. doi:10.1097/00005053-198007000-00002

75. Rapp SR, Case LD, Peiffer A, Naughton MM, Chan MD, Stieber VW, et al. Donepezil for irradiated brain tumor survivors: a phase III randomized placebo-controlled clinical trial. J Clin Oncol. 2015;33(15):1653-9. doi:10.1200/JCO.2014.58.4508

76. Boele FW, Klein M, Verdonck-de Leeuw IM, Cuijpers P, Heimans JJ, Snijders TJ, et al. Internet-based guided self-help for glioma patients with depressive symptoms: a randomized controlled trial. J Neurooncol. 2018;137(1):191-203. doi:10.1007/s11060-017-2712-5

77. Boele FW, Rooney AG, Bulbeck H, Sherwood P. Interventions to help support caregivers of people with a brain or spinal cord tumour. Cochrane Database Syst Rev. 2019;7(7):CD012582. doi:10.1002/14651858.CD012582.pub2

78. Gehring K, Sitskoorn MM, Gundy CM, Sikkes SA, Klein M, Postma TJ, et al. Cognitive rehabilitation in patients with gliomas: a randomized, controlled trial. J Clin Oncol. 2009;27(22):3712-22. doi:10.1200/JCO.2008.20.5765

79. Meyers CA, Hess KR, Yung WK, Levin VA. Cognitive function as a predictor of survival in patients with recurrent malignant glioma. J Clin Oncol. 2000;18(3):646-50. doi:10.1200/JCO.2000.18.3.646

80. Meyers CA, Hess KR. Multifaceted end points in brain tumor clinical trials: cognitive deterioration precedes MRI progression. Neuro Oncol. 2003;5(2):89-95. doi:10.1093/neuonc/5.2.89

81. Pace A, Dirven L, Koekkoek JAF, Golla H, Fleming J, Rudà R, et al. European Association for Neuro-Oncology (EANO) guidelines for palliative care in adults with glioma. Lancet Oncol. 2017;18(6):e330-40. doi:10.1016/S1470-2045(17)30345-5

82. Triebel KL, Martin RC, Nabors LB, Marson DC. Medical decision-making capacity in patients with malignant glioma. Neurology. 2009;73(24):2086-92. doi:10.1212/WNL.0b013e3181c67bce

83. Mukaino M, Aguiar Branco C, Alghwiri A, Amato S, Kontaxakis A, Berteanu M, et al. Clinical functioning information tool - coronavirus disease 2019 (ClinFIT COVID-19): psychometric evaluation and development of an interval-scaled functioning score across the care continuum. J Rehabil Med. 2025;57:jrm43227. doi:10.2340/jrm.v57.43227

https://doi.org/10.55453/rjmm.2026.129.6.9

ARTICLE / PERSPECTIVE

Rethinking Interleukin-11 in Metabolic Liver Disease: A Critical Reappraisal of Biomarker Directionality

Ion Mereuță[1], Diana Mihaela Ciuc[2,3], Cristina Octaviana Daia[3,4], Madalina Codruta Verenca[*,5], Vladimir Cărăuș[1], Ion Bălan[1], Nicolae Roșca[1], Valeriu-Gabi Dincă[*,2,3], Cristian Daniel Marica[3], and Gabriel Petre Gorecki[2,3,6]

[1] Moldova State University, Institute of Physiology and Sanocreatology, MD-2028, Chișinău, Republica Moldova
[2] Faculty of Medicine, Titu Maiorescu University, 031593, Bucharest, Romania
[3] CF2 Clinical Hospital, 011464 Bucharest, Romania
[4] Faculty of Medicine, Carol Davila University of Medicine and Pharmacy, 050474, Bucharest, Romania;
[5] Research Center in the Medical-Pharmaceutical Field, Medicine and Pharmacy Faculty, "Dunărea de Jos" University of Galați, 800010 Galați, Romania
[6] National Institute for Research and Development in Microtechnologies, 077190, Voluntari, Ilfov, Romania
*Correspondence : MCV, madalinacodrutaverenca@gmail.com; VGD, dincagaby@yahoo.com

Abstract: Multi-target phytotherapeutic and nutraceutical interventions have been proposed as complementary strategies in metabolic dysfunction-associated steatotic liver disease (MASLD), yet the interpretation of treatment-associated changes in interleukin-11 (IL-11) remains uncertain. Historically associated with tissue protection and regeneration, IL-11 has sometimes been regarded as a potentially favorable biomarker; however, recent evidence challenges this interpretation. This Perspective critically reappraises the biological role of IL-11 in metabolic liver disease. A narrative critical appraisal was integrated with evidence-informed mapping of a representative twelve-component phytotherapeutic formula onto processes implicated in hepatic IL-11 induction. Current evidence links hepatic IL-11 signaling through the interleukin-11 receptor alpha (IL-11Rα)/gp130 complex to lipotoxic and oxidative stress, hepatocyte injury, hepatic stellate-cell activation, and fibrogenesis, while cross-sectional human data associate circulating IL-11 with fibrosis severity in MASLD. Four competing, not necessarily mutually exclusive, hypotheses are proposed: upstream suppression (H1), adaptive rise (H2), extrahepatic/off-axis effects (H3), and null/analytical variability (H4), generating testable predictions regarding IL-11 trajectories and biomarker relationships. A treatment-associated increase in circulating IL-11 should therefore not be interpreted a priori as a favorable regenerative response without independent evidence of reduced hepatic injury or fibrogenic activity. A staged validation strategy is proposed to prospectively distinguish among these interpretations.

Keywords: interleukin-11; metabolic dysfunction-associated steatotic liver disease; hepatic fibrosis; oxidative stress; biomarkers; phytotherapy; nutraceuticals

INTRODUCTION

The problem this article addresses

Metabolic dysfunction-associated steatotic liver disease (MASLD) is the most prevalent chronic liver disease worldwide and involves interacting metabolic, oxidative, inflammatory, and fibrogenic processes that drive hepatocellular injury and disease progression [1–6]. This complex pathophysiology has stimulated interest in multi-target approaches, including phytotherapeutic and nutraceutical interventions as adjuncts to conventional management. Several compounds used in such interventions, including curcumin, silymarin, and dietary polyphenols, have been investigated in clinical studies and systematic reviews [7–10].

A key challenge is the interpretation of biomarkers used to characterize treatment-associated responses. Interleukin-11 (IL-11), historically associated with tissue protection and regeneration, has sometimes been interpreted as a potentially favorable biomarker, with increased circulating concentrations attributed to

Citation: Mereuță I, Ciuc DM, Daia CO, Verenca MC, Cărăuș V, Bălan I, et al. *Rethinking Interleukin-11 in Metabolic Liver Disease: A Critical Reappraisal of Biomarker Directionality.* R. J. Mil. Med. 2026, CXXIX(6): 709-724. https://doi.org/10.55453/rjmm.2026.129.6.9

Academic Editor: Octavian Vasiliu

Received: 03 October 2026
Revised: 27 October 2026
Accepted: 01 November 2026

regenerative activity. However, recent species-matched experimental studies and emerging human evidence challenge this interpretation by implicating hepatic IL-11 signaling in lipotoxic injury, oxidative stress, hepatic stellate-cell activation, and fibrogenesis.

This Perspective examines this discrepancy without seeking to establish the efficacy of a specific formulation. We ask whether attenuation of processes associated with hepatic injury is accompanied by reduced hepatic IL-11 induction and whether such changes are reflected in circulating IL-11 concentrations. We therefore propose a conceptual framework of competing, not necessarily mutually exclusive, hypotheses for treatment-associated IL-11 dynamics.

Why the IL-11 activity pattern matters

The direction and temporal pattern of changes in circulating IL-11 are central to its interpretation as a potential response biomarker. If increased IL-11 is assumed to reflect regenerative activity, rising concentrations may be interpreted as favorable. Conversely, if hepatic IL-11 induction in MASLD occurs downstream of lipotoxic, oxidative, and transforming growth factor beta 1 (TGF-β1)-associated signaling, increased circulating IL-11 may be compatible with persistent hepatic stress and activation of pathways involved in hepatocellular injury and fibrogenesis. Thus, the same biomarker trajectory may support contrasting biological interpretations.

However, hepatic IL-11 signaling and circulating IL-11 concentrations are not interchangeable measures. Circulating IL-11 may reflect hepatic and extrahepatic production, release kinetics, distribution, clearance, and biological and analytical variability. An isolated change in circulating IL-11 therefore cannot be interpreted as a surrogate for hepatic pathway activity or used to guide clinical decisions. Its significance should be evaluated alongside markers of liver injury, oxidative and inflammatory activity, fibrosis-related measures, temporal response patterns, and biomarker variability. These relationships must be characterized before circulating IL-11 can be meaningfully evaluated as a response biomarker in prospective studies of metabolic liver disease.

Contribution of this work

This Perspective translates current evidence and uncertainties into four competing, but not necessarily mutually exclusive, hypotheses for treatment-associated IL-11 dynamics. We present an evidence-informed framework linking upstream processes to hepatic IL-11 induction and propose a prospective validation strategy incorporating predefined outcomes, explicit requirements for IL-11 measurement, and a staged study design. The aim is not to assign a priori biological meaning to a specific IL-11 trajectory, but to establish testable criteria for evaluating alternative interpretations prospectively.

MATERIALS AND METHODS

Approach to the narrative appraisal

This Perspective integrates selected experimental and clinical evidence with a methodological analysis of IL-11 biomarker interpretation. Targeted literature searches were conducted through 29 September 2026 using PubMed and relevant publisher sources. Search terms combined IL-11/IL11 with MASLD, nonalcoholic fatty liver disease (NAFLD), nonalcoholic steatohepatitis (NASH), circulating, serum, biomarker, and component-specific liver-disease terms, supplemented by citation tracing. Sources were selected for their relevance to hepatic IL-11 biology, circulating IL-11 measurement, and the mechanisms addressed in the proposed framework.

Throughout the appraisal, direct experimental findings are distinguished from extrapolations and assumptions regarding dose, exposure, and clinical applicability. The Scale for the Assessment of Narrative Review Articles (SANRA) domains informed the structure and reporting of the narrative appraisal [11].

Evidence Mapping Approach

The twelve components of the patent-pending encapsulated formulation developed by four of the authors (I.M., V.C., I.B., and N.R.) were mapped onto the upstream biological nodes defined in the proposed mechanistic framework. The formulation was examined because it was used in the clinical observation that prompted the present hypothesis, rather than as an independently selected representative formulation. For each component, evidence was appraised according to study design, mechanistic directness, studied exposure, and applicability to the formulation. Evidence sources included human randomized trials and meta-analyses, human non-randomized studies, animal experiments, in vitro studies, and mechanistic evidence. Constituent-to-node relationships were classified as direct, indirect, supported at the compound-class level, or extrapolated from non-hepatic experimental systems. This author-defined approach was used as an evidence-mapping framework and not as a validated certainty-of-evidence grading system.

RESULTS

1. Reappraisal of Hepatic IL-11 Biology

The historical view of IL-11 as a hepatoprotective cytokine has been challenged by studies using species-matched reagents and genetic or pharmacological loss-of-function approaches. In the experimental systems examined, these studies support a contrasting role for endogenous IL-11 signaling in liver injury [12–14].

1.1. Origins of the Regenerative Interpretation

Early interpretations of IL-11 as a tissue-protective and regenerative cytokine arose from several observations. IL-11 was initially characterized for its hematopoietic effects, and recombinant human IL-11 (rhIL-11) was subsequently developed as a thrombopoietic agent. In addition, IL-11 signals through a gp130-containing receptor complex, linking it to pathways involved in hepatic acute-phase responses and regeneration. Finally, IL-11 expression is strongly induced in experimental liver injury, while rhIL-11 administration was reported to reduce injury in rodents. Together, these findings supported the hypothesis that IL-11 represented an endogenous protective response that could be therapeutically enhanced.

This interpretation, however, requires reconsideration. Increased expression of a mediator during tissue injury does not establish a protective function and may also reflect injury progression or maladaptive repair. Moreover, the apparent protective effects of exogenous rhIL-11 in mice did not demonstrate that endogenous, species-matched IL-11 exerted the same biological effects.

1.2. The Species-Mismatch Finding

A major change in the interpretation of IL-11 biology came from recognizing important differences between human and mouse IL-11. In mouse hepatocytes, species-matched mouse IL-11 activated injury-related ERK and JNK signaling and caspase-3 cleavage, whereas recombinant human IL-11 (rhIL-11) did not produce the same effects [12]. Similar findings were observed in experimental acetaminophen-induced liver injury.

However, earlier experimental studies reported findings consistent with hepatoprotective or regenerative effects of IL-11. Nishina et al. showed that oxidative stress induced hepatocyte IL-11 production and that IL-11 promoted STAT3-dependent compensatory proliferation in adjacent hepatocytes after acute liver injury. IL-11 receptor agonism also reduced acetaminophen-induced injury, whereas IL-11Rα deficiency aggravated it [15]. Other mouse studies reported protective effects of rhIL-11 in hepatic ischemia–reperfusion injury, including reduced hepatocellular injury, apoptosis, and inflammatory signaling [16,17].

The species-mismatch hypothesis provides a plausible explanation for some of these apparently conflicting findings, because human IL-11 and endogenous mouse IL-11 may not produce equivalent signaling responses in mouse hepatocytes [12]. However, species mismatch may not fully explain all discordant observations, particularly studies involving receptor agonism, genetic IL-11Rα deficiency, or different injury models. The available evidence therefore supports a context- and model-dependent interpretation rather than a universally protective or universally detrimental role for IL-11.

1.3. Genetic and Pharmacological Loss-of-Function Evidence

Loss-of-function studies provide further evidence against a regenerative role for endogenous hepatic IL-11 signaling. In acetaminophen-induced liver injury, hepatocyte-specific deletion of the **IL-11 receptor alpha gene (Il11ra)** or germline deletion of the **IL-11 gene (Il11)** protected mice and reduced JNK and ERK activation [12]. Pharmacological inhibition of IL-11 signaling also reduced liver injury and improved survival, even when treatment was delayed after acetaminophen overdose. Importantly, IL-11 inhibition increased markers of hepatocyte proliferation, suggesting enhanced rather than impaired regeneration [12].

Experimental models of metabolic liver disease support a similar interpretation. Inhibition of IL-11 signaling reduced hepatocyte death, inflammation, steatosis, and fibrosis in mouse models of NASH [13], while hepatocyte-specific IL-11 signaling has been implicated in lipotoxicity and progression from NAFLD to NASH [14]. Mechanistically, injured hepatocytes can release IL-11, which may amplify cellular injury through NADPH oxidase 4 (NOX4)-dependent oxidative stress, mitochondrial dysfunction, and JNK activation [12–14].

Together, these findings support a role for hepatic IL-11 signaling in hepatocellular injury and maladaptive repair in the experimental systems studied [12–14,18–20]. However, they do not establish circulating IL-11 as a quantitative surrogate for intrahepatic IL-11 activity.

1.4. Human Evidence and Its Limitations

Human evidence linking circulating IL-11 to MASLD severity remains limited and predominantly observational. In a cross-sectional study of 375 outpatients with MASLD, liver stiffness was significantly higher in individuals with detectable serum IL-11 than in those with undetectable levels. Controlled attenuation parameter (CAP) values did not differ significantly between groups, while detectable serum IL-11 was independently associated with the study-defined advanced-fibrosis category [21].

Three limitations are particularly relevant. First, the cross-sectional design demonstrates an association between detectable circulating IL-11 and non-invasive measures of fibrosis severity but cannot establish whether changes in IL-11 reflect changes in fibrosis or hepatic IL-11 signaling over time.

Second, the reported difference was primarily between detectable and undetectable IL-11 rather than across a continuous concentration range. The large proportion of samples below the assay detection threshold raises important questions about assay sensitivity and the reliability of longitudinal measurements.

Third, the association was primarily related to fibrosis rather than steatosis. These findings therefore provide limited evidence for predicting short-term changes in circulating IL-11 during interventions targeting metabolic dysfunction or steatosis, particularly in patients without advanced fibrosis.

1.5. Remaining Uncertainties

Although recent species-matched loss-of-function studies support a detrimental role for endogenous hepatic IL-11 signaling, earlier genetic, receptor-agonist, and ischemia–reperfusion studies reported protective or regenerative effects. These discrepancies may partly reflect species mismatch, experimental context, injury model, ligand or agonist used, dose, and timing, but they remain incompletely resolved. Against this background, four uncertainties are particularly relevant to the framework developed below.

First, the quantitative relationship between intrahepatic IL-11 activity and circulating IL-11 concentrations has not been established. Circulating IL-11 therefore cannot currently be considered a validated surrogate for hepatic IL-11 pathway activity.

Second, IL-11 is produced by multiple extrahepatic tissues and cell types. Circulating IL-11 is therefore not liver-specific, and treatment-associated changes may reflect extrahepatic production, distribution, or clearance in addition to hepatic processes. This uncertainty provides the basis for the extrahepatic/off-axis hypothesis developed later in this framework.

Third, IL-11 biology is tissue-, disease-, and context-dependent [18–20]. **The present framework is therefore restricted to evidence relevant to metabolic and experimental liver disease and should not be generalized to other physiological or pathological settings.** Fourth, our targeted appraisal did not identify prospective MASLD intervention studies examining whether individual changes in circulating IL-11 parallel changes in hepatic injury, oxidative stress, or fibrogenic activity. The expected trajectory of circulating IL-11 during an effective intervention therefore remains **a conditional, mechanism-dependent prediction rather than an established treatment-response pattern.** Given the narrative nature of the search, this finding should not be interpreted as evidence that such studies definitively do not exist.

2. Evidence-Informed Mechanistic Framework

2.1. Mechanistic Reframing of IL-11 Nutrigenomodulation

For the purposes of this Perspective, IL-11 nutrigenomodulation refers to the hypothesis that dietary bioactive compounds may influence biological processes involved in hepatic IL-11 induction or signaling. Based on the evidence reviewed above, this concept should not assume that a favorable intervention increases IL-11. Instead, we consider whether bioactive compounds may influence upstream processes associated with hepatic IL-11 activity, including lipotoxic and mitochondrial stress, oxidative stress, TGF-β1/SMAD signaling in hepatic stellate cells, inflammatory signaling, and gut-derived inflammatory stimuli.

Within this framework, attenuation of relevant upstream drivers may reduce hepatic IL-11 induction or signaling when these pathways are active in the biological context studied. However, changes in circulating IL-11 cannot be predicted directly from hepatic signaling because they may also depend on extrahepatic production, release, distribution, and clearance. Circulating IL-11 is therefore treated as a candidate downstream signal whose interpretation requires comparison with upstream biological changes and independent measures of hepatic injury and fibrogenic activity.

2.2. Definition of the Upstream Nodes

For analytical purposes, we define five interconnected biological nodes through which a multi-target intervention may influence processes related to hepatic IL-11 induction (Figure 1). These nodes differ in their proximity to IL-11 signaling and should not be interpreted as independent causal pathways. Together, they provide a framework encompassing metabolic, oxidative, profibrogenic, inflammatory, and gut-derived processes.

N1 — Lipotoxic and mitochondrial stress in hepatocytes. Free fatty-acid overload, mitochondrial dysfunction, and associated reactive oxygen species (ROS) generation can promote hepatocellular stress and IL-11 expression [5,6,14,18].

N2 — NOX4-derived oxidative stress. NOX4-dependent ROS generation is linked to IL-11 signaling and may form a feed-forward circuit in which oxidative stress promotes IL-11 induction and IL-11 signaling further enhances ROS generation [12,18]. N2 may therefore act both upstream and downstream of IL-11 signaling.

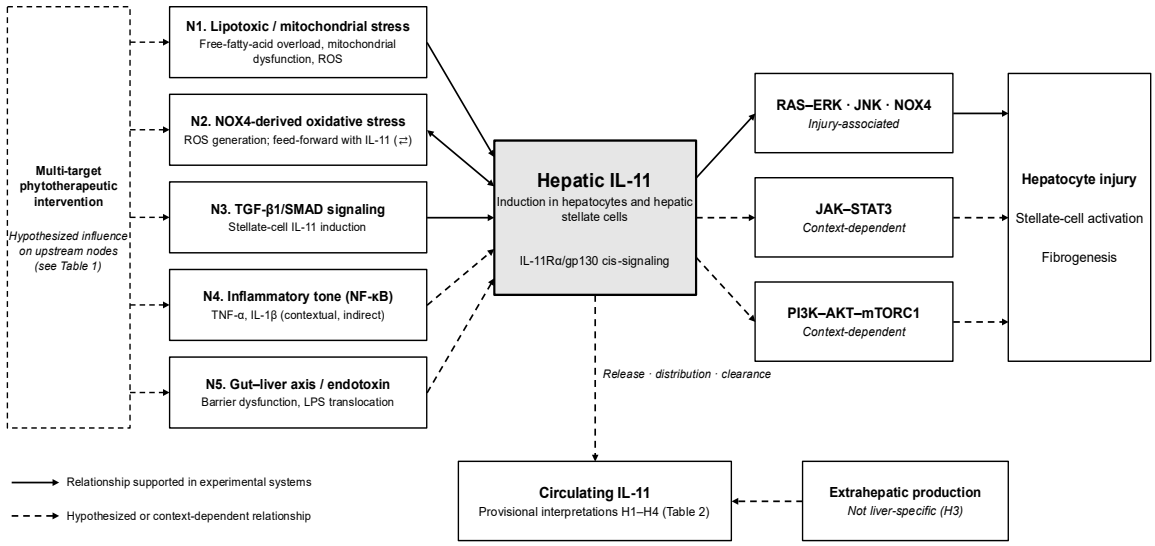
N3 — TGF-β1/SMAD signaling in hepatic stellate cells. TGF-β1 induces IL-11 expression in activated hepatic stellate cells, linking profibrogenic signaling to sustained IL-11 activity [13,18].

N4 — Inflammatory signaling and nuclear factor kappa B (NF-κB)-associated inflammatory tone. Proinflammatory mediators, including tumor necrosis factor alpha (TNF-α) and interleukin-1 beta (IL-1β), contribute to hepatic inflammation and interact with lipotoxic, oxidative, and profibrogenic pathways. Their relationship with IL-11 in this framework is considered primarily contextual and indirect [22].

N5 — Gut–liver axis and endotoxin exposure. Intestinal barrier dysfunction and translocation of microbial products, including lipopolysaccharide (LPS), can sustain hepatic inflammation and indirectly favor hepatic injury and IL-11 induction [3,4].

The proposed framework and the relationships among the five upstream nodes, hepatic IL-11 signaling, and downstream pathways are summarized in Figure 1.

Figure 1: Upstream determinants of hepatic IL-11 and hypothesized points of influence of a multi-target phytotherapeutic



Note: Five interconnected nodes (N1–N5) represent metabolic, oxidative, profibrogenic, inflammatory, and gut-derived processes that may converge on IL-11 induction in hepatocytes and hepatic stellate cells. IL-11Rα/gp130 cis-signaling is shown because no evidence of IL-11 trans-signaling was identified in the hepatocyte and NASH models examined [14]. The bidirectional relationship between N2 and hepatic IL-11 represents oxidative feed-forward amplification involving NOX4-derived ROS. Circulating IL-11 may reflect hepatic release, distribution, and clearance, as well as extrahepatic production, and therefore cannot be considered a direct surrogate for hepatic IL-11 activity. H1–H4 denote the provisional interpretations summarized in Table 2. Solid arrows indicate relationships supported in experimental systems; dashed arrows indicate hypothesized or context-dependent relationships. Abbreviations: AKT, protein kinase B; ERK, extracellular signal-regulated kinase; gp130, glycoprotein 130; IL-1β, interleukin-1 beta; IL-11, interleukin-11; IL-11Rα, interleukin-11 receptor alpha; JAK, Janus kinase; JNK, c-Jun N-terminal kinase; LPS, lipopolysaccharide; mTORC1, mechanistic target of rapamycin complex 1; NASH, nonalcoholic steatohepatitis; NF-κB, nuclear factor kappa B; NOX4, NADPH oxidase 4; PI3K, phosphoinositide 3-kinase; RAS, RAS family small GTPase; ROS, reactive oxygen species; SMAD, mothers against decapentaplegic homolog; STAT3, signal transducer and activator of transcription 3; TGF-β1, transforming growth factor beta 1; TNF-α, tumor necrosis factor alpha.

2.3. Constituent-to-Node Mapping and Evidence Appraisal

The twelve components of the patent-pending encapsulated formulation were mapped onto the upstream nodes defined above. Evidence varied substantially in study design, mechanistic directness, studied exposure, and applicability to the administered formulation. None of the available evidence establishes modulation of hepatic or circulating IL-11 by the complete formulation.

The formulation and complementary vegetable-based preparation were administered sequentially according to the protocol associated with the clinical observation described in Section 5. Full composition and administration details are provided in the Supplementary Material to ensure transparency and reproducibility.

Taxifolin, curcumin, and L-glutathione were specified as 98%, 95%, and 98%, respectively, whereas most botanical ingredients were characterized only by a 10:1 extract ratio. Because information on extraction solvents, standardization, and active-

compound content was unavailable, equivalence with standardized preparations or isolated compounds evaluated in published studies cannot be assumed.

The complementary vegetable-based preparation contained carrot, aronia or blueberries, dandelion root, chicory root, beetroot, dates, and ginger root. These components were mapped principally to N5 (dandelion and chicory), N1/N2 (anthocyanin-rich fruit and beetroot), and N4 (ginger). Evidence from randomized studies of ginger powder in NAFLD [23,24] cannot be directly extrapolated to fresh ginger root in this mixture, and aronia and blueberries were considered alternative rather than equivalent ingredients. Table 1 summarizes the constituent-to-node mapping together with the supporting evidence, studied exposures, and applicability to the administered formulation.

Table 1: Evidence-informed mapping of formula components to proposed upstream determinants of hepatic IL-11

Constituent (per capsule)	Node(s)	Evidence source	Measured outcome and node directness	Studied exposure	Applicability to formulation
Taxifolin 98%, 50 mg	N1, N2	Animal studies	Reduced oxidative stress and apoptosis in experimental hepatic injury [25,26]; IL-11 relationship extrapolated	Animal dosing	Human exposure and node/IL-11 effects unestablished
Curcumin 95%, 45 mg	N1, N3, N4	Human meta-analyses; in vitro studies	Liver biochemical outcomes [7]; TGF-β/SMAD effects in non-hepatic systems [27]; reduced ROS/steatosis with andrographolide in HepG2 cells [28]; node assignment partly indirect	~500–1500 mg/day; often bioavailability-enhanced [7,29]	Dose, preparation, and exposure equivalence unestablished
Silybum marianum extract (10:1), 45 mg	N1, N4	Human meta-analyses	Liver enzyme and metabolic outcomes in MASLD [7,8,30]; node assignment indirect	~140–800 mg/day standardized silymarin [7,8,30]	Extract mass not equivalent to standardized silymarin content
Rhaponticum carthamoides extract (10:1), 40 mg	N1	No direct study identified	Adaptogenic-class rationale; direct hepatic node or IL-11 evidence not identified	No supporting exposure identified	Applicability unestablished
Zingiber officinale extract (10:1), 40 mg	N4	Human randomized trials	Liver, inflammatory, and metabolic outcomes in NAFLD [23,24]; no IL-11 outcome	Ginger powder, 2 g/day for 12 weeks [23]	Powder exposure does not establish equivalence with this extract or regimen
Aronia melanocarpa extract (10:1), 35 mg	N1, N2	Human evidence, compound-class level	Polyphenol intervention evidence [9]; compound-class extrapolation without aronia-specific IL-11 evidence	Varied polyphenol preparations	Species, extract, and exposure equivalence unestablished
Cichorium intybus extract (10:1), 35 mg	N5	Mechanistic/compound-class evidence	Inulin-type fructan gut–liver rationale [3,4]; extract-specific effect unestablished	Gram-scale prebiotic exposure	Fructan content and corresponding exposure unknown
Andrographis paniculata extract (10:1), 35 mg	N1, N4	In vitro study	Andrographolide with curcumin reduced steatosis and ROS in HepG2 cells [28]; node assignment indirect	Cell-culture exposure	Andrographolide content and clinical exposure unknown
Glycyrrhiza glabra extract (10:1), 35 mg	N4	No direct study identified	Anti-inflammatory class rationale; direct node or IL-11 evidence not established	No supporting exposure identified	Active-compound content and exposure unestablished
Juglans regia extract (10:1), 30 mg	N1	No direct study identified	Phenolic-profile rationale; direct node or IL-11 evidence not established	No supporting exposure identified	Applicability unestablished
Phoenix dactylifera extract (10:1), 30 mg	—	No node-specific evidence	Nutritive component; no specific mechanistic claim	Not applicable	No IL-11 inference
L-glutathione 98%, 55 mg	N1, N2	Human uncontrolled pilot	Reduced ALT in NAFLD [31]; variable oral bioavailability/systemic effects [32,33]; node assignment indirect	300 mg/day [31]	Dose equivalence and node/IL-11 effects unestablished

Abbreviations: ALT, alanine aminotransferase; IL-11, interleukin-11; MASLD, metabolic dysfunction-associated steatotic liver disease; NAFLD, nonalcoholic fatty liver disease; ROS, reactive oxygen species; TGF-β, transforming growth factor beta.

2.4. Main Findings of the Evidence Mapping

Three main findings emerge from the evidence mapping. First, clinical evidence is concentrated around curcumin and silymarin, supported by meta-analyses in MASLD [7,8], and ginger, evaluated in randomized NAFLD trials [23,24]. These studies report biochemical, inflammatory, or metabolic outcomes but do not demonstrate IL-11 modulation. Evidence for the remaining components is predominantly indirect, compound-class, in vitro, animal, or inferential.

Second, the targeted appraisal identified no direct evidence that the complete formulation modulates hepatic or circulating IL-11 and no human clinical evidence directly demonstrating modulation of the TGF-β1/SMAD–IL-11 pathway represented by N3. Such an effect would therefore require two unverified steps: that the administered components modify the proposed upstream nodes at clinically relevant exposures, and that these changes produce a measurable alteration in hepatic or circulating IL-11.

Third, the complementary vegetable-based preparation principally maps to the gut–liver axis (N5) and to oxidative and metabolic processes (N1/N2). Because it was introduced after initiation of the encapsulated formulation, its independent contribution cannot be determined from the sequential regimen. Future studies should therefore separate the individual and combined effects of the two intervention components.

3. Competing Hypotheses and Their Provisional Predictions

The framework developed above generates four competing, but not necessarily mutually exclusive, explanations for intervention-associated changes in circulating IL-11. Their consistency with observed data can be evaluated prospectively by considering IL-11 direction and temporal pattern, covariation with hepatic and oxidative-stress biomarkers, treatment exposure and withdrawal, and reproducibility across repeated observations.

Two outcomes should be considered separately: the randomized treatment effect on circulating IL-11 and the within-person association between IL-11 and prespecified biochemical markers. Change-score associations require cautious interpretation because correlated measurement error, regression to the mean, and common temporal trends may distort apparent relationships (Supplementary Methods S5).

H1 — Upstream-Suppression Hypothesis

The intervention attenuates one or more upstream drivers of hepatic IL-11 induction, particularly the lipotoxic, oxidative, inflammatory, and gut-derived processes represented by N1, N2, N4, and N5. If this reduces hepatic IL-11 induction, circulating IL-11 would be expected to decline when hepatic production contributes substantially to circulating concentrations and extrahepatic production and clearance remain sufficiently stable.

H2 — Adaptive-Rise Hypothesis

Based on the historical regenerative interpretation of IL-11, an alternative hypothesis is that a favorable intervention produces a transient increase in circulating IL-11 during an adaptive or regenerative response. Under this model, IL-11 would rise despite biochemical improvement. Such a pattern would not, however, establish regeneration, because persistent profibrogenic signaling, altered clearance, extrahepatic production, and analytical effects remain alternative explanations.

H3 — Extrahepatic or Off-Axis Hypothesis

Changes in circulating IL-11 may arise partly from extrahepatic sources and therefore correlate weakly with hepatic IL-11 activity. Alternatively, intervention components may influence IL-11 or related signaling pathways outside the upstream nodes N1–N5. An extrahepatic interpretation requires positive source-related evidence rather than merely the absence of correlation with hepatic markers.

Exploratory assessment could incorporate prespecified systemic inflammatory measures or source-related measurements. Soluble IL-11Rα may be investigated, but its concentration alone neither localizes IL-11 production nor establishes functional trans-signaling, which was not supported in the hepatocyte and NASH models examined in reference [14].

H4 — Null/Analytical Hypothesis

Observed changes in circulating IL-11 may reflect assay imprecision, preanalytical variability, biological fluctuation, assay interference, or batch effects rather than an intervention-related biological response. This possibility is particularly relevant because reported circulating IL-11 concentrations vary across studies and assay platforms, and some measurements may fall near or below detection or quantification limits.

In one exploratory adult series, median serum IL-11 concentrations ranged from approximately 62 to 95 pg/mL, with 6.8% of measurements below the assay detection limit [34]. In a large MASLD cohort, the principal analyzable comparison was between detectable and undetectable IL-11 [21]. These observations do not define analytical error or a reference interval for MASLD but emphasize the need for caution when interpreting small absolute changes. Values in the 18–28 pg/mL range therefore require

platform-specific evaluation of assay precision, detection and quantification limits, sample handling, storage, freeze–thaw exposure, and within-subject variability.

Table 2 summarizes the directional, temporal, and reproducibility patterns that would be consistent with each hypothesis; none of these patterns independently establishes mechanism.

Table 2: Table 2. Provisional patterns consistent with the four hypotheses; no pattern independently establishes mechanism

Observation	H1: Upstream suppression	H2: Adaptive rise	H3: Extrahepatic/off-axis	H4: Null/analytical
Direction of IL-11 change	Decrease, conditional on hepatic contribution and stable clearance	Transient increase; regeneration not established	Either direction; source requires separate assessment	Either direction; random or systematic analytical effects
Within-person biomarker association	Possible positive association as IL-11 and injury/oxidative markers decrease	Possible negative association during biochemical improvement	Weak hepatic association may occur; source-related evidence required	No stable association with random error; interference may mimic one
Temporal relationship	Decline with or after upstream-marker improvement	Rise before or during improvement; biological meaning unresolved	May track an extrahepatic source or off-axis effect	Random fluctuation or systematic batch/exposure-related pattern
Repeated exposure/withdrawal	Reproducible pattern supports exposure association	Reproducible rise supports exposure association, not regenerative benefit	Reproducibility does not localize the source	Inconsistency supports noise; reproducibility does not exclude interference
Longer-term fibrosis measures	Lower IL-11 with stable/improved measures is compatible with H1 but not confirmatory	Absence of worsening does not establish regeneration	Absent association does not establish an extrahepatic source	No relationship or potentially misleading analytical association
IL-6/systemic context	Broader inflammatory improvement may accompany IL-11 decline	Divergence between IL-11 and IL-6 is nonspecific	Independent source/context evidence is required	Analytical effects require independent exclusion

Abbreviations: IL-6, interleukin-6; IL-11, interleukin-11; H1, upstream-suppression hypothesis; H2, adaptive-rise hypothesis; H3, extrahepatic or off-axis hypothesis; H4, null/analytical hypothesis.

No single observation can distinguish these hypotheses. Direction, biomarker covariation, temporal ordering, and repeated exposure/withdrawal can test consistency with H1 and H2 but cannot establish mechanism or regenerative benefit. H3 requires positive source-related evidence, whereas H4 requires explicit assessment of analytical and preanalytical factors.

IL-11 trajectories also need not be monotonic; transient or biphasic responses are biologically plausible. Prospective testing should therefore prioritize serial measurements and prespecified temporal patterns rather than a single baseline-to-follow-up change. Reproducibility across exposure and withdrawal periods strengthens evidence for an exposure-associated signal but, without analytical controls and independent pathway assessment, does not establish its biological mechanism.

4. Hypothesis-Generating Clinical Observation

A single anonymized clinical observation is presented solely as the observation that prompted the present hypothesis and not as evidence of efficacy, causality, or biomarker validity.

A 68-year-old man with a dysmetabolic profile and documented hepatic steatosis showed decreases in alanine aminotransferase (ALT; 98 to 39 U/L), aspartate aminotransferase (AST; 94 to 36 U/L), gamma-glutamyl transferase (GGT; 214 to 42 U/L), C-reactive protein (CRP; 8.2 to 3.1 mg/L), and malondialdehyde (MDA; 4.2 to 0.8 µmol/L), while circulating interleukin-11 (IL-11) increased from 18.0 to 28.0 pg/mL.

The retrospective records did not permit reliable reconstruction of the sampling interval and corresponding treatment phases, the biological matrix or analytical platform used for IL-11 measurement, the method used for MDA determination, or the imaging method and grading system used to characterize steatosis. The marked MDA change should therefore be interpreted with particular caution. Additional limitations include the absence of repeated IL-11 measurements and incomplete information on medication stability and other potential confounders.

These limitations preclude quantitative interpretation of the biomarker trajectories or attribution of the observed changes to the intervention. Accordingly, this observation is not used as evidence for any of the competing hypotheses; it serves only to define the question addressed by the prospective validation strategy proposed in Section 6.

5. Proposed Validation Strategy

5.1. Design Principles

The proposed strategy comprises three sequential stages, with progression conditional on the reliability and reproducibility of the preceding findings (Figure 2). The initial objective is not to establish clinical efficacy, but to determine whether circulating IL-11 can be measured reliably, whether it shows a reproducible intervention-associated trajectory, and whether that trajectory is consistent with H1–H4. Biomarker patterns alone cannot establish mechanism.

Stage 1 — Analytical and biological variability. A non-interventional study in 25–30 adults with MASLD at increased fibrosis risk is proposed to characterize analytical and within-subject variability under stable conditions. Participants should undergo four standardized fasting assessments over six weeks. Age-adjusted Fibrosis-4 Index (FIB-4) thresholds (≥1.3, or ≥2.0 in individuals aged >65 years) should prompt vibration-controlled transient elastography (VCTE); liver stiffness ≥8 kPa indicates increased fibrosis risk rather than a confirmed histological stage [35]. Duplicate IL-11 measurements, preferably within a single analytical run and kit lot for each participant, with a subset assessed on a second platform, should be used to estimate analytical variability, within-subject biological variability, quantification frequency, and the 95% reference change value (RCV). **The primary outcome is the within-subject variability of circulating IL-11 and the corresponding RCV. The proposed sample of 25–30 participants, each providing four repeated measurements, is intended as a precision-oriented feasibility sample for estimating within-subject variability and its uncertainty rather than for hypothesis testing; the resulting confidence intervals will determine whether the RCV is sufficiently precise for subsequent interventional use.**

Progression gate 1. Interventional testing should proceed only if assay precision, quantification frequency, and the precision of the estimated RCV are adequate for longitudinal interpretation. The IL-11 change described in Section 5 should not be treated as an expected effect size. Inadequate measurement performance should prompt assay refinement or an alternative biomarker strategy before intervention testing.

Stage 2 — Exposure/withdrawal feasibility and randomized N-of-1 series. Conditional on Stage 1, dense sampling during initial exposure and withdrawal should characterize onset, offset, reversibility, and potential carry-over. If the observed kinetics permit, 8–12 randomized N-of-1 trials are proposed, each comprising at least three paired active-treatment/placebo periods. The encapsulated formulation should be compared with matched placebo without the vegetable-based preparation, allowing the capsule intervention to be evaluated separately. Period and washout durations should be determined from observed intervention-associated kinetics and carry-over. The N-of-1 series should follow the CONSORT extension for N-of-1 trials [36]. **The primary outcome is the within-participant difference in circulating IL-11 between randomized active and placebo periods over a prespecified measurement window.**

This design reduces interindividual variability and allows assessment of within-person reproducibility across repeated randomized exposures. Participant-level estimates may be combined hierarchically to examine consistency across the series. If IL-11 kinetics are too slow or carry-over cannot be adequately controlled, a randomized parallel-group design with serial sampling should replace the N-of-1 approach. Successful placebo matching, including color, odor, and taste, should be formally assessed.

Progression gate 2. Progression should require an analytically credible intervention-associated signal, interpretable prespecified biomarker trajectories, and acceptable safety and feasibility. These findings may support exposure association and mechanistic consistency but cannot independently establish biological mechanism or clinical benefit.

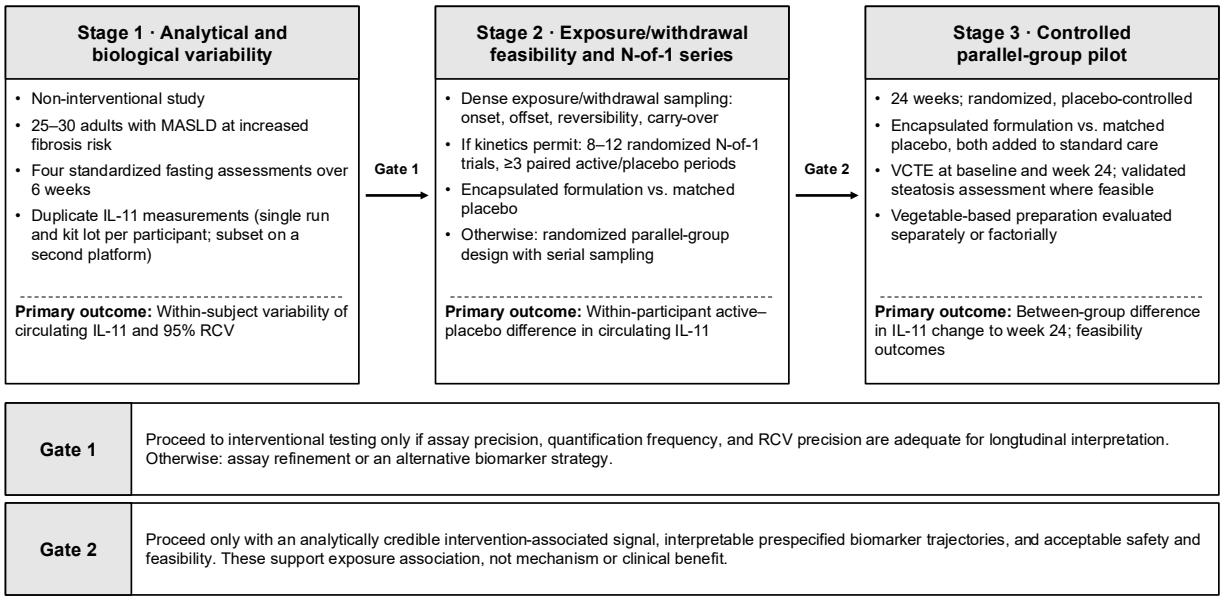
Stage 3 — Controlled parallel-group pilot. A 24-week randomized, placebo-controlled parallel-group pilot should compare the encapsulated formulation with matched placebo, both added to standard care. Concomitant treatment, dietary recommendations, physical activity, and relevant medications should be prospectively documented. VCTE should be performed at baseline and week 24, together with a validated assessment of hepatic steatosis where feasible. **The primary mechanistic outcome is the between-group difference in the change in circulating IL-11 from baseline to week 24; feasibility outcomes include recruitment, retention, adherence, and completeness of longitudinal biomarker assessment.**

Stage 3 is intended as a mechanistic feasibility pilot rather than a definitive efficacy trial. Its sample size should therefore be determined prospectively from the variance and intervention-associated IL-11 estimates obtained in Stages 1 and 2, together with predefined precision, recruitment, and retention criteria, rather than from an assumed clinical effect size.

The complementary vegetable-based preparation should be evaluated separately or within a design capable of distinguishing the effects of the encapsulated formulation, the vegetable-based preparation, and their combination.

The complete outcome panel, sampling schedule, IL-11 analytical specifications, safety monitoring, and statistical analysis plan are provided in the Supplementary Material.

Figure 2: Staged validation strategy and progression gates.



Note: Stage 1 characterizes analytical and within-subject biological variability in circulating IL-11 and establishes assay detectability and the reference change value (RCV). Conditional on adequate measurement performance, Stage 2 evaluates intervention-associated kinetics, reversibility, and carry-over through exposure/withdrawal sampling and, where appropriate, randomized N-of-1 trials. Stage 3 is a 24-week randomized, placebo-controlled mechanistic feasibility pilot. Progression between stages requires an analytically credible and reproducible signal together with acceptable safety and feasibility. Biomarker trajectories may support exposure association and mechanistic consistency but do not independently establish mechanism or clinical efficacy. Abbreviations: IL-11, interleukin-11; RCV, reference change value.

5.2. Interpretive Rule Set

The proposed framework is intended to prevent circulating IL-11 trajectories from being interpreted independently of their biological, analytical, and temporal context. Four principles should guide future studies.

1. An increase in circulating IL-11 should not, by itself, be interpreted as evidence of a favorable or regenerative response.

2. IL-11 trajectories should be interpreted alongside validated fibrosis-related measures and conventional hepatic, metabolic, inflammatory, and oxidative-stress biomarkers. Circulating IL-11 should not be used as a surrogate for fibrosis progression or regression.

3. A single pre–post change in circulating IL-11 is insufficient to establish an intervention-associated biological signal. Analytical verification and, where feasible, repeated within-subject measurements are required.

4. Interpretation should integrate the magnitude of IL-11 change relative to the RCV, assay precision, temporal relationship to exposure and withdrawal, covariation with prespecified biomarkers, reversibility, and reproducibility.

This staged strategy is designed to establish whether an intervention-associated IL-11 signal is reproducible while distinguishing upstream-suppression, adaptive-rise, extrahepatic/off-axis, and analytical explanations before larger efficacy studies are undertaken.

DISCUSSION

Implications of the Reframing

The principal implication of this reappraisal is a change in how circulating IL-11 trajectories should be interpreted during interventions targeting metabolic liver injury. Current evidence does not support interpreting an increase in circulating IL-11 as inherently favorable or regenerative. Its biological significance should instead be assessed in relation to upstream processes, concurrent hepatic and oxidative-stress markers, temporal patterns, and analytical reliability.

Under the upstream-suppression hypothesis (H1), attenuation of lipotoxic, oxidative, and inflammatory stress would be expected to reduce hepatic injury. A corresponding decline in circulating IL-11, however, remains conditional on hepatic contribution and

sufficiently stable extrahepatic production and clearance. Conversely, improvement in ALT, GGT, MDA, or inflammatory markers accompanied by increased IL-11 represents a discordant pattern requiring further investigation rather than evidence of regeneration.

The evidence mapping provides stronger clinical support for selected components, particularly curcumin, silymarin, and ginger, but does not establish that the complete formulation modulates hepatic IL-11 or its proposed upstream determinants at the administered exposures. The framework therefore does not predict that the formulation necessarily reduces circulating IL-11. Rather, it defines the biological conditions under which such a reduction would be consistent with H1 and the evidence required to evaluate this prediction.

Relation to the Multi-Target Rationale

This reappraisal does not evaluate the clinical efficacy of multi-target interventions in MASLD. The rationale for such approaches derives from the multifactorial nature of the disease, involving interacting metabolic, lipotoxic, oxidative, inflammatory, fibrogenic, and gut–liver processes [2,3,9,10,37]. Whether a specific combination produces clinically meaningful benefit requires direct evaluation.

The central methodological issue is not whether multi-target interventions are intrinsically beneficial, but whether the proposed biological relationships are explicit, evidence-based, and testable. A biomarker cannot validate an intervention when the expected direction and biological meaning of its change have not themselves been established.

The evidence matrix makes these inferential steps explicit. Evidence that a component improves selected outcomes in MASLD does not establish modulation of its assigned upstream node, and evidence of an upstream effect does not establish downstream modulation of IL-11. Likewise, evidence derived from compound-class, non-hepatic, in vitro, or theoretical sources should not acquire greater certainty simply because a component is included in a multi-ingredient formulation. The same principle applies to interactions and synergy: biological plausibility alone does not demonstrate effects beyond those of the individual components.

Limitations

This work is conceptual and methodological and generates no new experimental evidence. Its conclusions therefore depend on the literature identified, the validity of the proposed biological relationships, and their prospective testability.

First, the evidence mapping was based on a targeted narrative appraisal rather than a systematic review with duplicate screening and independent risk-of-bias assessment. Individual node assignments may therefore change as additional evidence emerges. Moreover, evidence of a clinical or biochemical effect does not establish modulation of the assigned node or of IL-11 itself. Much of the experimental evidence central to the revised interpretation of hepatic IL-11 derives from overlapping research groups [12–14], emphasizing the importance of independent replication.

Second, the relationship between circulating and intrahepatic IL-11 remains insufficiently characterized. Circulating concentrations cannot currently be considered a validated surrogate for hepatic production or cell-specific IL-11 pathway activity. Human evidence in MASLD remains limited, with the principal circulating IL-11 evidence derived from cross-sectional data [21], while mechanistic support includes human hepatocyte and liver-tissue studies alongside animal models [14]. The proposed reframing should therefore be regarded as a testable interpretation rather than an established model of human MASLD.

Third, the clinical observation in Section 5 is inherently hypothesis-generating. Its single-patient, uncontrolled, sequential design, concurrent supportive management, limited temporal sampling, and non-replicated IL-11 measurements preclude causal interpretation of either the biochemical changes or the IL-11 trajectory.

Fourth, analytical uncertainty remains substantial. Assay sensitivity, sample handling and storage, batch effects, and within-subject biological variability may influence apparent longitudinal changes in circulating IL-11. Their magnitude and clinical relevance remain insufficiently characterized, which is why the proposed validation strategy begins with analytical and biological variability rather than intervention testing.

Finally, IL-11 biology is tissue-, disease-, and context-dependent [18–20]. The framework and interpretive rules proposed here are restricted to metabolic liver disease and should not be extrapolated to other organs, diseases, or therapeutic settings without independent evidence.

Future Directions

Future research should first establish the analytical reliability of circulating IL-11 at concentrations relevant to longitudinal studies. Comparative assay studies should define precision, detection and quantification limits, preanalytical stability, and within-subject biological variability.

Experimental studies should then examine the effects of individual components and the complete formulation on IL11 transcription, IL-11 protein production, and downstream signaling in human hepatocytes and hepatic stellate cells. These studies should distinguish modulation of upstream oxidative, inflammatory, and TGF-β-related pathways from direct effects on IL-11 signaling.

Paired hepatic and circulating measurements would help determine whether circulating IL-11 reflects intrahepatic IL-11 activity. Where liver tissue is obtained for clinical indications, tissue expression, protein levels, and downstream signaling could be compared with circulating concentrations.

Prospective intervention studies should assess the reproducibility, timing, and biomarker relationships of IL-11 trajectories and their consistency with H1–H4. The staged strategy proposed in Section 6 provides a framework for this evaluation before larger efficacy trials.

Finally, the complementary vegetable-based preparation should be evaluated independently rather than inferred from sequential administration. Factorial or other interaction-capable designs could distinguish the effects of the encapsulated formulation, the vegetable-based preparation, and their combination, including any evidence of interaction or synergy.

CONCLUSION

Current evidence challenges the historical interpretation of IL-11 as an inherently protective or regenerative cytokine in metabolic liver disease. Experimental studies implicate hepatic IL-11 signaling in lipotoxic and oxidative stress, fibrogenic signaling, hepatocyte injury, and hepatic stellate-cell activation, while human evidence suggests an association between circulating IL-11 and fibrosis severity.

Within the upstream-suppression hypothesis, attenuation of these processes may be accompanied by a decline in circulating IL-11, provided that hepatic production contributes substantially and extrahepatic production and clearance remain sufficiently stable. This remains a testable hypothesis rather than an established treatment-response pattern. Adaptive-rise, extrahepatic/off-axis, and analytical explanations therefore require prospective evaluation through serial measurements, temporal assessment, within-subject replication, and appropriate analytical controls.

Before circulating IL-11 can be used as a response biomarker, its analytical and biological variability and the magnitude of change that can be reliably detected must be established. Until then, an intervention-associated increase in circulating IL-11 should be considered an unexplained finding rather than evidence of therapeutic benefit. In metabolic liver disease, the biological meaning of an IL-11 trajectory must be demonstrated rather than assumed.

PATENTS

A patent application related to the encapsulated composition, vegetable-based preparation, and administration protocol described in this manuscript has been filed with the State Agency on Intellectual Property of the Republic of Moldova (AGEPI). The application is pending, and no patent has been granted.

Conflicts of interest and sources of funding

I.M., V.C., I.B., and N.R. are inventors and owners of a patent application relating to the encapsulated phytotherapeutic composition, the complementary vegetable-based formula, and the administration protocol discussed in this manuscript. The application has been filed with the State Agency on Intellectual Property of the Republic of Moldova (AGEPI) and is currently pending; no patent has yet been granted. The inventors report no commercial role related to the formulation. D.M.C., C.O.D., M.C.V., V.-G.D., C.D.M., and G.P.G. declare no competing interests. This work received no external funding.

Acknowledgments

Generative artificial intelligence was used solely to assist with language editing, grammatical correction, and improvement of clarity and readability. It was not used to generate research data, perform analyses, select or interpret evidence, or formulate the scientific conclusions of the manuscript. All AI-assisted text was critically reviewed and revised by the authors, who take full responsibility for the final content.

All figures and tables were created by the authors specifically for this manuscript and are original. No copyrighted figures, images, or tables from other sources were reproduced or adapted.

Authors' contribution

Author contributions. Conceptualization, I.M., D.M.C. and C.O.D.; methodology, I.M., V.C., I.B., N.R. and C.O.D.; validation, C.O.D., D.M.C. and M.C.V.; formal analysis, C.O.D., I.M. and M.C.V.; investigation, I.M., V.C., I.B. and N.R.; resources, I.M., V.C., I.B. and N.R.; data curation, I.M., V.C., I.B., N.R. and C.O.D.; writing—original draft preparation, I.M., V.C., I.B., N.R. and C.O.D.; writing—review and editing, C.O.D., D.M.C., M.C.V., V.-G.D., C.D.M. and G.P.G.; visualization, C.O.D. and M.C.V.; supervision, I.M., D.M.C. and G.P.G.; project administration, I.M., D.M.C. and C.O.D. All authors have read and agreed to the published version of the manuscript. I.M. and D.M.C. contributed equally to this work and share first authorship.

Ethics approval and consent to participate

This article reports no new experimental research involving human participants. The single anonymized clinical observation described in Section 5 arose from routine individualized clinical practice. The use of anonymized clinical and laboratory data from this observation for scientific purposes was approved by the Ethics Committee of Clinical Hospital CF2 Bucharest, Bucharest, Romania (approval no. 3/13.10.2025). The individual provided written informed consent for the publication of the anonymized clinical and laboratory data presented in this article.

Patient consent for publication

Written informed consent was obtained from the patient for the publication of the anonymized clinical and laboratory data presented in this manuscript.

References

1. Portincasa P, Baffy G. Metabolic dysfunction-associated steatotic liver disease: evolution of the final terminology. Eur J Intern Med. 2024;124:35-39. doi:10.1016/j.ejim.2024.04.013

2. Svobodová G, Horní M, Velecká E, Boušová I. Metabolic dysfunction-associated steatotic liver disease-induced changes in the antioxidant system: a review. Arch Toxicol. 2025;99(1):1-22. doi:10.1007/s00204-024-03889-x

3. Schnabl B, Damman CJ, Carr RM. Metabolic dysfunction-associated steatotic liver disease and the gut microbiome: pathogenic insights and therapeutic innovations. J Clin Invest. 2025;135(7):e186423. doi:10.1172/JCI186423

4. An L, Wirth U, Koch D, Schirren M, Drefs M, Koliogiannis D, et al. The role of gut-derived lipopolysaccharides and the intestinal barrier in fatty liver diseases. J Gastrointest Surg. 2022;26(3):671-683. doi:10.1007/s11605-021-05188-7

5. Karkucinska-Wieckowska A, Simoes ICM, Kalinowski P, Lebiedzinska-Arciszewska M, Zieniewicz K, Milkiewicz P, et al. Mitochondria, oxidative stress and nonalcoholic fatty liver disease: a complex relationship. Eur J Clin Invest. 2022;52(3):e13622. doi:10.1111/eci.13622

6. LeFort KR, Rungratanawanich W, Song BJ. Contributing roles of mitochondrial dysfunction and hepatocyte apoptosis in liver diseases through oxidative stress, post-translational modifications, inflammation, and intestinal barrier dysfunction. Cell Mol Life Sci. 2024;81(1):34. doi:10.1007/s00018-023-05061-7

7. Huang Q, An Z, Xin X, Gou X, Tian X, Hu Y, et al. The effectiveness of curcumin, resveratrol, and silymarin on MASLD: a systematic review and meta-analysis. Food Sci Nutr. 2024;12(12):10010-10029. doi:10.1002/fsn3.4595

8. Malik A, Malik M, Qureshi S. Effects of silymarin use on liver enzymes and metabolic factors in metabolic dysfunction-associated steatotic liver disease: a systematic review and meta-analysis. Can Liver J. 2024;7(1):40-53. doi:10.3138/canlivj-2023-0021

9. Ranneh Y, Bedir AS, Abu-Elsaoud AM, Al Raish S. Polyphenol intervention ameliorates non-alcoholic fatty liver disease: an updated comprehensive systematic review. Nutrients. 2024;16(23):4150. doi:10.3390/nu16234150

10. Vrentzos E, Pavlidis G, Korakas E, Kountouri A, Pliouta L, Dimitriadis GD, et al. Nutraceutical strategies for metabolic dysfunction-associated steatotic liver disease (MASLD): a path to liver health. Nutrients. 2025;17(10):1657. doi:10.3390/nu17101657

11. Baethge C, Goldbeck-Wood S, Mertens S. SANRA—a scale for the quality assessment of narrative review articles. Res Integr Peer Rev. 2019;4:5. doi:10.1186/s41073-019-0064-8

12. Widjaja AA, Dong J, Adami E, Viswanathan S, Ng B, Pakkiri LS, et al. Redefining IL11 as a regeneration-limiting hepatotoxin and therapeutic target in acetaminophen-induced liver injury. Sci Transl Med. 2021;13(597):eaba8146. doi:10.1126/scitranslmed.aba8146

13. Widjaja AA, Singh BK, Adami E, Viswanathan S, Dong J, D'Agostino GA, et al. Inhibiting interleukin 11 signaling reduces hepatocyte death and liver fibrosis, inflammation, and steatosis in mouse models of nonalcoholic steatohepatitis. Gastroenterology. 2019;157(3):777-792.e14. doi:10.1053/j.gastro.2019.05.002

14. Dong J, Viswanathan S, Adami E, Singh BK, Chothani SP, Ng B, et al. Hepatocyte-specific IL11 cis-signaling drives lipotoxicity and underlies the transition from NAFLD to NASH. Nat Commun. 2021;12:66. doi:10.1038/s41467-020-20303-z

15. Nishina T, Komazawa-Sakon S, Yanaka S, Piao X, Zheng DM, Piao JH, et al. Interleukin-11 links oxidative stress and compensatory proliferation. Sci Signal. 2012;5(207):ra5. doi:10.1126/scisignal.2002056

16. Zhu M, Lu B, Cao Q, Wu Z, Xu Z, Li W, et al. IL-11 attenuates liver ischemia/reperfusion injury (IRI) through STAT3 signaling pathway in mice. PLoS One. 2015;10(5):e0126296. doi:10.1371/journal.pone.0126296

17. Yu J, Feng Z, Tan L, Pu L, Kong L. Interleukin-11 protects mouse liver from warm ischemia/reperfusion (WI/Rp) injury. Clin Res Hepatol Gastroenterol. 2016;40(5):562-570. doi:10.1016/j.clinre.2015.11.009

18. Chen Z, Yu F, Qiu Y, Lin J, Yu M, Yan J, Liu X. Interleukin-11 signaling in liver disease: mechanisms, cellular crosstalk, and therapeutic potential. Biomolecules. 2026;16(9):1309. doi:10.3390/biom16091309

19. Cook SA. Understanding interleukin 11 as a disease gene and therapeutic target. Biochem J. 2023;480(23):1987-2008. doi:10.1042/BCJ20220160

20. Zhang J, Leng Y, Li W, Wang B, Yang B, Li W. The role of IL-11 in chronic diseases. Front Immunol. 2026;17:1763360. doi:10.3389/fimmu.2026.1763360

21. Xue Y, Fu H, Wu H, Wang Z, Shen L, Zhu J, et al. Serum level of interleukin-11 is associated with the severity of hepatic fibrosis in adults with metabolic dysfunction-associated steatotic liver disease. J Interferon Cytokine Res. 2026;46(7):204-211. doi:10.1177/10799907261432064

22. Yang M, Zhang CY. Interleukins in liver disease treatment. World J Hepatol. 2024;16(2):140-145. doi:10.4254/wjh.v16.i2.140

23. Rahimlou M, Yari Z, Hekmatdoost A, Alavian SM, Keshavarz SA. Ginger supplementation in nonalcoholic fatty liver disease: a randomized, double-blind, placebo-controlled pilot study. Hepat Mon. 2016;16(1):e34897. doi:10.5812/hepatmon.34897

24. Rafie R, Hosseini SA, Hajiani E, Saki Malehi A, Mard SA. Effect of ginger powder supplementation in patients with non-alcoholic fatty liver disease: a randomized clinical trial. Clin Exp Gastroenterol. 2020;13:35-45. doi:10.2147/CEG.S234698

25. Bilge H, Yildizhan E. Protective effects of taxifolin against oxidative stress and apoptosis in liver ischemia-reperfusion injury: an experimental animal study. Ann Surg Treat Res. 2025;109(1):53-60. doi:10.4174/astr.2025.109.1.53

26. Wei H, Zhao T, Liu X, Ding Q, Yang J, Bi X, et al. Mechanism of action of dihydroquercetin in the prevention and therapy of experimental liver

injury. Molecules. 2024;29(15):3537. doi:10.3390/molecules29153537

27. Ashrafizadeh M, Zarrabi A, Hushmandi K, Zarrin V, Rahmani Moghadam E, Hashemi F, et al. Toward regulatory effects of curcumin on transforming growth factor-beta across different diseases: a review. Front Pharmacol. 2020;11:585413. doi:10.3389/fphar.2020.585413

28. Pipitone RM, Zito R, Lupo G, Javed A, La Mantia C, Di Maria G, et al. Curcumin and andrographolide co-administration safely prevent steatosis induction and ROS production in HepG2 cell line. Molecules. 2023;28(3):1261. doi:10.3390/molecules28031261

29. Yaikwawong M, Jansarikit L, Jirawatnotai S, Chuengsamarn S. Curcumin for inflammation control in individuals with type 2 diabetes mellitus and metabolic dysfunction-associated steatotic liver disease: a randomized controlled trial. Nutrients. 2025;17(12):1972. doi:10.3390/nu17121972

30. Shahsavari K, Ardekani SS, Ardekani MRS, Esfahani MM, Kazemizadeh H, Jamialahmadi T, et al. Are alterations needed in Silybum marianum (silymarin) administration practices? A novel outlook and meta-analysis on randomized trials targeting liver injury. BMC Complement Med Ther. 2025;25(1):134. doi:10.1186/s12906-025-04886-y

31. Honda Y, Kessoku T, Sumida Y, Kobayashi T, Kato T, Ogawa Y, et al. Efficacy of glutathione for the treatment of nonalcoholic fatty liver disease: an open-label, single-arm, multicenter, pilot study. BMC Gastroenterol. 2017;17(1):96. doi:10.1186/s12876-017-0652-3

32. Allen J, Bradley RD. Effects of oral glutathione supplementation on systemic oxidative stress biomarkers in human volunteers. J Altern Complement Med. 2011;17(9):827-833. doi:10.1089/acm.2010.0716

33. Richie JP Jr, Nichenametla S, Neidig W, Calcagnotto A, Haley JS, Schell TD, et al. Randomized controlled trial of oral glutathione supplementation on body stores of glutathione. Eur J Nutr. 2015;54(2):251-263. doi:10.1007/s00394-014-0706-z

34. Porr C, Vidrighin A, Preda EM, Iancu GM, Harris DM, Iovin VC, et al. Circulating interleukin-11 across allergic and non-allergic airway disease phenotypes: a single-center exploratory study. Life (Basel). 2026;16(9):1497. doi:10.3390/life16091497

35. European Association for the Study of the Liver (EASL), European Association for the Study of Diabetes (EASD), European Association for the Study of Obesity (EASO). EASL–EASD–EASO Clinical Practice Guidelines on the management of metabolic dysfunction-associated steatotic liver disease (MASLD). J Hepatol. 2024;81(3):492-542. doi:10.1016/j.jhep.2024.04.031

36. Vohra S, Shamseer L, Sampson M, Bukutu C, Schmid CH, Tate R, et al. CONSORT extension for reporting N-of-1 trials (CENT) 2015 Statement. BMJ. 2015;350:h1738. doi:10.1136/bmj.h1738

37. Elsayed Abouzed DE, Ezelarab HAA, Selim HMRM, Elsayed MMA, El Hamd MA, Aboelez MO. Multimodal modulation of hepatic ischemia/reperfusion-induced injury by phytochemical agents: a mechanistic evaluation of hepatoprotective potential and safety profiles. Int Immunopharmacol. 2024;138:112445. doi:10.1016/j.intimp.2024.112445

Supplementary Material

Rethinking Interleukin-11 in Metabolic Liver Disease: A Critical Reappraisal of Biomarker Directionality

Ion Mereuță, Diana Mihaela Ciuc, Cristina Octaviana Daia, Madalina Codruta Verenca, Vladimir Cărăuș, Ion Bălan, Nicolae Roșca, Valeriu-Gabi Dincă, Cristian Daniel Marica, and Gabriel Petre Gorecki

Contents: Supplementary Methods S1–S5; Supplementary Table S1; Supplementary References S1–S3. References cited as [n] refer to the reference list of the main article; references cited as [Sn] refer to the Supplementary References below.

Supplementary Methods S1. Composition and Administration Protocol

The patent-pending intervention comprised an encapsulated phytotherapeutic formulation and a complementary vegetable-based preparation. The encapsulated formulation contained, per capsule: taxifolin 98%, 50 mg; curcumin 95%, 45 mg; *Silybum marianum* extract (10:1), 45 mg; *Rhaponticum carthamoides* extract (10:1), 40 mg; *Zingiber officinale* extract (10:1), 40 mg; *Aronia melanocarpa* extract (10:1), 35 mg; *Cichorium intybus* extract (10:1), 35 mg; *Andrographis paniculata* extract (10:1), 35 mg; *Glycyrrhiza glabra* extract (10:1), 35 mg; *Juglans regia* extract (10:1), 30 mg; *Phoenix dactylifera* extract (10:1), 30 mg; and L-glutathione 98%, 55 mg.

The complementary vegetable-based preparation was prepared from the following raw ingredients per 1000 mL of final preparation: fresh carrot 400 g, aronia or blueberries 150 g, dandelion root 150 g, chicory root 120 g, beetroot 100 g, dates 100 g, and ginger root 15 g. Aronia and blueberries were used as alternative rather than equivalent ingredients.

The administration protocol comprised a 7–10-day initiation phase (one capsule/day), a 60-day active phase (two capsules/day plus 200 mL/day of the vegetable-based preparation), and a 30-day stabilization phase (one capsule/day plus 50 mL/day of the vegetable-based preparation), followed by a 30-day treatment-free period.

Most botanical ingredients were characterized only by a 10:1 extract ratio; extraction solvents, standardization, and active-compound content were unavailable. Therefore, equivalence with standardized preparations used in published studies cannot be assumed.

Supplementary Methods S2. Proposed Outcome Panel and Sampling Schedule

The proposed outcome panel assesses circulating IL-11 alongside hepatic injury, fibrosis, inflammation, oxidative stress, metabolic status, and safety. IL-11 is considered a candidate mechanistic biomarker rather than a clinical endpoint.

Stage 1. Adults with MASLD at increased fibrosis risk (n = 25–30) should be identified using age-adjusted FIB-4 thresholds (≥1.3, or ≥2.0 in individuals aged >65 years), followed by VCTE; liver stiffness ≥8 kPa indicates increased fibrosis risk rather than a confirmed histological stage [35]. Participants should remain on stable therapy and body weight and undergo four standardized fasting assessments over six weeks. IL-11 should be measured in duplicate at each visit, preferably within a single analytical run and kit lot for each participant, with a subset of samples assessed on a second platform. The primary outcome is the within-subject variability of circulating IL-11 and the corresponding 95% RCV.

Stage 2. IL-11 and prespecified biochemical markers should be measured repeatedly during active and placebo periods, including measurements near period transitions to assess onset, reversibility, and potential carry-over. At least two pretreatment measurements should be obtained

before randomized exposure. The encapsulated formulation should be compared with matched placebo without the vegetable-based preparation, and the N-of-1 series should be reported according to the CONSORT extension for N-of-1 trials [36]. The primary outcome is the within-participant difference in circulating IL-11 between randomized active and placebo periods over a prespecified measurement window.

Stage 3. Supplementary Table S1 presents the proposed schedule for the 24-week Stage 3 pilot, in which the encapsulated formulation is compared with matched placebo, both added to standard care. The primary mechanistic outcome is the between-group difference in the change in circulating IL-11 from baseline to week 24.

Supplementary Table S1. Proposed outcome panel and measurement schedule for Stage 3

Domain	Measure	BL	W4	W12	W24	Post-W
Primary mechanistic biomarker	Serum IL-11, duplicate measurement	X	X	X	X	X
Hepatocellular	ALT, AST, GGT, ALP, bilirubin	X	X	X	X	X
Fibrosis-related	FIB-4, liver stiffness by VCTE	X	—	—	X	—
Inflammatory	hs-CRP, TNF-α, IL-1β, IL-6	X	X	X	X	X
Oxidative	MDA, SOD, GPx, total antioxidant capacity	X	X	X	X	X
Metabolic	HbA1c, fasting insulin, HOMA-IR, lipid panel, BMI, waist circumference	X	—	X	X	—
Steatosis	CAP or MRI-PDFF	X	—	—	X	—
Adherence/co-exposure	Capsule count, diet, medications, lifestyle changes	Continuous				
Safety	Adverse events; hepatic, renal, hematological, electrolyte, and blood-pressure monitoring	X	X	X	X	X

Abbreviations: ALP, alkaline phosphatase; ALT, alanine aminotransferase; AST, aspartate aminotransferase; BL, baseline; BMI, body mass index; CAP, controlled attenuation parameter; FIB-4, Fibrosis-4 Index; GGT, gamma-glutamyl transferase; GPx, glutathione peroxidase; HbA1c, glycated hemoglobin; HOMA-IR, Homeostatic Model Assessment for Insulin Resistance; hs-CRP, high-sensitivity C-reactive protein; IL, interleukin; MDA, malondialdehyde; MRI-PDFF, magnetic resonance imaging proton density fat fraction; Post-W, post-withdrawal; SOD, superoxide dismutase; TNF-α, tumor necrosis factor alpha; VCTE, vibration-controlled transient elastography; W, week.

BL includes two pretreatment biomarker measurements. Post-W denotes an optional post-withdrawal assessment timed according to Stage 2 findings.

Supplementary Methods S3. Analytical and Preanalytical Specification for IL-11

A single biological matrix should be used throughout each study. Collection, processing, centrifugation, aliquoting, storage at −80 °C, and freeze–thaw exposure should be standardized and documented.

Samples from the same participant should preferably be analyzed within the same run and kit lot, in duplicate. The assay platform, manufacturer, analytical range, limit of detection (LoD), lower limit of quantification (LLOQ), and intra- and inter-assay precision should be reported. Measurements below the LoD or LLOQ should be reported and handled according to a prespecified statistical plan.

At least two baseline IL-11 measurements should be obtained before randomized exposure. Absolute concentrations and changes from baseline should be interpreted relative to assay precision, quantification limits, and the reference change value established in Stage 1. Laboratory personnel should remain blinded to treatment period and clinical response where feasible.

Supplementary Methods S4. Safety Monitoring

Because the formulation contains components associated with potential hepatic or systemic adverse effects, prospective safety monitoring is required in Stages 2 and 3. Turmeric-containing products have been associated with liver injury [S1], *Andrographis paniculata* has been associated with changes in liver biochemistry [S2], and *Glycyrrhiza glabra* may increase the risk of hypertension and hypokalemia [S3]. Concomitant medications should be reviewed for potential interactions.

Liver enzymes, bilirubin, renal function, blood count, potassium, and blood pressure should be monitored at prespecified visits (Supplementary Table S1). Suspected hepatic adverse events should prompt clinical assessment, additional testing, and evaluation of alternative causes. Treatment-withholding criteria should be predefined in the study protocol and adapted to baseline liver-test abnormalities and the characteristics of the study population.

Supplementary Methods S5. Analysis Plan

The primary Stage 1 analysis should estimate within-subject biological variability in circulating IL-11 and the corresponding 95% reference change value (RCV), together with confidence intervals reflecting the precision of these estimates.

The primary Stage 2 analysis should estimate the within-participant difference in circulating IL-11 between randomized active and placebo periods. Repeated observations should be analyzed using models appropriate for N-of-1 data, accounting for participant, treatment, period/time,

serial correlation, and potential carry-over where relevant.

For Stage 3, the primary mechanistic analysis should estimate the between-group difference in change in circulating IL-11 from baseline to week 24, with corresponding confidence intervals. Feasibility outcomes should include recruitment, retention, adherence, and completeness of longitudinal biomarker assessment. The Stage 3 sample size should be determined prospectively using variance and intervention-associated IL-11 estimates obtained in Stages 1 and 2, together with predefined precision and feasibility criteria.

Associations between IL-11 and prespecified hepatic or oxidative-stress biomarkers should be considered secondary mechanistic analyses. These analyses should distinguish within-person changes from between-person differences and common temporal trends. Change-score associations should be interpreted cautiously because correlated measurement error between baseline and follow-up values, regression to the mean (particularly in participants selected for elevated baseline values), and shared temporal trends may produce spurious correlations; mixed-effects models using repeated measurements, with baseline values included as covariates, are preferred over simple correlations of change scores. Directional associations should be interpreted as consistency checks for H1–H4 rather than evidence of mechanism.

The statistical analysis plan should prespecify the primary analysis for each stage, biomarker hierarchy, handling of missing and below-quantification values, repeated measurements, and criteria for progression between study stages.

Supplementary References

S1. Halegoua-DeMarzio D, Navarro V, Ahmad J, Avula B, Barnhart H, Barritt AS, et al. Liver injury associated with turmeric—a growing problem: ten cases from the Drug-Induced Liver Injury Network [DILIN]. Am J Med. 2023;136(2):200-206. doi:10.1016/j.amjmed.2022.09.026

S2. Kaewdech A, Nawalerspanya S, Assawasuwannakit S, Chamroonkul N, Jandee S, Sripongpun P. The use of Andrographis paniculata and its effects on liver biochemistry of patients with gastrointestinal problems in Thailand during the COVID-19 pandemic: a cross sectional study. Sci Rep. 2022;12:18213. doi:10.1038/s41598-022-23189-7

S3. Penninkilampi R, Eslick EM, Eslick GD. The association between consistent licorice ingestion, hypertension and hypokalaemia: a systematic review and meta-analysis. J Hum Hypertens. 2017;31(11):699-707. doi:10.1038/jhh.2017.45

https://doi.org/10.55453/rjmm.2026.129.6.10

ARTICLE

Unravelling the serum calcium-to-magnesium ratio: a study in 474 individuals with/without adrenal tumors in relationship with central DXA results

Mihai-Lucian Ciobica[1,2], Mihai Costachescu[3,4,*], Anda Dumitrascu[5], Ana-Maria Gheorghe[6], Gabi Voicu[5], Dana Manda[7], Sorina Violeta Schiopor[7], Mara Carsote[3,6,8], Luminita Suveica[9], Alexandra-Ioana Trandafir[6,10]

[1] Department of Internal Medicine and Gastroenterology, "Carol Davila" University of Medicine and Pharmacy, 020021 Bucharest, Romania
[2] Department of Internal Medicine I and Rheumatology, "Dr. Carol Davila" Central Military University Emergency Hospital, 010825 Bucharest, Romania lucian.ciobica@umfcd.ro
[3] PhD Doctoral School of "Carol Davila" University of Medicine and Pharmacy, 020021 Bucharest, Romania
[4] Department of Radiology and Medical Imaging, "Dr. Carol Davila" Central Military University Emergency Hospital, 010825 Bucharest, Romania, mihai.costachescu@drd.umfcd.ro
[5] Department of Radiology and Medical Imaging, C.I. Parhon National Institute of Endocrinology, 011683 Bucharest, Romania anda.dumitrascu@gmail.com, voicugabi@gmal.com
[6] Department of Clinical Endocrinology V, C.I. Parhon National Institute of Endocrinology, 011683 Bucharest, Romania, ana-maria.gheorghe@drd.umfcd.ro
[7] Department of Research, C.I. Parhon National Institute of Endocrinology, 011683 Bucharest, Romania dana.manda@gmail.com, sorina.schipor@parhon.ro
[8] Department of Endocrinology, "Carol Davila" University of Medicine and Pharmacy, 020021 Bucharest, Romania, carsote_m@hotmail.com
[9] Department of Family Medicine, State "Nicolae Testemiţanu" University of Medicine and Pharmacy, 2004 Chisinau, Republic of Moldova, luminita.suveica@usmf.md
[10] Clinica Medica Endoprovision,alexandra-ioana.trandafir@drd.umfcd.ro

*Correspondence to: mihai.costachescu@drd.umfcd.ro

Abstract: Background/Objective: In order to address the current knowledge gap with regard to serum calcium-to-magnesium ratio (Ca/Mg) in patients with adrenal incidentalomas, we aimed to analyze Ca/Mg in menopausal women diagnosed with these tumors versus (tumor-free) controls across DXA categories. Methods. This is a retrospective, real-world, cross-sectional study in 474 menopausal women admitted at a single tertiary center of endocrinology. Results. Tumor group (N=111) had osteoporosis/osteopenia/normal DXA prevalence: 17.1%, 36.9% and 46%, respectively, control group: 13.8%, 45.5%, and 40.8%. Ca/Mg ratio was similar between DXA sub-groups in each group. Tumor group: Ca/Mg corelated with age (r=0.288, p=0.047), P1NP (r= -0.459, p=0.011), osteocalcin (r= -0.37, p=0.026) and CrossLaps (r= -0.446, p=0.006) in subjects with normal DXA (N=51), while in those osteoporotic (N=19), with glycated hemoglobin A1c (r=0.596, p=0.025). Control group (N=363): Ca/Mg corelated with age (N=165, r=0.178, p=0.034), fasting glycemia (r=0.253, p=0.003), glycated hemoglobin A1c (r=0.22, p=0.045), osteocalcin (r= -0.196, p=0.03), and CrossLaps (r= -0.193, p=0.034) in osteopenic subjects (N=165) and with P1NP (r= -0.249, p=0.027) in normal DXA (N=148). Conclusion. Osteopenic subjects (regardless tumor diagnosis) showed a direct age-Ca/Mg association, while the ratio was correlated with the bone turnover biomarkers distinctively across DXA sub-groups. Additionally, the ratio might reflect a more severe glucose profile.

Keywords: adrenocortical adenoma, calcium, magnesium, calcium-to-phosphorus ratio, adrenal, incidentaloma, DXA, cortisol, ACTH, CT

Citation: Ciobica ML, Costachescu M, Dumitrascu A, Gheorghe AM, Voicu G, Manda D, et al. *Unravelling the serum calcium-to-magnesium ratio: a study in 474 individuals with/without adrenal tumors in relationship with central DXA results.* R. J. Mil. Med. 2026, CXXIX(6): 725-740. https://doi.org/10.55453/rjmm.2026.129.6.10

Academic Editor: Octavian Vasiliu

Received: 01 October 2026
Revised: 27 October 2026
Accepted: 01 November 2026

INTRODUCTION

Contemporary scientific and non-scientific community points out the importance of a healthy lifestyle, including an adequate amount of minerals such as calcium, magnesium or phosphorus [1-3]. These elements are related to food, drinking water and other drinks (e.g. milk, etc.) and their abnormal/inadequate intake is reflected in the mineral metabolism anomalies, negative cardiovascular and neurologic outcomes, development of kidney stones, etc. in both pediatric and adult population

[4-6]. A higher osteoporotic fracture risk under certain circumstances that also involves a dysregulation of the vitamin D status and/or parathyroid hormone (PTH) has been reported, too [7-12]. In addition, an abnormal magnesium/calcium intake disturbs their serum and cellular balance during pregnancy, further displaying, not only maternal consequences, but, also, a negative impact on the newborn (e.g. eclampsia/pre-eclampsia, pregnancy-related diabetes mellitus, on one hand, and, on the other hand, restriction of the intra-uterine growth, preterm birth, and metabolic/mineral ailments during early childhood) [13-16].

In addition to the dietary consumption and the connected reflection in the metabolic and mineral pathways, the calcium-to-magnesium ratio is also analyzed in the serum according to their circulating levels (mostly involving total serum calcium, not ionized calcium), the ratio being studied in patients with metabolic syndrome, primary hyperparathyroidism, osteoporosis, nephrolithiasis, etc. [17-20]. Moreover, the circumstances that alter the digestive absorption and the overall metabolism of calcium and magnesium may be related to a glucocorticoid excess, such as endogenous or exogenous Cushing's syndrome, which associates an impairment of the bone status and of the cardio-metabolic risk [21-25]. However, the data in mild cortisol excess, as found in patients with adrenal incidentalomas, remain scarce, while the condition has an increasing incidence due to an easy access to abdominal scans, thus the importance of analyzing alternative biomarkers, such as those easy-to-access e.g. calcium-to-magnesium ratio [26,27].

AIM

In order to address the current gap of knowledge with regard to serum calcium-to-magnesium ratio in patients with apparently non-functional adrenal tumors, we aimed to analyze the ratio in menopausal women diagnosed with these tumors versus (tumor-free) controls, sub-analyzing the population based on Dual-Energy X-Ray Absorptiometry (DXA) categories of osteoporosis, osteopenia and normal.

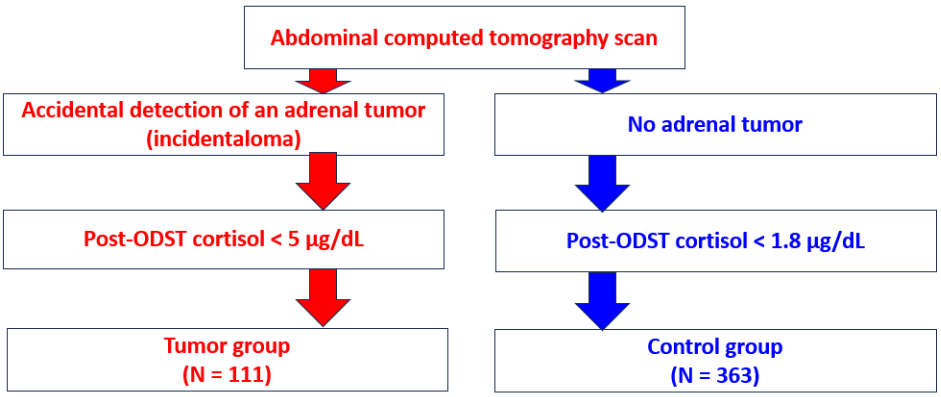
MATERIALS AND METHODS

This is a retrospective, real-world, cross-sectional study in menopausal women admitted at a single tertiary center of endocrinology (university hospital) with ethical approvals from hospital (number 37 from 09/22/2025) and associated university (number 7634 from 04/04/2025). We included women of 50 years or older who were in menopause (either surgical or physiological menopause) and who were diagnosed with non-functional adrenal tumors (adrenal incidentalomas) after their detection at abdominal computed tomography. We excluded patients with active (secretor) adrenal tumors (including Cushing's syndrome), any type of endocrine dysfunction (e.g., hyperthyroidism, hypothyroidism, primary hyperparathyroidism), active/prior malignancies, renal, hepatic and bone metabolic disorders; prior medication against osteoporosis, insulin therapy, anti-obesity drugs, and corticotherapy.

The subjects underwent central DXA (GE Lunar Prodigy device) and were grouped into osteoporosis, osteopenia, and normal DXA based on the lowest lumbar (L1-L4) T-score, according to the current World Health Organization (WHO) criteria for menopause [28-30]. The control group included patients with similar inclusion/exclusion criteria, except for the fact that they did not present any adrenal tumor at abdominal computed tomography scan.

The collected data were: age, years since last menstruation, body mass index; baseline morning adrenocorticotropic hormone (ACTH) and plasma cortisol, as well cortisol levels after 1-mg overnight dexamethasone test (post-ODST) (which were of less than 5 μg/dL for the group with tumors and of less than the normal cutoff of 1.8 μg/dL for the control group); the largest diameter at computed tomography (tumor group); the prior/concurrent diagnosis of type 2 diabetes, arterial hypertension, dyslipidemia; biochemical parameters (fasting glycemia, glycated hemoglobin A1c, serum total calcium, magnesium, phosphorus); mineral metabolism-related hormones: 25-hydroxyvitamin D (25OHD) and PTH; DXA-based parameters (lumbar T-score and bone mineral density), thyroid profile [thyroid stimulating hormone (TSH) and free thyroxine (FT4)], and circulating bone turnover markers (osteocalcin, P1NP, total alkaline phosphatase, and CrossLaps). We calculated the serum total calcium-to-magnesium ratio, as well as the serum total calcium-to-phosphorus ratio, for the tumor group and the control group, respectively. Prevalent fragility (osteoporotic) fractures were registered from prior medical history/records, screening thoracic-lumbar spine X-ray, or opportunistic detection on abdominal computed tomography scans. Obesity, overweight, and normal weight were defined based on standard body mass index values [28].

Figure 1: Flow chart diagram of the study



The parameters were introduced as mean ± standard deviation (in case of normal distribution); correlations between numerical variables were evaluated based on Spearman coefficient; student t-test was used to determine the statistical significance with a cutoff of < 0.05. (Figure 1)

RESULTS

We included 474 patients, 111 in the tumor group and 363 in (tumor-free) control group. Tumor group had 17.1% subjects with osteoporosis, 36.9% with osteopenia and 46% with normal DXA (a similar age and menopause duration was found between these three sub-groups). Body mass index was statistically significant higher in normal DXA versus osteoporosis sub-group (31.56 ± 5.60 versus 26.30 ± 4.59 kg/sqm, p = 0.011) and a higher prevalence of obesity was identified in normal DXA versus osteoporosis sub-group (60% versus 23%, p = 0.019), respectively, versus osteopenia sub-group (37%, p = 0.046).

Type 2 diabetes prevalence varied between 15% and 25% per (DXA-based) sub-group. While total serum calcium, magnesium and phosphorus were similar between DXA sub-groups, the calcium-to-phosphorus ratio was statistically significant lower in osteoporosis versus osteopenia (2.40 ± 0.39 versus 2.70 ± 0.46 mg/dL, p = 0.035), respectively, versus normal DXA sub-group (2.72 ± 0.36 mg/dL, p = 0.018), with similar calcium-to-magnesium ratio. Among the panel of bone turnover markers, osteocalcin was statistically significant higher in osteoporosis versus osteopenia sub-group (33.03 ± 13.45 versus 20.62 ± 8.29 ng/mL, p = 0.002), respectively CrossLaps (0.614 ± 0.23 versus 0.410 ± 0.16 ng/mL, p = 0.027), respectively, osteocalcin was higher in osteoporosis versus normal DXA sub-group (21.24 ± 10.78 ng/mL, p = 0.003). (Table 1)

Table 1: Analysis of the study population diagnosed with adrenal tumors (N = 111, 100%)

Parameter, unit	Osteoporosis	Osteopenia	Normal DXA	p-value osteoporosis-osteopenia	p-value osteoporosis-normal DXA	p-value osteopenia-normal DXA
Number of patients (N, %)	19, 17.1%	41, 36.9%	51, 46%			
Age (years) (mean ± SD)	59.78 ± 8.52	63.39 ± 8.06	62.21 ± 8.25	0.900	0.842	0.127
Years since menopause (mean ± SD)	12.66 ± 7.82	15.90 ± 8.35	12.80 ± 5.84	0.845	0.900	0.283
Body mass index (kg/sqm) (mean ± SD)	26.30 ± 4.59	28.68 ± 5.87	31.56 ± 5.60	0.572	**0.011**	0.068
Obesity (N, %)	3, 23%	14, 37.8%	27, 60%	0.499	**0.019**	**0.046**
Overweight (N, %)	5, 38.5%	11, 29.7%	14, 31.1 %	0.731	0.740	0.892
Normal weight (N, %)	5, 38.5%	12, 32.4%	4, 8.9%	0.741	**0.020**	**0.007**

Type 2 diabetes (N, %)	3, 15.8%	7, 17.5%	12, 24%	0.900	0.534	0.453
Dyslipidaemia (N, %)	13, 68.4%	31, 77.5%	45, 88.2%	0.528	0.074	0.171
Arterial hypertension (N, %)	12, 63.2%	32, 78%	42, 82.4%	0.225	0.114	0.605
Fasting glycemia (mg/dL) (mean ± SD)	99.00 ± 17.04	99.49 ± 12.27	105.31 ± 19.04	0.900	0.625	0.408
Glycated haemoglobin A1c (%) (mean ± SD)	5.61 ± 0.66	5.76 ± 0.42	6.01 ± 0.65	0.900	0.110	0.373
Serum total calcium (mg/dL) (mean ± SD)	9.33 ± 0.48	9.50 ± 0.41	9.58 ± 0.43	0.500	0.105	0.900
Serum phosphorus (mg/dL) (mean ± SD)	3.95 ± 0.55	3.60 ± 0.09	3.58 ± 0.45	0.058	**0.034**	0.900
Serum magnesium (mg/dL) (mean ± SD)	1.95 ± 0.23	1.98 ± 0.18	1.97 ± 0.21	0.900	0.900	0.990
Calcium-to-magnesium ratio (mean ± SD)	4.87 ± 0.83	4.83 ± 0.53	4.92 ± 0.65	0.990	0.900	0.900
Calcium-to-phosphorus ratio (mean ± SD)	2.40 ± 0.39	2.70 ± 0.46	2.72 ± 0.36	**0.035**	**0.018**	0.900
PTH (pg/mL) (mean ± SD)	49.32 ± 17.09	40.57 ± 16.20	44.65 ± 12.02	0.303	0.900	0.982
25OHD (ng/dL) (mean ± SD)	25.23 ± 8.19	26.46 ± 10.73	22.11 ± 9.73	0.900	0.981	0.218
P1NP (ng/mL) (mean ± SD)	60.93 ± 10.19	53.60 ± 25.17	52.91 ± 22.85	0.990	0.800	0.800
Alkaline phosphatase (U/L) (mean ± SD)	84.11 ± 42.07	75.44 ± 24.46	80.13 ± 26.69	0.921	0.900	0.900
Osteocalcin (ng/mL) (mean ± SD)	33.03 ± 13.45	20.62 ± 8.29	21.24 ± 10.78	**0.002**	**0.003**	0.900
CrossLaps (ng/mL) (mean ± SD)	0.614 ± 0.23	0.410 ± 0.16	0.443 ± 0.26	**0.027**	0.069	0.900
Lumbar (L1-4) bone mineral density	0.813 ± 0.10	0.978 ± 0.05	1.183 ± 0.11	**<0.001**	**<0.001**	**<0.001**
Lumbar (L1-4) T-score	-3.13 ± 0.79	-1.65 ± 0.37	0.12 ± 0.85	**<0.001**	**<0.001**	**<0.001**
Lumbar (L1-L4) Z-score	-1.95 ± 0.77	-0.51 ± 0.57	0.74 ± 1.00	**<0.001**	**<0.001**	**<0.001**
Fragility fractures (N, %)	3, 15.8%	3, 7.3%	5, 9.8%	0.370	0.674	0.728
ACTH (pg/mL) (mean ± SD)	18.82 ± 17.87	15.96 ± 10.93	13.83 ± 8.97	0.800	0.457	0.700

Plasma morning cortisol (µg/dL) (mean ± SD)	13.77 ± 7.39	12.88 ± 5.18	13.66 ± 6.14	0.700	0.800	0.900
Post-ODST cortisol (µg/dL) (mean ± SD)	1.66 ± 0.78	1.84 ± 1.33	1.90 ± 1.26	0.880	0.900	0.880
Bilateral tumours (N, %)	4, 23.5%	15, 38.5%	18, 35.3%	0.278	0.368	0.757
Largest tumour diameter (cm) (mean ± SD)	2.00 ± 0.70	2.29 ± 1.15	2.17 ± 0.84	0.990	0.900	0.800
TSH (µUI/mL) (mean ± SD)	1.63 ± 0.95	1.54 ± 1.02	2.02 ± 2.36	0.800	0.880	0.900
FT4 (pmol/L) (mean ± SD)	13.07 ± 3.61	14.06 ± 1.62	13.67 ± 2.46	0.530	0.800	0.700

Normal ranges for the blood parameters: ACTH: 3 - 66 pgmL; morning plasma cortisol: 6.2 - 19.4 µg/dL; post-ODST cortisol < 1.8 µg/dL; serum total calcium: 8.4 - 10.2 mg/dL; serum magnesium: 1.6 – 2.3 mg/dL; serum phosphorus: 2.3 - 4.7 mg/dL; PTH: 15 - 65 pg/mL; fasting glycemia: 70 – 105 mg/dL; glycated haemoglobin A1c: 4.8 - 5.9%; 25OHD: 30 - 100 ng/mL; P1NP: 20.25 - 76.31 ng/mL; osteocalcin: 15 - 46 ng/mL; total alkaline phosphatase: 35 - 104 U/L; CrossLaps: 0.33 - 0.782 ng/mL; TSH: 0.35 - 4.95 µUI/mL; FT4: 9 – 19 pmol/L . Normal T-score at central DXA > -1)

Control group (N = 363) included 13.8% patients with osteoporosis, 45.5% with osteopenia and 40.8% with normal DXA (no between-group difference was registered with respect to age and menopause duration). Body mass index was statistically significant different between each sub-group (the highest was in normal DXA sub-group). Obesity prevalence was statistically significant higher in normal DXA versus osteoporosis (50.4% versus 21.9%, p = 0.037), respectively, versus osteopenia (34.9%, p = 0.015). The mineral metabolism and adrenal parameters were similar between the three sub-groups, including calcium-to-magnesium and calcium-to-phosphorus ratios. (Table 2)

Table 2: Analysis of the control group (N = 363, 100%)

Parameter, unit	Osteoporosis	Osteopenia	Normal DXA	p-value osteoporosis-osteopenia	p-value osteoporosis-normal DXA	p-value osteopenia-normal DXA
Number of patients (N, %)	50, 13.8%	165, 45.5%	148, 40.8%			
Age (years) (mean ± SD)	62.02 ± 8.13	61.89 ± 7.3	60.44 ± 7.91	0.900	0.625	0.286
Years since menopause (mean ± SD)	13.77 ± 8.01	12.90 ± 7.29	11.66 ± 8.30	0.700	0.500	0.695
Body mass index (kg/sqm) (mean ± SD)	25.42 ± 5.11	27.93 ± 4.70	30.00 ± 5.39	**0.037**	**<0.001**	**0.005**
Obesity (N, %)	7, 21.9%	44, 34.9%	58, 50.4%	0.159	**0.004**	**0.015**
Overweight (N, %)	9, 28.1%	46, 36.5%	36, 31.3%	0.374	0.730	0.394
Normal weight (N, %)	16, 50%	36, 28.6%	21, 18.3%	**0.021**	**<0.001**	0.060
Type 2 diabetes (N, %)	7, 14.3%	20, 12.1%	33, 22.3 %	0.689	0.227	**0.017**
Dyslipidemia (N, %)	30, 60%	107, 65.2%	101, 68.2%	0.499	0.287	0.575

Arterial hypertension (N, %)	29, 58%	94, 57%	97, 65.5%	0.897	0.338	0.121
Fasting glycemia (mg/dL) (mean ± SD)	100.79 ± 27.52	99.86 ± 19.44	104.64 ± 25.89	0.910	0.986	0.252
Glycated haemoglobin A1c (%) (mean ± SD)	5.65 ± 0.45	5.71 ± 0.55	5.89 ± 0.66	0.880	0.342	0.123
Serum total calcium (mg/dL) (mean ± SD)	9.41 ± 0.65	9.58 ± 0.42	9.52 ± 0.49	0.108	0.512	0.949
Serum phosphorus (mg/dL) (mean ± SD)	3.63 ± 0.57	3.56 ± 0.46	3.60 ± 0.53	0.900	0.800	0.870
Serum magnesium (mg/dL) (mean ± SD)	1.99 ± 0.18	2.03 ± 0.46	2.51 ± 0.61	0.990	0.943	0.913
Calcium-to-magnesium ratio (mean ± SD)	4.74 ± 0.48	4.82 ± 0.60	4.77 ± 0.82	0.899	0.777	0.800
Calcium-to-phosphorus ratio (mean ± SD)	2.66 ± 0.44	2.73 ± 0.39	2.71 ± 0.44	0.877	0.760	0.900
PTH (pg/mL) (mean ± SD)	43.71 ± 13.64	43.66 ± 11.65	44.71 ± 11.93	0.890	0.900	0.700
25OHD (ng/dL) (mean ± SD)	21.59 ± 9.43	24.47 ± 9.53	23.28 ± 8.94	0.212	0.893	0.899
P1NP (ng/mL) (mean ± SD)	64.45 ± 23.25	60.08 ± 28.27	53.86 ± 22.08	0.920	0.181	0.309
Alkaline phosphatase (U/L) (mean ± SD)	76.27 ± 21.90	78.27 ± 30.01	76.72 ± 19.89	0.990	0.890	0.780
Osteocalcin (ng/mL) (mean ± SD)	25.76 ± 10.76	24.59 ± 9.36	22.74 ± 13.06	0.880	0.482	0.608
CrossLaps (ng/mL) (mean ± SD)	0.488 ± 0.18	0.529 ± 0.80	0.419 ± 0.21	0.900	0.990	0.429
Lumbar (L1-4) bone mineral density	0.808 ± 0.08	0.969 ± 0.08	1.186 ± 0.14	**<0.001**	**<0.001**	**<0.001**
Lumbar (L1-4) T-score	-3.05 ± 0.51	-1.68 ± 0.38	0.06 ± 1.01	**<0.001**	**<0.001**	**<0.001**
Lumbar (L1-L4) Z-score	-1.72 ± 0.75	-0.68 ± 0.64	0.61 ± 1.14	**<0.001**	**<0.001**	**<0.001**
Fragility fractures (N, %)	10, 20.4%	12, 7.3%	3, 2%	0.700	0.600	0.670
ACTH (pg/mL) (mean ± SD)	12.75 ± 4.67	15.29 ± 6.37	20.81 ± 7.15	0.670	0.084	0.112
Plasma morning cortisol (µg/dL) (mean ± SD)	12.35 ± 2.86	13.31 ± 5.08	11.55 ± 4.37	0.890	0.850	0.923

Post-ODST cortisol (µg/dL) (mean ± SD)	0.92 ± 0.07	0.77± 0.10	0.74 ± 0.07	0.473	0.256	0.880
TSH (µUI/mL) (mean ± SD)	2.61 ± 3.80	1.98 ± 2.73	2.75 ± 3.55	0.715	0.930	0.124
FT4 (pmol/L) (mean ± SD)	13.35 ± 3.21	13.89 ± 2.74	17.02 ± 31.45	0.870	0.911	0.625

Normal ranges for the blood parameters: ACTH: 3 - 66 pgmL; morning plasma cortisol: 6.2 - 19.4 µg/dL; post-ODST cortisol < 1.8 µg/dL; serum total calcium: 8.4 - 10.2 mg/dL; serum magnesium: 1.6 – 2.3 mg/dL; serum phosphorus: 2.3 - 4.7 mg/dL; PTH: 15 - 65 pg/mL; fasting glycemia: 70 – 105 mg/dL; glycated haemoglobin A1c: 4.8 - 5.9%; 25OHD: 30 - 100 ng/mL; P1NP: 20.25 - 76.31 ng/mL; osteocalcin: 15 - 46 ng/mL; total alkaline phosphatase: 35 - 104 U/L; CrossLaps: 0.33 - 0.782 ng/mL; TSH: 0.35 - 4.95 µUI/mL; FT4: 9 – 19 pmol/L . Normal T-score at central DXA > -1)

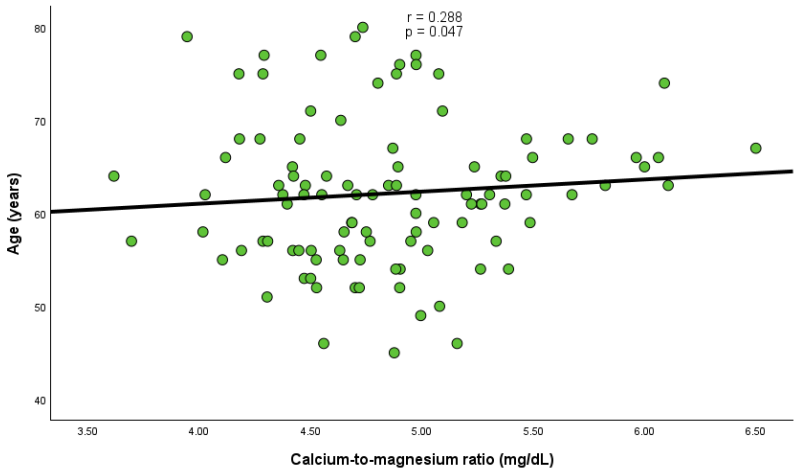
Calcium-to-phosphorus ratio was statistically significantly lower in osteoporotic patients from tumor group versus control group (2.40 ± 0.39 versus 2.66 ± 0.44 mg/dL, p = 0.036). (Table 3).

Table 3: Comparison between calcium-to-magnesium ratio, respectively, calcium-to-phosphorus ratio within the tumor group versus controls

Study group/sub-group	Calcium-to-magnesium ratio	Calcium-to-phosphorus ratio
Osteoporosis Tumor group versus control group	p-value = 0.426	**p-value = 0.036**
Osteopenia Tumor group versus control group	p-value = 0.916	p-value = 0.681
Normal DXA Tumor group versus control group	p-value = 0.248	p-value = 0.872

Calcium-to-magnesium ratio statistically significantly and positively corelated with the patients' age in tumor group with normal DXA (N = 51, r = 0.288, p = 0.047) and negatively with bone formation markers P1NP (r = -0.459, p = 0.011), osteocalcin (r = -0.37, p = 0.026) and bone resorption marker CrossLaps (r = -0.446, p = 0.006). (Figure 2)

Figure 2: Positive association between age (years) and calcium-to-magnesium ratio in the tumour group, specifically, in subjects with normal DXA results



In patients with adrenal incidentalomas, calcium-to-magnesium ratio statistically significantly associated with glycated hemoglobin A1c level (%) only in osteoporotic group (N = 19, r = 0.596, p = 0.025). On the other hand, calcium-to-phosphorus ratio displayed statistically significant inverse correlation coefficients with body mass index (r = -0.426, p = 0.011), P1NP (r = -0.509, p = 0.026), osteocalcin (r = -0.435, p = 0.018) in osteopenia sub-group (N = 41). (Table 4)

Table 4: Correlations between the calcium-to-magnesium ratio, respectively, calcium-to-phosphorus ratio and study parameters within the tumor group

	Calcium-to-magnesium ratio			Calcium-to-phosphorus ratio		
Parameter, unit, normal ranges	Osteoporosis	Osteopenia	Normal DXA	Osteoporosis	Osteopenia	Normal DXA
Age (years)	r = 0.041 p = 0.867	r = 0.039 p = 0.809	**r = 0.288** **p = 0.047**	r = 0.340 p = 0.167	r = -0.250 p = 0.130	r = 0.140 p = 0.355
Years since menopause	r = -0.012 p = 0.973	r = -0.069 p = 0.717	r = 0.136 p = 0.423	r = 0.462 p = 0.210	r = -0.296 p = 0.126	r = -0.048 p = 0.782
Body mass index (kg/sqm)	r = 0.201 p = 0.511	r = 0.175 p = 0.300	r = 0.174 p = 0.252	r = 0.343 p = 0.275	**r = -0.426** **p = 0.011**	r = -0.130 p = 0.411
Fasting glycemia (mg/dL)	r = 0.372 p = 0.172	r = 0.281 p = 0.113	r = 0.079 p = 0.632	r = 0.277 p = 0.337	r = -0.159 p = 0.394	r = 0.176 p = 0.298
Glycated hemoglobin A1c (%)	**r = 0.596** **p = 0.025**	r = 0.069 p = 0.749	r = 0.282 p = 0.132	r = -0.143 p = 0.642	r = -0.191 p = 0.408	r = 0.106 p = 0.591
PTH (pg/mL)	r = 0.098 p = 0.762	r = -0.407 p = 0.067	r = -0.210 p = 0.265	r = 0.100 p = 0.770	r = -0.230 p = 0.344	r = 0.315 p = 0.102
25OHD (ng/mL)	r = - 0.253 p = 0.405	r = -0.030 p = 0.874	r = -0.274 p = 0.092	r = 0.154 p = 0.633	r = 0.332 p = 0.078	r = -0.113 p = 0.499
P1NP (ng/mL)	r = - 0.267 p = 0.488	r = -0.104 p = 0.670	**r = -0.459** **p = 0.011**	r = -0.333 p = 0.420	**r = -0.509** **p = 0.026**	r = -0.740 p = 0.698
Alkaline phosphatase (U/L)	r = 0.027 p = 0.916	r = 0.006 p = 0.973	r = -0.053 p = 0.726	r = -0.416 p = 0.097	r = -0.018 p = 0.917	r = 0.206 p = 0.174
Osteocalcin (ng/mL)	r = 0.063 p = 0.846	r = -0.253 p = 0.170	**r = -0.370** **p = 0.026**	r = -0.400 p = 0.223	**r = -0.435** **p = 0.018**	r = -0.080 p = 0.649
CrossLaps (ng/mL)	r = - 0.201 p = 0.510	r = -0.168 p = 0.376	**r = -0.446** **p = 0.006**	r = 0.200 p = 0.533	r = -0.213 p = 0.276	r = -0.123 p = 0.483
Lumbar (L1-4) bone mineral density	r = 0.368 p = 0.216	r = -0.124 p = 0.477	r = 0.211 p = 0.164	r = 0.578 p = 0.049	r = -0.003 p = 0.988	r = 0.028 p = 0.858
Lumbar (L1-4) T-score	r = -0.089 p = 0.717	r = 0.057 p = 0.724	r = 0.076 p = 0.602	r = 0.483 p = 0.042	r = 0.065 p = 0.697	r = 0.064 p = 0.665
Lumbar (L1-L4) Z-score	r = - 0.252 p = 0.314	r = -0.123 p = 0.468	r = 0.237 p = 0.113	r = 0.216 p = 0.406	r = 0.235 p = 0.174	r = 0.163 p = 0.291
ACTH (pg/mL)	r = -0.079 p = 0.781	r = 0.330 p = 0.065	r = 0.190 p = 0.228	r = 0.415 p = 0.124	r = -0.074 p = 0.701	r = 0.179 p = 0.269
Plasma morning cortisol (µg/dL)	r = -0.036 p = 0.899	r = 0.152 p = 0.399	r = 0.104 p = 0.504	r = 0.273 p = 0.324	r = 0.010 p = 0.958	r = 0.062 p = 0.694
Post-ODST cortisol (µg/dL)	r = 0.210 p = 0.513	r = 0.144 p = 0.535	r = 0.118 p = 0.500	r = -0.102 p = 0.753	r = -0.095 p = 0.708	r = 0.034 p = 0.848
TSH (µUI/mL)	r = - 0.111 p = 0.652	r = 0.086 p = 0.601	r = 0.087 p = 0.550	r = -0.197 p = 0.432	r = -0.086 p = 0.616	r = 0.058 p = 0.698
FT4 (pmol/L)	r = 0.379 p = 0.147	r = -0.078 p = 0.647	r = -0.032 p = 0.850	r = -0.450 p = 0.092	r = 0.050 p = 0.777	r = 0.096 p = 0.566

In control group, osteopenic subjects (N = 165) showed a calcium-to-magnesium ratio positively and statistically significantly corelated with the subjects' age (N = 165; r = 0.178, p = 0.034), fasting glycemia (r = 0.253, p = 0.003), glycated hemoglobin A1c (r = 0.22, p = 0.045), and negatively with osteocalcin (r = -0.196, p = 0.03), and CrossLaps, respectively (r = -0.193, p = 0.034). Calcium-to-phosphorus ratio also positively associated with fasting glycemia (r = 0.239, p = 0.004) and glycated hemoglobin A1c (r = 0.342, p = 0.001), as well as negatively with bone turnover markers: osteocalcin (r = -0.287, p = 0.001), alkaline phosphatase (r = -0.169, p = 0.047), and CrossLaps (r = -0.263, p = 0.003). In addition, the same sub-group (N = 165) showed a statistically significant correlation between this ratio and body mass index (r = 0.242, p = 0.012). Individuals with normal DXA (N = 148) were found to present a statistically significant, negative correlation between calcium-to-magnesium ratio and P1NP (r = -0.249, p = 0.027), respectively, between calcium-to-phosphorus ratio and CrossLaps (r = -0.271, p = 0.009). Osteoporotic tumor free patients showed a correlation between calcium-to-phosphorus ratio and PTH (N = 50; r = 0.473, p = 0.005). (Table 5)

Table 5: Correlations between the calcium-to-magnesium ratio, respectively, calcium-to-phosphorus ratio and study parameters within the control group

	Calcium-to-magnesium ratio			Calcium-to-phosphorus ratio		
Parameter, unit, normal ranges	Osteoporosis	Osteopenia	Normal DXA	Osteoporosis	Osteopenia	Normal DXA
Age (years)	r = 0.136	**r = 0.178**	r = 0.085	r = -0.112	r = 0.152	r = 0.049

	p = 0.363	**p = 0.034**	p = 0.345	p = 0.458	p = 0.067	p = 0.584
Years since menopause	r = 0.079 p = 0.668	r = 0.166 p = 0.094	r = 0.036 p = 0.745	r = -0.159 p = 0.392	r = 0.060 p = 0.543	r = 0.099 p = 0.365
Body mass index (kg/sqm)	r = -0.171 p = 0.366	r = 0.188 p = 0.054	r = -0.026 p = 0.803	r = 0.078 p = 0.694	**r = 0.242** **p = 0.012**	r = 0.067 p = 0.526
Fasting glycemia (mg/dL)	r = 0.065 p = 0.670	**r = 0.253** **p = 0.003**	r = 0.168 p = 0.072	r = -0.004 p = 0.978	**r = 0.239** **p = 0.004**	r = -0.012 p = 0.899
Glycated haemoglobin A1c (%)	r = 0.141 p = 0.566	**r = 0.220** **p = 0.045**	r = -0.098 p = 0.386	r = -0.159 p = 0.516	**r = 0.342** **p = 0.001**	r = -0.100 p = 0.374
PTH (pg/mL)	r = 0.145 p = 0.422	r = -0.019 p = 0.856	r = -0.198 p = 0.071	**r = 0.473** **p = 0.005**	r = 0.119 p = 0.247	r = 0.159 p = 0.146
25OHD (ng/mL)	r = -0.017 p = 0.912	r = -0.074 p = 0.405	r = 0.026 p = 0.792	r = 0.245 p = 0.122	r = 0.059 p = 0.503	r = -0.063 p = 0.525
P1NP (ng/mL)	r = -0.099 p = 0.631	r = -0.193 p = 0.082	**r = -0.249** **p = 0.027**	r = -0.264 p = 0.202	r = -0.257 p = 0.021	r = -0.139 p = 0.239
Alkaline phosphatase (U/L)	r = -0.188 p = 0.246	r = -0.047 p = 0.589	r = -0.175 p = 0.070	r = 0.169 p = 0.290	**r = -0.169** **p = 0.047**	r = -0.237 p = 0.012
Osteocalcin (ng/mL)	r = 0.082 p = 0.642	**r = -0.196** **p = 0.030**	r = -0.147 p = 0.166	r = 0.077 p = 0.658	**r = -0.287** **p = 0.001**	r = -0.180 p = 0.089
CrossLaps (ng/mL)	r = 0.187 p = 0.268	**r = -0.193** **p = 0.034**	r = -0.145 p = 0.166	r = 0.045 p = 0.790	**r = -0.263** **p = 0.003**	**r = -0.271** **p = 0.009**
Lumbar (L1-4) bone mineral density	r = -0.015 p = 0.931	r = 0.036 p = 0.701	r = -0.047 p = 0.163	r = 0.126 p = 0.457	r = 0.008 p = 0.927	r = -0.175 p = 0.061
Lumbar (L1-4) T-score	r = 0.140 p = 0.347	r = 0.035 p = 0.676	r = 0.004 p = 0.963	r = 0.210 p = 0.161	r = -0.014 p = 0.867	r = -0.159 p = 0.076
Lumbar (L1-L4) Z-score	r = 0.183 p = 0.229	r = 0.031 p = 0.724	r = 0.030 p = 0.746	r = 0.054 p = 0.729	r = -0.035 p = 0.694	r = -0.122 p = 0.185
ACTH (pg/mL)	r = 0.500 p = 0.391	r = -0.095 p = 0.748	r = 0.139 p = 0.701	r = 0.800 p = 0.104	r = -0.280 p = 0.354	r = 0.200 p = 0.555
Plasma morning cortisol (µg/dL)	r = 0.029 p = 0.957	r = 0.119 p = 0.713	r = -0.139 p = 0.701	r = -0.400 p = 0.505	r = -0.343 p = 0.276	r = 0.491 p = 0.150
Post-ODST cortisol (µg/dL)	r = -0.200 p = 0.998	r = -0.400 p = 0.900	r = -0.300 p = 0.890	r = -0.720 p = 0.789	r = -0.120 p = 0.897	r = -0.460 p = 0.895
TSH (µUI/mL)	r = 0.194 p =0.196	r = 0.011 p = 0.895	r = -0.072 p = 0.429	r = 0.157 p = 0.302	r = -0.084 p = 0.324	r = -0.042 p = 0.644
FT4 (pmol/L)	r = -0.050 p = 0.752	r = 0.098 p = 0.271	r = 0.050 p = 0.597	r = -0.093 p = 0.570	r = 0.068 p = 0.448	r = -0.122 p = 0.199

DISCUSSION

In this study, we included 474 patients with adrenal incidentalomas (N = 111), who displayed a post-ODST cortisol less than 5 µg/dL, respectively, < 1.8 µg/dL in control group (N = 363). The cohort with tumors actually involved two sub-categories: those with a true non-functional profile (a post-ODST cortisol level less than 1.8 µg/dL) and those with a mild autonomous cortisol secretion (a post-ODST cortisol value between 1.8 and 5 µg/dL) [31,32]. (Figure 3A+B+C+D)

Figure 3A: Case sample analysis: abdominal CT scan with a left adrenal incidentaloma – yellow arrow (arterial phase, transversal plane) in a menopausal woman who underwent CT scan for osteoporotic vertebral fractures-related persistent pain

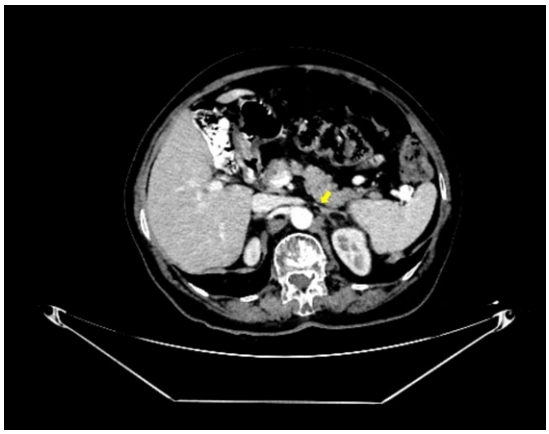


Figure 3B: A menopausal woman with a right adrenal incidentaloma on CT – yellow arrow

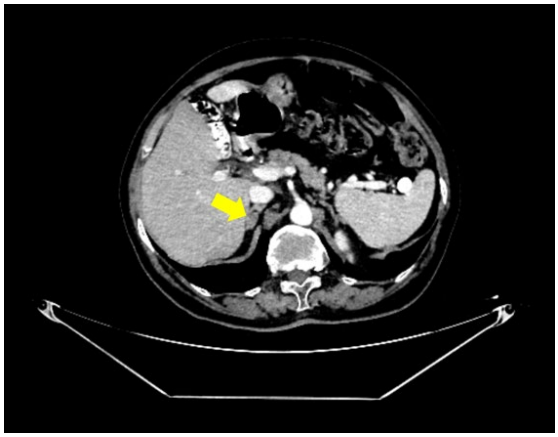


Figure 3C: Osteopenia at central (lumbar) DXA (GE Lunar Prodigy device) showing a T-score at L1-L4 lumbar spine of -1.2

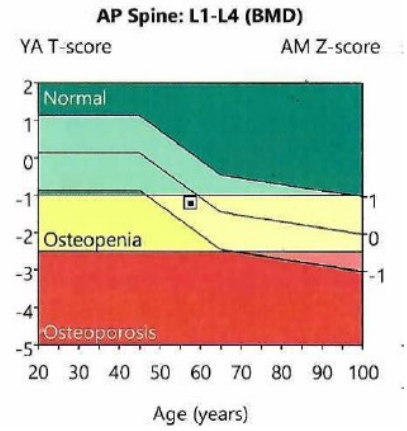


Figure 3D: Red arrows point T8, T9, T10 thoracica vertebral fractures at CT scan with intravenous contrast (bone window, sagittal plane) in a menopausal female



We enrolled them across the same cluster of analysis since, recently, alternative biomarkers of ACTH-cortisol axis exploration have been proposed to help the characterization of these tumors in addition to the cutoffs of post-ODST cortisol measurements [33-37]. For instance, adrenal androgens suppression, the combination of post-ODTS cortisol with baseline morning ACTH value, different assays of urinary and salivary cortisol, etc. suggested that post-ODST might not be a stand-alone marker of the hormonal profile in adults with adrenal cortex adenomas that were incidentally detected (in the absence of a fully manifested clinical picture of Cushing's syndrome) [38-41]. Notably, we found no particular association between post-ODST or baseline cortisol and calcium-to-magnesium/calcium-to-phosphorus ratios, nor with morning plasma ACTH.

Calcium-to-magnesium ratio was similar between DXA sub-groups in each study group. In tumor group: the ratio corelated with age ($r = 0.288$, $p = 0.047$), P1NP ($r = -0.459$, $p = 0.011$), osteocalcin ($r = -0.37$, $p = 0.026$) and CrossLaps ($r = -0.446$, $p = 0.006$) in subjects with normal DXA (N = 51), while in osteoporotic females (N = 19), it associated with glycated hemoglobin A1c ($r = 0.596$, $p = 0.025$). In control group: the ratio corelated with age ($r = 0.178$, $p = 0.034$), fasting glycemia ($r = 0.253$, $p= 0.003$), glycated hemoglobin A1c ($r = 0.22$, $p = 0.045$), osteocalcin ($r = -0.196$, $p = 0.03$), and CrossLaps ($r= -0.193$, $p = 0.034$) in osteopenic subjects (N = 165), respectively, with P1NP ($r = -0.249$, $p = 0.027$) in normal DXA sub-group (N = 148).

Interestingly, we pointed out that the ratio gains a distinct significance depending on the DXA category, not in comparing between-group differences, but in the correlations with circulating bone markers. This aspect may be related to an abnormal level of calcium, magnesium or both, noting that patients with prior medication against osteoporosis were ruled out, but we could not quantify the calcium/magnesium intake via food and supplements, and this might come as a potential bias [42]. Of note, we found no correlation with bone mass at DXA, and some prior data suggested that calcium intake might be more important in this matter (not the circulating level), but not all authors agree [43].

The association between calcium-to-magnesium ratio and glycemia, respectively, glycated hemoglobin A1 (that was found in some sub-groups, not all) pinpoints its metabolic contribution irrespective of the DXA results, since a low magnesium and a higher calcium are prone to endothelial dysfunction, increased oxidative stress and impairment of insulin release and peripheral actions [44,45]. Whether the additional contribution of tumor-related cortisol represents a co-loop is still an open matter. For instance, Alsheikh et al. [18] analyzed the impact of serum calcium-to-magnesium ratio in adults diagnosed with metabolic syndrome. This was a cross-sectional analysis in 9693 residents from Qatar amid prior data collection at Qatar Biobank. 19% of the study population fulfilled the criteria of metabolic syndrome. Serum magnesium was statistically significant higher in the patients confirmed with the syndrome versus those who were syndrome-free (0.83 ± 0.06 mmol/L versus 0.81 ± 0.08 mmol/L, $p < 0.05$). On the contrary, the serum calcium-to-magnesium ratio was higher in the group with metabolic syndrome versus controls (2.30 ± 0.08 mmol/L, 2.77 ± 0.23 mmol/L, $p < 0.05$). An inverse association between magnesium quartiles and the presence of metabolic syndrome was found, as opposite to a positive dose-response with respect to calcium-to-magnesium ratio, respectively, serum total calcium and the diagnosis of the metabolic syndrome [18].

Other applications of the calcium-to-magnesium ratio involve the association with the risk of kidney stones in primary hyperparathyroidism, which was proposed as a novel biomarker under these specific circumstances (in addition to the traditional value of 24-hour urinary calcium). Yalçın et al. [20] studied 367 patients diagnosed with primary hyperparathyroidism, and

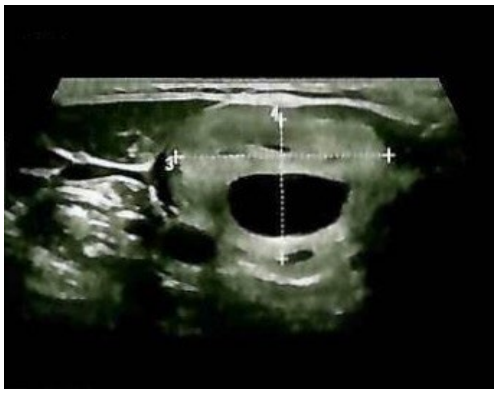
receiver operating characteristics showed an optimal cutoff of 6.35, while multivariate regression proved the ratio to be an independent predictor of nephrolithiasis [20]. In addition, Kabaswa et al. [17] analyzed the calcium-to-magnesium ratio, not only according the studied population's intake, but, also, in albuminuria, noting that both minerals homeostasis involves a normal kidney function [46-48]. This was a cross-sectional, community-based study in Japan (N = 6,849 patients of 40 years or older, with an average age of 68.8 years, and more than a half were women). A lower intake of both minerals was corelated with a log-transformed albumin-to-creatinine ratio, while, after adjustment, only calcium remained statistically significant. These findings suggested that magnesium should be cautiously interpreted depending on the calcium intake, and their ratio might become more relevant for practical purposes than individually analyzing each of them [17].

A second analysis involved the calcium-to-phosphorus ratio in menopausal females who, of note, were excluded if they presented traditional anomalies of the mineral metabolism. In the tumor group: the ratio was lower in osteoporosis versus osteopenia (N = 19, 2.40 ± 0.39 versus N = 41, 2.70 ± 0.46 mg/dL, p = 0.035), respectively, versus normal DXA sub-group (N = 51, 2.72 ± 0.36 mg/dL, p = 0.018). Only in osteopenia patients (N = 41) the ratio corelated with body mass index (r = -0.426, p = 0.011), P1NP (r = -0.509, p = 0.026), and osteocalcin (r = -0.435, p = 0.018).

In control group, osteopenic subjects (N = 165) had this ratio associated with body mass index (r = 0.242, p = 0.012), fasting glycemia (r = 0.239, p = 0.004), glycated hemoglobin A1c (r = 0.342, p = 0.001), osteocalcin (r = -0.287, p = 0.001), CrossLaps (r = -0.263, p = 0.003), alkaline phosphatase (r = -0.169, p = 0.047); in women with normal DXA (N = 148) the ratio correlated with CrossLaps (r = -0.271, p = 0.009). Osteoporotic tumor-free patients showed a correlation between the ratio and PTH (N = 50; r = 0.473, p = 0.005). The ratio was decreased in osteoporotic females with tumors versus those who were osteoporotic, but tumor-free (N = 19, 2.40 ± 0.39 versus N = 50, 2.66 ± 0.44 mg/dL, p = 0.036). Notably, a lower phosphorus might involve an anomaly of vitamin D metabolism; however, in the present cohort, we found no correlations of the studied ratios with 25OHD. Also, PTH might increase calcium and decrease phosphorus, which potentially explains the association with the hormone. The calcium-to-phosphorus ratio might be more important in patients under hemodialysis or those with recurrent kidney stones [49-53].

The limits of the current study involve the transversal design. An interesting analysis should expand the panel of metabolic issues that have been co-diagnosed in the patients with apparently non-functional adrenal tumours/mild autonomous cortisol secretion (e.g. criteria for metabolic syndrome). The distinction of the tumours with mild autonomous cortisol secretion (post-ODST cortisol between 1.8 and 5 μg/dL) potentially show a distinct profile with respect to calcium-to-magnesium ratio and further multiple regression models could reveal a multifactorial model, including imaging interplay [54-57]. Of note, this is a study in accidentally detected adrenal masses in patients who were evaluated amid an endocrine (clinical) setting and we did not provide an analysis of the primary endocrine condition on first admission such as goiter. (Figure 4)

Figure 4: This is a post-menopausal woman who was detected with an adrenal incidentaloma starting from the assessment of the thyroid gland; the goiter has indication for thyroidectomy; in this capture: thyroid ultrasound showing isoechoic, inhomogeneous pattern; right thyroid lobe with a isoechoic, inhomogeneous macro-nodule, with necrosis areas and peripheral and mild intra-nodular vascularization of 4.23/1.84/2.84 cm (transverse plane)



Future inclusion of calcium, magnesium and phosphorus intake in the analysis of their blood levels may improve their practical approach, including the interpretation of the circulating levels. Bone-specific alkaline phosphatase potentially reflects more accurately the bone turnover rather than total alkaline phosphatase, an assay which is not available in our university hospital. In the light of a wider frame of assessments to characterize the adrenal profile, adrenal androgens, urinary free cortisol and midnight salivary cortisol assays might help, as well as urinary metabolomic analysis of the steroidogenesis-related markers [58-64].

CONCLUSION

In this study of 474 menopausal women, we pointed out that the calcium-to-magnesium ratio potentially gains distinct significance depending on the DXA sub-category in an exploratory analysis, not in comparing between-group differences, but in the correlations with circulating bone markers. The mentioned subgroup correlations remain exploratory at this point. Osteopenic (tumor-negative) and normal DXA (tumor-positive) subjects showed a direct association between the ratio and patients' age, while the ratio was correlated with the bone turnover biomarkers distinctly across DXA subgroups. Additionally, the ratio might reflect a more severe glucose profile, as shown by glycated hemoglobin A1c. Notably, we found no particular association between baseline or post-ODST cortisol, nor ACTH and calcium-to-magnesium/calcium-to-phosphorus ratios. No direct correlation with bone mass at DXA was established. Osteoporotic tumor-free patients showed a positive correlation between the calcium-to-phosphorus ratio and PTH. This ratio was decreased in osteoporotic females with adrenal incidentalomas versus those who were osteoporotic, but tumor-free, which highlights potential influence of the adrenal-related status.

Conflicts of interest and sources of funding

The authors declare no conflict of interest. This research received no external funding.

Acknowledgments

This is part of PhD research no. no. 27859 from 30 September 2024. This is a collaboration with the project "Biomarkers in endocrine tumours—limits of the clinical decision" (ethical approval no. 37 from 26 November 2024).

Authors' contribution

Conceptualization, M.-L.C., A.-I.T., A.D., A.-M.G., G.V., D.M., M.C., and L.S.; methodology, M.-L.C., A.-I.T., A.D., A.-M.G., G.V., D.M., M.C., and L.S.; software, M.-L.C., A.-I.T., and L.S.; validation, M.-L.C., A.-I.T., A.D., A.-M.G., M.C., and L.S.; formal analysis, M.-L.C., A.-I.T., A.D., A.-M.G., G.V., M.C., and L.S.; investigation, M.-L.C., A.-I.T., A.-M.G., G.V., D.M., M.C., and L.S.; resources, M.-L.C., A.-I.T., A.D., D.M., M.C., and L.S.; data curation, M.-L.C., A.-I.T., A.D., A.-M.G., G.V., D.M., M.C., and L.S.; writing—original draft preparation A.-I.T.; writing—review and editing, M.-L.C., A.-I.T., A.D., A.-M.G., M.C., and L.S.; visualization, M.-L.C.; supervision, M.-L.C.; project administration, M.-L.C.; funding acquisition, M.-L.C. All authors have read and agreed to the published version of the manuscript.

Ethics approval and consent to participate

The Ethics Committee of Scientific Research of Carol Davila University of Medicine and Pharmacy, Bucharest, Romania, approved this study (No. 29336 from 17 October 2025) and C.I Parhon National Institute of Endocrinology, Bucharest, Romania (no. 37 from 26 November 2024).

Patient consent for publication

Patient consent was waived due to retrospective design.

References

1. Zhang Y, Luo J, Tan Y, Wang Z, Qian K, Chen W, et al. Impact of Calcium-Magnesium Ratio in Purified Water Remineralization on Calcium Oxalate Crystal Formation and Renal Injury. Nutrients. 2026;18(5):792. https://doi.org/10.3390/nu18050792. PMID: 41829962. PMCID: PMC12986501.

2. Shahsavani Z, Masoumi SJ, Barati-Boldaji R, Shamshirgardi E, Kafipour R, Sohrabi Z, et al. Dietary Calcium to Magnesium Ratio and Risk of Cardiovascular Diseases. Biol Trace Elem Res. 2025;203(11):5581-5588. https://doi.org/10.1007/s12011-025-04587-0. PMID: 40123040.

3. Deng K, Liu J, Miao Y, Wang G, Wang X, Liu S, et al. The effects of magnesium and vitamin D/E co-supplementation on inflammation markers and lipid metabolism of obese/overweight population: a systematic review and meta-analysis. Front Nutr. 2025;12:1563604. https://doi.org/10.3389/fnut.2025.1563604. PMID: 40959697. PMCID: PMC12433974.

4. Moradmand Z, Mirzaei S, Asadi A, Akhlaghi M, Tirani SA, Saneei P. Dietary Magnesium and Calcium Intake in Relation to Metabolic Health Status in Iranian Adolescents with Overweight and Obesity. Curr Dev Nutr. 2026;10(2):107634. https://doi.org/10.1016/j.cdnut.2025.107634. PMID: 41674720. PMCID: PMC12887371.

5. Mitrica M, Vasiliu O, Plesa A, Sirbu OM. Multinodular and vacuolating neuronal tumor. Rom J Mil Med. 2025;CXXVIII(1):10-16. https://doi.org/10.55453/rjmm.2025.128.1.2.

6. Manea MM, Dragos D, Ghenu MI, Enache II, Stoican IC, Ciulavu C, et al. The Neurocardiogenic Impact of Ischemic Stroke: Intricacies of Cardiac Enzymes and the Vegetative System. Rom J Mil Med. 2025;CXXVIII(1):36-42. https://doi.org/10.55453/rjmm.2025.128.1.5.

7. Ahmed S, Sattar AA, Siddiqui I. Magnesium - The Silent Partner or the Next Vitamin D? Shifting Paradigm in Mineral Metabolism in Health and Disease. EJIFCC. 2026;37(1):5-8. PMID: 41659294. PMCID: PMC12882071.

8. Paduraru DN, Nica A, Carsote M, Valea A. Adrenalectomy for Cushing's syndrome: do's and don'ts. J Med Life. 2016;9(4):334-341.

9. Chiarello DI, Marín R, Proverbio F, Benzo Z, Piñero S, Botana D, et al. Effect of hypoxia on the calcium and magnesium content, lipid peroxidation level, and Ca2+-ATPase activity of syncytiotrophoblast plasma membranes from placental explants. Biomed Res Int. 2014;2014:597357. https://doi.org/10.1155/2014/597357. PMID: 25180187. PMCID: PMC4142282.

10. Cheung MM, Dall RD, Shewokis PA, Altasan A, Volpe SL, Amori R, et al. The effect of combined magnesium and vitamin D supplementation on vitamin D status, systemic inflammation, and blood pressure: A randomized double-blinded controlled trial. Nutrition. 2022;99-100:111674. https://doi.org/10.1016/j.nut.2022.111674. PMID: 35576873.

11. Valea A, Ghervan C, Morar A, Pop DD, Carsote M, Albu SE, et al. Hashimoto's thyroiditis and breast cancer: coincidence or correlation? Arch Balk Med Union. 2016;51(1):129-32.

12. Yilmaz E, Ünver S. Investigation of the relationship between magnesium level and vitamin D, bone mineral density, and chronic diseases in patients with knee osteoarthritis. Magnes Res. 2023;36(2):40-48. https://doi.org/10.1684/mrh.2023.0515. PMID: 37897257.

13. Nelson DJ, Sommerville LJ. Chronic Latent Magnesium Deficiency and an Unbalanced Calcium-to-Magnesium Ratio Impact Fetal Development and Maternal Health. J Diet Suppl. 2026;23(2):268-289. https://doi.org/10.1080/19390211.2026.2624107. PMID: 41618740.

14. Udenze IC, Arikawe AP, Azinge EC, Okusanya BO, Ebuehi OA. Calcium and Magnesium Metabolism in Pre-Eclampsia. West Afr J Med. 2014;33(3):178-82. PMID: 26070821.

15. Bjørklund G, Butnariu M, Gurgas L, Hangan T. Vitamin D and Diabetes: Exploring the Link, Prevention, and Management. Curr Med Chem. 2026;33(4):689-707. https://doi.org/10.2174/0109298673360987250621042131. PMID: 40641014.

16. Kovacs CS. Calcitriol's role in fetal bone and mineral metabolism: Evidence from human and animal studies. J Steroid Biochem Mol Biol. 2026;256:106896. https://doi.org/10.1016/j.jsbmb.2025.106896. PMID: 41223950.

17. Kabasawa K, Hosojima M, Nakamura K, Takachi R, Sawada N, Tsugane S, et al. Associations of calcium and magnesium intakes and their intake ratio with albuminuria in middle-aged and older adults. PLoS One. 2025;20(11):e0335412. https://doi.org/10.1371/journal.pone.0335412. PMID: 41296656. PMCID: PMC12654892.

18. Alsheikh R, Aldulaimi H, Hinawi R, Al-Sadi F, Al-Baker A, Alkuwari A, et al. Association of serum magnesium and calcium with metabolic syndrome: a cross-sectional study from the Qatar-biobank. Nutr Metab (Lond). 2025;22(1):8. https://doi.org/10.1186/s12986-024-00892-y. PMID: 39885554. PMCID: PMC11783880.

19. Sandru F, Dumitrascu MC, Albu SE, Carsote M, Valea A. Hyperpigmentation and ACTH – an overview of literature. Ro Med J. 2019;66(4):309-12. https://doi.org/:10.37897/RMJ.2019.4.20.

20. Yalçın N, Ertınmaz Özkan A, Güneş E, Koca N. Calcium to magnesium ratio as a superior biomarker for nephrolithiasis detection in primary hyperparathyroidism. Sci Rep. 2025;15(1):3545. https://doi.org/10.1038/s41598-025-86954-4. PMID: 39875421. PMCID: PMC11775213.

21. Lanna CM, Paula FJ, Montenegro RM Jr, Moreira AC, Foss MC. Parathyroid hormone secretion in chronic human endogenous hypercortisolism. Braz J Med Biol Res. 2002;35(2):229-36. https://doi.org/10.1590/s0100-879x2002000200012. PMID: 11847527.

22. da Silva MMR, Bilezikian JP, de Paula FJA. Phosphate metabolism: its impact on disorders of mineral metabolism. Endocrine. 2025;88(1):1-13. https://doi.org/10.1007/s12020-024-04092-9. PMID: 39527339.

23. Saillant A, Try M, Laparra A, Lecoq AL, Zaidan M. Electrolyte disorders in oncological patients. Bull Cancer. 2024;111(7-8):687-700. https://doi.org/10.1016/j.bulcan.2023.04.014. PMID: 37208250.

24. Prinzi A, Lombardo AM, Finocchiaro S, Galvano A, Vella V, Frasca F, et al. Expanding the Clinical Profile of Mild Autonomous Cortisol Secretion: New Diagnostic Markers and Emerging Complications. Endocr Pract. 2026;32(1):46-52. https://doi.org/10.1016/j.eprac.2025.09.009. PMID: 40972722.

25. Nicola (Marioara) OM, Popescu M, Vladoianu CN, Carlig V, Carsote M, Ghenea AE. Study of cognitive dyfunctions in thyroid pathology. Curr Health Sciences J. 2021;47(2):256-62. https://doi.org/10.12865?CHSJ.47.02.16.

26. Kanis JA, Cooper C, Rizzoli R, Reginster JY; Scientific Advisory Board of the European Society for Clinical and Economic Aspects of Osteoporosis and Osteoarthritis (ESCEO) and the Committees of Scientific Advisors and National Societies of the International Osteoporosis Foundation (IOF). Executive summary of the European guidance for the diagnosis and management of osteoporosis in postmenopausal women. Calcif Tissue Int. 2019;104(3):235-238. https://doi.org/10.1007/s00223-018-00512-x. PMID: 30796490. PMCID: PMC6422308.

27. Hiligsmann M, Reginster JY, Tosteson ANA, Bukata SV, Saag KG, Gold DT, et al. Recommendations for the conduct of economic evaluations in osteoporosis: outcomes of an experts' consensus meeting organized by the European Society for Clinical and Economic Aspects of Osteoporosis, Osteoarthritis and Musculoskeletal Diseases (ESCEO) and the US branch of the International Osteoporosis Foundation. Osteoporos Int. 2019;30(1):45-57. https://doi.org/10.1007/s00198-018-4744-x. PMID: 30382319. PMCID: PMC6331734.

28. American Diabetes Association Professional Practice Committee for Obesity. Pharmacologic treatment of obesity in adults: Standards of care in overweight and obesity. BMJ Open Diabetes Res Care. 2026;13(Suppl 1):e005729. https://doi.org/10.1136/bmjdrc-2025-005729. PMID: 41529914. PMCID: PMC12815056.

29. Yoshida Y, Horiuchi K, Otsuki M, Okamoto T. Diagnosis and management of adrenal incidentaloma: use of clinical judgment and evidence in dialog with the patient. Surg Today. 2024;54(12):1417-1427. https://doi.org/10.1007/s00595-023-02781-y. PMID: 38091063. PMCID: PMC11582175.

30. Poiana C, Musat M, Carsote M, Chirita C. Premenstrual dysphoric disorder: neuroendocrine interferences, Rev Med Chir Soc Med Nat Iasi. 2009;113(4):996-1000. PMID: 20191865.

31. Rowe NE, Kumar R, Schieda N, Siddiqi F, McGregor T, McAlpine K, et al. Diagnosis, Management, and Follow-Up of the Incidentally Discovered Adrenal Mass: CUA Guideline Endorsed by the AUA. J Urol. 2023;210(4):590-599. https://doi.org/10.1097/JU.0000000000003644. PMID: 37556768.

32. Fassnacht M, Tsagarakis S, Terzolo M, Tabarin A, Sahdev A, Newell-Price J, et al. European Society of Endocrinology clinical practice guidelines on the management of adrenal incidentalomas, in collaboration with the European Network for the Study of Adrenal Tumors. Eur J Endocrinol. 2023;189(1):G1-G42. https://doi.org/10.1093/ejendo/lvad066. PMID: 37318239.

33. Dumitru N, Ghemigian A, Carsote M, Albu SE, Terzea D, Valea A. Thyroid nodules after initial evaluation by primary health care practitioners: an ultrasound pictorial essay. Arch Balk Med Union. 2016;51(3):434-8.

34. Issa BG, Hanna FWF, Fryer AA, Ensah G, Ebere I, Marshall D, et al. The Utility of Salivary Cortisone in the Overnight Dexamethasone Suppression Test in Adrenal Incidentalomas. J Clin Endocrinol Metab. 2023;108(10):e937-e943. https://doi.org/10.1210/clinem/dgad242. PMID: 37155577.

35. Vasiliu O. Impact of SGLT2 inhibitors on metabolic status in patients with psychiatric disorders undergoing treatment with second-generation

antipsychotics (Review). Exp Ther Med. 2023;25(3):125. https://doi.org/10.3892/etm.2023.11824. PMID: 36845949. PMCID: PMC9947579.

36. Muth A, Sundin A, Zedenius J. Many adrenal incidentalomas are not adequately evaluated - updated guidelines to improve follow-up are presented. Lakartidningen. 2023;120:23045. PMID: 37337898.

37. Vasiliu O, Panea CA, Mangalagiu AG, Petrescu BM, Cândea CA, Manea MM, et al. Case Management of Delirium in Patients with Major Neurocognitive Disorders. Rom J Mil Med. 2025;CXXVIII(1):67-77. https://doi.org/10.55453/rjmm.2025.128.1.9.

38. Annesi CA, Talutis SD, Goldman AL, Childs E, Knapp PE, McAneny D, et al. Point-of-care access to clinical guidelines may improve management of incidental findings in the primary care setting. J Eval Clin Pract. 2023;29(4):632-638. https://doi.org/10.1111/jep.13806. PMID: 36602429.

39. Rebelo JFD, Costa JM, Junqueira FD, Fonseca AO, de Almeida ABABS, Moraes AB, et al. Adrenal incidentaloma: Do patients with apparently nonfunctioning mass or autonomous cortisol secretion have similar or different clinical and metabolic features? Clin Endocrinol (Oxf). 2023;98(5):662-669. https://doi.org/10.1111/cen.14861. PMID: 36514987.

40. Jackson BS. Adrenal Incidentaloma Controversial Size Recommendations. Urol Res Pract. 2023;49(2):96-99. https://doi.org/10.5152/tud.2023.22245. PMID: 37877855. PMCID: PMC10192718.

41. Chen AX, Burt MG. Cardio-metabolic pathophysiology in mild glucocorticoid excess: Potential implications for management of adrenal incidentaloma. Clin Endocrinol (Oxf). 2023;98(2):153-164. https://doi.org/10.1111/cen.14850. PMID: 36367077.

42. Costello RB, Rosanoff A, Dai Q, Saldanha LG, Potischman NA. Perspective: Characterization of Dietary Supplements Containing Calcium and Magnesium and Their Respective Ratio-Is a Rising Ratio a Cause for Concern? Adv Nutr. 2021;12(2):291-297. https://doi.org/10.1093/advances/nmaa160. PMID: 33367519. PMCID: PMC8264923.

43. Fouhy LE, Mangano KM, Zhang X, Hughes BD, Tucker KL, Noel SE. Association between a Calcium-to-Magnesium Ratio and Osteoporosis among Puerto Rican Adults. J Nutr. 2023;153(9):2642-2650. https://doi.org/10.1016/j.tjnut.2023.05.009. PMID: 37164266. PMCID: PMC10550845.

44. Moia MN, Lima SCVC, da Silva Nunes FL, Queiroz SIML, Marchioni DML, Pedrosa LFC, et al.

Plasma Levels of Magnesium, Calcium, Calcium to Magnesium Ratio, and Associations with Metabolic Syndrome and Cardiometabolic Risk Factors. Biol Trace Elem Res. 2024;202(12):5307-5318. https://doi.org/10.1007/s12011-024-04088-6. PMID: 38347294.

45. Lv Y, Aihemaiti G, Guo H. Effect of Dietary Approaches to Stop Hypertension (DASH) on Patients with Metabolic Syndrome and Its Potential Mechanisms. Diabetes Metab Syndr Obes. 2024;17:3103-3110. https://doi.org/10.2147/DMSO.S477739. PMID: 39206416. PMCID: PMC11350064.

46. Ahmed HS. Vitamin D and Mineral Ion Regulation. Adv Exp Med Biol. 2026;1493:69-89. https://doi.org/10.1007/978-3-032-04357-3_6. PMID: 41219599.

47. Bjørklund G, Butnariu M, Gurgas L, Hangan T. Vitamin D and Diabetes: Exploring the Link, Prevention, and Management. Curr Med Chem. 2026;33(4):689-707. https://doi.org/:10.2174/0109298673360987250621042131. PMID: 40641014.

48. Silva TDBD, Vieira GMM, Fraga LTS, Fernandes WD, Sakane EN, Maeda SS. Supplements for bone health. Arch Endocrinol Metab. 2025;70(Spe1):e20250374. https://doi.org/10.20945/2359-4292-2025-0374. PMID: 41370665. PMCID: PMC12714311.

49. Bubulac L, Zivari M, Eremia IA, Erena C, Gheorghe CM, Gheorghe IR, et al. Stress, Anxiety, and Self-Efficacy in Hypertension: Evidence from a Romanian Case-Control Study. Diseases. 2025;13(11):373. https://doi.org/10.3390/diseases13110373. PMID: 41294913.

50. Li J, Hu Y, Yang Y, Lin D, He X, Hu L, et al. Analysis of risk factors related to osteoporosis in maintenance hemodialysis patients. Clin Nephrol. 2026;105(1):1-11. https://doi.org/10.5414/CN111686. PMID: 41208347.

51. Bogdan-Andreescu CF, Bubulac L, Albu CC, Slăvescu DA, Bănăţeanu AM, Botoacă O, et al. Toward Smart Salivary Diagnostics: A Comprehensive Review of Heavy Metal Biomarkers and Digital Risk Modeling. Diagnostics (Basel). 2026;16(4):635. https://doi.org/10.3390/diagnostics16040635. PMID:41750781.

52. Wawrzyniak A, Klimczyk P, Woźniak A, Anyżewska A, Leonkiewicz M. Assessment of differences in nutrients consumption in women diagnosed with osteoporosis as compared to a healthy control group. Rocz Panstw Zakl Hig. 2017;68(2):143-149. PMID: 28646831.

53. Bubulac L, Gheorghe IR, Ungureanu E, Bogdan-Andreescu CF, Albu CC, Gheorghe CM, et al. Promoting Re-Epithelialization in Diabetic Foot Wounds Using Integrative Therapeutic Approaches. Bioengineering (Basel). 2025;12(10):1053. https://doi.org/10.3390/bioengineering12101053. PMID:41155052.

54. Anichini M, Grazzini G, Mattolini L, Codignola G, Paolucci S, Pradella S, et al. xsCT-based radiomics for adrenal incidentaloma characterization. Radiol Med. 2026. https://doi.org/10.1007/s11547-026-02278-x. PMID: 42753040.

55. Bubulac L, Seche E, Zivari M, Erena C, Popescu-Spineni DM, Bogdan-Andreescu CF, et al. Psychological Stress and Anxiety in Autoimmune Diseases: A Cross-Sectional Case-Control Study. Healthcare (Basel). 2026;14(16):2584. https://doi.org/10.3390/healthcare14162584. PMID: 42651355.

56. Frisina P, Ricci P, Valentini F, Messineo D. Radiomic Characterization of Adrenal Incidentalomas on NECT: Retrospective Exploratory Study and Systematic Review. J Imaging. 2026;12(4):151. https://doi.org/10.3390/jimaging12040151.

57. Russu EA, Popa LG, Păunică S, Bubulac L, Giurcăneanu C, Albu CC. Patient-Reported Outcomes on Quality of Life in Older Adults with Oral Pemphigus. Healthcare (Basel). 2025;13(22):2843. https://doi.org/10.3390/healthcare13222843. PMID: 41302231.

58. Nakao H, Yokomoto-Umakoshi M, Nakatani K, Umakoshi H, Ogata M, Fukumoto T, et al. Adrenal steroid metabolites and bone status in patients with adrenal incidentalomas and hypercortisolism. EBioMedicine. 2023;95:104733. https://doi.org/10.1016/j.ebiom.2023.104733. PMID: 37543511. PMCID: PMC10505782.

59. Bogdan-Andreescu CF, Albu ŞD, Slăvescu DA, Bubulac L, Tudor V, Botoacă O, et al. Periodontitis-Induced Immune Reprogramming: Implications for Cancer Immunotherapy Response. Biomedicines. 2026;14(2):480. https://doi.org/10.3390/biomedicines14020480. PMID:

41751379.

60. Araujo-Castro M, Pascual-Corrales E, García Cano AM, Marchan M, Casals G, Hanzu FA, et al. Evaluation of Body Composition in Patients With and Without Adrenal Tumors and Without Overt Hypersecretory Syndromes. Endocr Pract. 2023;29(2):110-118. https://doi.org/10.1016/j.eprac.2022.11.009. PMID: 36455692.

61. Bubulac L, Georgescu T, Zivari M, Popescu-Spineni DM, Albu CC, Bobu A, et al. An Integrative Review of Computational Methods Applied to Biomarkers, Psychological Metrics, and Behavioral Signals for Early Cancer Risk Detection. Bioengineering (Basel). 2025;12(11):1259. https://doi.org/10.3390/bioengineering12111259. PMID: 41301215.

62. Bloomgarden NA, Berkenblit R. Adrenal Incidentalomas: Modern Tools to Address a Condition of Modern Times. Endocrinol Metab Clin North Am. 2026;55(2):239-257. https://doi.org/10.1016/j.ecl.2026.01.003. PMID: 42067268.

63. Montalvão PVG, Mangueira IM, Alves GDM, Cordeiro JVF, Costa MHS, Ravanini GAG. Evaluation of adrenal tumors and analysis of the metabolic profile of patients with incidentaloma. Rev Col Bras Cir. 2025;51:e20243685. https://doi.org/10.1590/0100-6991e-20243685-en. PMID: 39841720. PMCID: PMC11702972.

64. Mu D, Qian X, Ma Y, Wang X, Gao Y, Ma X, et al. Plasma Steroid Profiling Combined With Machine Learning for the Differential Diagnosis in Mild Autonomous Cortisol Secretion From Nonfunctioning Adenoma in Patients With Adrenal Incidentalomas. Endocr Pract. 2024;30(7):647-656. https://doi.org/10.1016/j.eprac.2024.04.008. PMID: 38657794.

Guidelines for authors

Thank you for your interest in the Romanian Journal of Military Medicine. Please read the complete Author Guidelines carefully before submission, including the section on copyright.

To ensure fast peer review and publication, manuscripts that do not adhere to the following instructions will be returned to the corresponding author for technical revision before undergoing peer review. Note that submission implies that the content has not been published or submitted for publication elsewhere except as a brief abstract in the proceedings of a scientific meeting or symposium. Once you have prepared your submission following the Guidelines, manuscripts should be submitted online at office@rjmm.ro.

EDITORIAL AND CONTENT CONSIDERATIONS

Aims and Scope

Romanian Journal of Military Medicine (RJMM) is the official journal of the Romanian Association of Military Physicians. The Journal publishes peer-reviewed original papers, reviews, meta-analyses, systematic reviews, and editorials concerned with clinical practice and research in the fields of medicine. Papers may cover the medical, surgical, radiological, pathological, biochemical, physiological, ethical, and historical subject areas. Clinical trials are afforded expedited publication if deemed suitable. RJMM also covers the basic sciences and experimental work, particularly those with clear relevance to disease mechanisms and new therapies. Case reports and letters to the Editor may not be considered for publication.

Editorial Review and Acceptance

The acceptance criteria for all papers and reviews are based on the quality and originality of the research and its clinical and scientific significance to our readership. All manuscripts are peer-reviewed under the direction of an Academic Editor. The Editor-in-Chief reserves the right to refuse any material for review that does not conform to the submission guidelines detailed throughout this document, including ethical issues, completion of an Exclusive License Form, and stipulations as to length.

ETHICAL CONSIDERATIONS

Principles for Publication of Research Involving Human Subjects

Manuscripts must contain a statement to the effect that all human studies have been reviewed by the appropriate ethics committee and have therefore been performed following the ethical standards laid down in an appropriate version of the Declaration of Helsinki (as revised in Brazil 2013), available at: http://www.wma.net/en/30publications/10policies/b3/index.html. It should also state clearly in the text that all persons gave their informed consent before their inclusion in the study. Details that might disclose the identity of the subjects under the study should be omitted. Photographs need to be cropped sufficiently to prevent human subjects from being recognized (or an eye bar should be used).

Registration of Clinical Trials

We strongly recommend, as a condition of consideration for publication, registration in a public trials registry. Trials register at or before the onset of patient enrolment. This policy applies to any clinical trial. We define a clinical trial as any research project that prospectively assigns human subjects to intervention or comparison groups to study the cause-and-effect relationship between a medical intervention and a health outcome. Studies designed for other purposes, such as to study pharmacokinetics or major toxicity (e.g., phase 1 trials), are exempt.

We do not advocate one particular registry, but registration with a registry that meets the following minimum criteria:

– Accessible to the public at no charge;

– Searchable by standard, electronic (Internet-based) methods;

– Open to all prospective registrants free of charge or at minimal cost;

– Validates registered information;

– Identifies trials with a unique number; and

– Includes information on the investigator(s), research question or hypothesis, methodology, intervention and comparisons, eligibility criteria, primary and secondary outcomes measured, date of registration, anticipated or actual start date, anticipated or actual date of the last follow-up, a target number of subjects, status (anticipated, ongoing or closed) and funding source(s).

Plagiarism Detection

The journal uses a plagiarism-detection system. By submitting your manuscript to this journal, you accept that your manuscript may be screened for plagiarism against previously published works.

All figures, images, and tables should be original and acknowledged as such by the authors. However, if figures, images, or tables from other sources are included, the copyright must be obtained from the authors of the original article, and proof of the copyright waiver must be provided to the Editors of RJMM. In case of any uncertainty regarding the copyright, the Editors may request the authors to remove from the article certain figures/tables/images.

Generative AI use

The journal requires a statement from the authors confirming that no generative AI tools were used to produce the articles. Still, if AI tools have been used to generate the main text, then this aspect should be clearly disclosed in the acknowledgments, specifying the purpose, specific areas of use, and acknowledging that the final responsibility for the text remains with the authors.

Committee on Publication Ethics

The Journal subscribes to the principles of the Committee on Publication Ethics (COPE).

MANUSCRIPT CATEGORIES AND SPECIFICATIONS

All articles, except for Editorials, must contain an abstract of no more than 200 words. Abstracts for original articles should be formatted as detailed in the Word form. Titles must not be longer than 120 characters (including spaces). In every article, there must be three to ten pertinent keywords specific to the article yet reasonably common within the subject discipline.

Editorials

These are invited by the Editor-in-Chief or their delegated editor and should be a brief review of the subject concerned, with reference to and commentary about one or more articles published in the same issue of RJMM. Editorials are generally 1200–1500 words, may contain one table or figure, and cite up to 15 references, including the source article. This should be cited as Rom. J. Mil. Med. (year); (vol): [issue].

Review Articles

RJMM welcomes reviews of important topics across the scientific basis of medicine and advances in clinical practice. Most published reviews are in response to the editorial invitation, including thematically related "miniseries" of reviews. Authors considering submitting a review for RJMM are advised to canvas their possible review with the Editor-in-Chief or a colleague editor; this avoids early rejection if the subject matter is not deemed a high priority for the Journal at the time of submission. Reviews are suggested to limit to 3500–5000 words, with an abstract of up to 200 words and up to 100 references and figures or tables.

Meta-Analyses or Systematic Reviews

RJMM particularly welcomes the submission of Meta-Analyses and Systematic Reviews, which underpin evidence-based medicine. Guidelines for the preparation of meta-analyses and Systematic Reviews are similar to other reviews, and articles are subject to the usual peer review process. Meta-analyses and Systematic Reviews are suggested to be limited to 3500–5000 words, with an abstract of up to 200 words and up to 100 references and figures or tables.

Original Articles (including clinical trials)

RJMM welcomes original articles concerned with clinical practice and research in the fields of medicine. Papers can cover the medical, surgical, radiological, pathological, biochemical, physiological, ethical, and/or historical subject areas. Clinical trials are afforded expedited publication if deemed suitable. RJMM also deals with the basic sciences and experimental work, particularly that with clear relevance to disease mechanisms and new therapies. Original articles are suggested to be limited to 3000 words, with an abstract of up to 200 words and up to 100 references and figures or tables.

Education and Imaging

The Editors welcome contributions to the Education and Imaging section. The purpose is to present imaging for the evaluation of unusual features of common conditions or the diagnosis of unusual cases. Contributions will be reviewed by the Executive Editors. The format of the Images pages involves two parts, each of which will occupy up to one journal page. In Part 1, a case will be described briefly, including a summary of the presentation, clinical features, and key laboratory results. One to two key images will then be presented. It is helpful to the reader if the author responds to questions that follow from the images of the case, such as 'What is your diagnosis? What are the features indicated on the CT scan? What is the differential diagnosis?' Part 2 will briefly describe the imaging features, particularly those that lead to a diagnosis or are critical for management. Differential diagnosis should be mentioned. It will be useful to include either further images or pathological details that validate the imaging diagnosis. Occasionally, the presentation of analogous cases or related images from a similar case might be appropriate.

Please include between one and three references to definitive studies and appropriate reviews of the subject. The format of the Images page involves a brief background and description of the disorder of interest, together with two figures of high quality. Colored photographs are encouraged. The submission may take the form of a case report or may illustrate particular features from more than one patient.

MANUSCRIPT PREPARATION

Style

Manuscripts should follow the style of the Vancouver agreement detailed in the International Committee of Medical Journal Editors' revised 'Uniform Requirements for Manuscripts Submitted to Biomedical Journals: Writing and Editing for Biomedical Publication, as presented at http://www.ICMJE.org/.

Spelling

The journal uses US spelling and authors should, therefore, follow the latest edition of Merriam-Webster's Collegiate Dictionary.

Units

All measurements must be given in SI units as outlined in the latest edition of Units, Symbols, and Abbreviations: A Guide for Biological and Medical Editors and Authors (Royal Society of Medicine Press, London).

Abbreviations

Abbreviations should be used sparingly and only where they ease the reader's task by reducing the repetition of long technical terms. Initially, use the word in full, followed by the abbreviation in parentheses. Thereafter, use the abbreviation.

Trade names

Trade names should not be used. Drugs should be referred to by their generic names, rather than brand names.

Parts of the Manuscript

The manuscript should be submitted in separate files: the title page and the main text file according to the Word model.

Title page

The title page should contain (i) a short informative title that contains the major keywords. The title should not contain abbreviations; (ii) the full names of the authors (if possible, not more than 5 authors per title); (iii) the author's institutional affiliations at which the work was carried out; (iv) the full postal and email address, plus telephone number, of the author to whom correspondence about the manuscript should be sent; (v) disclosure statement; and (vi) acknowledgments. The present address of any author, if different from that where the work was carried out, should be supplied in a footnote.

Disclosure statement

The source of financial grants and other funding should be acknowledged, including a frank declaration of the authors' industrial links and affiliations. In the case of clinical trials or an article describing the use of a commercial device, therapeutic substance, or food must state whether there are any potential conflicts of interest for each of the authors: failure to make such a statement may jeopardize the article being sent out for peer review.

Acknowledgments

The contribution of colleagues or institutions should also be acknowledged. Thanks to anonymous reviewers are not allowed.

Main text

As papers are double-blind peer-reviewed, the main text file should not include any information that might identify the authors. The main text of the manuscript should be presented according to the word model. Figures and supporting information should be submitted as separate files. Footnotes to the text are not allowed, and any such material should be incorporated into the text as parenthetical matter.

Abstract and keywords

Original articles must have a structured abstract that states in 200 words or fewer the purpose, basic procedures, main findings, and principal conclusions of the study. If appropriate, divide the abstract with the headings: Background and Aim, Methods, Results, and Conclusions. The abstracts of reviews need not be structured. The abstract should not contain abbreviations or references. Three to ten keywords should be supplied below the abstract and should be taken from those recommended by the US National Library of Medicine's Medical Subject Headings (MeSH) browser – http://www.nlm.nih.gov/mesh/meshhhome.html.

Text

Authors should use the word form when editing the submitted material.

References

The Vancouver system of referencing should be used. In the text, references should be cited using Arabic numerals in square parentheses in the order in which they appear. If cited only in tables or figure legends, number them according to the first identification of the table or figure in the text. In the reference list, the references should be numbered and listed in order of appearance in the text. Cite the names of all authors when there are six or fewer; when seven or more, list the first three followed by et al. Names of journals should be abbreviated in the style used in MEDLINE. References to unpublished data and personal communications should appear in the text only.

Use Index Medicus as the style guide for references and other journal abbreviations.

Always insert the DOI of the article, if available.

Tables

Tables should be self-contained and complement, but not duplicate, the information contained in the text. Number tables consecutively in the text in

Arabic numerals. Type tables on a separate page with the legend above. Legends should be concise but comprehensive – the table and legend must be understandable without reference to the text. Column headings should be brief, with units of measurement in parentheses; all abbreviations must be defined in footnotes. Footnote symbols: †, ‡, •, ▪ should be used (in that order) and *, **, *** should be reserved for P-values. Statistical measures such as SD or SEM should be identified in the headings.

Figure legends

Type figure legends on a separate page. Legends should be concise but comprehensive – the figure and its legend must be understandable without reference to the text. Include definitions of any symbols used and define/explain all abbreviations and units of measurement. Indicate the stains used in histopathology. Identify statistical measures of variation, such as standard deviation and standard error of the mean.

Figures

All illustrations (line drawings and photographs) are classified as figures. Figures should be numbered using Arabic numerals and cited in consecutive order in the text. Each figure should be supplied as a separate file, with the figure number incorporated in the file name.

Preparation of Electronic Figures for Publication:

Although low-quality images are adequate for review purposes, publication requires high-quality images to prevent the final product from being blurred or fuzzy.

SUBMISSION REQUIREMENTS

Manuscripts should be submitted online at office@rjmm.ro. A cover letter containing an authorship statement should be included. The cover letter should include a statement covering each of the following areas:

– Confirmation that all authors have contributed to and agreed on the content of the manuscript, and the respective roles of each author. It is not accepted that the idea of equal contribution.

– Confirmation that the manuscript has not been published previously, in any language, in whole or in part, and is not currently under consideration elsewhere.

– A statement outlining how ethical clearance has been obtained for the research, particularly concerning studies involving human subjects and animal experimentation.

The institutional ethics committees approving this research must comply with acceptable international standards (such as the Declaration of Helsinki), and this must be stated.

– For research involving pharmacological agents, devices, or medical technology, a clear Conflict of Interest statement about any funding from or pecuniary interests in companies that could be perceived as a potential conflict of interest in the outcome of the research.

– For clinical trials, these have been registered in a publicly accessible database (see more under 'ETHICAL CONSIDERATIONS (Further Information)' later in these guidelines).

If the above items are not included in the cover letter, manuscripts cannot be sent for review. Please also note that the cover letter does not require a detailed or lengthy description of the content or structure of the manuscript itself.

Two Word files need to be included upon submission: A title page file and the main text file that includes all parts of the text in the sequence indicated in the section 'Parts of the manuscript', including tables and figure legends but excluding figures, which should be supplied separately.

The main text file should be prepared using the Word model that is to be found on the web page (https://revistamedicinamilitara.ro/author-submission/).

Each figure should be supplied as a separate file, with the figure number incorporated in the file name. For submission, high-resolution figures (at least 300 d.p.i.) saved as .eps, .jpg, or .tif files are required.

PUBLICATION PROCESS AFTER ACCEPTANCE

Accepted Articles

Accepted Articles are published online after final acceptance, and appear in PDF format only.

Proofs

Once the paper has been typeset, the corresponding author will receive an email alert containing the proof of acceptance. It is therefore essential that a working e-mail address is provided for the corresponding author.

COPYRIGHT, LICENSING, AND ONLINE OPEN

Details are on the Copyright Agreement Form that must be completed and signed when the Article is submitted

Romanian Journal of
Military Medicine

New Series, Vol. 129, No 6/2026, November
ISSN-L 1222-5126; eISSN 2501-2312; pISSN 1222-5126